The mechanistic basis of susceptibility and resistance to the antitubercular drug *para*-aminosalicylic acid

A DISSERTATION
SUBMITTED TO THE FACULTY OF
THE UNIVERSITY OF MINNESOTA
BY

Shannon Lynn Kordus

IN PARTIAL FULFILLMENT OF THE REQUIREMENTS
FOR THE DEGREE OF
DOCTOR OF PHILOSOPHY

Advisor: Anthony David Baughn

May 2019

Acknowledgements

First, I would like to thank my advisor, Anthony “Tony” Baughn. When I first started, I was passionate about structural biology and biochemistry. Thank you for letting me pursue those passions in your research program. Your high expectations empowered me to become an independent scientist and, more importantly, paved the way for me to obtain my dream post-doctoral position. Thank you for fostering an environment of scientific rigor while placing a importance of having fun. I will not forget all the whiskey Friday nights, Tough Mudders, flossing, the Tony Tangents, and our unique mentor-mentee relationship. Thank you for accepting my Shannonisms, I think you will miss them. But, more important, just think of how much cleaner your office carpet is going to be!

I would like to thank all of the Baughn lab members past and present. It was a joy to work alongside you throughout the years. Zombie movie nights, beer nights, Tough Mudders, soccer games, volleyball games, and everything I am missing made completing my PhD a much more memorable experience. Thank you for listening to practice talks and for helping me with my prelim. I would like to give a shout out to the mouse team people Elise Lamont, Michael Howe, and (I guess) Tony. Working in the BSL3 for 12+ hours could have been a nightmare, but you made it bearable. I will not forget our songs, our games, and the mice! I would like to thank all of the undergrads I have mentored over the years in the Baughn lab. You taught me so much about mentoring and I am so proud of each of you. I have really enjoyed watching all of you grow into great scientists.

I would like to thank members of the Tischler and Aldrich labs for our joint group meetings and your invaluable advice for this body of work. Thank you for

listening to countless practice talks. Special shout out to Dylan White, Sarah Elliot, Sarah Namugenyi, and Anna Tischler for all the help with the mouse training!

I would like to thank my thesis committee (Tony Baughn, Jeff Gralnick, Anna Tischler, Courtney Aldrich, Gary Dunny, and Barry Finzel), thank you for providing me with different points of view and making this thesis as great as it is. Thank you, Tony, Anna, and Courtney for writing countless letters of recommendation and for all of your career advice over the years. Anna, thank you for being a great female role model!

Thank you to everyone associated with the Microbiology, Immunology, and Cancer Biology PhD program. You have made it a fun and supportive community. I would like to thank Beth Adamowicz, Tijana Martinov, Sarah Namugenyi, Kelsey Binder, and Katrina Jackson for all of the support over the years. Thank you for always listening to talks, reading fellowship proposals, always listening (and drinking) when I was having a rough day. I could not have done it without you. Also thank you for the dinner, drinks and dance nights, for including me in Pathfinders.

I would like to thank my best friend Dana Palm for her never ending support over the years! I would also like to thank Amy Rymaszewski for not only introducing me to my husband but also introducing me to research opportunities while I was in undergrad.

I would like to thank my family for all of their support. Specifically my parents, Art and Sandy Kordus ,from a young age you fostered my love for the sciences,

although I am still waiting for a chemistry set you promised me. Thank you for always telling me to shoot for the stars, to ignore the naysayers, and instilling a hard work ethic. All of these traits are essential to complete a PhD. I would like to thank my brother Andrew Kordus, MD. Just for the record PhDs were the first doctors, so yes, I am a real doctor. I would like to thank my Uncle Colin. My in-laws Kris, John, and Callan, thank you for always making me feel like a member of the Krystofiak family.

I would like to thank those closest to me, Tesla Kordus (aka Taco), Newton Krystofiak, and my partner in crime Evan Krystofiak, PhD. I would not have completed my PhD without your support. Evan, I know it has been difficult to be in a long-distance relationship for the better of nine years but I know the best is yet to come! I know the doggos cannot wait for us to be together. I cannot wait to see what The Vandy has in store for us. We are going to rock it!

Dedication

I would like to dedicate this dissertation to everyone who has believed in me throughout the years. I would also like to dedicate this thesis to those who did not believe in me. Your doubts fueled a fire to succeed and never, ever give up.

Abstract

Tuberculosis (TB) is responsible for the deaths of 1.6 million people worldwide each year and is the leading cause of death by the pathogen *Mycobacterium tuberculosis*. The treatment regimen for *M. tuberculosis* involves lengthy, intensive drug therapy that causes severe side-effects. The antimicrobial *para*-aminosalicylic acid (PAS) is used to treat drug-resistant *M. tuberculosis* infections. Despite the use of PAS to treat *M. tuberculosis* for over 70 years, the biochemical mechanisms which govern PAS susceptibility and resistance in *M. tuberculosis* are incomplete. The focus of this dissertation is to determine these mechanisms and can be summarized into three interrelated studies: 1) The mechanism of action of PAS on the *M. tuberculosis* folate metabolic pathway; 2) Understanding the mechanisms of PAS resistance; and 3) Examining the drug-drug interactions between PAS and other anti-folate drugs that are used to treat opportunistic infections in patients with HIV-*M. tuberculosis* co-infections.

Chapter 2 shows that PAS is a pro-drug and is converted, via the *M. tuberculosis* folate biosynthetic pathway, to hydroxy-dihydrofolate. The folate biosynthesis pathway is an essential metabolic pathway used maintain the production of DNA, RNA, and proteins. Results showed that hydroxy-dihydrofolate acted as a potent inhibitor for dihydrofolate reductase and confirm the biochemical mode of action of PAS. Although PAS was originally found to be effective at inhibiting *M. tuberculosis* and showed no activity against other bacterial species. PAS activity

was tested against other bacterial pathogens. While *M. tuberculosis* was extraordinarily sensitive to PAS, other bacteria resisted PAS-mediated killing. Chapter 2 found these bacterial species could utilize PAS as a fully functional folate analog into one-carbon metabolism. The folate biosynthesis precursor, *para*-aminobenzoic acid (PABA), is a known antagonist of antifolates, namely sulfonamides. Since PAS was shown to act similarly to PABA in folate biosynthesis, PAS-sulfonamide interactions were tested against a panel of bacterial pathogens. PAS could antagonize sulfonamides in all of these organisms. HIV-infected individuals are given numerous drugs to both treat the HIV infection and prophylactically treat and prevent opportunistic infections. The most commonly prescribed prophylactic drugs are the sulfonamides. These findings strongly support that PAS and sulfonamides should cease to be used in combination in individuals with HIV-*M. tuberculosis* co-infections.

Many patients discontinue treatment of PAS because of the side effects, namely, gastrointestinal distress. Bacteria must make their own folates and many bacteria in the human colon excrete folate to supply human enterocytes with folates. All rapidly dividing human cells require folates for the synthesis of new DNA, RNA, and proteins. All human cells contain folate receptors which recognize the metabolites dihydrofolate or folate. Purified human dihydrofolate reductase enzyme and could use hydroxy-dihydrofolate but much less effectively than the native substrate. Since enterocytes require a large amount of folates for rapid cell

growth, enterocytes using hydroxy-dihydrofolate as a source of folates may not be able to grow as fast leading to severe gastrointestinal distress. Indeed, hydroxy-dihydrofolate, not PAS, was cytotoxic to enterocytes and hepatocytes. These findings will allow us to ultimately to design better ways to administer PAS to prevent patients from discontinuing PAS treatment.

In Chapter 3, we hypothesized mice could be co-treated with sulfonamides to prevent PAS bioactivation and resulting PAS toxicity. Surprisingly, sulfonamides antagonized the anti-mycobacterial action of PAS in mice, resulting in the unrestricted growth of *M. tuberculosis* in the lungs and dissemination of *M. tuberculosis* into the liver and spleen. Taken together, these data indicate that combining PAS with sulfonamide in the clinic would not be useful, could be detrimental to patient outcome, and further highlights the need for mechanistic studies of drug-drug interactions.

.

Chapter 4 established that PAS resistance in *M. tuberculosis* primarily mapped to the folate biosynthetic pathway. The most prevalent mutations mapped to *thyA* and *folC,* a thymidylate synthase and dihydrofolate synthase, respectively. We hypothesized that *folC* mediated resistance occurred through an increase in PABA biosynthesis. Indeed PABA biosynthesis genes were upregulated in *folC* resistant mutants but not in *thyA* resistant mutants. The *folC* mutants had restored susceptibility to PAS when PABA biosynthesis was disrupted.

Furthermore, it was found that disruptions in PABA biosynthesis were bactericidal in *M. tuberculosis*. These data represent a novel intrinsic mechanism of resistance to PAS and highlights a novel drug target in *M. tuberculosis.*

This dissertation is the first to determine that PAS selectively inhibits *M. tuberculosis* dihydrofolate reductase enzyme and subsequently, the folate biosynthetic pathway. The work presented in this dissertation found that using PAS and sulfonamides together prevented both drugs from working correctly in *M. tuberculosis* and in other bacterial pathogens. The results generated from this dissertation will be used to inform the current clinical practices in combination therapy and foster a paradigm shift in the treatment regimen administered to HIV-*M. tuberculosis* co-infected patients, leading to decreased mortality rates among this population.

TABLE OF CONTENTS

List of Tables

List of Figures

Chapter 1:

The mechanistic basis for susceptibility and resistance to *para*-aminosalicylic acid and other antifolates

This chapter is a reprint, with alterations, of a published manuscript.

Kordus, S.L. and Baughn A. B. 2019. Revitalizing antifolates through understanding mechanisms that govern susceptibility and resistance. *MedChemComm*. Accepted.

Impact of Mycobacterium tuberculosis

Mycobacterium tuberculosis is the causative agent of tuberculosis (TB). TB was responsible for 1.6 million deaths and yielded 10 million new active cases in 2017(WHO, 2018). TB is one of the top 10 causes of death worldwide and is the leading cause of death due to a single infectious agent. Although a highly effective treatment regimen for TB exists, therapy remains challenging due to the protracted treatment duration that requires multiple antibiotics. The minimum treatment duration for TB is 6 months with drugs that are associated with adverse reactions. Standard treatment can cure 95% of drug susceptible TB cases. Drug resistant strains of *M. tuberculosis* can emerge in the 5% of patients that cannot be effectively treated by standard therapy. Drug resistant TB is multifactorial and can occur from treatment errors and poor quality or supply of antitubercular drugs. Furthermore, drug-resistant strains of TB can only be cured in about 50% of patients. Treatment of drug-resistant TB can last more than 2 years with chemotherapeutics that are associated with even more adverse side effects. Treatment duration and costs make curing drug resistant TB challenging. Therefore, there is an increased interest in studying drugs used to treat drug-resistant TB.

para-aminosalicylic acid (PAS) is an antimicrobial agent used to treat *M. tuberculosis* infections. Despite the use of PAS to treat TB for over 70 years, the biochemical knowledge which govern PAS susceptibility and resistance in *M.*

tuberculosis are incomplete. The focus of this dissertation is to determine these mechanisms and can be summarized into three interrelated studies: 1) Understanding the mechanisms that govern PAS resistance and susceptibility; 2) Examining the drug-drug interactions between PAS and other antifolate drugs that are used to treat opportunistic infections in patients with HIV-*M. tuberculosis* co-infections; and 3) Probing *para*-aminobenzoic acid biosynthesis for novel drug targets. Determining the mechanisms that govern resistance and susceptibility to current anti-tubercular drugs will allow the discovery of new therapeutic approaches to shorten treatment times and counter drug-resistant TB.

The disease tuberculosis

In the 1880s, Robert Koch discovered *M. tuberculosis* was the causative agent of TB. The disease generally affects the lungs and has symptoms that include chronic cough, fever, night sweats, and weight loss(WHO, 2018). Historically, TB was called consumption or wasting away disease due to the severe weight loss patients experienced. The cough is not productive during the initial phase of the disease. As the disease progresses, inflammation and tissue necrosis increase, and causes a productive cough with blood tinged sputum. The word TB was derived from the tubercle lesions people with *M. tuberculosis* had in their lungs. The early period during the infection can be misdiagnosed as other pulmonary diseases. TB is thought to latently infect between one-third to one-fourth of the world's population(WHO, 2018). In 5-10% of these infected individuals, the

bacterium will cause active disease that can be transmitted via coughing or sneezing. Although many pathogenic bacteria have devised strategies to prevent immune recognition, *M. tuberculosis* has evolved multiple mechanisms to be recognized by and exploit the host immune system.

M. *tuberculosis* first emerged in Africa around 70,000 years ago and spread across the world by human migration(Hershberg *et. al*., 2008; M Cristina *et. al*., 2005). *M. tuberculosis* is believed to have evolved from an ancient environmental strain of mycobacteria(Gagneux, 2018). A close relative of this ancestral strain can be isolated in east Africa. This common ancestor of *Mycobacterium* is thought to have been unable to be transmitted from person to person but was capable of causing a chronic infection in an immune-competent person(Supply *et. al*., 2013). In contrast, *M. tuberculosis* can only spread by human to human transmission (Brites and Gagneux, 2012; Ebert and Bull, 2003). Furthermore, *M. tuberculosis* has no known animal or environmental reservoir, unlike many other bacterial pathogens. Taken together, these observations suggests that *M. tuberculosis* evolved to become an intercellular pathogen and environmental mycobacteria initially evolved to survive inside of a free-living protozoa that fed on environmental bacteria(Jang *et. al*., 2008). Additionally, while this strain survived inside of protozoa, it evolved the ability to survive and multiply intracellularly in a macrophage; however, this strain could not be transmitted from person to person(VanderVen *et. al*., 2017). This *Mycobacterium* is thought to

have evolved the ability to spread from person to person, via aerosol droplets, facilitated by increased human social interactions that resulted from the agricultural revolution(Chisholm *et. al*., 2016).

Some Mycobacteria can also cause disease in animals. These strains of Mycobacteria are thought to have evolved similarly to *M. tuberculosis* after domestication of animals. For instance, humans infected with *M. tuberculosis* were able to transmit the pathogen to cattle, this strain of *M. tuberculosis* evolved into the bacterium *Mycobacterium bovis*(Brosch *et. al*., 2002). *M. bovis* has also maintained the ability to be transmitted to humans.

The Biology of Mycobacteria

Mycobacteria are a member of the Actinobacteria phylum. They are non-motile, aerobic rods, with a high G+C DNA content (62-70% depending on species). The word *Mycobacterium* describes the fungal, pellicle-like hyphal colony morphology when grown on solid medium. Most Mycobacteria are environmental, soil-dwelling organisms and are generally classified into two groups, fast-growing and slow-growing(Fedrizzi *et. al*., 2017; Gagneux, 2018; Rogall *et. al*., 1990). Fast growing Mycobacteria require less than seven days to form colonies on agar plates, while slow-growing Mycobacteria require over seven days. Some slow-growers are human pathogens including *M. tuberculosis* (the causative agent of TB) and *Mycobacterium leprae* (the causative agent of leprosy). Although, it is

noted that *M. leprae* cannot be grown in pure culture. *M. tuberculosis* has a doubling time of 18-24 hours while *Mycobacterium smegmatis*, a fast growing Mycobacterium, has a doubling time of roughly 2.5 hours. The mechanistic basis for Mycobacterium slow growth is not understood.

The immune response to M. tuberculosis *infection*

M. tuberculosis is spread through aerosol droplets released from an infected individual either through coughing or sneezing. The aerosols are inhaled by another individual and *M. tuberculosis* is phagocytized by alveolar phagocytic cells within the lung. While most research has focused on interaction of *M. tuberculosis* with monocyte derived macrophages, neutrophils and dendritic cells can also phagocytize the bacterium, and less is known about the infection of these other immune cells. The information in this section will be focused within the context of alveolar macrophages. *M. tuberculosis* is phagocytized by binding to receptors on macrophages such as C-type lectin receptors, scavenger receptors, and complement receptors(Philips and Ernst, 2012; Schäfer *et. al*., 2009; Wolf *et. al*., 2007). Interestingly, *M. tuberculosis* binding to distinct receptors dictates their intracellular fate. For instance, binding to a C-type lectin (specifically, dendritic cell-specific intracellular adhesion molecule 3–grabbing nonintegrin) or a complement receptor results in lysosomal delivery of the bacteria. Binding to a C-type lectin receptor (specifically, macrophage mannose receptor) prevents phagolysosomal maturation(Armstrong and Hart, 1975; Kang

et. al., 2005; Philips and Ernst, 2012). Taken together, *M. tuberculosis* has evolved multiple strategies to gain entry into phagocytic cells that serve as a niche for replication and persistence within the host.

After gaining entry into the macrophage, there are multiple intracellular fates of *M. tuberculosis.* Once phagocytized, *M. tuberculosis* employs multiple mechanisms to prevent phagosomal maturation and remain in an early endosome-like environment(Russell, 2001). In some instances, *M. tuberculosis* is unable to prevent the phagosome-lysosome fusion leading to bacterial death. Furthermore, in some instances, the bacterium can replicate in the phagolysosome(17, 23). An early endosome environment allows *M. tuberculosis* to acquire nutrients, such as iron, while preventing acidification and fusion with the lysosome(Philips, 2008). The early endosome-like environment allows *M. tuberculosis* to replicate and eventually allows transmission to other cells.

Once in the phagosome, *M. tuberculosis* can express and secrete proteins through Esx-1, a type VII secretion system. Esx-1 allows for escape and replication of *M. tuberculosis* into the cytosol. It is only present in pathogenic strains of *M. tuberculosis* and absent in the attenuated vaccine strain *M. bovis* BCG(Philips and Ernst, 2012; van der Wel *et. al*., 2007). One Esx-1 secreted protein of interest is the early secreted antigenic target 6kDa (ESAT-6) that inhibits antigen presentation by macrophages(Samten *et. al*., 2009; Volkman *et.*

al., 2010). ESAT-6 can also bind culture filtrate protein-10 (CFP-10) and allows *M. tuberculosis* to escape the phagosome during acidic conditions(De Jonge *et. al*., 2007). Bacterial escape into the cytosol, allows for growth and transmission of *M. tuberculosis* to neighboring alveolar macrophages. In the closely related *Mycobacterium*, *Mycobacterium marinum*, a model bacterium for studying the immune response to *M. tuberculosis*, cytosolic bacteria can also be ubiquitinated and are killed by autophagy(Collins *et. al*., 2009). It is not clear whether cytosolic ubiquitinated *M. tuberculosis* are killed by autophagy similar to *M. marinum*.

M. tuberculosis can replicate inside of resting macrophages. Specific host factors (such as interferon gamma, tumor necrosis factor, and vitamin D) can activate the resting macrophages which results in the killing of *M. tuberculosis*(Jouanguy *et. al*., 1999). Interferon gamma can activate production of reactive nitrogen and oxygen species. Both reactive nitrogen and oxygen species are toxic to the bacterium and can result in the limitation of iron and other metals(Chan *et. al*., 1992). Furthermore, in an activated macrophage, *M. tuberculosis* will switch its metabolism to allow for the utilization of host cholesterol, as a primary carbon source(Chang *et. al*., 2009; Pandey and Sassetti, 2008; Schnappinger *et. al*., 2003). In an interferon gamma activated macrophage, the bacteria must acquire iron through siderophore production. Tumor necrosis factor is essential for controlling *M. tuberculosis* replication and works synergistically with interferon gamma to activate macrophages. However, *M. tuberculosis* can manipulate

macrophage production of tumor necrosis factor to enhance lung inflammation in mice(Agarwal *et. al*., 2009). Taken together *M. tuberculosis* employs multiple mechanisms to survive, replicate, and escape death by macrophages to promote disease and spread to new phagocytic cells.

Once *M. tuberculosis* has replicated to a high titer in the macrophage or if they have escaped the macrophage, they spread to an uninfected phagocytic cell to propagate the infection(30). *M. tuberculosis* can escape the macrophage through two mechanisms, apoptosis and necrosis. Multiple studies found that the bacteria promote necrotic death of the macrophage(Keane *et. al*., 2000a; Molloy *et. al*., 1994a). Attenuated and mutant strains of *M. tuberculosis* promote macrophage apoptosis that results in the release of fewer bacteria(Keane *et. al*., 2000b; Molloy *et. al*., 1994b). Apoptosis allows for the presentation of *M. tuberculosis* antigens to $CD8^+$ T cells that would promote an adaptive immune response and limit the spread of infection(Divangahi *et. al*., 2010). During necrosis, macrophages will release signals to recruit additional phagocytic cells allowing for the spread of *M. tuberculosis*. Furthermore, *M. tuberculosis* infected macrophages that promote necrosis are taken up by newly recruited phagocytic immune cells causing the infection to spread(Philips and Ernst, 2012). *M. tuberculosis* also has multiple mechanisms to prevent apoptosis, via modulating the regulation of pro-and anti-apoptosis and inflammation responses(Balcewicz-Sablinska *et. al*., 1998; Kremer *et. al*., 2007; Oddo *et. al*., 1998; Sly *et. al*., 2014).

Specifically, *M. tuberculosis* upregulates the anti-apoptotic genes *mcl-1* and *A1*, as well as the protein complex NF-KB(Kremer *et. al*., 2007; Sly *et. al*., 2014). *M. tuberculosis* can also downregulate pro-apoptotic proteins such as Fas and tumor necrosis factor receptor 2(Balcewicz-Sablinska *et. al*., 1998; Oddo *et. al*., 1998). During this initial phase of the infection, there is little restriction of bacterial growth in the lung. This phase of the infection is dynamic and varies depending on individual immune response.

Following the initial innate response, a delayed adaptive immune response is thought to be a mechanism employed by *M. tuberculosis* to expand the initial bacterial population in the lungs thereby establishing a chronic infection(Wolf *et. al*., 2008). Activation of $CD4^+$ T cells results in the arrest of bacterial growth(Wolf *et. al*., 2008). In most humans, this arrest results in a latent bacterial infection. During latency, the cell mediated immune response coupled with the innate response forms the granuloma.

Granulomas represent the hallmark histopathological lesions during a TB infection. Simply, the granuloma is an ordered assemblage of dendritic cells, T cells, B cells and several types of macrophages including mature macrophages, foamy macrophages, and multinucleated (Langhans) giant cells. Foamy macrophages are found in areas of the necrotic regions of the granuloma and are associated with large amounts of lipids(Peyron *et. al*., 2008). Interestingly, a

small proportion of macrophages in the granuloma are infected with *M. tuberculosis*. The granuloma is a “stalemate” between the host immune system and the bacterium. Granuloma formation is thought to be beneficial for *M. tuberculosis* survival, as the granuloma allows for the recruitment of additional phagocytic cells that allows for bacterial growth(Davis and Ramakrishnan, 2009). Similarly, the granuloma is thought to be beneficial to the host because it allows for close interactions between the bacterium and the immune system. The cell mediated immune response coupled with the innate response maintains the bacterial population and prevents dissemination to other areas of the host; however, it does not clear the infection.

Although the initial infection primarily involves the innate immune response, the adaptive immune response is of paramount importance for controlling the infection. One feature of the adaptive immune response is the delay in the T cell response during an *M. tuberculosis* infection in humans and in mice(Grange and Yates, 1995). The delay is due to the lag in the migration of antigen presenting cells, from the lung to the lymph nodes. *M. tuberculosis* antigens are recognized by $CD4^+$ T cells(Wolf *et. al*., 2008). These $CD4^+$ T cells are a subset of T-cells that recognize antigen bound to major histocompatibility class (MHC) II molecules found on antigen presenting cells. Binding of a $CD4^+$ T cell to its cognate antigen, via MHC II, allows the $CD4^+$ T cell to activate phagocytic cells such as macrophages and dendritic cells. Therefore, $CD4^+$ T cells are essential

for protective immunity against *M. tuberculosis*. $CD4^+$ T cells are equally important in preventing reactivation of *M. tuberculosis* to an active infection, especially in the context of an HIV-TB co-infection (see section *TB and HIV/AIDS Co-infection*). *M. tuberculosis* employs several mechanisms to prevent antigen presentation to $CD4^+$ T cells such as down-regulating antigen production, preventing antigen loading onto the MHC II, and preventing trafficking of MHC II to the membrane(Harding and Boom, 2010). There are multiple subsets of $CD4^+$ T cells such as T_h1, T_h17, and Tregs that are also important for an effective immune response against *M. tuberculosis*(Harding and Boom, 2010; Khader *et. al*., 2005, 2007). $CD4^+$ T cells activate another type of T cell, called $CD8^+$ T cells that recognize MHC I molecules. MHC I is expressed on all host cells and expresses a peptide from degraded cytosolic proteins and also antigens from intracellular pathogens, like *M. tuberculosis*. When $CD8^+$ T cells, or cytotoxic T cells, bind their cognate antigen they release cytotoxins such as perforin, granzymes, and granulysins to kill *M. tuberculosis* infected host cells by apoptosis(Lewinsohn *et. al*., 2003; Philips and Ernst, 2012). $CD8^+$ T cells are important in controlling *M. tuberculosis* infection and, similarly to $CD4^+$ T cells, depletion of $CD8^+$ T cells can also cause a latent infection to become active(van Pinxteren *et. al*., 2000).

Although $CD4^+$ and $CD8^+$ T cells are essential to control intracellular infections, another important immune cell for controlling infection and for vaccine

development are B cells. B cells are a population of white blood cells that are both antigen presenting cells and secrete antibodies. B cells recognize antigen through a B cell receptor that can bind extracellular antigen. Once antigen is bound to a B cell receptor, the B cell can present the antigen to antigen presenting cells and secrete cytokines(Blum *et. al*., 2013). After binding antigen, the B cell can undergo a class switch and affinity maturation to ultimately secrete high affinity antibodies to target the antigen(Mårtensson *et. al*., 2010). Antibody binding can have outcomes including opsonization of the surface of bacterial cell, neutralization of a pathogen, agglutination and precipitation of antigens to allow for phagocytosis to occur. One study found treating SCID mice (lacking T and B cells) with polyclonal antibodies against *M. tuberculosis* provided protection against disease relapse(Guirado *et. al*., 2006). During an infection many intracellular pathogens, including *M. tuberculosis*, will become extracellular therefore exposing antibodies to potential antigens(Achkar *et. al*., 2015). As the immune response is not capable of eliminating *M. tuberculosis*, people can be reinfected after the disease is treated and cleared.

The complex interplay between *M. tuberculosis* and the host makes designing effective vaccines and discovery of new drugs challenging. The Bacillus Calmette-Guérin (BCG) vaccine is the only vaccine approved and given to prevent *M. tuberculosis* infection. The vaccine is given to infants worldwide in areas where TB is common(WHO, 2018). The vaccine is derived from an

attenuated strain of *M. bovis*, a strain of *Mycobacterium* that causes TB in bovines. *M. bovis* can also infect humans and cause TB(JM *et. al*., 1996). *M. bovis* BCG lacks many virulence factors found in *M. tuberculosis* such as the RD-1 locus that encodes for many secreted proteins essential for virulence, such as ESX-1(Ganguly *et. al*., 2008; Stanley *et. al*., 2003). Children and adults can also receive the vaccine if they have not been previously infected with *M. tuberculosis* but are frequently exposed to drug resistant strains of *M. tuberculosis*(Davenne and McShane, 2016). The efficacy of the *M. bovis* BCG vaccine varies widely depending on the study. The vaccine protects an estimated 20% of people from getting a latent infection and it prevents an estimated 50% of people from developing the disease(Bjartveit, 2003; Hawn *et. al*., 2014). The vaccine is most effective at preventing extrapulmonary disease (Colditz *et. al*., 1995; Fine, 1995). One obstacle in creating new vaccines is the lack of a convenient animal model that fully recapitulates various aspects of the human immune response to *M. tuberculosis*. Standard lab mice do not exhibit the hallmark granuloma within the lung and succumb to the disease much slower than humans(Ernst, 2012; Ramakrishnan, 2012).

For many years, a diagnosis of latent TB was defined as a reactivity to the tuberculin skin test without signs or symptoms of active disease. Briefly, this test uses purified protein derivatives that are injected intradermally. The tuberculin skin test measures the delayed-type hypersensitivity response elicited to these

proteins. Patients could test positive due to the presence or exposure to non-pathogenic mycobacterial antigens such as those found in the *M. bovis* BCG vaccine(Barry *et. al*., 2009; Mazurek *et. al*., 2001). Recently, more specific tests, such as QuantiFERON gold and T-spot test have been developed for diagnosis *M. tuberculosis* exposure. QuantiFERON measures the amount of interferon gamma level produced by circulating T cells in response to *M. tuberculosis* antigens early secretory antigenic target 6 (ESAT-6), culture filtrate protein 10 (CFP-10), and TB7.7. Interferon gamma levels are elevated in patients that have elicited a cell-mediated immune response to the previously mentioned *M. tuberculosis* antigens. One major drawback to the QuantiFERON gold test is that depending upon the level of T cell depletion, HIV-positive individuals may lack an effective cell-mediated immune response, to any infection, and will test negative. In this patient cohort, an (ELISPOT) assay is performed termed T-spot TB. Specifically, the T-spot measures the number of interferon gamma producing T cells after exposure to ESAT-6 and CFP-10 (Wang *et. al*., 2007). As previously described both of these proteins are only found in *M. tuberculosis* and are absent in non-pathogenic mycobacteria. Importantly, the T-spot assay can be used to evaluate patients who are HIV-positive, as the assay does not require high amounts of reactive $CD4^+$ T cells(Lawn *et. al*., 2007). One problem with all of the previously mentioned diagnostic tests is that they do not distinguish between active and latent disease(Barry *et. al*., 2009).

The definition of a latent infection is quite diverse. Some define latency as metabolically active bacteria contained in the host in the absence of clinical symptoms, compared to those who have cleared the infection(Young *et. al*., 2009). Similarly, even active TB is broadly characterized by the presence of caseous hypoxic lesions with dynamic bacterial burden or liquid cavities with massive loads of replicating bacteria. Therefore, TB is thought to be a spectrum of disease(Barry *et. al*., 2009). Recently, there has been a shift in our understanding of what a latent infection might be. Several studies have shown that TB reactivity can occur even after an *M. tuberculosis* infection has cleared(Behr *et. al*., 2018). A recent study found individuals who test positive for latent TB might never reactivate to an active infection. Furthermore, these individuals had no viable bacilli even with sequence positive results in the lesions, in the lung. In some individuals considered latently infected, no bacilli were found with negative sequencing results(Behr *et. al*., 2018).

Bacterial reactivation can be influenced by certain genetic or pathophysiological factors, such as HIV co-infection, aging, and cancer(WHO, 2018). These factors decrease the cell mediated immune response and allow the bacteria to grow and breakdown the granuloma structure. Deterioration of the granuloma can allow the bacteria to escape the confinement of necrotized host cells allowing for the transmission into the airways. Once in the airways *M. tuberculosis* is able to be transmitted person to person. In some cases, the infection can go systemic and

spread to other parts of the body such as spleen, liver, bones and central nervous system. Approximately 15-20% of new cases of TB are extrapulmonary(Lee, 2015; WHO, 2018). Symptoms of extrapulmonary TB are similar to pulmonary TB and can include fever, weight loss, anorexia and general weakness (WHO, 2018). Systemic infections are associated with higher morbidity and mortality rates especially in immunocompromised individuals.

Mycobacterial cell wall

A distinct feature of Mycobacteria is their unique cell envelopes. Functionally similar to Gram-negative bacteria, *M. tuberculosis* cell envelope consists of an asymmetric lipid bilayer made of long chain fatty acids (mycolic acids), a layer of peptidoglycan, arabinogalactan, and waxy components that surround the plasma membrane (Brennan, 2003; Hett and Rubin, 2008). The mycobacterial cell wall inner layer extending from the plasma membrane is composed of, in order, peptidoglycan and arabinogalactan, linked together. Peptidoglycan provides a scaffold to allow the bacteria to maintain their shape(Brennan, 2003; Hett and Rubin, 2008). Arabinogalactan, composed of arabinan and galactan, is the most abundant polysaccharide of the mycobacterial cell wall. Arabinogalactans anchor the peptidoglycan layer to the mycolic acid layer and is important for mycomembrane integrity(Brennan, 2003; Hett and Rubin, 2008).

Lastly, the mycomembrane, is composed of two layers the inner layer and the outer layer(Vincent *et. al*., 2018). The inner layer is composed of mycolic acids that are long (between 60 and 90 carbon atoms), branched-chain hydroxy fatty acids; therefore, mycolic acids are hydrophobic. Mycolic acids are also primarily responsible for mycomembrane impermeability(Vincent *et. al*., 2018). For instance, mycolic acids are impervious to traditional Gram staining, and, for this reason, have been termed Gram indeterminate. In order to detect mycobacteria, an acid-fast stain is used. Briefly, acid fast staining uses heat and a phenol-basic dye which allows the stain to be retained in the membrane. The stain is not easily washed out due to the hydrophobic mycolic acid membrane. Notably, the inner mycomebrane is a target for many antitubercular drugs (See *Treatment of tuberculosis*, and Table 1.1).

The mycomembrane outer layer is comprised lipids, lipoglycans, and proteins(Chiaradia *et. al*., 2017; Vincent *et. al*., 2018). The outer layer is not well characterized due to its complexity and many low abundance proteins. Some of the lipids found in the outer layer include phthiocerol dimycocerosate, phenolic glycolipid, and lipooligosaccharides. These lipids also help *M. tuberculosis* evade the host immune response and are virulence factors(Forrellad *et. al*., 2013; Reed *et. al*., 2004). The outer layer is associated via hydrophobic interactions with the inner mycomembrane layer(Grzegorzewicz *et. al*., 2016). The lipids in the outer membrane make mycobacteria more resistant to damage from certain sterilizing

chemicals and can prevent hydrophilic antibiotics from diffusing into the cell(Brennan and Nikaido, 1995).

TB and HIV/AIDS Co-infection

Opportunistic infections, such as TB, are the leading cause of death in individuals with HIV/AIDS. Individuals infected with HIV and latently infected with TB are 20 times more likely than HIV-negative people to develop active disease(WHO, 2018). In 2017, 9% of active TB diseases were in individuals who were HIV-positive and caused an estimated 300,000 deaths among HIV-positive individuals(WHO, 2018). Therefore, individuals with HIV are not only placed on anti-retroviral therapy, but also a lifetime prophylactic combination of co-trimoxazole, a broad spectrum anti-folate that is used to prevent opportunistic infections. HIV infections are a strong risk factor for developing active TB infections and are associated with poorer treatment outcomes. With the increase in antiretroviral therapy, the TB incidence rates have decreased among HIV-positive individuals since 2010 (Williams *et. al*., 2010).

HIV is a member of the *Lentivirus* genera of retroviruses. A retrovirus is a type of RNA virus that encodes its own reverse transcriptase to produce DNA from its RNA genome. The DNA is then integrated into the host DNA and the host transcription and translational machinery can express viral protein. HIV infects

$CD4^+$ helper T cells. In healthy HIV-negative individuals, proliferating $CD4^+$ T cells are long lived (Okoye and Picker, 2013). During HIV infection, these cells are quickly turned over either by pyroptosis, the killing of infected cells by $CD8^+$ T cells or by apoptosis(Doitsh *et. al*., 2013; Garg *et. al*., 2012; Okoye and Picker, 2013). Without treatment HIV is fatal after 9-13 years and generally results in acquired immunodeficiency syndrome (AIDS) when the $CD4^+$ T cell count is below 200 cells per µL of blood. Without treatment the mean survival period, of people with AIDS is less than 3 years.

As discussed above in *The disease tuberculosis*, controlling *M. tuberculosis* infection requires both $CD4^+$ T cells and $CD8^+$ T cells. Depletion of both cell types results in TB activation and rapid disease progression. Specifically, declining $CD4^+$ T cells results in poor granuloma formation and an increase in dissemination of *M. tuberculosis*(Diedrich and Flynn, 2011). The advent of effective antiretroviral therapy to treat HIV prevents the rapid decline in $CD4^+$ T cells. Although, the $CD4^+$ T cell function is not as robust as in a TB-positive HIV-negative individual (Chang *et. al*., 2013; Suthar *et. al*., 2012). Patients who are HIV-positive with diagnosed latent TB are started on a treatment regimen to prevent the reactivation of TB. Furthermore, although TB is the leading cause of death in HIV-positive individuals, there are a variety of other opportunistic infections that can cause death in HIV-positive individuals.

To protect against opportunistic infections, HIV-infected individuals are given the chemotherapeutic agent co-trimoxazole, a combination of sulfamethoxazole (SMX) and trimethoprim (TMP) in a 5:1 ratio, respectively. Co-trimoxazole is given as life-long prophylactic therapy to HIV-positive individuals even when the viral titers are undetectable. The combination of SMX/TMP is used to treat a variety of bacterial infections including respiratory tract infections, urinary tract infections, *Staphylococcal* infections, and cholera. Co-trimoxazole has also been given as lifetime prophylactic therapy to treat and prevent *Pneumocystis* pneumonia and *Toxoplasma gondii* which commonly infect individuals with AIDS. When SMX is not well tolerated dapsone is used as a surrogate. Given the success and global availability of highly active antiretroviral therapy for HIV, there is a debate regarding the need for lifelong co-trimoxazole prophylactic therapy. More information on antifolates will be discussed in *Folate biosynthesis as a drug target*.

Treatment for M. tuberculosis

Treatment of *M. tuberculosis* is more complex than treatment for any other bacterial infection. For drug susceptible *M. tuberculosis* infections, patients are treated with short course antitubercular therapy of rifampicin, isoniazid, ethambutol, and pyrazinamide for 2 months followed by treatment with isoniazid and rifampicin for an additional 4 months(WHO, 2018). Each drug is associated with a unique mechanism of action for targeting different metabolic

processes(Table 1.1). Each of the previously mentioned drugs are associated with numerous adverse reactions(Table 1.1). Extensive clinical trials have shown that this short course therapy will provide a cure to drug susceptible strains of *M. tuberculosis* in more than 95% of cases, if the drugs are taken correctly. However, a small subset of *M. tuberculosis* cells are able to “persist” in low numbers for long periods of time despite the presence of antitubercular therapy. These “persisters” can take months to fully eradicate and can lead to disease relapse if not fully resolved.

Isoniazid is considered the best bactericidal drug while rifampicin is considered the best sterilizing drug. If resistance occurs to both of these instrumental agents, patients will be infectious longer, proloning treatment from 6 months to possibly longer than 24 months. Multiple types of drug resistance are wide spread across the globe and must be considered during TB treatment. Multidrug resistant TB (MDR-TB) is defined as being resistant to both isoniazid and rifampicin. While extensively drug resistant TB (XDR-TB) is defined as being resistant to isoniazid, rifampicin, a second-line fluoroquinolone, and an injectable second line drug such as amikacin, kanamycin, or capreomycin. In some areas of the world, totally drug resistant strains of *M. tuberculosis* exist that cannot be cured by existing drug regimens. The factors that contribute to the emergence of MDR-TB are still not fully understoodinclude treatment errors and patient noncompliance. MDR-TB drugs are prescribed by the following considerations, (i) the percentage of drug

resistance in the local region, (ii) previous anti-tubercular drugs taken by the patient and adverse reactions to those drugs, and (iii) patient medical history (Lange *et. al*., 2014).

Drug discovery in *M. tuberculosis* has been challenging. First, drugs must be able to travel to the lung, travel through the granuloma, and ultimately travel into a macrophage in high enough dosage to inhibit or, ideally, kill *M. tuberculosis*. These “ideal” drug candidates should inhibit various physiological states of the bacterium and *M. tuberculosis* should have low evolvable resistance to these candidates. The bacterium can be found in many diverse environments (such as hypoxia and low pH). Therefore, the drug candidates should be stable (not prone to degradation). Ideally, the drug candidates should inhibit both replicating and non-replicating states of *M. tuberculosis*. As described above, the cell wall of *M. tuberculosis* is waxy, lipid rich, and can be impenetrable to many drug-like compounds. Furthermore, a relatively inexpensive animal model recapitulating the various microenvironments inhabited by *M. tuberculosis* does not exist. Also, the drugs must be well tolerated in patients for extended periods of time, be inexpensive, and have minimal drug-drug interactions with the current treatment regimen and HIV antiretroviral therapy. This coupled with the slow growth rate of *M. tuberculosis* and requiring Biosafety Level 3 culturing and animal facilities have resulted in very few drugs entering into the development pipeline and ultimately into the clinic(Koul *et. al*., 2011; Kumar *et. al*., 2017; Zuniga *et. al*.,

2015). There have been numerous recent advances in understanding *M. tuberculosis* biology, including models for understanding bacterial physiology and genetics of *M. tuberculosis*.

para-Aminosalicylic acid inhibits M. tuberculosis

para-Aminosalicylic acid (PAS) was synthesized in 1902; however, its therapeutic potential was not recognized until 1940(Seidel and Bittner, 1902). Frederick Bernheim found salicylic acid stimulated oxygen consumption in *M. tuberculosis*, while other structural analogs of salicylic acid decreased oxygen consumption(BERNHEIM, 1940). Jörgen Lehmann followed up on these studies and screened over 50 benzoic acid structural analogs, synthesized by K. G. Rosdahl from Ferrosan Company(Donald and Diacon, 2015). He identified PAS as a potent antitubercular agent(Lehmann, 1946). In March 1944, after PAS was found to be efficacious in treating TB in animals, it was given to 20 patients with pulmonary TB. Although bacterial counts were not reported, patients gained weight, had reduced fevers, and decreased erythrocyte sedimentation rates (a correlative measure of bacterial burden)(Donald and Diacon, 2015; Lehmann, 1946). Although, PAS was the first antitubercular agent tested in humans, no controls were used in the study. Interestingly, PAS has been shown to only have activity against *M. tuberculosis*, although the mechanistic basis for this high level of selectivity is not known(Ivanovics *et. al*., 1948; Ragaz, 1948; Sievers, 1946;

Tobie and Jones, 1949; Wyss, 1943). PAS entered clinical use as a bacteriostatic antitubercular agent in 1946(Youmans *et. al*., 1947b).

While Lehmann was testing the antitubercular activity of PAS, Albert Schatz, a PhD student in the laboratory of Selman A. Waksman, isolated the antibiotic streptomycin. Streptomycin showed potent antitubercular activity(Schatz *et. al*., 1944). Shortly thereafter, streptomycin was used in randomized clinical trials to treat patients with TB and showed excellent efficacy.

Before the discovery of PAS and streptomycin, 50-80% of patients who tested positive for TB would die within 10 years(Tiemersma *et. al*., 2011). The discovery of streptomycin and PAS had dramatically improved TB survival rates. However, resistance to streptomycin in *M. tuberculosis* emerged shortly after its introduction into the clinic. PAS was found to be effective against streptomycin-resistant strains of *M. tuberculosis*(Youmans *et. al*., 1947b). PAS was used in combination with streptomycin, which reduced the emergence of drug resistance, and is considered the first multi-drug therapy. The antitubercular agent isoniazid, discovered in the early 1950s, was highly effective in treating *M. tuberculosis* and was often included in the streptomycin-PAS treatment regimen. The three-drug combination was found to be highly effective in curing *M. tuberculosis* and decreased the emergence of drug resistant strains.

Unfortunately, treatment with PAS was often associated with gastrointestinal (GI) distress. During the first clinical trial of PAS 75% of patients taking PAS reported severe GI distress, and 20-25% reported nausea, vomiting and diarrhea(Erdei and Snell, 1948; Vallentin and Tronell, 1950). Clinical trials in the US resulted in almost half of patients discontinuing PAS treatment(Pfuetze and Pyle, 1949). During these clinical trials researchers speculated that this GI distress was due to impurities during the synthesis or deterioration of PAS by opening storage containers(Mitchell *et. al*., 1954). To counter these severe side effects, PAS was given intravenously in Europe and was found to be much bettered tolerated(Jones, 1954). Furthermore, PAS was found to be quickly inactivated in the liver either through acetylation, to produce mono- or di-acetyl-PAS, or carboxylated, to produce glycine-PAS(Jenne *et. al*., 1961). In addition, the mean serum life of PAS is 1hr. With the advent of better tolerated and superior antitubercular agents, such as ethambutol, rifampicin, and pyrazinamide, PAS fell out of use to treat TB in the 1960s.

In 1994, with the global spread of MDR and XDR strains of *M. tuberculosis*, PAS has re-entered antitubercular drug regimens to treat drug resistant strains of *M. tuberculosis*. Furthermore, PAS was reformulated into a new delayed release gastro-resistance formulation, to help prevent GI distress. PAS is given as the free base. The acid resistant granules should be taken with acidic food. Once the granules enter the small intestines, the coating is dissolved at neutral pH and the

coat allows for delayed release of PAS, so that the serum levels do not immediately peak. However, patients still must take 10-12g of PAS per day to reach inhibitory levels in the lung and still 20% of patients will discontinue PAS treatment due to GI distress. In response to the revitalization of PAS, there is a need for understanding of the molecular details of susceptibility and resistance of *M. tuberculosis* to PAS. Initial observations suggested that PAS disrupted a salicylic acid-linked metabolic pathway; however, recent studies have suggested that PAS inhibits folate biosynthesis.

Folate biosynthesis as a drug target

In prokaryotes and eukaryotes, folate (vitamin B_9) is an essential metabolic cofactor required for all actively growing cells. Specifically, folate serves as a one-carbon carrier in the synthesis of amino acids (such as methionine, serine, and glycine), N-formylmethionyl-tRNA, coenzyme A, purines and thymidine (Figure 1.1). Many microbes are unable to acquire folates from their environment and rely on *de novo* folate biosynthesis. In contrast, mammals lack the *de novo* folate biosynthesis pathway and must obtain folate from commensal microbiota or the environment using proton-coupled folate transporters. The essentiality and dichotomy between mammalian and bacterial folate biosynthesis and utilization pathways make it an ideal drug target for the development of antimicrobial agents and cancer chemotherapeutics.

De novo folate biosynthesis begins with the synthesis of *para*-aminobenzoic acid (PABA, Figure 1.2) and 6-hydroxymethyl-7,8-dihydropterin pyrophosphate (DHPPP, Figure 1.3). Although both pathways are largely absent in mammals and essential in bacteria, protozoa and fungi, there are no antimicrobial agents in clinical use that target PABA or DHPPP biosynthesis.

Later steps in folate synthesis involve the conversion of 7,8-dihydropteroate (DHP) to 5,6,7,8-tetrahydrofolate (THF) in three ordered steps by DHP synthase (FolP), dihydrofolate synthase (FolC), and dihydrofolate reductase (DHFR in mammals and FolA in bacteria) (Figure 1.4). The only approved therapeutic agents in clinical use that target this portion of the pathway inhibit FolP and dihydrofolate reductase.

Antifolates, agents that impair folate biosynthesis, were the first class of antimetabolites to enter clinical use. They were used to treat a variety of cancers and inflammatory disorders in humans and were among the first antimicrobial agents used to treat bacterial infections. Historically, antifolates have targeted the enzymes FolP (sulfonamides and sulfones) and DHFR (methotrexate, proguanil and trimethoprim). Resistance to antifolates was reported shortly after their introduction into clinic use. Since some antifolates can be associated with adverse reactions, some have been replaced with safer more effective drugs. With the rise in resistance to many chemotherapeutics and antimicrobial agents

and with the advent of better-tolerated antifolates, there has been a renewed interest in using this drug class to treat many diseases.

Sulfonamides were introduced into the clinic in 1935 to treat a variety of bacterial infections. However, some sulfonamides, such as sulfamethoxazole (SMX), were associated with rare adverse reactions such as blood dyscrasias, hypoglycemia, hyperkalemia, and inhibition of cytochrome P450(KEISU *et. al*., 1990; Strevel *et. al*., 2006; Wen *et. al*., 2002). In 1962, TMP was introduced into the clinic as a bacterial FolA inhibitor. Shortly after introduction of TMP into clinic use, it was noted that SMX and TMP showed potent synergistic activity, permitting the use of lower dosages of SMX that resulted in fewer adverse reactions(Smilack, 1999). Consequently, co-administration of SMX with TMP (co-trimoxazole) became standard of care for treating many infections. Since co-trimoxazole is generally well-tolerated, relatively inexpensive and can target a broad spectrum of microbes, it is commonly used for prophylactic treatment against opportunistic infections in immunocompromised individuals.

Targeting para-*Aminobenzoic Acid Biosynthesis in Microbes*

In most bacteria, fungi, protozoans and plants, folates are synthesized from the convergence of two pathways, the PABA biosynthesis pathway and pterin biosynthesis pathway. The PABA biosynthesis pathway is generally absent in the metazoan lineage. The first step of PABA biosynthesis involves the conversion of

chorismate to aminodeoxychorismate (ADC) (Figure 1.2). Chorismate is a product of the shikimate pathway, the pathway from which aromatic amino acids, quinones and salicylic acid are also derived. In the synthesis of PABA, chorismate and glutamine are converted to ADC and glutamate by the action of ADC synthase. ADC synthase is comprised of two enzymatic subunits PabA and PabB encoded by *pabA* and *pabB*, respectively. Both enzymes require physical interaction for optimal catalysis. PabA catalyzes glutamine lyase activity and is typically only active in the presence of stoichiometric amounts of PabB(Roux and Walsh, 1993; Viswanathan *et. al*., 1995). In the absence of PabA and glutamine, PabB is able to catalyze the amination of chorismate in the presence of vast molar excess ammonia(Roux and Walsh, 1993). Both *pabA* and *pabB* are predicted to be essential in many bacterial species.

Interestingly, some bacteria do not encode a defined PabA homolog and instead there is functional overlap with an analogous enzyme TrpG from the tryptophan biosynthetic pathway. In tryptophan biosynthesis TrpG functions in conjunction with TrpE to catalyze synthesis of anthranilate from chorismate and glutamine in a reaction similar to that for synthesis of ADC(Kaplan *et. al*., 1984; Knöchel *et. al*., 1999; Morollo and Eck, 2001; Mugumbate *et. al*., 2015; Slock *et. al*., 1990). As TrpG and PabA show a high degree of sequence conservation and have mechanistically identical enzymatic function(Morollo and Eck, 2001; Slock *et. al*., 1990), organisms such as *Bacillus subtilis*, *Acinetobacter calcoaceticus* and

Salmonella enterica express a bi-functional (amphibolic) glutamine ammonium lyase that operates as a subunit of both anthranilate synthase and ADC synthase.

The last step in PABA biosynthesis is the conversion of ADC to PABA by ADC lyase encoded by *pabC*(Green and Nichols, 1991; Green *et. al*., 1992). This reaction proceeds with the elimination of the pyruvyl moiety of ADC enabling subsequent aromatization to PABA. Since elimination of pyruvate from ADC can occur spontaneously, disruption of *pabC* is not predicted to be essential in many bacteria.

In *M. tuberculosis* disruption of PABA biosynthesis, specifically through mutagenesis of *pabB* or *pabC,* results in enhanced susceptibility to antifolates, including sulfa-drugs and the diaminophenylsulfone, dapsone(Thiede *et. al*., 2016). There are multiple natural products that inhibit PabB including abyssomicin C and anthelminthicin C and their derivatives (Figure 1.5)(Bihelovic *et. al*., 2013; Freundlich *et. al*., 2010; Keller *et. al*., 2007a, 2007b; Matovic *et. al*., 2014). These compounds show inhibitory activity against *M. tuberculosis* and methicillin resistant *Staphylococcus aureus* (MRSA) in whole cell assays (Bihelovic *et. al*., 2013; Freundlich *et. al*., 2010; Matovic *et. al*., 2014; Riedlinger *et. al*., 2004; Wang *et. al*., 2010a). Evaluation of their activity in animal models of infection has not been reported. Abyssomicin C and some of its derivatives

display a high level of cytotoxicity against mammalian cells(Bihelovic *et. al*., 2013). Although, atrop-*O*-benzyl-desmethylabyssomicin C was found to have significantly reduced cytotoxicity whilst retaining activity against MRSA and may represent a promising lead(Matovic *et. al*., 2014). In addition to these derivatized natural products, the synthetic dichloronitrophenyl propanone, MAC173979, was found to inhibit PABA biosynthesis in *E. coli* both enzymatically and in whole cell assays(Zlitni *et. al*., 2013). MAC173979 exhibited time-dependent inhibition in a one-pot assay using purified recombinant PabA, PabB, and PabC, yet, the exact target of MAC173979 is not known(Zlitni *et. al*., 2013). MAC173979 also showed potent activity against *M. tuberculosis* that could be antagonized by exogenously supplied PABA (Figure 1.5) (Thiede *et. al*., 2016). Consistent with genetic studies described above, synergistic inhibition of growth was observed when *M. tuberculosis* was treated with MAC173979 in combination with various sulfa-drugs or dapsone(Thiede *et. al*., 2016). Taken together, the PABA biosynthesis pathway remains a promising drug target especially in combination with sulfa-drugs.

Targeting Pterin Biosynthesis in Prokaryotes and Eukaryotes

Prokaryotes and eukaryotes synthesize pterins, albeit, the metabolic functions they serve can be quite distinct. For instance, in humans, guanine cyclohydrolase (encoded by *GCH1*) catalyzes GTP hydrolysis, isomerization and cyclization to form 7,8-dihydroneopterin triphosphate (Figure 1.3), a precursor in

tetrahydrobiopterin synthesis. Tetrahydrobiopterin is a critical co-factor for the synthesis of aromatic amino acids and multiple neurotransmitters(Kappock and Caradonna, 1996). Deficiencies in the production of tetrahydrobiopterin results in dystonia, or sustained muscle contractions. Bacteria, fungi, protozoans and plants also encode a guanine hydrolase (FolE, encoded by *folE*) that performs the same biochemical function as GCH1. However, in this context, 7,8-dihydroneopterin triphosphate is essential for folate biosynthesis (Figure 1.3). FolE requires a zinc ion to be bound that allows for subsequent binding of the purine ring of GTP. Following binding, GTP is cleaved and isomerized to allow for the closure of the dihydropyrazine ring(Auerbach *et. al*., 2000; Gräwert *et. al*., 2013; Tanaka *et. al*., 2005). Interestingly, 8-aminoguanosine triphosphate and other structural analogs of GTP, can competitively inhibit bacterial FolE and GCH1 by mimicking the transition state between GTP and 7,8-dihydroneopterin triphosphate (Figure 1.6)(Blau and Niederwieser, 1986; Tanaka *et. al*., 2005).

In the next step of DHPPP synthesis, 7,8-dihydroneopterin triphosphate is dephosphorylated by a cytoplasmic Nudix hydrolase to produce 7,8-dihydroneopterin (Figure 1.3). Nudix hydrolases form a superfamily of pyrophosphatases that are often involved in detoxifying toxic metabolites. The first 7,8-dihydroneopterin triphosphate pyrophosphatase Nudix hydrolase enzyme to be described was YlgG, encoded by *ylgG*, in *Lactococcus lactis*(Klaus *et. al*., 2005). Since YlgG did not show sufficient sequence similarity to Nudix

enzymes of bacteria with known genome sequences, identifying other Nudix hydrolases involved in pterin synthesis has been quite challenging. The product of the gene *orf17*, NudB (or NtpA), was the first dihydroneopterin triphosphate pyrophosphatase described in *E. coli*(Gabelli *et. al*., 2007; O'Handley *et. al*., 1998). Nudix enzymes hydrolyze substrates through the use of a nucleophilic substitution and require a metal ion for coordination of GTP, though the specific metal varies between Nudix enzymes(Gabelli *et. al*., 2007; Hill *et. al*., 2017; Klaus *et. al*., 2005; O'Handley *et. al*., 1998). Since dihydroneopterin triphosphate pyrophosphatases have only been recently discovered, inhibitors of this enzyme have yet to be identified. Nevertheless, deletion of *nudB* in *E. coli* has been shown to dramatically enhance susceptibility to both SMX and TMP (Li *et. al*., 2017; Minato *et. al*., 2018). Thus, these recent discoveries open avenues for novel therapeutic development.

Once formed, 7,8-dihydroneopterin is converted to 6-hydroxymethyl-7,8-dihydropterin by dihydroneopterin aldolase (FolB) yielding glyceraldehyde as a byproduct (Figure 1.3). FolB, encoded by *folB*, is predicted to be essential in bacteria. Most aldolases require a Schiff base for the cleavage of the carbon-carbon double bond and a zinc ion for catalysis, both of these features are targets for selective aldolase inhibitors(Daher and Therisod, 2010). FolB is a unique aldolase as it requires neither a Schiff base for cleavage nor a zinc ion for catalysis(Blaszczyk *et. al*., 2007; Wang *et. al*., 2006). Because of its novel

characteristics, designing FolB inhibitors has been challenging. In some organisms, dihydroneopterin aldolase is a bi-, or in some parasites, a tri-functional enzyme. For instance, in *Streptococcus pneumonia*, dihydroneopterin aldolase (SulD, encoded by *sulD*) is a bi-functional enzyme that encodes 6-hydroxymethyl-7,8-dihydropterin pyrophosphokinase that can convert 6-hydroxymethyl-7,8-dihydropterin to 7,8-dihydroneopterin(Garçon *et. al*., 2006; Lopez and Lacks, 1993). The opportunistic pathogen *Pneumocystis jiroveci* encodes a tri-functional enzyme that functions not only as a dihydroneopterin aldolase and 6-hydroxymethyl-7,8-dihydropterin pyrophosphokinase but also as a dihydropteroate synthase(Volpe *et. al*., 1993). These multi-functional enzymes have been extensively targeted for development of antimicrobial inhibitors.

Most FolB inhibitors mimic the pterin or pyrimidine moiety of 7,8-dihydroneopterin (Figure 1.6) (Zimmerman *et. al*., 1977). A high-throughput X-ray crystallography screen and structure-directed lead optimization discovered multiple potent inhibitors of dihydroneopterin aldolase from *S. aureus*(Sanders *et. al*., 2004) (Figure 1.6). It has not yet been reported whether these compounds possess whole cell inhibitory activity against intact bacteria.

The last step in pterin biosynthesis for folates requires the conversion of 6-hydroxymethy-7,8-dihydropterin to DHPPP via the enzyme 6-hydroxymethyl-7,8-dihydropterin pyrophosphokinase (FolK, encoded by *folK* in bacteria) (Figure

1.3). In bacteria, disruption of FolK results in a pronounced growth defect. FolK is a unique pyrophosphokinase because it transfers a pyrophosphate from the beta phosphate of ATP rather than a more conical gamma phosphate yielding AMP(Blaszczyk *et. al*., 2000). FolK has been studied for the development of novel bisubstrate analog inhibitors allowing for selective inhibition of this target (Figure1.6) (Parang and Cole, 2002; Shi *et. al*., 2012b, 2012a). Most of the bisubstrate inhibitors developed mimic the ATP phosphate donor and acceptor (serine, threonine, or tyrosine). Despite these compounds potently inhibiting purified FolK, they showed limited whole cell activity. 8-mercaptoguanine has also been shown to inhibit *S. aureus* FolK by acting as a non-competitive inhibitor (Figure 1.6) (Chhabra *et. al*., 2012, 2013). Although 8-mercaptoguanine is a potential scaffold for discovery, its activity against *S. aureus* has not been reported and it is likely to show polypharmacology through interaction with other proteins with purine binding domains (Figure 1.6). In bacteria, the pterin biosynthetic pathway is highly conserved, however, the enzymes are structurally distinct and may ultimately allow for selective targeting (Bourne, 2014).

Targeting Folate Biosynthesis in Prokaryotes and Eukaryotes

DHP is produced from the condensation of PABA and DHPPP with elimination of pyrophosphate via DHP synthase (DHPS, FolP in bacteria, encoded by *folP*) (Figure 1.4). FolP is a target of many antimicrobial agents including sulfonamides and diaminodiphenyl sulfones (Figure 1.7). Both drug classes are analogs of

PABA. Sulfonamides, such as SMX, are broad spectrum antimicrobial agents that inhibit FolP by creating the dead-end product sulfamethoxazole-dihydropterin(Hevener *et. al*., 2011; Palmer and Kishony, 2014; Zhao *et. al*., 2016). Another inhibitor of FolP is 8-mercaptoguanine that has been shown to have promiscuous activity by inhibiting many enzymes that have a substrate bearing a purine moiety (Figure 1.7) (Dennis *et. al*., 2018). Since FolP is an important drug target, there have been many structural and biochemical studies focused on designing more potent FolP inhibitors(Hammoudeh *et. al*., 2013; Yun *et. al*., 2012) During the catalytic cycle DHPPP binds first, and the pyrophosphate is removed in a magnesium dependent reaction(Baca *et. al*., 2000; Hevener *et. al*., 2011; Yun *et. al*., 2012; Zhao *et. al*., 2016). Once the pyrophosphate is eliminated, the PABA binding pocket opens and allows for binding of PABA, sulfonamides or diaminodiphenyl sulfones(Babaoglu *et. al*., 2004; Hevener *et. al*., 2011; Levy *et. al*., 2008; Yun *et. al*., 2012). Sulfonamides and sulfones bind the PABA binding pocket that is separate from the pterin binding pocket. To develop novel classes of inhibitors, there is an increased interest in targeting the pterin binding pocket. Recently, a series of novel compounds were designed to inhibit the pterin binding pocket of purified recombinant *Bacillus anthracis* FolP (Figure 1.7) (Zhao *et. al*., 2012). These compounds potently inhibited through binding within the pterin binding pocket and provided structure activity relationship information for designing new inhibitors.

Many sulfonamides and sulfonylurea-based drugs, such as sulfasalazine, sulfathiazole, sulfapyridine, SMX, and chloropropamide, can show toxicity through off target effects in humans. These compounds have been found to inhibit the NADPH dependent enzyme sepiapterin reductase(Haruki *et. al*., 2013; Yang *et. al*., 2015). Sepiapterin reductase is an essential enzyme that is required for synthesis of tetrahydropterin, a critical co-factor for neurotransmitter synthesis in mammals.

DHP is converted to 7,8 dihydrofolate (DHF) by the ligation of L-glutamate using the ATP-dependent enzyme DHF-synthase (DHFS, FolC in bacteria, encoded by *folC*) (Figure 1.4). In many organisms, such as *E. coli*, *Corynebacterium* sp., and *P*. *falciparum*, DHFS is a bi-functional enzyme that can catalyze the gamma linkage of additional L-glutamate residues to fully reduced folate species(Bognar *et. al*., 1985; Salcedo *et. al*., 2001; Shane, 1979). Folylpolyglutamates are important in bacteria for methionine synthesis(Watson *et. al*., 2007). In humans, folates are polyglutamylated by the enzyme downstream of dihydrofolate reductase, folylpolyglutamate synthase (FPGS). In eukaryotes, polyglutamylation is important for retaining reduced folates in subcellular compartments. The role of polyglutamylation has not been extensively studied in bacteria, but, it is conceivable that the negatively charged polyglutamate tail may prevent folate species from diffusing across the cytoplasmic membrane.

Both FolC and FPGS are members of the Mur superfamily of enzymes and both contain an ATPase domain(Bourne, 2014; Mathieu *et. al*., 2005). ATP is positioned in a narrow channel and is stabilized by two magnesium ions(Young *et. al*., 2008). In the crystal structure of many apo-FolC enzymes the pterin binding site is not well resolved, however, the active site becomes more ordered upon the binding of DHP(Mathieu *et. al*., 2005; Sheng *et. al*., 2008a; Young *et. al*., 2008). Interestingly, in bacteria, FolC has an induced fit pterin binding pocket to allow mono- and poly-glutamylated folates to bind(Sheng *et. al*., 2008b; Smith *et. al*., 2006a; Sun *et. al*., 2001a). The conversion of DHP to DHF generates a tetrahedral intermediate through the transfer of a phosphate from ATP to DHP(Smith *et. al*., 2006b; Sun *et. al*., 2001b). Glutamate will react with the intermediate to produce DHF. Attempts to target the tetrahedral transition state have yielded initial hits against purified FolC but none have shown whole cell activity(Banerjee *et. al*., 1988; Wang *et. al*., 2010b).

The last step in folate biosynthesis is the reduction of DHF to THF by the NADPH dependent enzyme dihydrofolate reductase (Figure 1.4) (DHFR, FolA in bacteria encoded by *folA*) (Figure 3). DHFR is a small 18kDa protein containing 8 β-sheets and 4 α-helices and has no disulfide bonds. Although most enzymes in the folate biosynthesis pathway are essential, FolA in bacteria can be conditionally essential. In *E. coli*, *folA* can be deleted following disruption of the gene for thymidylate synthase (Howell *et. al*., 1988), a folate-dependent enzyme

required for thymidine synthesis. Unlike other folate-dependent enzymes thymidylate synthase yields DHF rather than THF. Thus, while elimination of this activity confers thymidine auxotrophy, it decreases the demand for folate reduction which can be inefficiently catalyzed by FolM(Giladi *et. al*., 2003).

DHFR reduces DHF using NADPH as an electron donor to THF and with the release of $NADP^+$ (Figure 1.8 and Figure 1.9). Under steady state reaction conditions, the catalytic mechanism of DHFR is stepwise (Figure 1.8) (Fierke *et. al*., 1987; Schnell *et. al*., 2004). The reaction begins with NADPH bound to the enzyme (E:NADPH), next DHF binds which creates the Michaelis complex (E:NADPH:DHF) (Figure 1.8). Once DHF binds, the hydride transfer occurs ($E:NADP^+$:THF). The exact biochemical mechanism of the hydride transfer is not well understood. To date there are two proposed mechanisms, the first states the hydride transfer is pH dependent and occurs by an ionizable side chain in the active site(Cannon *et. al*., 1997). The second mechanism states the pH dependent hydride transfer is solvent dependent(Chen *et. al*., 1994). $NADP^+$ is released (E:THF), another NADPH binds (E:NADPH:THF), and finally THF is released in the rate determining step to prime the enzyme for another catalytic cycle.

DHFR is a highly dynamic enzyme and multiple structures of DHFR exist with multiple ligands bound. Therefore, the movement of DHFR has been extensively

studied using x-ray crystallography, NMR and neutron diffraction(Schnell *et. al*., 2004). The protein is made up of two structural domains, the adenosine binding domain and the major subdomain. The adenosine binding domain allows for the adenosine moiety of NADPH to bind. The major subdomain is made up of other smaller domains that are located around the active site. These subdomains consist of the Met20 loop (residues 1-20), the F-G loop, and the G-H loop. The subdomains movement is controlled by Lys38 and Val88, in *E. coli*(Behiry *et. al*., 2014). Both amino acids act as hinges to allow the adenosine binding domain to move relative to the major subdomain upon ligand binding.

The Met20 loop lies over the active site preventing solvent exposure, as both NADPH and DHF bind in a hydrophobic binding pocket. The Met20 loop allows both DHF and NADPH to bind in close proximity of one another. Specifically, the NADPH is within van der Waals contact of the hydride acceptor DHF(Schnell *et. al*., 2004). The Met20 loop is important for the structure of the active site by stabilizing hydrogen bonding between the F-G loop and the G-H loop. The Met20 loop forms four different confirmations based on X-ray studies: occluded, closed, open, and disordered (Figure 1.8). The occluded and closed have also been observed in solution NMR studies(Schnell *et. al*., 2004). The confirmation is determined by a specific ligand that is bound. The loop is considered open when NADPH is bound and forms a wide binding area to allow DHF to bind and allow for subsequent release of $NADP^+$. When THF is only bound in the active site,

DHFR forms an occluded conformation to allow for increased binding affinity to NADPH. When NADPH binds the Met20 domain moves to “pack” the NADPH into the closed active site confirmation allowing for the release of THF. Lastly, the Met20 loop has not been resolved in crystallized apo-enzyme structures or in structures where methotrexate, a DHFR inhibitor, is bound(Schnell *et. al*., 2004).

DHFR is an important folate biosynthesis chemotherapeutic target. There are many drugs that selectively inhibit DHFR in humans, bacteria, fungi, and protozoa. DHFR inhibitors in humans and protozoans generally mimic the substrate folate (Figure 1.7). One class of inhibitors, the diaminopteridines, include methotrexate (MTX) and aminopterin, both are used to treat cancers and autoimmune disorders (Figure 1.7) (Cronstein, 2005). Diaminopteridines are transported into human cells by folate receptors. Since, folate receptors are highly upregulated by as much as 100-fold in cancer cells, MTX and other diaminopteridines potently target these cells compared to non-cancerous cells(Sudimack and Lee, 2000). Not only do folate receptors recognize folate and folate analogs but they also recognize polyglutamylated folate species. As described above, polyglutamylated species are retained within cellular compartments. Thus, this mechanism for retention of folates has been co-opted to promote accumulation of DHFR inhibitors, such as pralatrexate, within target cells(Visentin *et. al*., 2013).

Aminopterin was the first human DHFR inhibitor to enter clinical use for the treatment of childhood lymphocytic leukemia (Figure 1.7) (Figure 3). Aminopterin was associated with high toxicity and was quickly replaced with MTX which was found to be as effective, but less toxic. MTX is known to inhibit all purified DHFRs, including those from bacteria, fungi and protozoans, and is characterized as a slow, time-dependent, tight-binding competitive inhibitor (Figure 3)(Morrison and Walsh, 1988; Williams *et. al*., 1979). Binding of MTX results in a slow conformational change in the enzyme active site and is known to bind almost identically to folate by forming similar hydrogen bonding within the active site. One notable difference occurs when the pterin ring of MTX is flipped 180º with respect to DHF. This flip allows hydrogen bonding with the ionizable group in the active site(Bennett *et. al*., 2006).

Since most pathogenic bacteria lack folate receptors and cannot actively take up this cofactor, antibacterial FolA inhibitors are not close structural analogs of folate. In general, bacterial FolA inhibitors must diffuse across the cell envelope or require folate independent transport(Floyd *et. al*., 2010; Kok *et. al*., 1996). The structure of many of these inhibitors leaves them vulnerable to numerous efflux pumps (Figure 1.10) (Floyd *et. al*., 2010; Kok *et. al*., 1996). One notable bacterial FolA inhibitor, trimethoprim (TMP), contains a 2,4-diaminopyrimidine ring that allows for critical hydrogen bonding in the active site. TMP binds much more tightly (about 10^5) to bacterial FolA than mammalian DHFR (Figure 1.7)(Burchall

and Hitchings, 1965). The benzyl ring of TMP undergoes a thermodynamically unfavorable flip in the apo-enzyme. However, in the presence of NADPH the flipping of the benzyl ring is decreased. Therefore, in bacteria, TMP is a competitive inhibitor with respect to DHF and a non-competitive inhibitor with respect to NADPH. Conversely, mammalian DHFR can bind TMP but cannot form key hydrogen bond contacts within the active site(Matthews *et. al*., 1985).

TMP was first introduced into the clinic in 1962. Resistance was described as early as 1968, therefore, TMP derivatives were synthesized and explored for antimicrobial activity. Two notable TMP derivatives are tetroxoprim used for the treatment of *Pneumocystis pneumonia and* iclaprim for treatment of methicillin and vancomycin resistant strains of *Staphylococcus aureus* as well as drug resistant strains of *Streptococcus* species (Figure 1.7) (Aschhoff and Vergin, 1979; Sincak and Schmidt, 2009). Trimetrexate is a quinazoline derivative and is a chimera of pterin moiety of methotrexate and contains the benzyl ring of TMP. Iclaprim, like TMP, is a diaminopyrimidine that contains a chromene ring in place of the benzyl ring of TMP. The chromene ring allows for additional hydrogen bonding to occur within the active site of FolA(Sincak and Schmidt, 2009).

The first anti-malarial antifolate drug discovered was the biguanide proguanil which is one of the components of the widely used malaria prophylactic drug malarone (Figure 1.7). Shortly after its discovery, proguanil was found to be a

pro-drug that is metabolized by the host CYP2C19 to cycloguanil (Figure 1.7)(Carrington *et. al*., 1951; Desta *et. al*., 2002). This activated form was found to inhibit *Plasmodium falciparum*, the most prevalent causative agent of malaria, through targeting of DHFR. Many proguanil derivatives, including the cycloguanil structural analog pyrimethamine, have since been developed to counter drug resistant strains of *P. falciparum* (Figure 1.7) (Hitchings *et. al*., 1950). Pyrimethamine showed excellent efficacy in humans because of the low dosage required for treatment and paucity of side effects(Hoekenga, 1954). However, pyrimethamine resistance quickly emerged which diminished its use in treatment of malaria. Pyrimethamine has been repurposed to treat toxoplasmosis and is used in combination with dapsone to treat *Pneumocystis* pneumonia in HIV infected individuals.

The dihydrotriazine, WR99210, is an anti-malarial DHFR inhibitor that was developed after emergence of resistance to pyrimethamine and cycloguanil (Figure 1.7). WR99210 potently inhibits DHFR at very low concentrations, in the nano- to picomolar range. Unfortunately, in human clinical trials, daily administration of 200 mg of WR99210 for three days resulted in severe gastrointestinal distress. As a result, further clinical investigation into WR99210 was abandoned. To counter WR99210 toxicity, the biguanide pro-form PS-15 ((N-(3-(2,4,5-trichlorophenoxy)propyloxy)-N'-(1-methylethyl)-imidocarbonimidic diamide hydrochloride) was synthesized based on proguanil that could be

activated *in vivo* (Figure 1.7) (Canfield *et. al*., 1993). PS-15 showed improved antimalarial activity and it is anticipated that it will be better tolerated than WR99210. Importantly, PS-15 was found to selectively inhibit *P*. *falciparum* DHFR and had little activity against mammalian DHFR. Unfortunately, large-scale synthesis of PS-15 is challenging for drug production and has caused its development to lag. However, with this scaffold, other WR99210 analogs have been explored as novel DHFR inhibitors not only in *Plasmodia* species, but also in *M. tuberculosis*, *Mycobacterium avium* and *P*. *jiroveci*(Gerum *et. al*., 2002; Kumar *et. al*., 2015).

Antifolate Synergy

Currently, TMP and SMX are rarely given in monotherapy. When used in combination, TMP and SMX (co-trimoxazole) exhibit highly synergistic antimicrobial activity. For several decades it was presumed that the basis for synergy between SMX and TMP was exclusively due to the ability of SMX to prevent DHF synthesis and enhance the ability of TMP to inhibit FolA (Bushby and Hitchings, 1968; Minato *et. al*., 2018; Wormser *et. al*., 1982). While this model explains how SMX is able to enhance microbial susceptibility to TMP, it is not sufficient to explain the ability of TMP to enhance susceptibility of microbes to SMX(Harvey, 1978). It was recently demonstrated that TMP treatment results in depletion of DHPPP through impairment of GTP synthesis and is the basis for potentiation of SMX susceptibility (Minato *et. al*., 2018). Thus, it is the cyclic

nature of the folate biosynthetic pathway that enables the potent synergy between SMX and TMP (Minato *et. al*., 2018).

Antifolates for treating drug resistant M. tuberculosis

Although the folate biosynthesis pathway is not the current target of first line therapy, there is renewed interest in targeting folate biosynthesis to treat drug resistant strains of *M. tuberculosis.* Shortly after the discovery of the broad spectrum antifolates, sulfonamides were used to treat *M. tuberculosis*; however, they were found to be ineffective(Freilich *et. al*., 1939). Recently, with the increasing challenge of treating MDR- and XDR-TB there has been a renewed interest of using co-trimoxazole, because both are well tolerated drugs and are cost effective for long term use. Several studies have found that co-trimoxazole is a viable treatment option for treating MDR- and XDR-TB(Alsaad *et. al*., 2013; Forsman *et. al*., 2014; Vilchèze and Jacobs, 2012). Although, these studies also suggest that co-trimoxazole should only be given during the initial treatment of *M. tuberculosis*. SMX have limited intracellular activity in macrophages (MIC_{90}=76µg/ml) compared to extracellular treatment (MIC_{90}=23µg/ml) suggesting that the therapeutically relevant concentrations may not be reached in the macrophages. Therefore, this drug combination should be used during the initial infection when *M. tuberculosis* is more extracellular.

PAS targets folate metabolism

PAS is a structural analog of PABA, possessing a hydroxyl-group in the *ortho*-position to the carboxylic acid. Soon after its discovery, PAS was thought to disrupt folate biosynthesis based on the observation that exogenous PABA could antagonize its inhibition of *M. tuberculosis* growth(Youmans *et. al*., 1947a). Initially, PAS was thought to act as a FolP inhibitor similar to sulfonamides. However, no cross-resistance between PAS and sulfonamides in *M. tuberculosis* was observed(Yegian and Long, 1951). Further, in contrast to sulfonamides, PAS was found to only weakly inhibit purified FolP enzymatic activity and was later demonstrated to be converted to a hydroxylated version of DHP, hydroxy-DHP (Figure 1.4, Figure 1., and Figure 1.11) (Chakraborty *et. al*., 2013; Zhao *et. al*., 2014; Zheng *et. al*., 2013). FolC was found to catalyze the glutamylation of hydroxy-DHP to hydroxy-DHF (Figure 1.4 and Figure 1.11), which suggested that FolC is not the target of bioactivated PAS and the target was likely downstream within the folate pathway (Chakraborty *et. al*., 2013; Zhao *et. al*., 2014; Zheng *et. al*., 2013). Indeed, it was predicted and later confirmed that hydroxy-DHF could potently inhibit FolA (Figure 1.4, Figure 1., and Figure 1.11), (Chakraborty *et. al*., 2013; Dawadi *et. al*., 2017; Zheng *et. al*., 2013).

Antifolate Resistance

While folate metabolism remains a powerful target for drug discovery and development, there has been a surge in resistance to many antifolates. There are multiple mechanisms that can confer broad resistance to sulfonamides and

were found to emerge shortly after entrance of this drug class into clinical use. One such resistance mechanism involves single amino acid point mutations in the chromosomal *folP* (Figure 1.10). Among clinically resistant isolates, many have been characterized that have mutations that result in alteration of the ternary structure and prevent productive interaction with sulfonamides(Padayachee and Klugman, 1999). In the case of the respiratory pathogen *S. pyogenes*, clinical resistance to sulfonamides emerged much faster than in most other organisms and was the result of horizontal acquisition of a plasmid encoding a sulfonamide resistant FolP variant (Swedberg *et. al*., 1998). Similarly, in many Gram-negative bacteria, resistance to sulfonamides has been traced to mobile genetic elements bearing *sul* genes that encode fully functional FolP variants that fail to interact with sulfonamides (Figure 1.10)(Sköld, 2000). In early reports of this resistance mechanism, *E. coli* was found to transfer sulfonamide resistance to *Shigella* species via a Tn*21* family transposon encoding *sul1* or *sul2*(Akiba *et. al*., 1960). Tn*21* family transposons have since been found to be broadly distributed amongst enteric bacteria that are resistant to sulfonamides(Shin *et. al*., 2014). Recent evidence suggests that the *sul* genes originated in the Gram-negative bacterial orders *Rhodobiaceae* and *Leptospiraceae* prior to the development of sulfonamides and were subsequently distributed amongst human associated microbes with broad clinical use of sulfonamides(Sánchez-Osuna *et. al*., 2019).

Another factor that limits the use of sulfonamides is intrinsic resistance through methionine-associated metabolism. Shortly after discovery of the sulfonamides, it was found that exogenously supplied methionine could potently antagonize the antimicrobial action of these drugs in numerous bacterial species(Henry, 1944). While the mechanism governing this antagonism has not been fully elucidated, it has been presumed to occur through methylation-dependent inactivation. In the context of *M. tuberculosis*, sulfonamides are known to inhibit purified recombinant FolP, yet, they show poor activity against intact bacilli (Nopponpunth *et. al*., 1999). The related drug dapsone was initially developed as an antitubercular agent and also inhibits purified recombinant *M. tuberculosis* FolP, but, like sulfonamides shows limited activity against whole cells(Nopponpunth *et. al*., 1999). In support of a model for methyl inactivation, it has been demonstrated that *M. tuberculosis* rapidly metabolizes sulfonamides and dapsone to *N*-methyl and *N,N*-dimethyl species(Chakraborty *et. al*., 2013). In addition to methyl inactivation, it has recently been demonstrated in *E. coli* and *M. tuberculosis* that methionine also mediates antagonism of antifolates through affecting synthesis of folate precursors(Howe *et. al*., 2018; Minato *et. al*., 2018). Beyond the problem of intrinsic resistance, sulfonamides show limited activity against intracellular bacilli, suggesting that it may be difficult to achieve therapeutically relevant concentrations needed to target organisms like *M. tuberculosis* in their *in vivo* niche (Forsman *et. al*., 2014).

Like SMX, TMP resistance can occur by a variety of mechanisms including intrinsic resistance, target modification or overexpression, and acquisition of mobile genetic elements (Figure 1.10). Many bacterial species are naturally resistant to therapeutically relevant concentrations of TMP including *M. tuberculosis*, *Bacteroides* species, *Clostridium* species, and *Neisseria* species(Huovinen *et. al*., 1995; Minato *et. al*., 2015). In the case of *M. tuberculosis*, it was found that the native FolA Tyr100 residue was responsible for the weak binding of TMP(Dias *et. al*., 2014). Modification of Tyr100 to phenylalanine resulted in increased affinity for TMP(Dias *et. al*., 2014). It has been reported that some strains of *E. coli*, *S. aureus*, and *Haemophilus influenzae* harbor spontaneous mutations in the promoter region of *folA* that confer resistance through increased expression of FolA(de Groot *et. al*., 1996; Huovinen *et. al*., 1995; Nurjadi *et. al*., 2014). In addition, it has been shown that TMP resistance in *S. aureus*, *S. pneumonia* and *H. influenzae* can arise from mutations that result in a single amino acid substitution in FolA(Dale *et. al*., 1997; de Groot *et. al*., 1996; Pikis *et. al*., 1998). The mechanism that is primarily associated with TMP resistance in Gram-negative bacteria involves acquisition of mobile genetic elements encoding variants of FolA (encoded by *dfr*). To date there are over 30 different mobile genetic elements encoding unique *dhfr* genes and are classified as either type I or type II variants (Seputiene *et. al*., 2010). The type I variants share sequence similarity with bacterial *folA* and are typically located on the site-specific integron *Tn*7 (Heikkila *et. al*., 1991). In contrast, type

II variants are often found on conjugal R plasmids and that lack discernable sequence similarity to *folA*(Stone and Smith, 1979).

In mammalian cells, resistance to MTX can arise and can lead to treatment failure. Several MTX resistance mechanisms have been described to date. One common mechanism for acquired MTX resistance stems from a defect in transport of the drug into target cells and is frequently observed in the context of acute lymphocytic leukemia (Figure 1.10) (Trippett *et. al*., 1992). Another observed MTX resistance mechanism associated with acute non-lymphoblastic leukemia involves impaired polyglutamylation, a process that is normally associated with cytosolic retention of folates (Figure 1.10) (Li *et. al*., 1992; Lin *et. al*., 1991; Rhee *et. al*., 1993; Visentin *et. al*., 2013). To overcome this resistance mechanism, analogs of MTX that show better intracellular retention independent of polyglutamylation, such as pralatrexate, have been employed(Gonen and Assaraf, 2012) Other mammalian antifolate resistance mechanisms involve overexpression and missense mutations in DHFR (Figure 1.10) (Göker *et. al*., 1995; Schimke, 1988). Interestingly, increased DHFR expression has been linked to mutations in *p53* (a tumor suppressor gene), E2F (a transcription factor in cell cycle regulation), and genes that are involved in regulation of thymidylate synthase(Banerjee *et. al*., 2002; Göker *et. al*., 1995; Li *et. al*., 1995). Similar to that which is observed for PAS resistance in *M. tuberculosis*, DHFR active site

mutations that confer MTX resistance are rare but have been observed in the laboratory(Ercikan-Abali *et. al*., 1996; Srimatkandada *et. al*., 1989).

Resistance to PAS

Resistance to PAS in *M. tuberculosis* arises exclusively through occurrence of spontaneous mutations in genes related to folate synthesis and metabolism. Most frequently, PAS resistance mutations are identified in *folC*, *ribD* and *thyA* (Mathys *et. al*., 2009; Zhang *et. al*., 2015; Zhao *et. al*., 2014).

Mutations in *folC* are the most prevalent mutations identified in PAS resistant clinical isolates(Mathys *et. al*., 2009; Zhang *et. al*., 2015). *folC* mutations typically map to positions corresponding to substrate binding and nucleoside binding pockets of the ATP domain in FolC(Mathys *et. al*., 2009; Zhang *et. al*., 2015; Zhao *et. al*., 2014). Both of these positions are essential for proper enzymatic function. Purified recombinant FolC variants from resistant strains were found to have reduced enzymatic activity (10 to 20% of wild type activity)(Zhao *et. al*., 2014). When these variants were analyzed for the ability to glutamylate hydroxy-DHP, no detectable hydroxy-DHF was observed (Zhao *et. al*., 2014). Similarly, PAS resistant *M. tuberculosis folC* mutant strains were found to produce substantially less hydroxy-DHF than the wild type control(Zhao *et. al*., 2014). Thus, *folC*-linked PAS resistance occurs via impaired synthesis of hydroxy-DHF.

Another common PAS resistance mechanism involves loss-of-function mutations in *thyA*, encoding a non-essential thymidylate synthase (ThyA) in *M. tuberculosis* that is responsible for the 5,10-methylene-tetrahydrofolate dependent conversion of dUMP to dTMP (Mathys *et. al*., 2009; Zhang *et. al*., 2015; Zhao *et. al*., 2014). When functional, ThyA releases DHF that must be re-reduced to be utilized in folate metabolism. *M. tuberculosis* encodes an alternate thymidylate synthase (ThyX, encoded by *thyX*) that regenerates THF from 5,10-methylene-THF following catalysis (Myllykallio *et. al*., 2002). Thus, in contrast to ThyA, ThyX places limited demand of FolA for maintaining reduced folate pools. In contrast to other pathogens that do not encode a ThyX ortholog and are attenuated mutation of *thyA* (Cersini *et. al*., 1998; Kok *et. al*., 2001), *M. tuberculosis thyA* loss-of-function mutants are not compromised for fitness growth and survival *in vivo*.

To date, few *folA* missense mutations associated with PAS resistance have been reported(Myllykallio *et. al*., 2002). Numerous studies have reported that alterations in the FolA active site can be highly deleterious to the overall enzyme function. Thus, it could be rare for *folA* point mutations to confer resistance to PAS without compromising FolA enzymatic activity. One paper recently described five independent clinical PAS resistant isolates containing a deletion of the *folA*-*thyA* coding sequence(Moradigaravand *et. al*., 2016). These strains were 26 times more resistant to PAS than susceptible control strains. Unlike many bacteria, *M. tuberculosis* does not encode a FolM ortholog that would be

expected to compensate for loss of FolA activity. Instead, this compensation likely comes from weak DHF reductase activity that can be catalyzed by the 5-amino-6-(5-phosphoribosylamino)uracil reductase RibD that normally functions in riboflavin synthesis(Salcedo *et. al*., 2001; Zhao *et. al*., 2014). Consistent with this model, *ribD* promoter mutations have been described that confer PAS resistance and were shown to render *folA* as non-essential in *M. tuberculosis*(Zhang *et. al*., 2015; Zhao *et. al*., 2014).

Like TMP, PAS is prone to exclusion from the cytoplasm by the action of efflux pumps (Figure 1.10). Overexpression of the major facilitator superfamily protein Tap (Rv1258c) in *Mycobacterium bovis* BCG was found to confer resistance to PAS(Ramón-García *et. al*., 2012a). Furthermore, overexpression of Tap in *M. tuberculosis, M. fortuitum* and *M. bovis* BCG was found to confer resistance to a variety of other antimicrobial agents that do not target folate biosynthesis including streptomycin, vancomycin, and tetracycline(Aínsa *et. al*., 1998; Ramón-García *et. al*., 2012b),(Siddiqi *et. al*., 2004).

Main hypothesis

Numerous groups have shown PAS is converted to hydroxy-dihydrofolate via the folate biosynthesis pathway to inhibit dihydrofolate reductase. Due to the lack of analytically pure compound, hydroxy-dihydrofolate has never evaluated for inhibitory activity against purified recombinant FolA from *M. tuberculosis*. We

hypothesize that hydroxy-dihydrofolate potently inhibits dihydrofolate reductase in *M. tuberculosis*. Furthermore, although PAS was discovered to be specific for *M. tuberculosis*, we propose that bacteria which are resistant to PAS can utilize PAS *in lieu* of PABA in folate biosynthesis. Since antifolates work better in combination, such as TMP and SMX, we hypothesize that PAS and SMX will also work better in combination. The mechanism by which this occurs is similar to TMP and SMX. As such PAS will decrease flux through PABA biosynthesis and SMX will decrease metabolic flux through pterin biosynthesis. Since PAS has been described to be toxic and many patients discontinue PAS therapy, we propose to find novel ways to shorten PAS treatment or find drug combinations to use smaller dosages of PAS. Furthermore, we propose that by blocking PABA biosynthesis we can potentiate the antitubercular activity of PAS. The ultimate goal is to determine novel drug targets to use in combination with PAS.

TABLE 1. Prescription, adverse reaction and mechanism of actions of anti-TB drugs.

Name of Drug (abbreviation)	WHO Guidelines for treatment	Mechanism of action	Adverse reactions
Rifampicin (RIF)	First line 6 months for DS TB	Inhibits RNA polymerase(CALVORI *et. al*., 1965)	Liver toxicity Nausea Diarrhea
Isoniazid (INH)	First line 6 months for DS TB	Inhibits InhA and thereby mycolic acid synthesis(Banerjee *et. al*., 1994)	Peripheral neuropathy Gastrointestinal distress Aplastic anemia Liver toxicity
Ethambutol (EMB)	First line 2 months for DS TB	Inhibits arabinosyl transferase and thereby arabinogalactan synthesis(Takayama and Kilburn, 1989)	Liver toxicity Kidney toxicity Peripheral neuropathy
Pyrazinamide (PZA)	First line 2 months for DS TB	Not known. Many have been proposed but the Baughn group and others keep disproving them(Boshoff *et. al*., 2002; Dillon *et. al*., 2017; Peterson *et. al*., 2015; Shi *et. al*., 2011; Zimhony *et. al*., 2000)[1]	Joint pain Liver toxicity Gout Nausea Vomiting
Streptomycin	First or second line 2+months	Protein synthesis inhibitor specifically the 30S ribosomal subunit(Luzzatto *et. al*., 1968)	Deafness *in utero* Kidney toxicity Tinnitus Vertigo

Kanamycin A	Second line 12+months	Protein synthesis inhibitor specifically the 30S ribosomal subunit(Misumi and Tanaka, 1980)	Deafness *in utero* Kidney toxicity Tinnitus Vertigo
Moxifloxacin	Second line 12+months	DNA replication specifically by inhibiting DNA gyrase(Drlica and Zhao, 1997)	Tendonitis Hepatitis Peripheral neuropathy

DS-drug susceptible

[1]Because if the Baughn lab cannot determine the mode of action of PZA no other lab should be able to.

Figures:

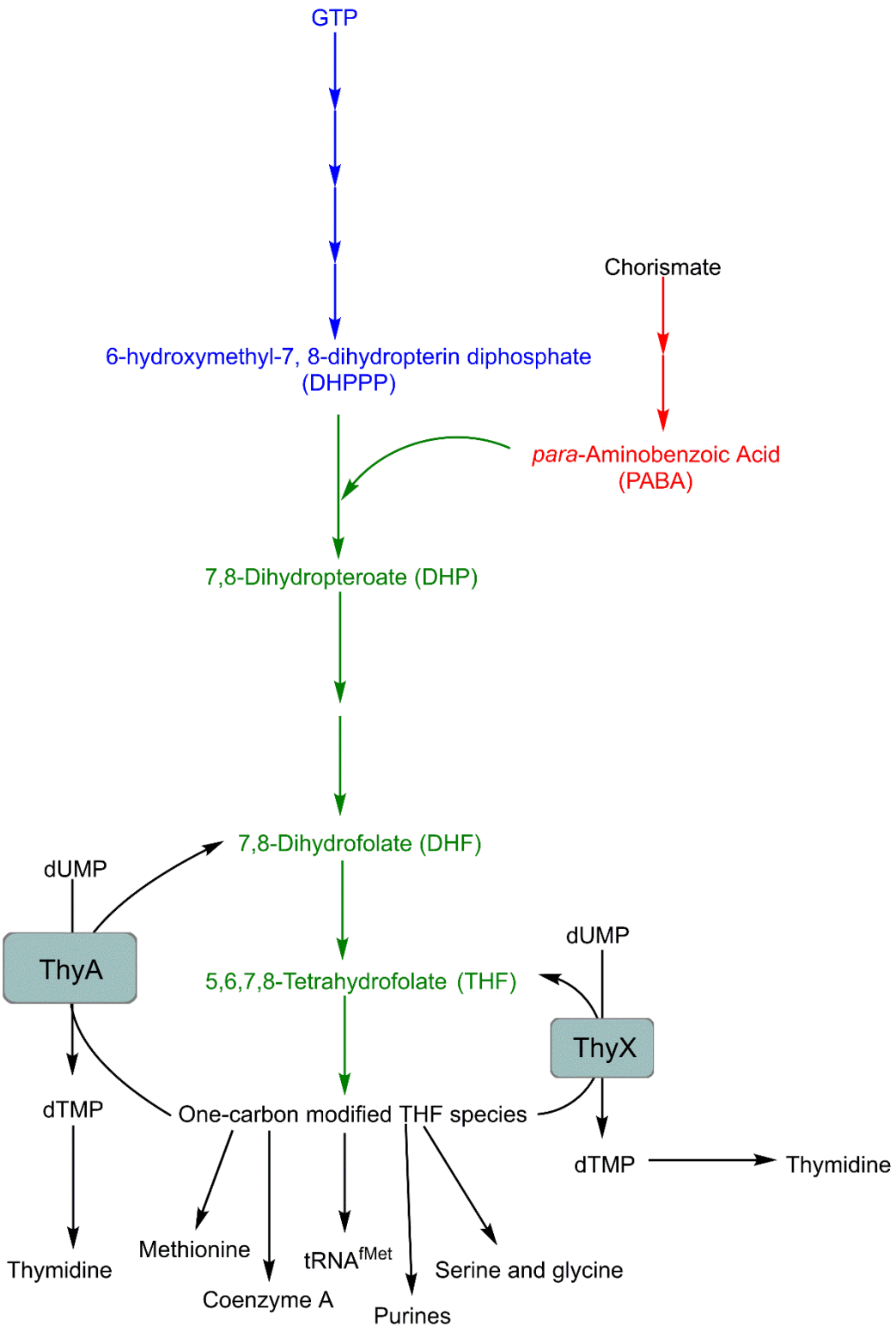
GTP
Chorismate
6-hydroxymethyl-7, 8-dihydropterin diphosphate
(DHPPP)
para-Aminobenzoic Acid
(PABA)
7,8-Dihydropteroate (DHP)
7,8-Dihydrofolate (DHF)
dUMP
ThyA
5,6,7,8-Tetrahydrofolate (THF)
dUMP
ThyX
dTMP
One-carbon modified THF species
dTMP
Thymidine
Thymidine
Methionine
tRNA^{fMet}
Serine and glycine
Coenzyme A
Purines

Figure 1.1. Folate biosynthesis and one carbon metabolism in bacteria. Blue indicates pterin biosynthesis. Red indicates PABA biosynthesis. Green indicates folate biosynthesis. Black indicates one carbon metabolism.

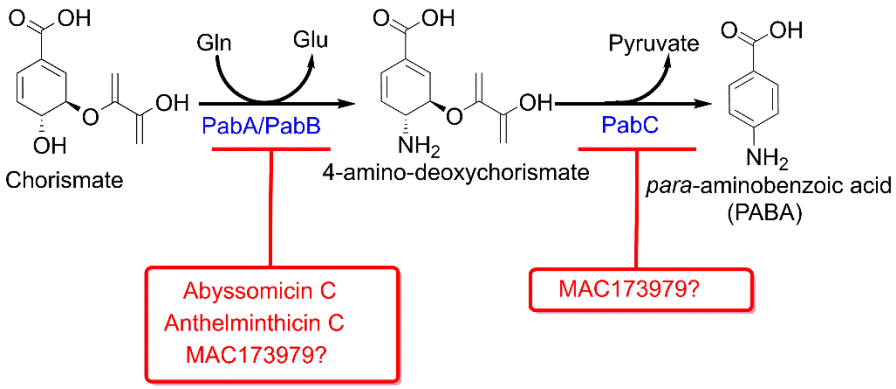

Figure 1.2. *para*-Aminobenzoic acid biosynthesis pathway in bacteria with known inhibitors.

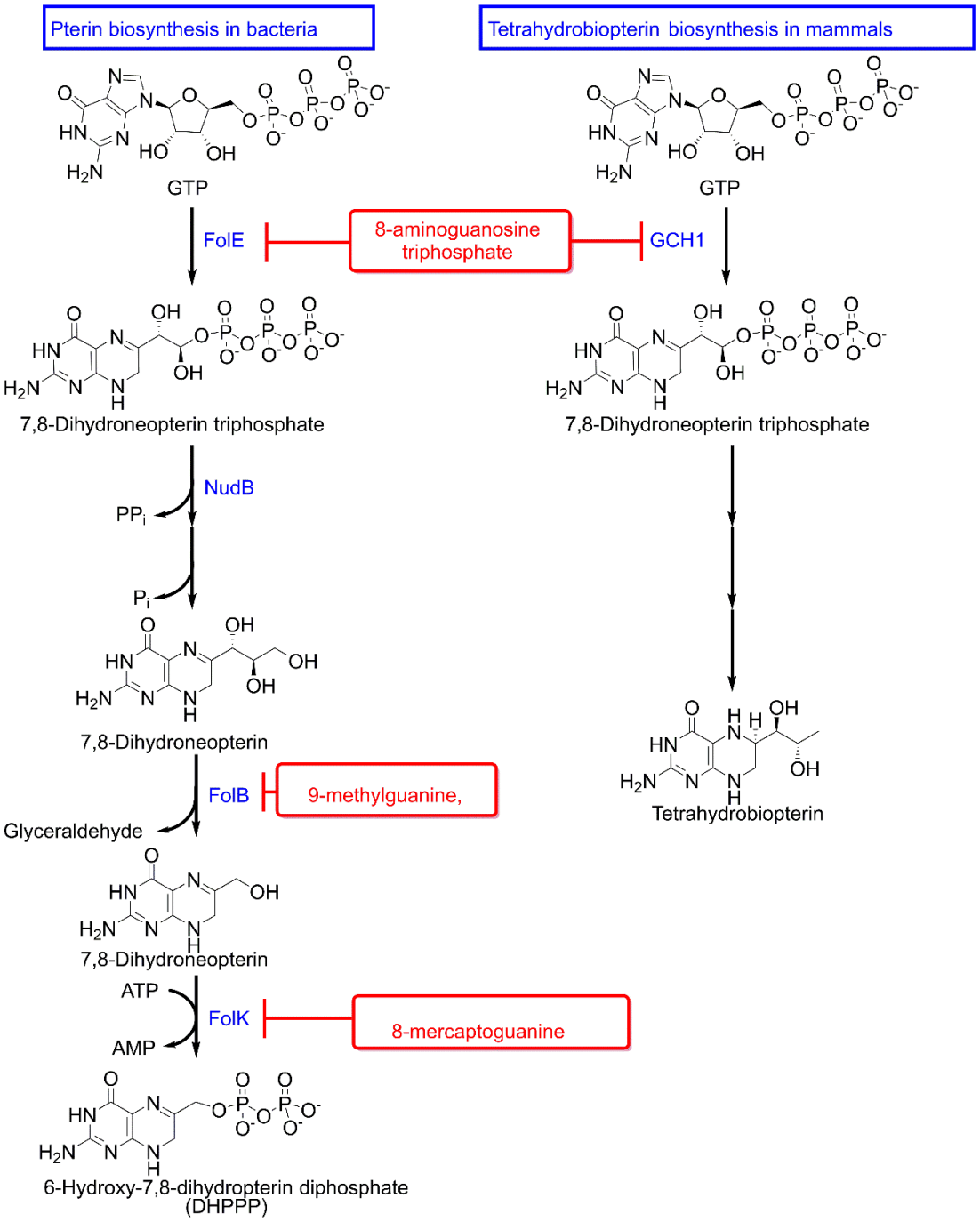

Figure 1.3. Pterin and tetrahydropterin biosynthesis and inhibitors in bacteria and mammals

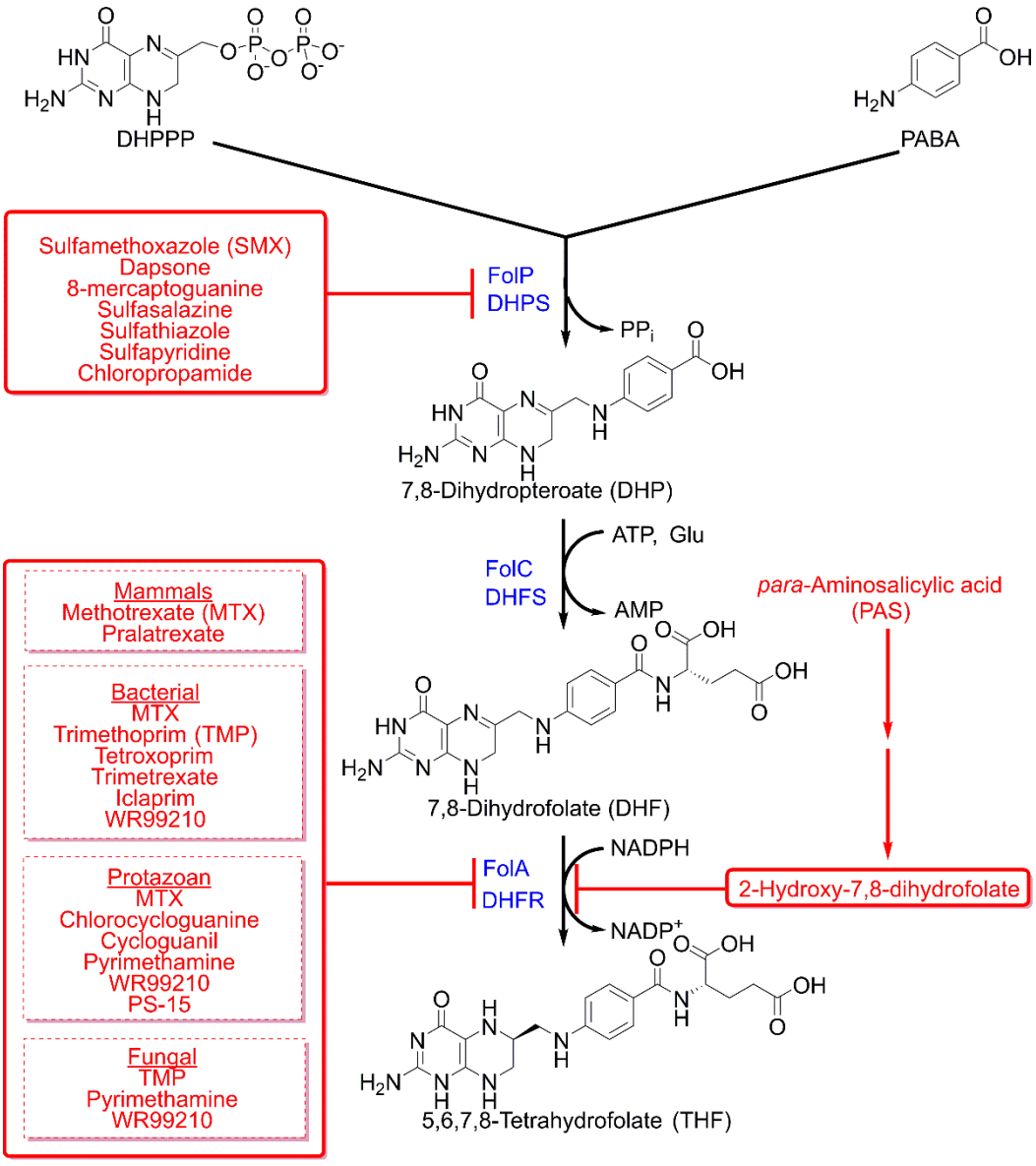

Figure 1.4. Folate biosynthesis and inhibitors in bacteria and eukaryotes.

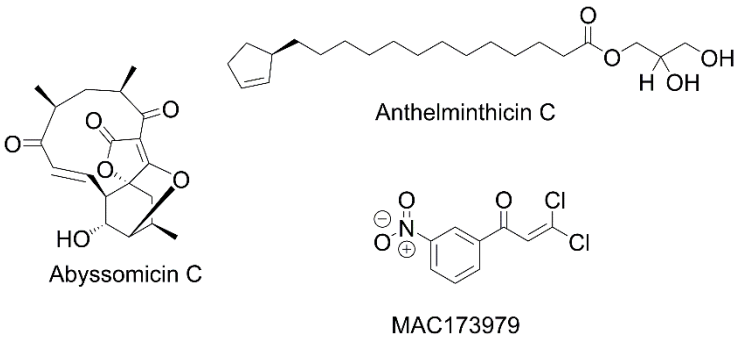

Figure 1.5. Chemical structures of inhibitors of PABA biosynthesis.

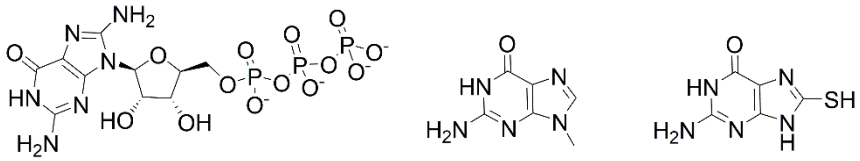

Figure 1.6. Chemical structures of pterin biosynthesis inhibitors.

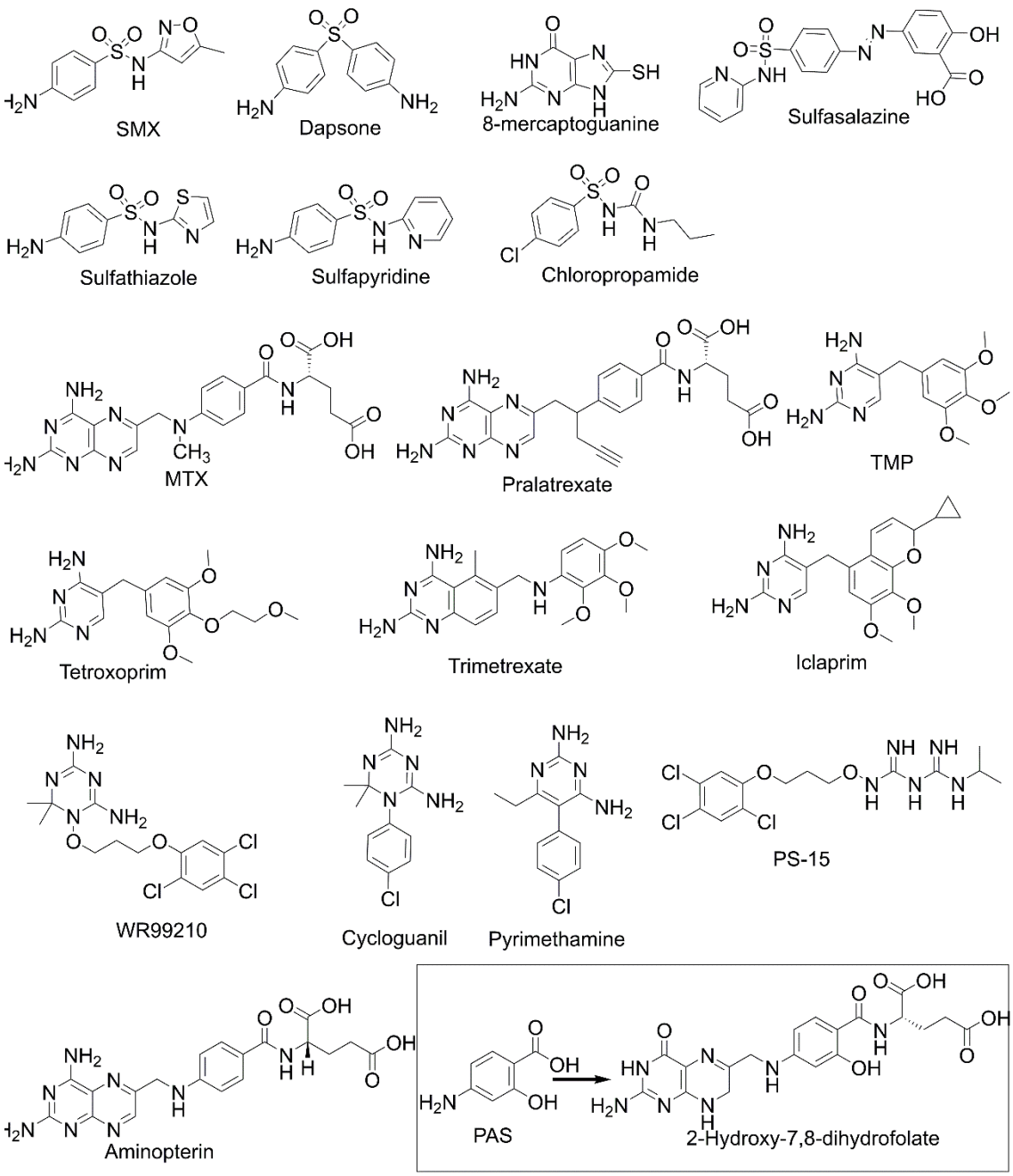

Figure 1.7. Chemical structures of folate biosynthesis inhibitors.

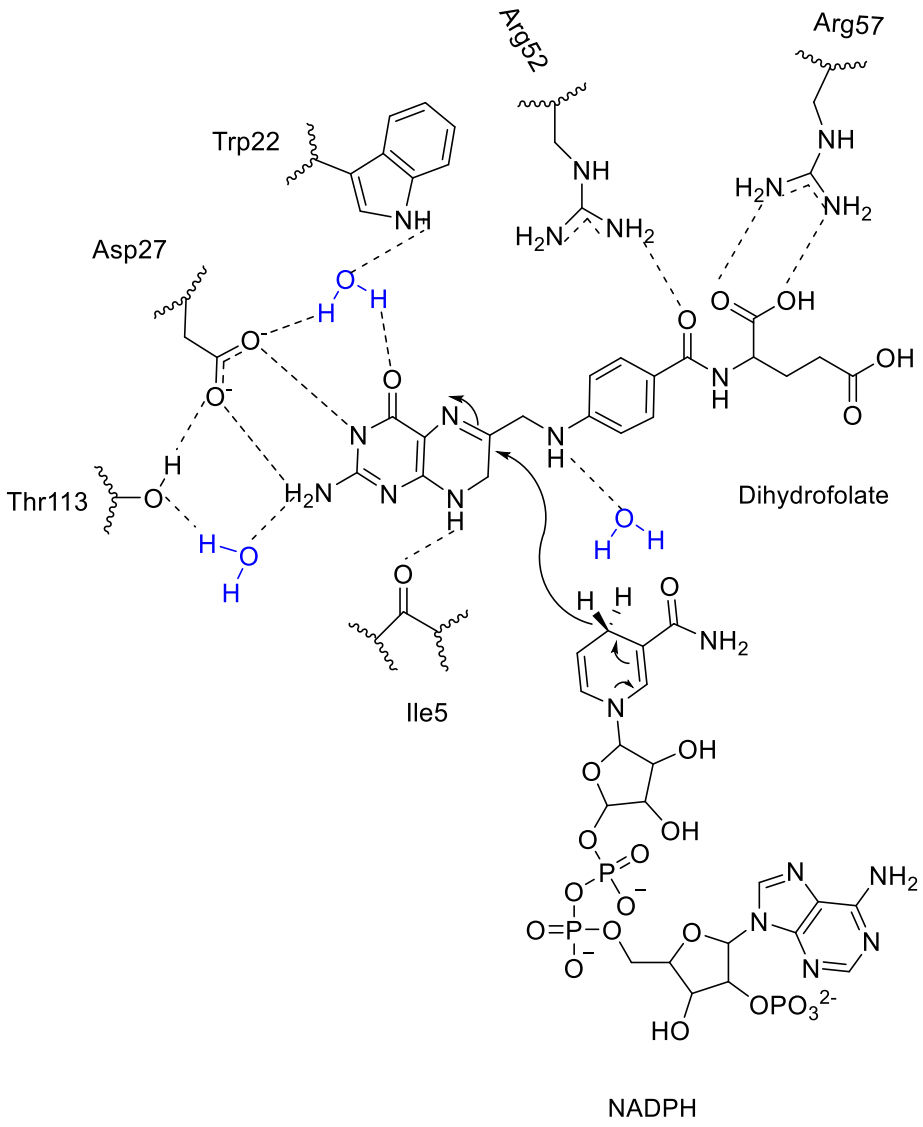

Figure 1.8. Catalytic mechanism of FolA$_{Mtb}$. Water molecules are indicated in blue. .

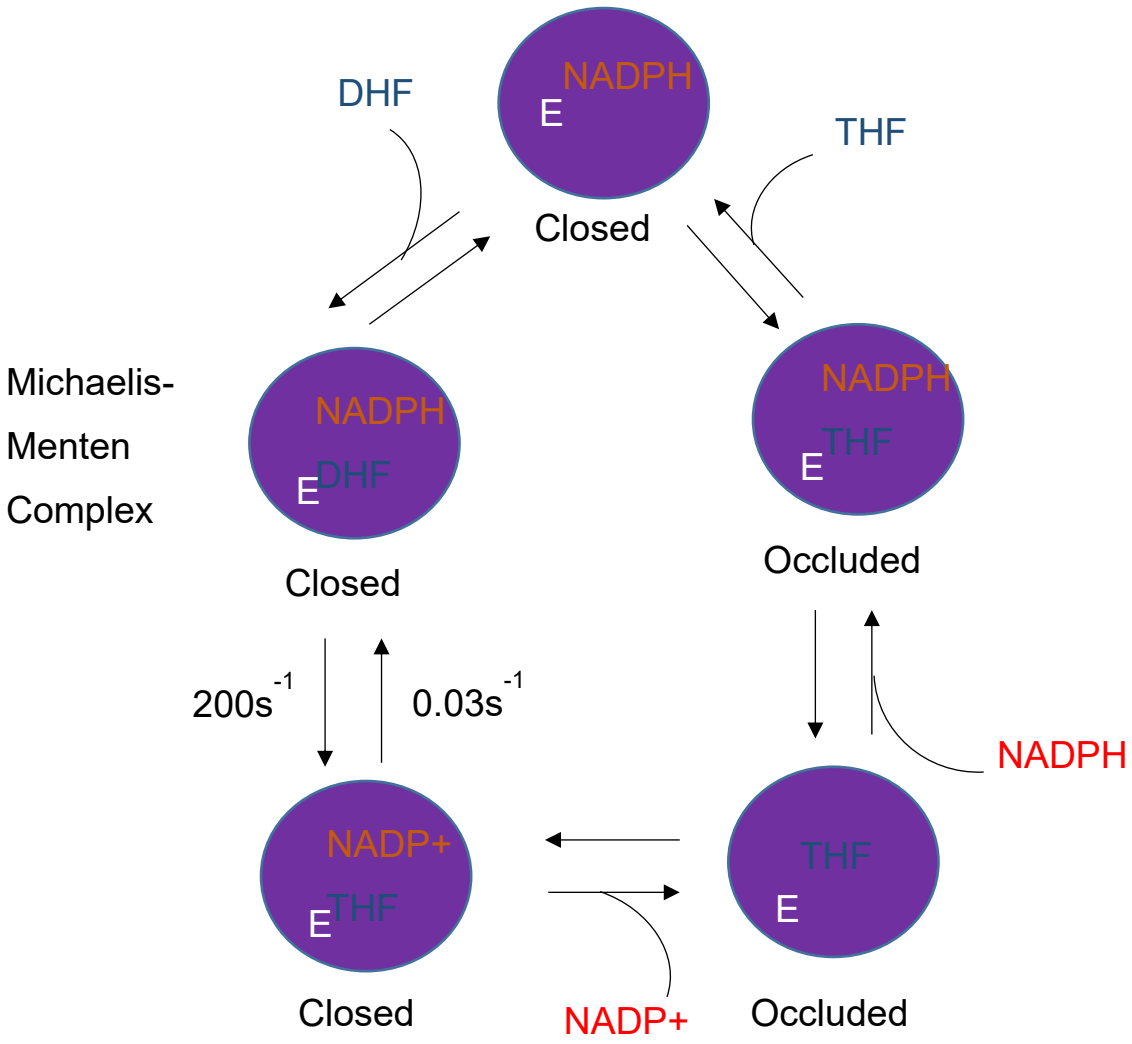

Figure 1.9. Biochemical catalytic transition states of dihydrofolate reductase.

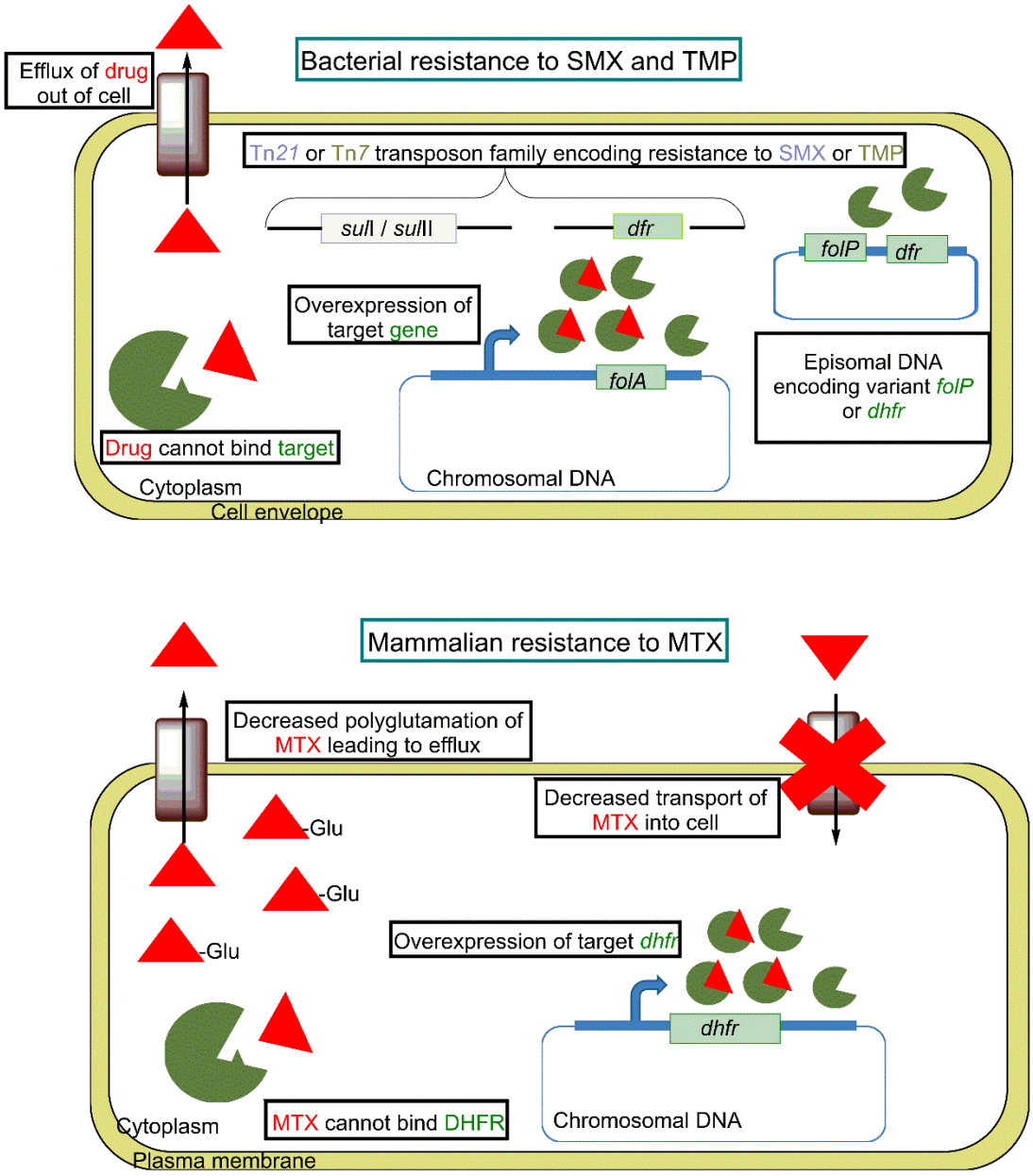

Figure 1.10. Mechanisms of antifolate resistance in bacterial and mammalian cells.

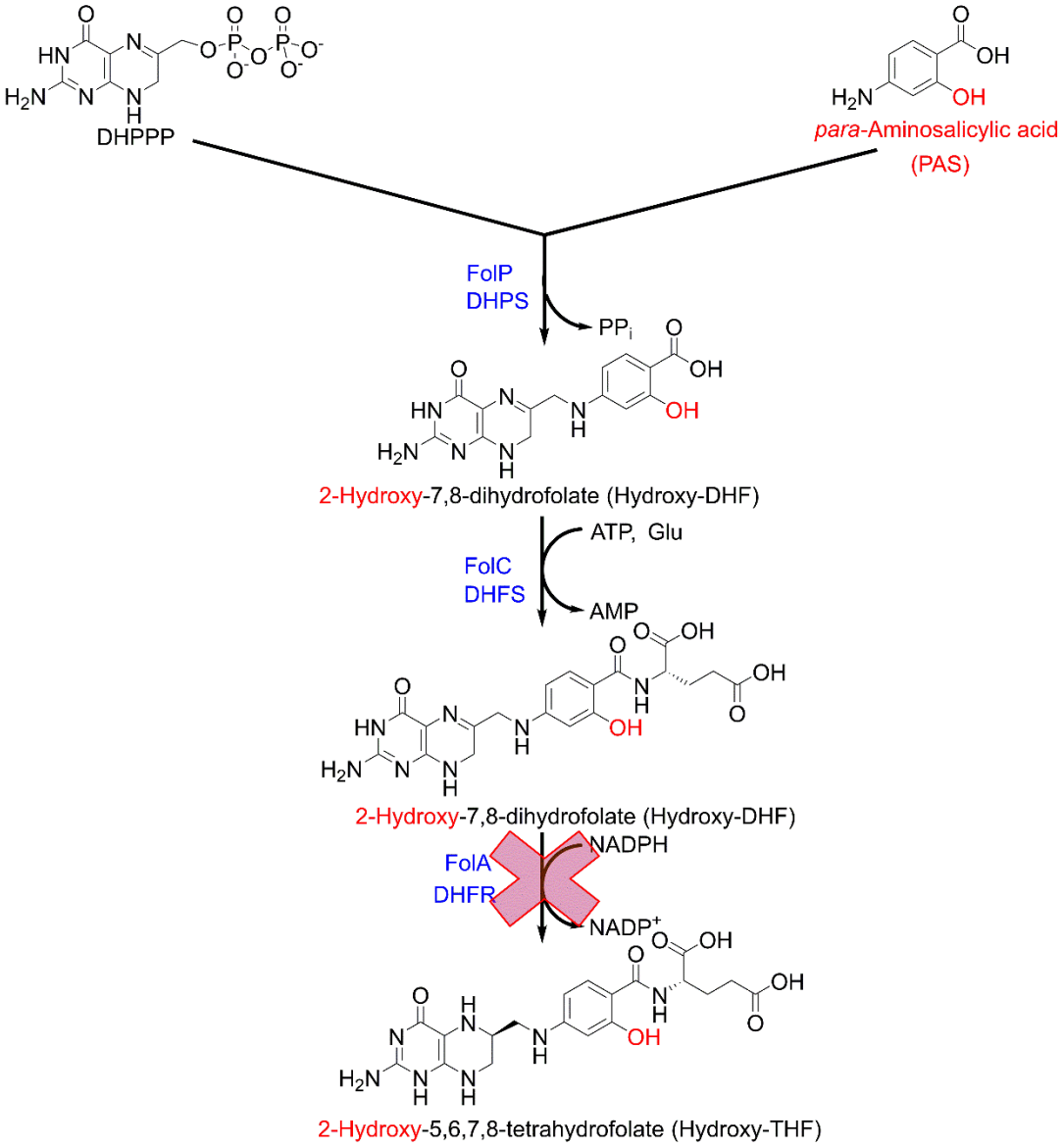

Figure 1.11. Bioactivation of PAS.

Chapter 2:

para-Aminosalicylic acid selectively inhibits *Mycobacterium tuberculosis* dihydrofolate reductase

This chapter is a reprint, with alterations, of a published manuscript.

Dawadi S*, Kordus SL*, Baughn AD, Aldrich CC. Synthesis and analysis of bacterial folate metabolism intermediates and antifolates. Org Lett. 2017;19(19).

*Denotes equal contribution.

Specific contributions from *Organic Letters* manuscript

Dawadi, S devised synthetic route for hydroxy-dihydrofolate (Figure 2.1) and wrote methods for synthesis

Kordus, SL tested inhibitory activity of hydroxy-dihydrofolate against purified recommbinant dihydrofolate reductase from *Mycobacterium tuberculosis* (Figure 2.2) wrote the methods for the purification and inhibitory concnetration.

The rest of the chapter has not published when the thesis was submitted. All experiments, experimental design, intellectual contributations were performed by Shannon Lynn Kordus. One exception is the docking studies were performed in collaboration with Bill McCue and the methods were written by Bill McCue.

Synopsis

para-Aminosalicylic acid (PAS) was one of the first drugs to enter clinical use for treatment of tuberculosis. Despite for over 70 years of study, the precise mode of action of PAS is still not fully understood. PAS is known to selectively inhibit *Mycobacterium tuberculosis* and has limited to no activity against other microorganisms. Previous studies have shown that PAS can be incorporated *in lieu* of PABA by the *M. tuberculosis* folate biosynthetic pathway. PAS is ultimately converted to hydroxy-dihydrofolate that is predicted to inhibit *M. tuberculosis* dihydrofolate reductase. Using a biochemical approach, we demonstrate for the first time, that hydroxy-dihydrofolate potently inhibits dihydrofolate reductase. Furthermore, we show that other bacteria can also utilize PAS for synthesis of hydroxy-dihydrofolate. In contrast to *M. tuberculosis*, these organisms are capable of using PAS-containing folate species as a co-factor for one carbon metabolism. One previously unforeseen consequence of this selectivity is that PAS can antagonize the activity of sulfa-drugs in many bacterial species. Since sulfa-drugs are used as prophylactic therapy to treat and prevent opportunistic infections in HIV-infected individuals, co-treatment with PAS needs to be reevaluated.

Introduction

In 1940, Frederick Bernheim discovered that salicylic acid stimulated oxygen consumption in *Mycobacterium tuberculosis*(Bernheim, 1940). Following up on these studies, Jörgen Lehmann performed a screen of 50 structural analogs of salicylic acid for compounds that could potently inhibit growth of *M. tuberculosis*. From this screen PAS was identified as the most potent salicylic acid analog and was found to be safe and effective in treatment of human tuberculosis in a small scale clinical trial (Lehmann, 1946)..PAS entered clinical use for treatment of tuberculosis in 1946 and was typically given with streptomycin to prevent the emergence of drug resistance.

PAS was given orally and often associated with gastrointestinal distress. By the mid-1960s, PAS was replaced with the better-tolerated and more efficacious companion drug ethambutol (Ferebee *et. al*., 1966) With the increased incidence of drug resistant strains of *M. tuberculosis*, PAS has regained more frequent clinical use. Consequently, there has been renewed interest in understanding the mechanisms that govern susceptibility and resistance to PAS.

Multiple studies have shown that PAS disrupts folate metabolism. PAS is a structural analog of the folate precursor, *para*-aminobenzoic acid (PABA). Like PABA, PAS is a substrate for the *M. tuberculosis* folate biosynthesis pathway (Chakraborty *et. al*., 2013; Dawadi *et. al*., 2017; Rengarajan *et. al*., 2004; Zhao

et. al., 2014; Zheng *et. al*., 2013). In this pathway, PAS is ligated to 6-hydroxymethyl dihydropterin pyrophosphate by the enzyme dihydropteroate synthase (FolP) to produce hydroxy-dihydropteroate (Chakraborty *et. al*., 2013; Zhao *et. al*., 2014; Zheng *et. al*., 2013). Hydroxy-dihydropteroate is then converted to the dihydrofolate analog hydroxy-dihydrofolate (hydroxy-DHF) via dihydrofolate synthase (FolC)(Chakraborty *et. al*., 2013; Zhao *et. al*., 2014; Zheng *et. al*., 2013). In normal folate metabolism, the native substrate dihydrofolate is reduced by the enzyme dihydrofolate reductase (encoded by DfrA in *M. tuberculosis*, herein referred to as $FolA_{Mtb}$ for simplicity) to produce tetrahydrofolate, a critical cofactor for the synthesis of DNA, RNA, and proteins. Although multiple studies have suggested that hydroxy-DHF inhibits $FolA_{Mtb}$, there has been no biochemical validation due to the lack of analytically pure hydroxy-DHF. In this study, hydroxy-dihydrofolate was synthesized by the coupling of N^2-acetyl-6-formylpterin obtained from the degradation of folic acid and appropriately functionalized arylamines. The sequential chemoselective reduction of the imine and pterin ring led to the formation of hydroxy-DHF. Using this pure hydroxy-DHF, we have confirmed it to be a potent inhibitor of $Fol_{Mtb,}$

PAS has been shown to only have inhibitory activity against *M. tuberculosis*, although the mechanistic basis for this exquisite selectivity is not known(Ivanovics *et. al*., 1948; Ragaz, 1948; Sievers, 1946; Tobie and Jones, 1949; Wyss, 1943). Previous studies of the selectivity of PAS were extended to

test a variety of organisms including Gram positive, Gram negative, and non-tuberculous mycobacteria. Next, PABA auxotrophic strains of *Escherichia coli*, *Acinetobacter baumannaii*, and *Mycobacterium smegmatis* were used to determine if PAS could be utilized in folate synthesis and one carbon metabolism. In addition, purified recombinant *E. coli* and *M. smegmatis* dihydrofolate reductase ($FolA_{Ec}$ and $FolA_{Ms}$, respectively) were tested for the ability to utilize hydroxy-dihydrofolate as a substrate.

To understand if $FolA_{Mtb}$ is the principal target for hydroxy-DHF, $folA_{Mtb}$ and $folA_{Ms}$ were expressed *in trans* in PABA auxtrophic strains of *M. tuberculosis* and were grown in the presence of PAS. A similar experiment was performed in *E. coli* using strains that lacked *folA* but contained plasmid borne copies of $folA_{Mtb}$ or $folA_{Ec}$ and grown in the presence of PAS. (Howell *et. al*., 1988a). The structure of both $FolA_{Ec}$ and $FolA_{Mtb}$ bound to hydroxy-DHF was analyzed using molecular docking and evolutionary coupling was performed to predict important residues for binding of DHF compared to hydroxy-DHF.

If PAS can act as a fully functional PABA analog in one carbon metabolism then PAS, like PABA, would be predicted to antagonize FolP inhibitors. Antagonism of FolP inhibitors, including sulfa-drugs and sulfones, was tested in the presence of exogenously supplied PAS for a variety of bacterial species. The present study

reveals the mechanistic basis for PAS selectivity and previously unrecognized antifolate interactions.

Materials and Methods

Bacterial strains, media, and growth conditions

All information regarding primers, plasmids and bacterial strains used in this study can be found in Tables 2.1-2.3.

M. tuberculosis and *M. abscessus* strains were grown at 37 ºC in 7H9 broth (Difco) supplemented with 0.2% (wt/vol) glycerol (Fisher Scientific), 10% oleic acid-albumin-dextrose-catalase (OADC) (BD), and 0.05% tyloxapol (Sigma) or on 7H10 agar (Difco) supplemented with 0.2% (wt/vol) glycerol (Fisher) and 10% oleic acid-albumin-dextrose-catalase (OADC) (Difco). *E. coli*, *S. enterica, B. cenocepacia, Stenotrophomonas maltophilia*, *and A. baumannii* were grown at 37 ºC in either lysogeny broth (LB) (Difco) or M9 minimal media supplemented with 0.2% (wt/vol) glucose (Fisher Scientific). *M. smegmatis* was grown at 37 ºC in 7H9 supplemented with 0.05% tyloxapol, and 0.2% (wt/vol) glucose. *S. aureus* was grown as previously described (Minato *et. al*., 2018). *S*. *parasanguinis* was grown at 37 ºC in Mueller-Hinton Broth (Difco) and Iso-sensitest broth (Oxiod) both supplemented with 5% laked sheeps blood (BD). *B. fragilis* was grown at 37 ºC in an anaerobic chamber (Bactron IV, Sheldon Manufacturing, Inc.) with an atmosphere of 5% CO_2, 10% H_2, and 85% N_2 (Matheson, PA) in brain heart infusion broth (BHIS) (Difco) supplemented with 0.5% yeast extract (Fisher) and 15 µg/mL hematin (Sigma) and anaerobic minimal medium (AMMGluc) with 0.5% glucose with modifications described in Baughn and Malamy (Baughn and

Malamy, 2002). All media and plastics used to cultivate *B. fragilis* were equilibrated anaerobically for a minimum of 48 hrs to ensure minimal oxygen contamination. *E. coli* Δ*thyA* Δ*folA* strains were grown as described previously(Howell *et. al*., 1988b).

All antibiotics were purchased from Sigma and added, when appropriate, to final concentrations of 50 µg/mL for kanamycin, 150 µg/mL for penicillin G, and 150 µg/mL for hygromycin. PABA free media was created by baking glassware for a minimum of one hour at 180 ºC. PAS, PABA, trimethoprim (TMP), sulfamethoxazole (SMX), dapsone (DDS) sulfanilamide (SNL) were all purchased from Sigma and were dissolved in 100% DMSO (Sigma). Sulfathiazole (STZ) was purchased from Tokyo Chemical Industry and was dissolved in 100% DMSO (Sigma).

Synthesis of hydroxy-dihydrofolate

The following text was written and synthesis was performed by Dr. Surendra Dawadi. To a solution of N^2-acetyl-6-formylpterin (141 mg, 0.603 mmol, 1.0 equiv) in glacial acetic acid (6 mL) was added dimethyl-(4-amino-2-(benzoyloxy)benzoyl)glutamate, (275 mg, 0.664 mmol, 1.1 equiv) and the mixture was stirred briefly for 15 min at room temperature (rt) (Freisleben *et. al*., 2002; Thijssen, 1973). A solution of dimethylamine borane (56 mg, 0.950 mmol, 1.6 equiv) in glacial acetic acid (1 mL) was added and stirring was continued at rt for

20 min. The suspension was warmed to 60 °C for 10 min and cooled to rt. Acetic acid was evaporated under reduced pressure and the residue was dissolved in 20% methanol in methylene chloride and residual acetic acid was neutralized by adding a few drops of trimethylamine. The crude product was purified by column chromatography (silicon dioxide, 0:100 to 10:90 methanol/methylene chloride) yielding dimethyl-N^2-acetyl-2'-benzoyloxyfolate (220 mg, 57%) as a yellow solid.

A solution of dimethyl-N^2-acetyl-2'-benzoyloxyfolate (110 mg, 0.174 mmol) in 0.5 N sodium hydroxide (NaOH) (1 mL) was heated at 70 °C for 1.5 h and cooled to rt. In a separate flask, deoxygenated water (6 mL) was prepared by bubbling nitrogen for 15-20 min. Ascorbic acid (368 mg, 2.088 mmol) was added in one portion into the deoxygenated water and pH of the solution was adjusted to 6.5 by adding 1 N NaOH dropwise. Sodium dithionite (400 mg, 2.30 mmol) was added followed by the previously prepared solution of dimethyl N^2-acetyl-2'-benzoyloxyfolate in 0.5 N NaOH and pH of the solution was re-adjusted to 6.5 by adding 1N hydrochloric acid (HCl) (or 1N NaOH as needed) dropwise. An another portion of sodium dithionite (200 mg, 1.15 mmol) was added and the mixture was warmed to 40 °C and stirred at that temperature for 3 h. The mixture was cooled to rt and the pH was adjusted to ~2 by adding 1N HCl dropwise while S7 stirring. At that pH, precipitation occurred and the mixture was stored at 4 °C for overnight. The mixture was centrifuged, the supernatant was discarded and the residue was washed by vortex and centrifugation cycle twice with water,

twice with ethanol, and once with diethyl ether. The residue was dried under reduced pressure for 3-4 hr to obtain the product (69 mg, 86%) as a brown solid. The amber colored vial containing the product was filled with argon and stored at –80 °C. Hydroxy-DHF was resuspended in DMSO at a final concentration of 10 mg/mL.

Biochemical characterization of FolA$_{Mtb}$

Cloning of *M. tuberculosis folA* was performed similarly as described with the exception pET28b(+) (Novagen) was used instead of pET28a(+) (Argyrou *et. al*., 2006; Dias *et. al*., 2014). *M. tuberculosis folA*$_{Mtb}$ (Rv2763c) was amplified from H37Ra genomic DNA by PCR using the primers found in Table 2.1. The resulting DNA was cut with the restriction enzymes *Nde*I and *Hind*III and ligated into an already digested pET28b(+) using the same restriction enzymes. Expression and purification of FolA$_{Mtb}$ was similarly performed as previously described (Argyrou *et. al*., 2006; Dias *et. al*., 2014). Briefly, sequence-verified pET28b(+):*folA*$_{Mtb}$ was used to transform chemically competent *E. coli* BL21 (DE3) cells. *E. coli* BL21 pET28b(+):*folA*$_{Mtb}$ was inoculated into LB and grown overnight at 37 ºC. The cells were diluted 1:1000 into fresh LB (4 L) and were grown until mid-exponential phase (optical density at 600 nm (OD_{600}) 0.4–0.6) at 37 ºC. The cells were equilibrated to 18 ºC for 1 h. Next, 1 mM Isopropyl β-D-1-thiogalactopyranoside (IPTG) (GoldBio) was added to induce protein expression at 18 ºC for 20 h. The cells were collected by centrifugation at 5,000 rpm (Beckman Coulter, Avanti

JXN-30) at 4 ºC. The pellet was resuspended in 40 mL of lysis buffer (20 mM triethanolamine (TEA), 50 mM KCl, pH 7) and was disrupted by ultrasonication (Branson Sonifier 450) three times using 20 sec burst and 20 sec cooling (4 ºC). 40 mg chicken egg white lysozyme (MP Biomedicals, LLC) was added and incubated on ice for 30 min. The insoluble fraction was removed by centrifugation (Beckman Coulter, Avanti JXN-30) at 11,000 rpm at 4 ºC for 45 min. The supernatant was applied to a 4 ml of Ni-NTA Agarose (Qiagen) equilibrated with lysis buffer. The column was washed with 40 mL of wash buffer (20 mM TEA, 50 mM KCl, 50 mM imidazole (GoldBio), pH 7). The protein was eluted with 5 ml of elution buffer (20 mM TEA, 50 mM KCl, 500 mM imidazole (GoldBio), pH 7). Fractions containing pure $FolA_{Mtb}$ (>90% as judged by an SDS-PAGE gel) were pooled, and concentrated using an ultra-centrifugal filter (Millipore) into storage buffer (20 mM potassium phosphate, 50 mM KCl, pH 7.0) to 500 µg/ml. The protein was stored at –80 ºC.

Inhibition of $FolA_{Mtb}$ by hydroxy-DHF

All enzymatic assays were performed in storage buffer. 2.5 nM $FolA_{Mtb}$ was added to 50 µM NADPH (Sigma), 0.01% Triton X-100, and varying concentrations of hydroxy-DHF previously dissolved in 100% DMSO, and the mixture was incubated for 5 min at 25 ºC. The reaction was initiated with the addition of 25 µM DHF (Sigma). The reaction was performed under initial velocity conditions and monitored by following oxidation of NADPH through measuring

decrease in absorbance at 340 nm (BioTek Synergy H1) every 10 sec for 10 min. The percent activity was normalized to a no drug control. The Cheng-Prushoff equation was used to determine the K_i from the initial IC_{50} value (2.9 ± 1.2 µM) using the K_m of DHF of 1.6 µM as determined by Czekster and coworkers(Czekster *et. al*., 2011). The data represents 3 independent experiments using the average of 3 technical replicates. Biochemical characterization for type of inhibitor:

$$\mathrm{Ki} = \frac{\mathrm{IC50}}{1 + \frac{[\mathrm{S}]}{\mathrm{Km}}}$$

Purification of FolA$_{Ec}$ and *FolA*$_{Ms}$

E. coli BW25113 *folA* was amplified using primers in Table 2.1. The resulting DNA was cut with the restriction enzymes *Nde*I and *Bam*HI and ligated into an already digested pET28b(+) using the same restriction enzymes. Expression and purification of FolA$_{Ec}$ was similarly performed as previously described(Lee *et. al*., 2010). Briefly, sequence-verified pET28b(+):*folA*$_{Mtb}$ was transformed into competent *E. coli* BL21 (DE3) cells. E. coli BL21 pET28b(+)-*folA*$_{Ec}$ was inoculated into LB and grown overnight at 37 ºC. The cells were diluted 1:1000 into fresh LB (1 L) and were grown until mid-exponential phase (OD_{600} 0.4–0.6) at 37 ºC and 1 mM IPTG was added to induce protein expression at 37 ºC for 4 h. The cells were collected by centrifugation at 5,000 rpm at 4 ºC. The pellet was

resuspended in 10 mL of lysis buffer (50 mM NaH_2PO_4, 300 mM NaCl, and 10 mM imidazole (pH 8.0)) containing 10 mg chicken egg white lysozyme was added and incubated on ice for 30 min. The insoluble fraction was removed by centrifugation at 11,000 rpm at 4 ºC for 45 min. The supernatant was applied to a 1 mL of Ni-NTA Agarose (Qiagen) equilibrated with lysis buffer. The column was washed with 10 mL of wash buffer (50 mM NaH_2PO_4, 300 mM NaCl, and 20 mM imidazole (pH 8.0)). The protein eluted and collected in 5-1mL aliquots of elution buffer (50 mM NaH_2PO_4, 300 mM NaCl, and 250 mM imidazole (GoldBio) (pH 8.0)). Fractions containing pure $FolA_{Ec}$ (>90% as judged by an SDS-PAGE gel) were pooled, concentrated (Millipore) into storage buffer (25 mM Tris buffer (pH 7.5) with 10% glycerol and 1 mM DTT) to 10 mg/mL. The protein was stored at –80 ºC.

$FolA_{Ms}$ was purified similarly as the purification of $FolA_{Mtb}$. Briefly, *M. smegmatis* $folA_{Ms}$ was amplified using *M. smegmatis* genomic DNA by PCR. The resulting DNA was cut with the restriction enzymes *Nde*I and *BamH*1 and ligated into an already digested pET28b(+) using the same restriction enzymes. Briefly, sequence-verified pET28b(+):$folA_{Ms}$ was transformed into competent *E. coli* BL21 (DE3) cells. E. coli BL21 pET28b(+):$folA_{Mtb}$ was inoculated into LB and grown overnight at 37 ºC. The cells were diluted 1:1000 into fresh LB (1 L) and were grown until mid-exponential phase (optical density at 600 nm 0.4–0.6) at 37 ºC and 1 mM IPTG was added to induce protein expression at 37 ºC for 4 h. The

cells were collected by centrifugation at 5,000 rpm (Beckman Coulter, Avanti JXN-30) at 4 ºC. The pellet was resuspended in 10 mL of lysis buffer (20 mM triethanolamine (TEA), 50 mM KCl, pH 7) and was ultrasonicated (Branson Sonifier 450) three times using 20 sec burst (4 ºC) and 20 sec cooling. 10 mg chicken egg white lysozyme (MP Biomedicals, LLC) was added and incubated on ice for 30 min. The insoluble fraction was removed by centrifugation (Beckman Coulter, Avanti JXN-30) at 11,000 rpm at 4 ºC for 45 min. The supernatant was applied to a 1 mL of Ni-NTA Agarose (Qiagen) equilibrated with lysis buffer. The column was washed with 40 mL of wash buffer (20 mM TEA, 50 mM KCl, 50 mM imidazole (GoldBio), pH 7). The protein was eluted with 5 mL of elution buffer (20 mM TEA, 50 mM KCl, 500 mM imidazole (GoldBio), pH 7). Fractions containing pure $FolA_{Ms}$ (>90% as judged by an SDS-PAGE gel) were pooled, concentrated (Millipore) into storage buffer (20 mM potassium phosphate, 50 mM KCl, pH 7.0) to 5 mg/ml. The protein was stored at –80 ºC.

Biochemical utilization of DHF and hydroxy-DHF

All enzymatic assays were performed in flat bottom 96 well plates (Corning), with 200 µL reaction volume, and measured in a BioTek Synergy H1 spectrophotometer at 25 ºC. $FolA_{Ec}$ enzymatic assays were performed using 5 nM enzyme in MTEN buffer [50 mM 2-morpholinoethanesulfonic acid, 25 mM tris(hydroxymethyl)aminomethane, 25 mM ethanolamine, and 100 mM NaCl (pH 7.0)] containing 1 mM DTT and 0.01% (vol/vol) Triton-X 100. The enzyme was

preincubated with 67 µM of NADPH at room temperature for 5 min. The reaction was initiated with varying concentrations of dihydrofolate or hydroxy-dihydrofolate. The decrease in absorbance corresponding to NADPH oxidation was monitored at 340 nm every 10 sec for 10 min. Kinetic measurements for $FolA_{Ms}$ were performed identically as $FolA_{Ec}$ except the reaction was performed in 20 mM potassium phosphate, 50 mM KCl, pH 7.0 with 0.01% (vol/vol) Triton-X 100. The K_m were determined from 4 independent experiments performed in biological triplicate and analyzed using GraphPad Prism software.

Construction of PABA auxotrophic strains

E. coli Δ*pabB* and *A. baumannii* Δ*pabC* strains were constructed as previously described (Baba *et. al*., 2006). *M. smegmatis pabB* gene was replaced with a hygromycin resistance and *sacB* cassette using the specialized transduction method (Bardarov *et. al*., 2002). Briefly, ~1,000 bp regions upstream and downstream of *pabB* were amplified via PCR, digested with *Van*91I and ligated into previously digested p0004S. The resulting plasmid was sequenced to verify amplicons. The resulting plasmid was digested with *Pac*I and ligated into previously digested phAE159. The resulting temperature sensitive phage was propagated at 30 ºC in *M. smegmatis* to high titer and used to transduce *M. smegmatis.* The resulting transductants were plated on 10 µg/mL PABA and hygromycin and incubated at 37 ºC. The deletion was verified by PCR. H37Rv Δ*pabB* was created identically to *M. smegmatis* Δ*pabB* except using primers

found in Table 2.1 and the transduced H37Rv was plated on 1 µg/mL PABA and hygromycin.

PABA auxotroph growth curves

E. coli Δ*pabB* and *A. baumannii* Δ*pabC* were grown to mid-exponential phase (OD_{600} 0.4-0.6) in LB medium and washed three times with PABA-free M9 medium. The cells were subcultured in PABA-free M9 medium to OD_{600} 0.001 in the presence of 10 µg/mL PABA, 10 µg/mL PAS, or no addition, in technical triplicate, in round bottom 96-well plates (Corning). The cells were incubated at 37 ºC, with 200 rpm shaking, and OD_{600} were read every hour for 24 hrs. *M. smegmatis* Δ*pabB* was grown in PABA-free supplemented 7H9 containing 10 µg/mL PABA to mid-exponential phase (OD_{600} 0.4-0.6) and washed three times with PABA-free 7H9. The cells were subcultured in PABA-free 7H9 to an OD_{600} of 0.001 in the presence of 10 µg/mL PABA, 10 µg/mL PAS, or no addition, in technical triplicate, in round bottom 96-well plates (Corning). The cells were incubated at 37 ºC without shaking. Absorbance (OD_{600}) was read every 6 and 18 hours (Spectronic Genesys 5S). All growth curves were performed in biological triplicate.

E. coli ΔthyA ΔfolA *containing pUC19 constructs*

E. coli folA was amplified using primers in Table 2.1 using PCR. The resulting DNA was cut with the restriction enzymes *Bam*HI and *Xma*I and ligated into an already digested pUC19. The resulting plasmid was sequence verified and electroporated into *E. coli* Δ*thyA* Δ*folA*. *M. tuberculosis folA* was amplified from a codon optimized G Block (Invitrogen) using primers in Table 2.1 for PCR. The resulting DNA was cut with restriction enzymes *Bam*HI and *Eco*RI and ligated into an already digested pUC19. The resulting plasmid was sequence verified and electroporated into *E. coli* Δ*thyA* Δ*folA*.

H37Rv ΔpabB *containing pUMN002 constructs*

M. smegmatis folA and *M. tuberculosis folA* were amplified using primers in Table 2.1 for PCR. The resulting amplicons were cut with the restriction enzymes *Hind*III and *Eco*RI and ligated into an already digested pUMN002. The resulting plasmids was sequence verified and electroporated into H37Rv Δ*pabB*. The strains were plated on 7H10 containing 1 µg/mL PABA, hygromycin, and kanamycin.

folA *swap growth curves*

E. coli Δ*thyA* Δ*folA* containing either pUC19-$folA_{Ec}$ *or* pUC19-$folA_{Mtb}$ was grown in M9 medium supplemented with 200 µg/mL thymine (Sigma) and 50 µM IPTG to mid-exponential phase (OD_{600} 0.4-0.6) and washed three times in M9 medium. *E. coli* containing pUC19-$folA_{Ec}$ was subcultured to OD_{600} 0.001 and *E. coli*

containing pUC19-*folA*$_{Mtb}$ was subcultured to OD_{600} 0.01, in M9 supplemented with 200 µg/mL thymine (Sigma) and 50 µM IPTG, either alone or with 50 µg/mL PAS, in round bottom 96-well plates (Corning), in technical triplicate. The cells were incubated at 37 ºC with shaking at 200rpm. Absorbance (OD_{600}) was read every hour for 50 hours. All growth curves were performed in biological triplicate.

H37Rv Δ*pabB* containing pUMN002, pUMN002-*folA*$_{Mtb}$ or pUMN002-*folA*$_{Ms}$ was grown with 10 ng/mL PABA to mid-exponential phase and was subcultured to OD_{600} 0.01 with 10 ng/mL PABA. The strains were grown to mid-exponential phase and streaked on PABA-free 7H10 plates containing 5 µg/mL PAS or 5 µg/mL PABA. The plates were incubated for 3 weeks at 37 ºC.

Computational docking (Written by William McCue)

Dihydrofolate and hydroxy-DHF were each docked into the crystal structures of analogous FolA$_{Ec}$ and FolA$_{Mtb}$. Docking was performed using the Schrödinger Maestro suite [Schrödinger, LLC, New York, NY, 2018]. The X-ray crystal structures of *E. coli* DHFR with methotrexate and NADPH (PDB 4P66) and *Mtb* DHFR with methotrexate and NADPH (PDB 1DF7) were retrieved from the RCSB PDB (Berman *et. al*., 2000; Li *et. al*., 2000; Liu *et. al*., 2014). The PDB structures-were prepared for docking studies using the Maestro Protein Preparation Wizard to assign bond orders, create disulfide bonds, fill-in gaps in the protein structure, and add in hydrogens. Waters greater than 5 Å away from a

ligand or amino acid hetero group were removed and then an energy minimization was completed using the OPLS3 force field. The Maestro Receptor Grid Generation module was used to define a 25 × 25 × 25 Å grid centered on the methotrexate position in both structures. Dihydrofolate and hydroxy-DHF ligand structures for docking were prepared by adaptation from the methotrexate structure of 4P66 using the Maestro 3D Build Module. Docking was performed using the Maestro Glide module-with extra precision and flexible ligand sampling, but no additional constraints. 10 initial poses were generated for each molecule and subjected to a post-docking minimization using an OPLS3 force field. The resulting poses were ranked according to their Glide score, which is an approximation of binding energy.

Evolutionary coupling

The evolutionary coupling between pairs of residues in $FolA_{Mtb}$ was determined using EVcouplings (http://www.EVfold.org) (Marks *et. al*., 2012; Sander *et. al*., 2011). The amino acid sequence used was UniProt ID P9WNX1 and the PDB 1DG8 was used for the structural comparisons (Li *et. al*., 2000). All other default parameters were used. The majority of coupling pairs are required for structural folding of the protein and map outside of the active site. The only coupling pair found within the active site was Q28 and I20.

Testing of evolutionary coupling pairs with site directed mutagenesis and enzyme assays

pET28b(+)-*folA*$_{Mtb}$ described previously was mutated with primers described in Table 2.1 using QuikChange II Site-Directed Mutagenesis Kit (Agilent). Primers were designed according to the Agilent website using QuikChange II parameters To create the double mutant pET28b-*folA*$_{Mtb}$ I20M Q28L, pET28b-*folA*$_{Mtb}$ I20M was mutated with primers used to create pET28b-*folA*$_{Mtb}$ Q28L. The enzymes were induced and purified as previously described for pET28b(+)-*folA*$_{Mtb}$, with some alterations. Once the cells were grown to mid-exponential phase, they were incubated at 25 ºC for 2 hours and then induced at 18 ºC for 18hrs. The enzyme assays were performed similarly as described previously. One modification noted was the enzyme assays were performed in quartz cuvettes in a spectrophotometer (Genesys 10S) with a final volume of 500 µL. Variations in enzyme concentration, or substrate concentration were noted.

Determination of minimum inhibitory concentrations of antifolates for bacterial strains

Minimum inhibitory concentration (MIC_{90}) is defined as the minimum concentration of antimicrobial agent required to inhibit ≥90% of growth compared to a no drug control. MIC_{50} is defined as the minimum concentration of drug required to inhibit ≥50% of growth compared to a no drug control. Growth was

assessed spectrophotometrically (OD_{600}) (BioTek Synergy H1) or visually, when noted.

M. *tuberculosis* was grown to mid-exponential phase and subcultured to OD_{600} 0.01 in inkwell bottles. The MIC_{90} of PAS was determined using log_2 serial dilutions. The MIC_{90} was determined after 14 days of incubation. The MIC_{90} and checkerboards of PAS and SMX for *E. coli* and *S. aureus* were performed as previously described(Minato *et. al*., 2018) using log_2 serial dilutions. *M. smegmatis* was grown to mid-exponential phase and subcultured to OD_{600} 0.001 in a round bottom 96-well plate (Corning). The MIC_{90} and checkerboards for PAS and SMX were performed using log_2 serial dilutions and the MIC_{90} was determined after 3 days of static incubation. *A. baumannii*, *S. enterica, S. maltophilia*, and *B. cenocepacia* were grown in LB to mid-exponential phase and washed 3 times with M9 medium. The cells were diluted to OD_{600} 0.001 in M9 medium in round bottom 96-well plates (Corning). The MIC and checkerboards for PAS and SMX were performed using log_2 serial dilutions and the MIC (or MIC for *B. cenocepacia*) was determined visually after 24 hrs (or 3 days for *B. cenocepacia*) of static incubation. *B. fragilis* was grown in BHIS to mid-exponential phase and washed three times with AMMGluc. The cells were diluted to OD_{600} 0.001 in AMMGluc in round bottom 96-well plates (Corning). The MIC and checkerboards for PAS and SMX were performed using log_2 serial dilutions and the MIC was determined visually after 3 days of static incubation. *S.*

parasanguinis was grown in Mueller-Hinton broth to mid-exponential phase and washed three times with Iso-Sensitest broth. The cells were diluted to OD_{600} 0.001 in Iso-Sensitest broth in flat bottom 96-well plates (Corning). The MIC_{90} and checkerboards for PAS and SMX was performed using log_2 serially dilutions and the MIC_{50} was determined visually after 24 hrs of static incubation. All MICs were performed in biological triplicate.

Results

Hydroxy-dihydrofolate inhibits FolA$_{Mtb}$ but can be utilized as a substrate in other organisms

We were able to synthesize analytically pure hydroxy-DHF and tested whether it had inhibitory activity against purified recombinant *M. tuberculosis* FolA (FolA$_{Mtb}$) (Figure 2.1). Hydroxy-DHF was able to potently inhibit FolA$_{Mtb}$ with an IC_{50} of 2.9 ± 1.2 μM and a K_i of 74 nM (Table 2.4 and Figure 2.2).

We determined the minimum inhibitor concentration (MIC) of PAS required to inhibit growth in multiple bacteria including enteric commensal bacteria, Gram positive pathogens, Gram negative pathogens, non-pathogenic and non-tuberculosis mycobacteria were all resistant to PAS (Table 2.5). To determine if FolA from these bacteria could utilize hydroxy-DHF, we purified the FolA from *Escherichia coli* (FolA$_{Ec}$) and *Mycobacterium smegmatis* (FolA$_{Ms}$), and found that each of these enzymes could use both DHF and hydroxy-DHF as substrates (FolA$_{Ec}$ $K_{m\ DHF}$ 2.1 μM and $K_{m\ hydroxy\text{-}DHF}$ 17.2 μM, FolA$_{Ms}$ $K_{m\ DHF}$ 4.2 μM and $K_{m\ hydroxy\text{-}DHF}$ 22.5 μM) (Figure 2.3). Taken together, the data suggest that PAS is selective for *M. tuberculosis*, and its activated form hydroxy-DHF can be utilized as a substrate by FolA in *M. smegmatis* and *E. coli*.

To determine if PAS can be converted to hydroxy-DHF and utilized for folate metabolism, we used PABA auxotrophic strains *E. coli* Δ*pabB*, *M. smegmatis*

Δ*pabB*, and *Acetinobacter baumannii* Δ*pabC*. These strains cannot grow without addition of supplemental PABA to the growth medium (Figure 2.4). When the strains were supplemented with PAS, the growth defects of all of the strains were chemically complemented (Figure 2.4). These data indicate that PAS can be used *in lieu* of PABA in folate synthesis to support one carbon metabolism.

FolA$_{Mtb}$ *is the principle target for hydroxy-DHF*

To further understand if FolA$_{Mtb}$ is the principal target for hydroxy-DHF, we determined if PAS could be utilized in a *M. tuberculosis* Δ*pabB* expressing *folA*$_{Ms}$ or *folA*$_{Mtb}$ *in trans*. *M. tuberculosis* Δ*pabB* expressing *folA*$_{Mtb}$ could only grow in the presence of PABA, not PAS (Figure 2.5). Interestingly, *M. tuberculosis* Δ*pabB* expressing *folA*$_{Ms}$ could grow in the presence of both PAS and PABA(Figure 2.5). However, it is worth noting that growth on PAS was not as robust as growth on PABA, indicating that PAS-containing folates are not used as efficiently as native folates in this strain. Furthermore, these strains could not grow reliably in liquid medium in the presence of PAS (data not shown) but could grow on solid medium containing PAS. These observations indicate that FolA the molecular determinant for microbial PAS susceptibility and resistance.

We performed the converse experiment using *E. coli* Δ*folA*$_{Ec}$ Δ*thyA* expressing *folA*$_{Mtb}$ and *folA*$_{Ec}$ *in trans*. The strain cannot grow without supplemental thymidine because the strain also lacks thymidylate synthase (encoded by *thyA*),

a key enzyme in thymidine synthesis pathway(Howell *et. al*., 1988a). *E. coli* Δ*folA*$_{Ec}$ Δ*thyA* expressing *folA*$_{Ec}$ could grow in the presence of thymidine and PAS (Figure 2.6). As expected, *E. coli* Δ*folA*$_{Ec}$ Δ*thyA* expressing *folA*$_{Mtb}$ could grow in the presence of supplemental thymidine, but could not grow in the presence of thymidine and PAS (Figure 2.6). However, the strain has a much longer lag phase compared to the strain with expressing *folA*$_{Ec}$. Taken together, these data demonstrate that *folA*$_{Mtb}$ is the principal target of activated PAS.

FolA$_{Mtb}$ *forms additional hydrogen bonds with hydroxy-DHF compared to other bacterial FolAs*

DHF and hydroxy-DHF was docked into crystal structures of FolA$_{Mtb}$ and FolA$_{Ec}$. The docking score was determined for each confirmation of DHF and hydroxy-DHF. The docking score corresponds to the theoretical binding affinity K_d. The more negative binding score the higher binding affinity the enzyme has for the substrate. FolA$_{Mtb}$ formed an additional hydrogen bond with hydroxy-DHF compared to DHF (Figures 2.7 and 2.8). This additional hydrogen bond resulted in a more negative docking score (Figure 2.8). In contrast, FolA$_{Ec}$ could not form any additional hydrogen bonding with hydroxy-DHF and the docking score of hydroxy-DHF is similar to DHF (Figures 2.7 and 2.9). The addition of one hydrogen bond could explain how FolA$_{Ec}$ can utilize hydroxy-DHF while FolA$_{Mtb}$ is inhibited.

We also used evolutionary coupling as an approach to discover which residues were important in the selective binding of hydroxy-DHF. Evolutionary coupling predicted many residues to be conserved in FolA, however, only two residues were found to be coupled in the active site of $FolA_{Mtb}$ I20 and Q28 (Figure 2.10). Although the hydrophobic I20 position is conserved among FolA orthologs, Q28 is unique to $FolA_{Mtb}$ and could also hydrogen bond with hydroxy-DHF in the molecular docking studies (Figures 2.7 and Figure 2.10).

Based on the results from the molecular docking and evolutionary coupling experiments, we performed site directed mutagenesis to create the following variants $FolA_{Mtb}$ I20M, $FolA_{Mtb}$ Q28L, and $FolA_{Mtb}$ I20M Q28L, to determine if these enzymes could utilize hydroxy-DHF. $FolA_{Mtb}$ I20M was found to be enzymatically active in its ability to utilize DHF, however, it could not utilize hydroxy-DHF (Figures 2.11 and 2.12). $FolA_{Mtb}$ Q28L was not able to utilize DHF even at higher enzyme concentrations (Figure 2.11). $FolA_{Mtb}$ I20M Q28L did not show any enzymatic activity using DHF or hydroxy-DHF (Figure 2.12). Taken together, this data suggests $FolA_{Mtb}$ Q28 is predicted to be an important residue in conferring susceptibility to hydroxy-DHF. Although, mutations to Q28 could be detrimental to enzyme activity, additional compensatory mutations in $FolA_{Mtb}$ could be required to utilize hydroxy-DHF

Exogenous PAS can antagonize antifolates in various bacteria

Exogenous PABA can antagonize the activity of many FolP inhibitors such as sulfonamides and diaminodiphenyl sulfones (Figures 2.13 and 2.14). Since we have demonstrated that PAS can act *in lieu* of PABA in folate biosynthesis, we hypothesized that PAS can also antagonize the activity of sulfonamides and diaminodiphenyl sulfones. In *E. coli*, addition of exogenous PAS can antagonize the activity of sulfamethoxazole (SMX), sulfanilamide, sulfathiazole and the diaminodiphenyl sulfone dapsone (Figures 2.13 and 2.14). Exogenous PABA cannot antagonize the activity of TMP(Minato *et. al*., 2018). We examined the interaction, if any, between PAS and TMP and found exogenous PAS had no interaction with TMP in *E. coli* (Figures 2.13 and 2.14). Since SMX and TMP are most frequently given in combination, we tested if PAS could antagonize the activity of SMX and TMP given in a clinical 5:1 ratio. For *E. coli*, the MIC of SMX alone is 0.2 µg/mL and for TMP alone is 0.5 µg/mL (Figure 2.15). Since SMX and TMP work synergistically, the MIC of SMX and TMP in a 5:1 ratio is 0.194/0.0388 µg/mL, respectively (Figure 2.15). Surprisingly, PAS could antagonize the synergistic activity of SMX and TMP until the MIC of TMP (0.0388 µg/mL) is reached. (Figure 2.15).

SMX and TMP are used to treat a wide range of bacterial infections. We also determined if exogenous PAS could antagonize SMX activity in a variety of other bacterial species. Exogenous PAS did antagonize the activity of SMX in *M. smegmatis, Staphylococcus aureus*, *Streptococcus parasanguinis*, *Bacteroides*

fragilis, *Salmonella enterica* and *Burkholderia cenocepacia* (Figures 2.13 and 2.14). This suggests exogenous PAS, like PABA, is able to antagonize sulfa-drug activity.

Discussion

Hydroxy-DHF inhibits FolA$_{Mtb}$ *but can be utilized as a substrate in other organisms.*

Herein, we tested the hypothesis that hydroxy-DHF selectively inhibits FolA$_{Mtb}$ while other organisms can utilize hydroxylated folate species as a cofactor for one carbon metabolism. To test this hypothesis, we first needed to synthesize hydroxy-DHF, as no source for analytically pure material exists. We were able to develop a synthetic scheme and were able to subsequently demonstrate that hydroxy-DHF inhibits FolA$_{Mtb}$. We found that hydroxy-DHF potently inhibits FolA$_{Mtb}$ with an IC_{50} of 2.9 ± 1.2 μM and a K_i of 74 nM. The inhibitory data is similar to other reported dihydrofolate reductase inhibitors such as methotrexate, TMP and WR99210 (Burchall and Hitchings, 1965; Milhous *et. al*., 1985).

Previous work noted that PAS was selective at inhibiting *M. tuberculosis*. We followed up on these studies and found in most organisms tested PAS did not exhibit any inhibitory activity (>500 μg/mL). Although one organism, *S. parasanguinis*, did have a measurable PAS MIC of 250 μg/mL. The serum concentration of PAS ranges from 9-35 μg/mL with an average time to peak serum concentration levels of 6 hrs. Therefore, although PAS did display inhibitory activity against *S. parasanguinis*, the serum concentrations of PAS would be far below this MIC. Since PAS is given orally 3-4 times per day in 4

gram doses, it is possible that this level could be reached in the stomach or intestines. Although, one remaining question is, why does *S. parasanguinis* have a measurable MIC to PAS while the other bacteria tested do not? On explanation could be that hydroxy-DHF or a downstream hydroxy-folate species could be inhibitory at very high concentrations.

We extended this study and tested purified recombinant FolA from *E. coli* and *M. smegmatis* for utilization of hydroxy-DHF. We found that both enzymes could utilize hydroxy-DHF as a substrate, however, at a higher K_m. Since K_m is related to binding affinity, both enzymes cannot bind hydroxy-DHF as well as DHF. Interestingly, although they have a higher K_m for hydroxy-DHF, the amount of hydroxy-DHF required for growth must be very low.

To determine if the previously tested bacteria were utilizing PAS for folate biosynthesis, we used PABA auxotrophic strains of *E. coli* and *M. smegmatis* to test if these strains could utilize PAS. All strains could grow in the presence of both PABA and PAS. Thus, PAS can be utilized for folate biosynthesis and resulting folates can serve as cofactors for one carbon metabolism.

$FolA_{Mtb}$ is the principle target for hydroxy-DHF

In order to determine if FolA is the principle target for PAS, we used a strain of *E. coli* that lacked *folA* and *thyA*, an essential enzyme to make thymidine. Using this

strain we could express $FolA_{Ec}$ and $FolA_{Mtb}$ from a plasmid and determine whether these strains could grow in the presence of thymidine alone or in the presence of thymidine and PAS.. In order to ensure the enzyme was able to fold properly, we first grew both strains in the presence of thymidine. Although the strain containing $FolA_{Mtb}$ had a delayed growth phenotype it could still grow using thymidine. This suggests that when $FolA_{Mtb}$ is expressed in *E. coli*, it may not have the same kinetics as $FolA_{Ec}$. The fast growth rate of *E. coli*, relative to *M. tuberculosis*, likely demands an increased abundance of reduced folates. When we grew both strains in the presence of PAS, only the strain expressing $FolA_{Ec}$ was capable of growth, suggesting that we could transfer PAS susceptibility to *E. coli* with the expression of $FolA_{Mtb}$.

We performed a similar experiment in a PABA auxotrophic strain of *M. tuberculosis*. Instead of expressing *folA* from *E. coli*, we used $folA_{Ms}$ from *M. smegmatis*. We reasoned that expression of an ortholog from a more closely related bacterial species would have a greater chance of proper folding in *M. tuberculosis*. $FolA_{Ms}$ has more sequence identity with $FolA_{Mtb}$ then $FolA_{Ec}$ (~60% compared to ~30%). We grew both strains with the minimum amount of PABA to support growth so that the exogenous PABA would not antagonize the activity of PAS. We used plates containing 5 µg/mL of PABA or PAS, as previous literature has shown that PAS could have an alternative mechanism of action at high concentrations of 10 µg/mL or more(Moradigaravand *et. al*., 2016). We found that

the strain expressing FolA$_{Ms}$ could grow in the presence of both PABA and PAS. In contrast, the strain expressing FolA$_{Mtb}$ could grow in the presence of PABA, but could not grow in the presence of PAS. The ability of *M. tuberculosis* to utilize PAS *in lieu* of PABA when expressing FolA from a resistant organism demonstrates that FolA$_{Mtb}$ is the exclusive target and basis for the exquisite selectivity of activated PAS.

FolA$_{Mtb}$ *can form an additional hydrogen bond to hydroxy-DHF from the residue Q28*

To pinpoint the exact mechanisms of this selectivity, we used molecular docking to dock DHF and hydroxy-DHF into previously crystallized FolA$_{Mtb}$ and FolA$_{Ec}$. FolA$_{Mtb}$ is predicted to bind both DHF and hydroxy-DHF, however, hydroxy-DHF had a more negative docking score (-11.6 DHF compared to -12.6 hydroxy-DHF). This score correlates to a log order higher affinity binding of hydroxy-DHF compared to DHF in FolA$_{Mtb}$. Furthermore, this more negative docking score is likely attributed to an additional hydrogen bond with hydroxy-DHF at position Q28. Conversely, FolA$_{Ec}$ had a less negative binding score to DHF (-9.4 DHF compared to -9.1 hydroxy-DHF), suggesting that FolA$_{Ec}$ can bind to both substrates, but has a slightly higher affinity to DHF. This observation could explain the higher K_m of FolA$_{Ec}$ for utilization of hydroxy-DHF compared to DHF. Notably, FolA$_{Ec}$ had a residue L28 that could not hydrogen bond with hydroxy-DHF. This lack of hydrogen bonding at position 28 in FolA$_{Ec}$ could explain the

less negative binding score between DHF and hydroxy-DHF. Furthermore, the alpha helix, that binds DHF and hydroxy-DHF in FolA$_{Mtb}$ and FolA$_{Ec}$ are different. The alpha helix in FolA$_{Mtb}$ contains much more hydrophilic residues compared to FolA$_{Ec}$. Therefore, hydroxy-DHF undergoes a much more thermodynamically unfavorable rotation, in FolA$_{Ec}$, to place the hydroxyl-group on hydroxy-DHF into a more favorable environment.

Evolutionary coupling was performed using FolA$_{Mtb}$ to determine which amino acid residues on FolA had a larger evolutionary pressure to mutate. Interestingly, Q28 was predicted to be evolutionary coupled with I20. Q28 is the same residue that can hydrogen bond with hydroxy-DHF in the molecular docking studies. We constructed and purified these enzymes and tested the ability to utilize DHF or hydroxy-DHF as a substrate. We found that FolA$_{Mtb}$ I20M had reduced enzymatic activity compared to the wild type enzyme but could not utilize hydroxy-DHF as a substrate. The FolA$_{Mtb}$ Q28L mutant and FolA$_{Mtb}$ I20M Q28L double mutant could not utilize either DHF or hydroxy-DHF. One avenue of future research could be to exchange the alpha helix from FolA$_{Ec}$ with the alpha helix from FolA$_{Mtb}$. This modification could overcome any detrimental mutations in the active site. Another assay to address any overall structural changes to the enzyme, would be to perform an enzyme evolution assay using random mutagenesis where active variants could be selected in *E. coli*.

PAS, like PABA, can antagonize antifolates

We have previously demonstrated that PAS can act similarly to PABA in folate biosynthesis. Since PABA can antagonize the activity of sulfa-drugs, we tested drug-drug interactions between PAS and sulfa-drugs. Specifically, we tested if PAS could antagonize SMX, DDS, STZ and SNL. We found that in *E. coli* PAS could antagonize these drugs. Furthermore, PAS could antagonize SMX in a variety of bacterial species. Since previous studies have found that PABA cannot antagonize TMP activity, we also tested if PAS could antagonize TMP activity. Not surprisingly, PAS could not antagonize TMP activity. Since SMX and TMP are rarely given in monotherapy, we tested if PAS could antagonize SMX and TMP given in a clinical 5:1 ratio. Indeed PAS could antagonize SMX and TMP activity, however, once the MIC of TMP is reached the antagonism is abolished. This observation indicates that only SMX activity is being antagonized by PAS and that co-treatment with PAS and SMX/TMP may be similar to treating with TMP in monotherapy.

From a clinical perspective, these data suggest that PAS and sulfa drugs should not be used in combination. Patients who are HIV positive are given lifelong prophylactic therapy of SMX/TMP to prevent and treat opportunistic pathogens. In some areas of the world there is a high prevalence of HIV-TB co-infection. Therefore, treatment with PAS and SMX/TMP needs to be reevaluated as PAS could antagonize the activity of SMX/TMP.

Tables

Table 2.1. Oligonucleotide primers used in this study

Primer name	Primer sequence[1]	Source	Restriction enzyme
FolC seq For	CGTCGGGGGCCCGAGTGATGATG	(Zhao *et. al*., 2014)	NA
FolC seq internal	CCTACCGGGAGATCGAGCCG	This work	NA
FolC seq rev	GAACCTGCGCGATGCTATCGACG	(Zhao *et. al*., 2014)	NA
ThyA seq for	CGCCGCGCTTGCATCGCCCGCT	This work	NA
ThyA seq rev	TGT CGC TTG AGC CCA GAT CA	This work	NA
pet28b-*folA*-*Mtb* for	TTTTTTCATATGGTGGGGCTGATCTGGGCT	This work	*Nde*1
pet28b-*folA*-*Mtb* rev	TTTTTTGGATCCTCATGAGCGGTGGTAGCT	This work	*Bam*HI
pet28b-*folA*-*Ec* for	TTTTTTCATATGATGATCAGTCTG	This work	*Nde*1
pet28b-*folA*-*Ec* rev	TTTTTTGGATCCTTACCGCCGC	This work	*Bam*HI
pet28b-*folA*-*Mtb* for	TTTTTTCATATGATGAGACTGATCTGGGCCCA	This work	*Nde*1
pet28b-*folA*-*Mtb* rev	TTTTTTGGATCCTCAGCGCCGGTAGCTGCAGA	This work	*Bam*HI
*pabB*_Ms LL	TTTTTTTTCCATAAATTGGTTCTGGTTCAAGGGACGCAACCGCG	This work	*Van*91I
*pabB*_Ms LR	TTTTTTTTCCATTTCTTGGGCCATCAGCGTGGCAGATTGCTAGC	This work	*Van*91I
*pabB*_Ms RL	TTTTTTTTCCATAGATTGGAGTTCGCGCTTGGACGGCGCGCCCG	This work	*Van*91I
*pabB*_Ms RR	TTTTTTTTCCATCTTTTGGCCCAGGTTCAAGAACCGGGTGATCG	This work	*Van*91I
FolA$_{Mtb}$ I20M for	GCGCCAGGGCATGTCGCCGCCG	This work	NA
FolA$_{Mtb}$ I20M rev	CGGCGGCGACATGCCCTGGCGC	This work	NA
FolA$_{Mtb}$ Q28L for	CGGAAATGCGCCAGGTCCTCGGGCA	This work	NA
FolA$_{Mtb}$ Q28L rev	TGCCCGAGGACCTGGCGCATTTCCG	This work	NA
pUC19-*folA*-*Ec*-for	TTTTTTGGATCCATGATCAGTCTGATTGCGGCGTT	This work	*Bam*HI
pUC19-*folA*-*Ec*-rev	TTTTTTCCCGGGTTACCGCCGCTCCAGAATCTC	This work	*Xma*1
pUC19-*folA*-*Mtb*-for	TTTTTTGGATCCATGGTCGGCTTAATC	This work	*Bam*HI
pUC19-*folA*-*Mtb*-rev	TTTTTTGAATTCTCAACTACGATGGTAC	This work	*Eco*RI

pabB_Mtb LL	TTTTTTTTCCATAAATTGGCTCGCAAACTCGCGTCGTAGG	This work	*Van*91I
pabB_Mtb LR	TTTTTTTTCCATTTCTTGGGCACCGGACAGGCTCTCATAC	This work	*Van*91I
pabB-Mtb RL	TTTTTTTTCCATAGATTGGAGTGTGGCACCTGGTGTCCAC	This work	*Van*91I
pabB-Mtb RR	TTTTTTTTCCATCTTTTGGACTCCAGCGCGTTAACCGCAA	This work	*Van*91I
pUMN002-*folA-Ms*-for	TTTTTTAAGCTTATGATGAGACTGATCTGGGCCCA	This work	*Hind*III
pUMN002-*folA-Ms*-rev	TTTTTTGAATTCTCAGCGCCGGTAGCTGCAGA	This work	*Eco*RI
pUMN002-*folA-Mtb*-for	TTTTTTAAGCTTATGGTGGGGCTGATCTGGGCT	This work	*Hind*III
pUMN002-*folA-Mtb*-rev	TTTTTTGAATTCTCATGAGCGGTGGTAGCT	This work	*Eco*RI

[1]Underline corresponds to the restriction enzyme cut site. All primers are written in 5’ to 3’ orientation

Table 2.2. Plasmids used in this study

Plasmid	Relevant characteristics	Source
pET28b+	Bacterial high copy plasmid for protein overexpression containing C- and N-terminal 6X histidine tags inducible with *lacI*, Kan^r	Novagen
pET28b-*folA-Mtb*	pET28b+ containing *folA*$_{Mtb}$ with an N-terminal 6x-histidine tag, Kan^r	This work
pET28b-*folA-Ec*	pET28b+ containing *folA*$_{Ec}$ with an N-terminal 6x-histidine tag, Kan^r	This work
pET28b-*folA-Ms*	pET28b+ containing *folA*$_{Ms}$ with an N-terminal 6x-histidine tag, Kan^r	This work
pET28b-*folA-Mtb*-Q28L	pET28b+ containing *folA*$_{Mtb}$ containing the Q28L mutation with an N-terminal 6x-histidine tag, Kan^r	This work
pET28b-*folA-Mtb*-I20M	pET28b+ containing *folA*$_{Mtb}$ containing the I20M mutation with an N-terminal 6x-histidine tag, Kan^r	This work
pET28b-*folA-Mtb*-I20M Q28L	pET28b+ containing *folA*$_{Mtb}$ containing the I20M and Q28L double mutation with an N-terminal 6x-histidine tag, Kan^r	This work
p0004S	Plasmid used for allelic exchange, Hygro^r, *sacB*	(Baughn *et. al*., 2010)
phAE159	Phasmid used for specialized transduction, Pen^r	(Bardarov *et. al*., 2002)
pUC19	*E. coli* complementation plasmid, inducible with lacI, Pen^r	Lab stock
pUC19-*folA-Ec*	pUC19 containing *folA*$_{Ec}$, Pen^r	This work
pUC19-*folA-Mtb*	pUC19 containing *folA*$_{Mtb}$ that has been codon optimized for expression in *E. coli*, Pen^r	This work
pUMN002	Mycobacterial low copy number constitutively replicating plasmid, Kan^r	Lab stock
pUMN002- *folA*$_{Ms}$	pUMN002 containing *folA*$_{Ms}$, Kan^r	This work
pUMN002-*folA*$_{Mtb}$	pUMN002 containing *folA*$_{Mtb}$, Kan^r	This work

Table 2.3. Strains used in this study

Strain Name	Relevant characteristics	Source
E. coli		
DH5α	Cloning strain	Lab stock
BL21 (DE3)	Protein purification strain	Lab stock
pET28b-*folA*-*Mtb*	BL21 containing pET28b-*folA*-*Mtb* for overexpression of $FolA_{Mtb}$	This work
pET28b-*folA*-*Ec*	BL21 containing pET28b-*folA*-*Ec* for overexpression of $FolA_{Ec}$	This work
pET28b-*folA*-*Ms*	BL21 containing pET28b-*folA*-*Ms* for overexpression of $FolA_{Ms}$	This work
pET28b-*folA*-*Mtb*-Q28L	BL21 containing pET28b-*folA*-*Mtb*-Q28L for overexpression of $FolA_{Mb}$ Q28L	This work
pET28b-*folA*-*Mtb*-I20M	BL21 containing pET28b-*folA*-*Mtb*-I21M for overexpression of $FolA_{Mb}$ I20M	This work
pET28b-*folA*-*Mtb*-I20M Q28L	BL21 containing pET28b-*folA*-*Mtb*-I21M for overexpression of $FolA_{Mb}$ I20M Q28L	This work
BW25113	Wild-type lab stock	Lab stock
Δ*pabB*	BW25113 *pabB*::kan, Kan^r	Keio collection(Baba *et. al*., 2006)
Δ*thyA* Δ$folA_{Ec}$	LH18, Δ*thyA* Δ$folA_{Ec}$::kan, Kanr	(Howell *et. al*., 1988c)
Δ*thyA* Δ$folA_{Ec}$-pUC19-$folA_{Ec}$	Δ*thyA* Δ$folA_{Ec}$ containing pUC19-$folA_{Ec}$, Pen^r, Kan^r	This work
Δ*thyA* Δ$folA_{Ec}$-pUC19-$folA_{Mtb}$	Δ*thyA* Δ$folA_{Ec}$ containing pUC19-$folA_{Mtb}$, Pen^r, Kan^r	This work
M. tuberculosis		
H37Rv	Wild-type strain	Lab stock
H37Ra	Wild-type attenuated strain derived from H37Rv	Lab stock
Δ*pabB*	H37Rv *pabB*::hygro-sacB cassette, $Hygro^r$	This work
Δ*pabB*-pUMN002	Δ*pabB* containing pUMN002, Kan^r, $Hygro^r$	This work
Δ*pabB*-pUMN002- $folA_{Ms}$	Δ*pabB* containing pUMN002-$folA_{Ms}$, Kan^r, $Hygro^r$	This work
Δ*pabB*-pUMN002-$folA_{Mtb}$	Δ*pabB* containing-pUMN002 $folA_{Mtb}$, Kan^r, $Hygro^r$	This work
M. smegmatis		

mc^{2}155	Wild-type strain	(Baughn *et. al*., 2010)
Δ*pabB*	mc^{2}155 *pabB*::hygro-sacB cassette, Hygro^r	This work
M. abscessus		?
B. fragilis	G38A wild-type lab stock	?
B. cenocepacia	B7, Cystic fibrosis clinical isolate	(Tomich and Mohr, 2004)
S. enterica	Wild-type lab stock	(Adamowicz *et. al*., 2018)
S. maltophilia		
S. aureus	USA300 clinical isolate strain	(Minato *et. al*., 2018)
S. parasanguinis		

Table 2.4. Mechaelis-Menten kinetics of utilization of dihydrofolate and hydroxy-DHF in FolA

Organism	Dihydrofolate K_m (µM)	Hydroxy-dihydrofolate K_m (µM)
E. coli	2.1	17.2
M. smegmatis	4.2	22.5

Table 2.5. PAS Inhibitory concentrations against various bacterial species

Organism	PAS Inhibitory Concentration (μg/mL)
Mycobacterium tuberculosis	0.3
Mycobacterium smegmatis	>500
Mycobacterium abscessus	>500
Staphylococcus aureus	>500
Streptococcus parasanguinis	250
Salmonella enterica	>500
Bacteroides fragilis	>500
Escherichia coli	>500
Burkholderia cenocepacia	>500
Stenotrophomonas maltophilia	>500
Acinetobacter baumannii	>500

Figures

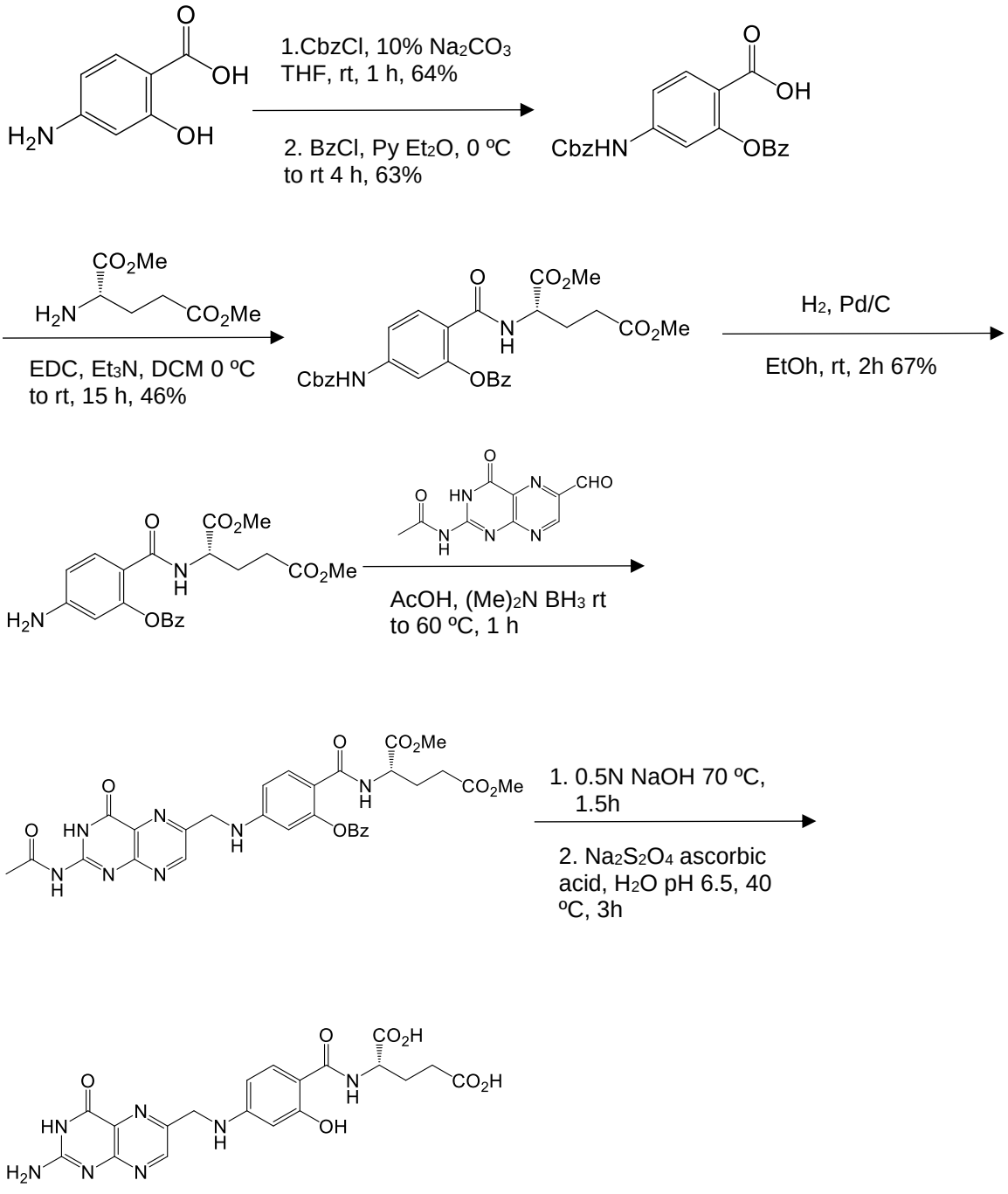
1.CbzCl, 10% Na2CO3
THF, rt, 1 h, 64%
2. BzCl, Py Et2O, 0 ºC
to rt 4 h, 63%
EDC, Et3N, DCM 0 ºC
to rt, 15 h, 46%
H2, Pd/C
EtOh, rt, 2h 67%
AcOH, (Me)2N BH3 rt
to 60 ºC, 1 h
1. 0.5N NaOH 70 ºC,
1.5h
2. Na2S2O4 ascorbic
acid, H2O pH 6.5, 40
ºC, 3h

Figure 2.1. Synthesis of hydroxy-DHF. Synthesis scheme by Dr. Surendra Dawadi.

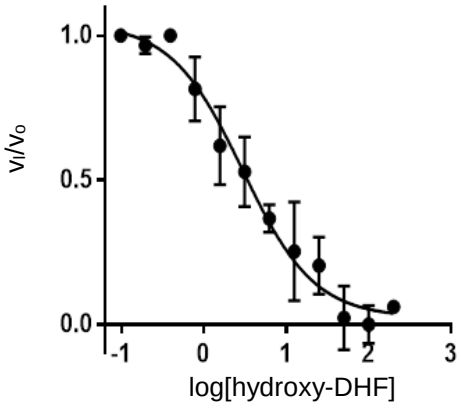

Figure 2.2. Hydroxy-DHF inhibits $FolA_{Mtb}$. An IC_{50} curve was generated using 2.5 nM of purified $FolA_{Mtb}$ against varying concentrations of hydroxy-DHF. The data shown represents 3 independent experiments using the average of 3 technical replicates. The IC_{50}(2.9 ± 1.2 μM) was calculated using GraphPad Prism software and K_i (74 nM) was calculated based on the Cheng-Prushoff equation.

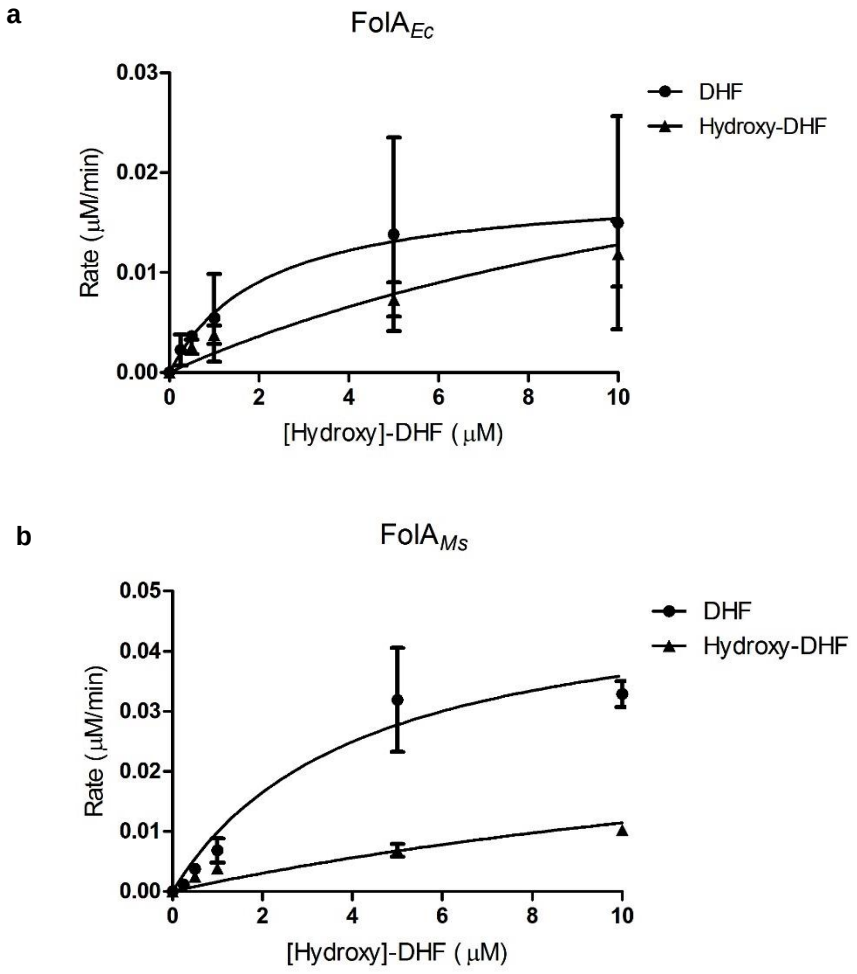

Figure 2.3. Mechaelis-Menten kinetics utilization of DHF or hydroxy-DHF. DHF or hydroxy-DHF utilization was measured in the presence of dihydrofolate or hydroxy-dihydrofolate using purified recombinant dihydrofolate reductase from *E. coli* and *M. smegmatis*. The data represents the average error of the mean performed in technical triplicate with a minimum of four biological replicates.

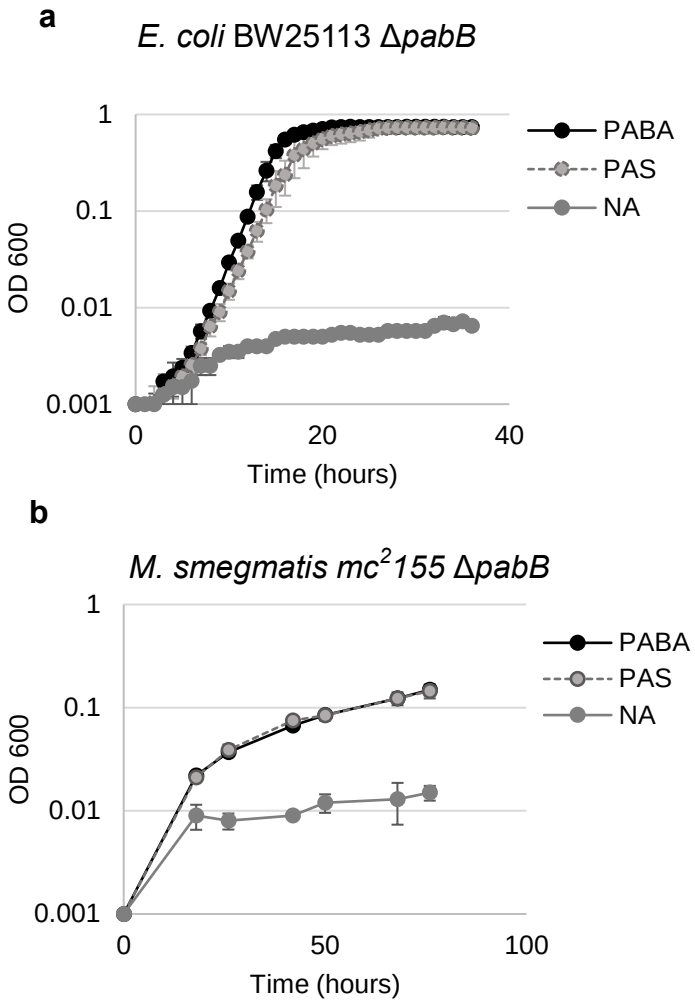
a
E. coli BW25113 ΔpabB
1
0.1
0.01
0.001
OD 600
0
20
40
Time (hours)
PABA
PAS
NA
b
M. smegmatis mc²155 ΔpabB
1
0.1
0.01
0.001
OD 600
0
50
100
Time (hours)
PABA
PAS
NA

Figure 2.4. PAS can be utilized *in lieu* of PABA for folate biosynthesis and is function in one carbon metabolism. a) *E. coli* or b) *M. smegmatis* PABA auxotrophs were grown in the presence of PABA or PAS (10 µg/mL). Both strains could not grow in the absence of PABA.

a

PABA free medium

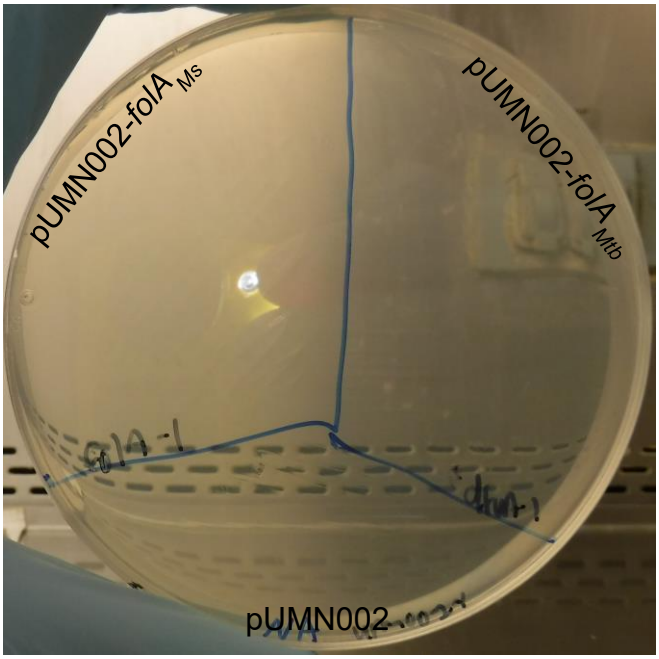

b

PABA 5µg/mL

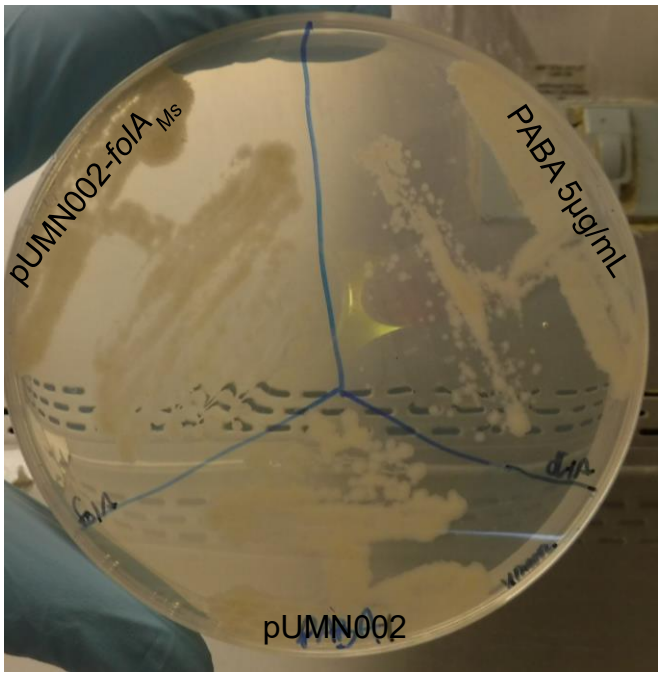

c PAS 5µg/mL

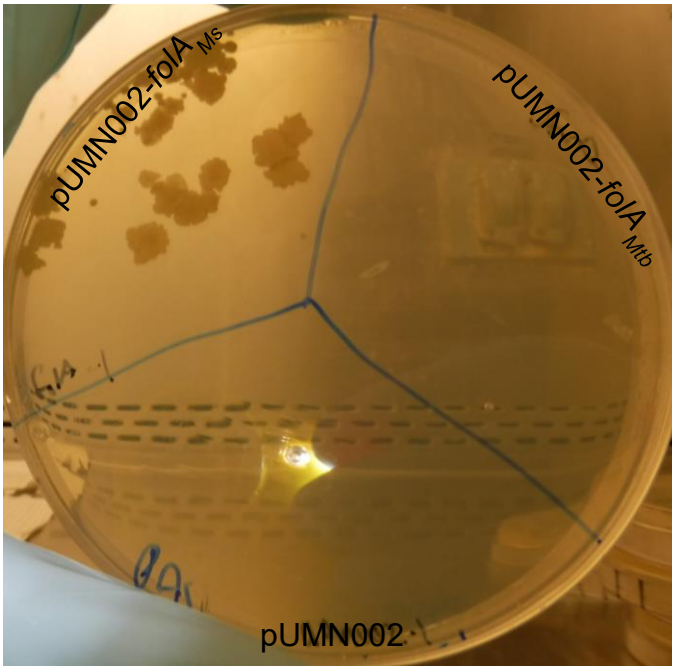

Figure 2.5. The mechanistic basis for PAS selectivity in *M. tuberculosis*. H37Rv Δ*pabB* pUMN002 expressing $folA_{Mtb}$ or $folA_{Ms}$ or empty vector were grown in the presence of a) no addition, 5 µg/mL of b) PABA or c) PAS. Plates were incubated at 37 ºC for 3 weeks. Picture represents one of three biological replicates.

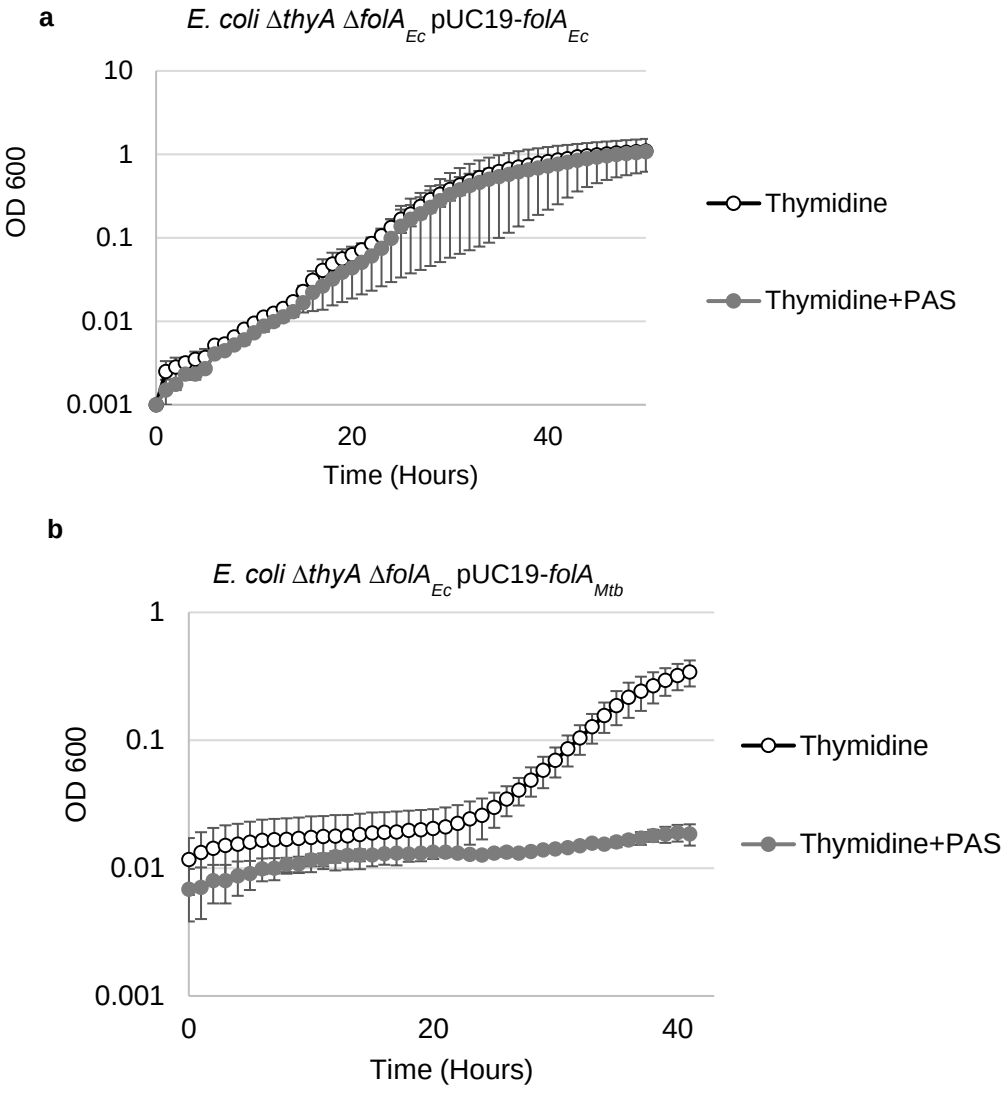

Figure 2.6. The mechanistic basis for PAS selectivity in *E. coli***.** a) *E. coli* Δ*thyA* Δ$folA_{Ec}$ pUC19-$folA_{Ec}$ can grow in the presence of thymidine and thymidine+PAS (50 µg/mL) in M9 minimal media. b) *E. coli* Δ*thyA* Δ$folA_{Ec}$ pUC19-$folA_{Mtb}$ can only grow in the presence of thymidine and not in the presence of thymidine+PAS (50 µg/mL) in M9 minimal media.

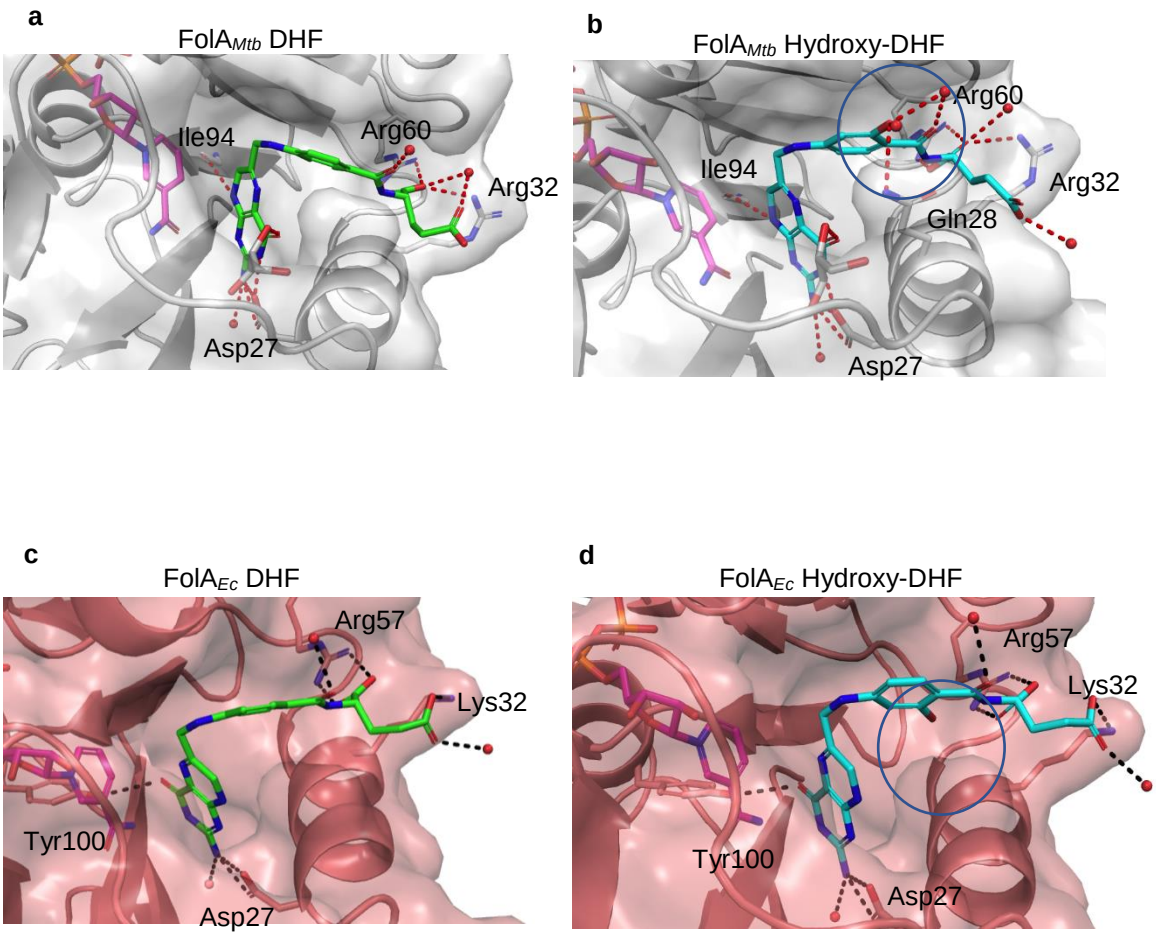

Figure 2.7. Molecular docking of DHF and hydroxy-DHF into FolA$_{Mtb}$ and FolA$_{Ec}$. Previously crystallized FolA$_{Mtb}$ (PDB:1DF7) was used to dock a) DHF or b)hydroxy-DHF. Previously crystallized FolA$_{Ec}$ (PDB 4P66) was used to dock c) DHF or d) hydroxy-DHF. Dashed lines represent key hydrogen bonds formed during the docking simulation. Red dots represent water molecules found in the crystal structures of the molecules used for docking. Circle indicated hydrogen bond formation present in FolA$_{Mtb}$ bound to hydroxy-DHF that is absent in FolA$_{Ec}$ bound to hydroxy-DHF

a FolA$_{Mtb}$ DHF

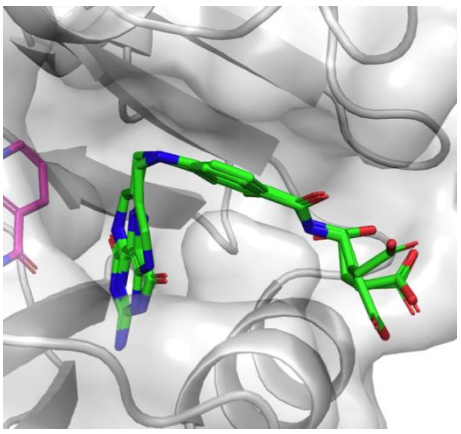

Pose	FolA$_{Mtb}$ Docking Score (DHF)
1	-11.639
2	-11.537
3	-11.403
4	-11.163
5	-11.020

b FolA$_{Mtb}$ hydroxy-DHF

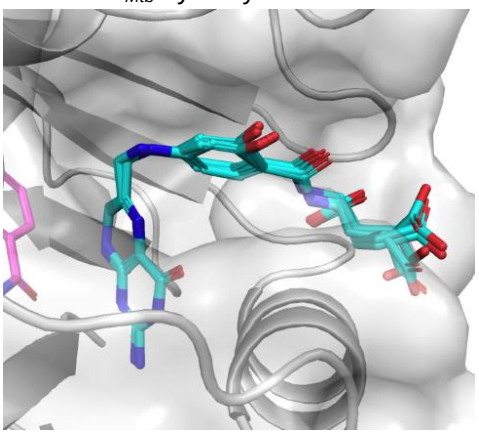

Pose	FolA$_{Mtb}$ Docking Score (hydroxy-DHF)
1	-12.591
2	-12.410
3	-12.017
4	-11.935
5	-11.929
6	-11.912

Figure 2.8. Molecular docking scores and positions of DHF and hydroxy-DHF in FolA$_{Mtb.}$ Previously crystallized FolA$_{Mtb}$ (PDB:1DF7) was used to dock a) DHF or b) hydroxy-DHF.

a

FolA$_{Ec}$ DHF

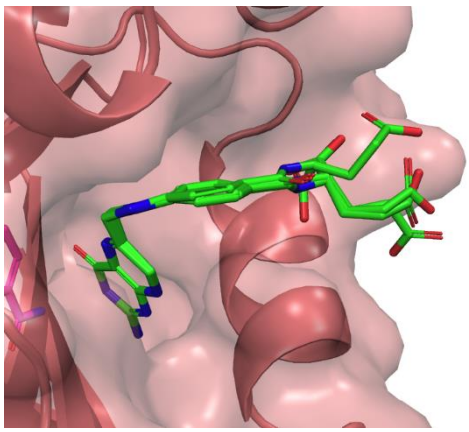

Pose	FolA$_{Ec}$ Docking Score (DHF)
1	-9.440
2	-9.370
3	-9.322
4	-9.028

b

FolA$_{Ec}$ hydroxy-DHF

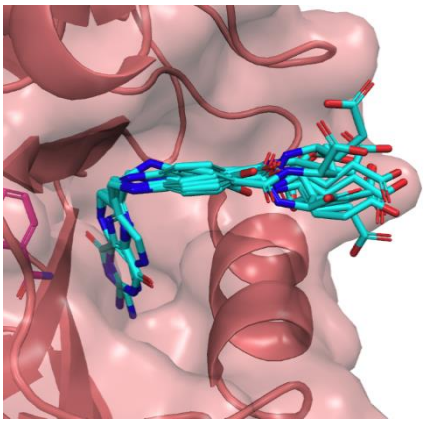

Pose	FolA$_{Ec}$ Docking Score (hydroxy-DHF)
1	-9.177
2	-8.948
3	-8.598
4	-8.483
5	-8.419
6	-8.219
7	-8.219
8	-8.040
9	-7.821
10	-7.116

Figure 2.9. Molecular docking scores and positions of DHF and hydroxy-DHF in FolA$_{Ec}$. Previously crystallized FolA$_{Ec}$ (PDB 4P66) was used to dock a) DHF or b) hydroxy-DHF.

a

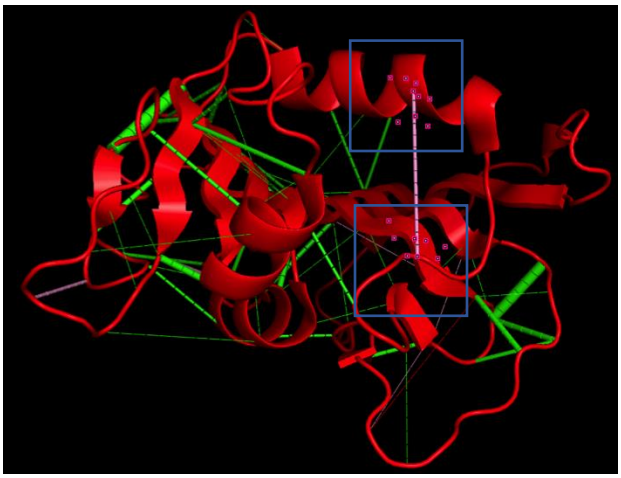

b

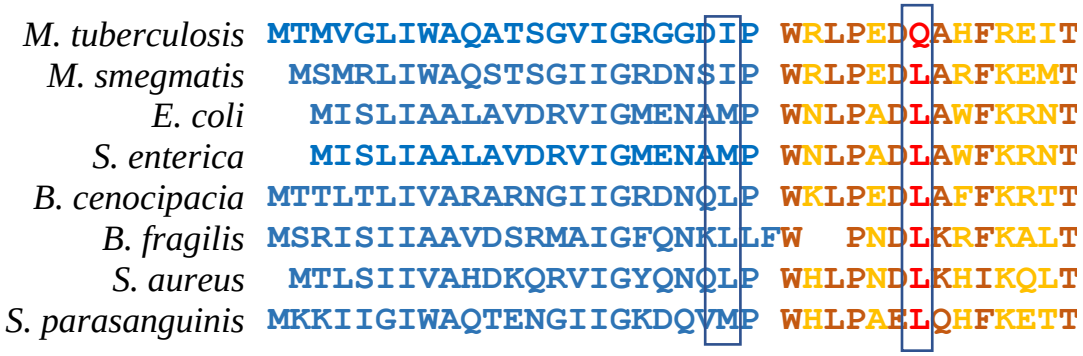

Figure 2.10. Evolutionary coupling predicts key contacts between Q28 and I20 uniquely found in FolA$_{Mtb}$. a) Evolutionary coupling was performed on FolA$_{Mtb}$, although multiple residues were considered coupled (green) the only residues in the active site found to be coupled were Q28 and I20. b) Amino acid sequence alignment of the M20 shows conservation of I20 amino acid among FolA (box). Q28 is only found in is the only residue not conserved in the amino acid sequence comparison (box).

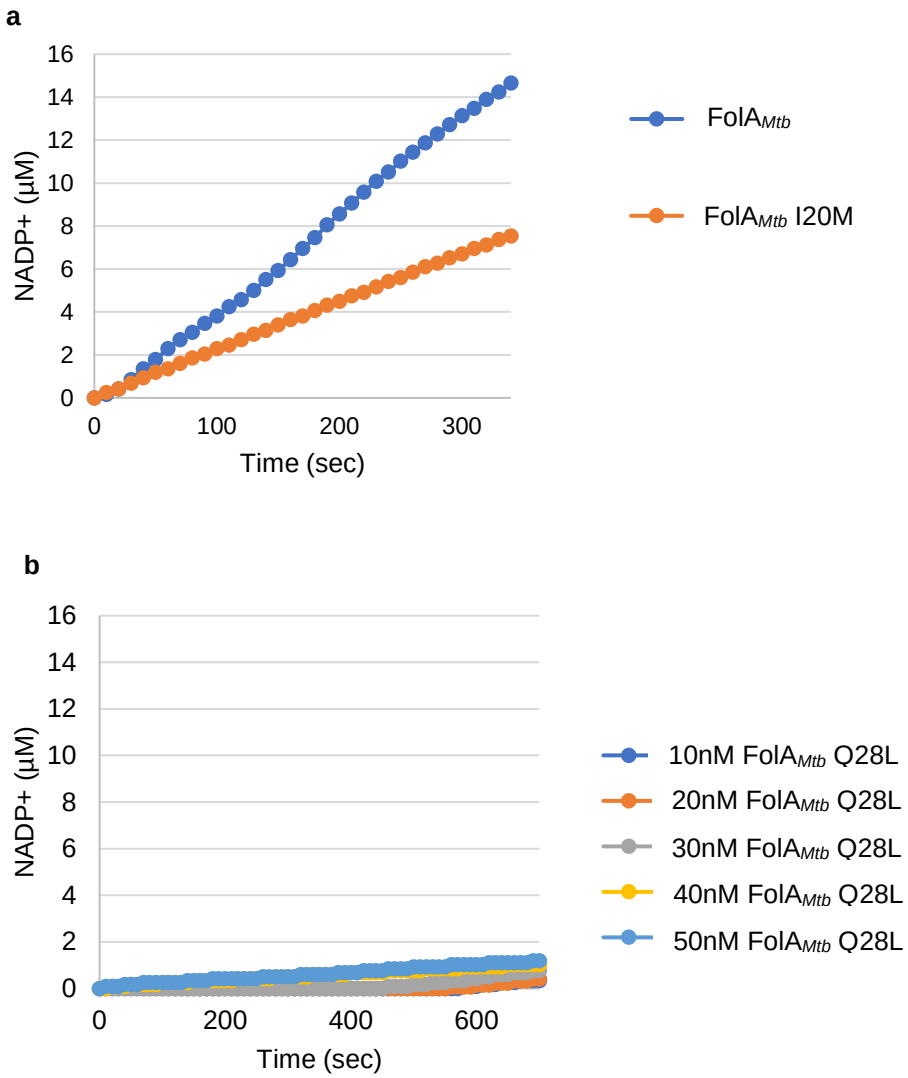

Figure 2.11. Progress curves of FolA$_{Mtb}$ I20M and FolA$_{Mtb}$ Q28L utilizing DHF. a) 10 nM of FolA$_{Mtb}$ and FolA$_{Mtb}$ I20M utilizing DHF as a substrate. b) Varying concentrations of FolA$_{Mtb}$ Q28L utilizing DHF as a substrate. All enzymes were preincubated with saturating concentrations of NADPH (90 µM) for 5 min. The reaction was initiated with saturating concentrations of DHF (76 µM) and the reaction was read by the depletion of NADPH at 340 nm every 10 sec for 700 sec. Results are an average of three independent experiments.

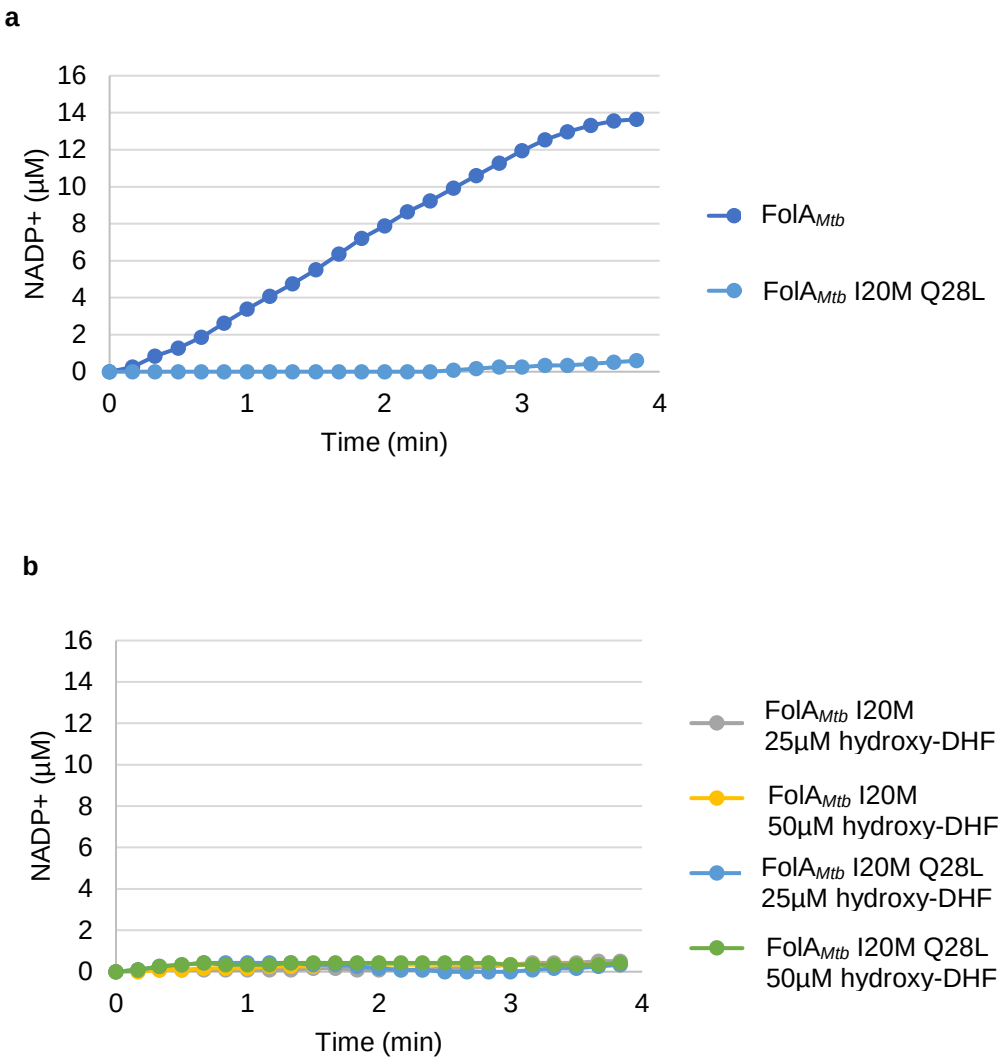

Figure 2.12. Progress curves of FolA$_{Mtb}$ I20M, FolA$_{Mtb}$ Q28L and FolA$_{Mtb}$ I20M Q28L utilizing hydroxy-DHF. a) 10 nM of FolA$_{Mtb}$ and FolA$_{Mtb}$ I20M Q28L utilizing DHF as a substrate. b) 10 nM FolA$_{Mtb}$ I20M, FolA$_{Mtb}$ Q28L and FolA$_{Mtb}$ I20M Q28L utilizing 25µM or 50µM of hydroxy-DHF. All enzymes were preincubated with saturating concentrations of NADPH (90µM) for 5 min. The reaction was initiated with saturating concentrations of DHF (25µM) or indicated amounts of hydroxy-dihydrofolate and the reaction was read by the depletion of NADPH at 340nm every 10 sec for 700 sec. Results are shown as the average of three independent experiments.

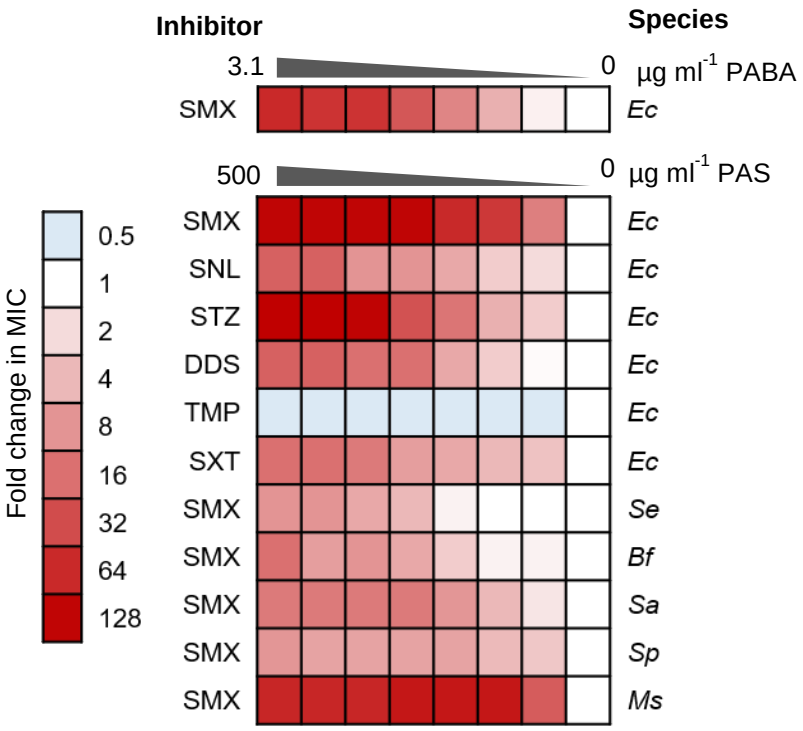

Figure 2.13. PAS, like PABA, can antagonize antifolates. *E. coli* (*Ec*)**,** *M. smegmatis* (*Ms*), *Staphylococcus aureus* (*Sa*), and *Bacteroides fragilis* (*Bf*) were grown in minimal media in the presence of varying concentrations of PAS and either sulfamethoxazole (SMX), sulfanilamide (SNL), sulfathiazole (STZ), dapsone (DDS), trimethoprim (TMP), or a 5:1 ratio of SMX/TMP. The heat map shows the fold change of the minimum concentration to inhibit growth.

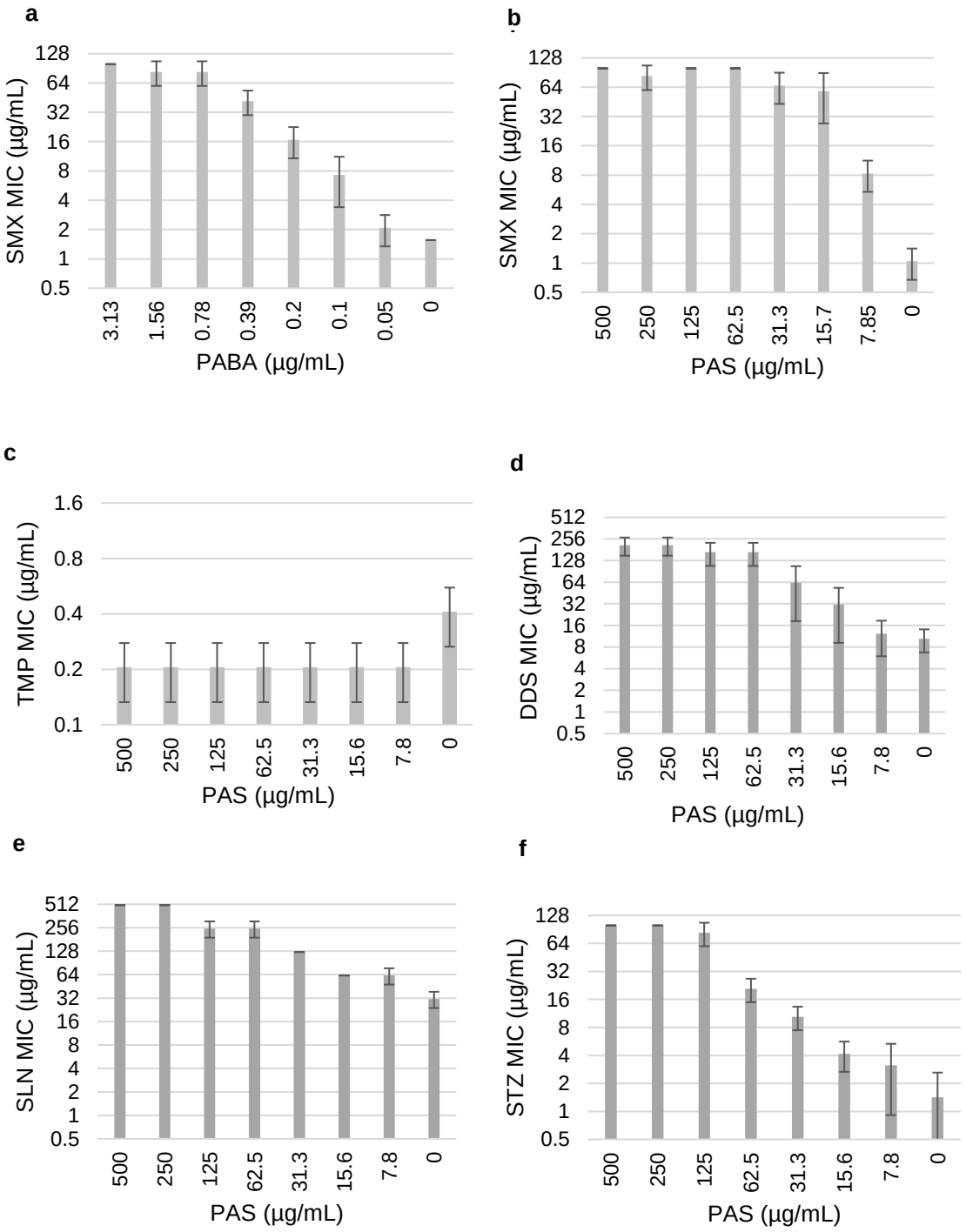
a
SMX MIC (µg/mL)
128
64
32
16
8
4
2
1
0.5
3.13
1.56
0.78
0.39
0.2
0.1
0.05
0
PABA (µg/mL)
b
SMX MIC (µg/mL)
500
250
125
62.5
31.3
15.7
7.85
0
PAS (µg/mL)
c
TMP MIC (µg/mL)
1.6
0.8
0.4
0.2
0.1
500
250
125
62.5
31.3
15.6
7.8
0
PAS (µg/mL)
d
DDS MIC (µg/mL)
512
256
128
64
32
16
8
4
2
1
0.5
500
250
125
62.5
31.3
15.6
7.8
0
PAS (µg/mL)
e
SLN MIC (µg/mL)
512
256
128
64
32
16
8
4
2
1
0.5
500
250
125
62.5
31.3
15.6
7.8
0
PAS (µg/mL)
f
STZ MIC (µg/mL)
128
64
32
16
8
4
2
1
0.5
500
250
125
62.5
31.3
15.6
7.8
0
PAS (µg/mL)

Figure 2.14. PAS, like PABA, can antagonize antifolates in *E. coli*. *E. coli* were grown in minimal M9 medium in the presence of varying concentrations of a) PABA and sulfamethoxazole (SMX). *E. coli* were grown in minimal M9 medium in the presence of varying concentrations of PAS and either b) sulfamethoxazole (SMX), c) trimethoprim (TMP), d) dapsone (DDS), e) sulfanilamide (SNL), f) sulfathiazole (STZ) for 24hrs at 37 ºC. The data represents the minimum concentration of drug required to inhibit growth in varying PAS concentrations. Each experiment represents an average of three biological replicates, error bar represents standard deviation.

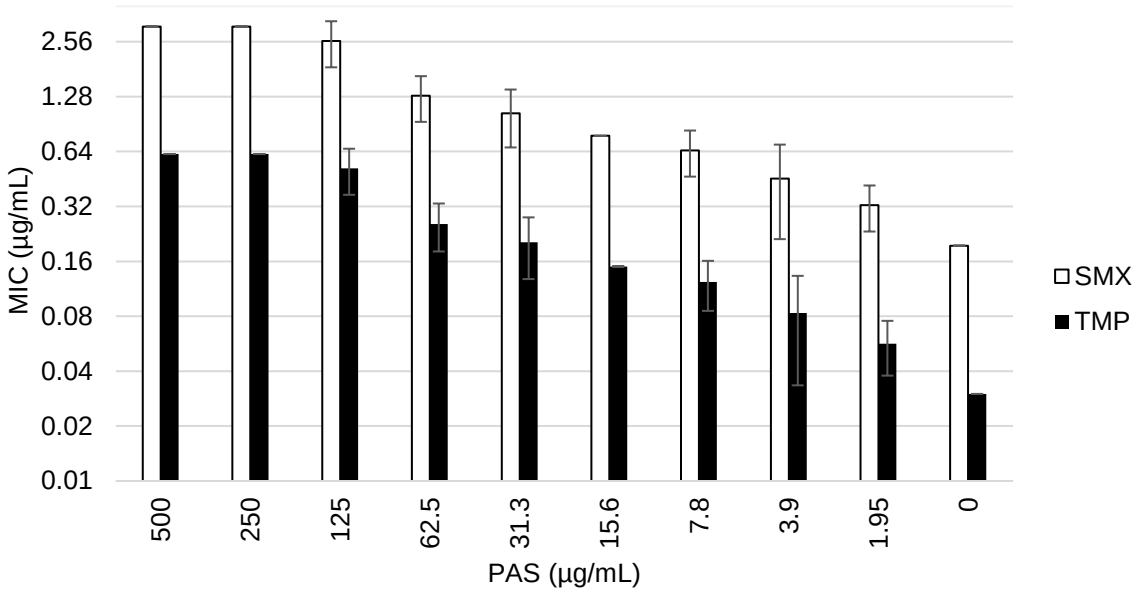

Figure 2.15. PAS can only partially antagonize a clinical combination of SMX and TMP. *E. coli* were grown in minimal media in the presence of varying concentrations of PAS and a 5:1 ratio of sulfamethoxazole (SMX) trimethoprim (TMP), respectively, for 24hrs at 37 ºC. The data represents the minimum concentration of drug required to inhibit growth in varying PAS concentrations. Each experiment represents an average of three biological replicates, error bar represents standard deviation.

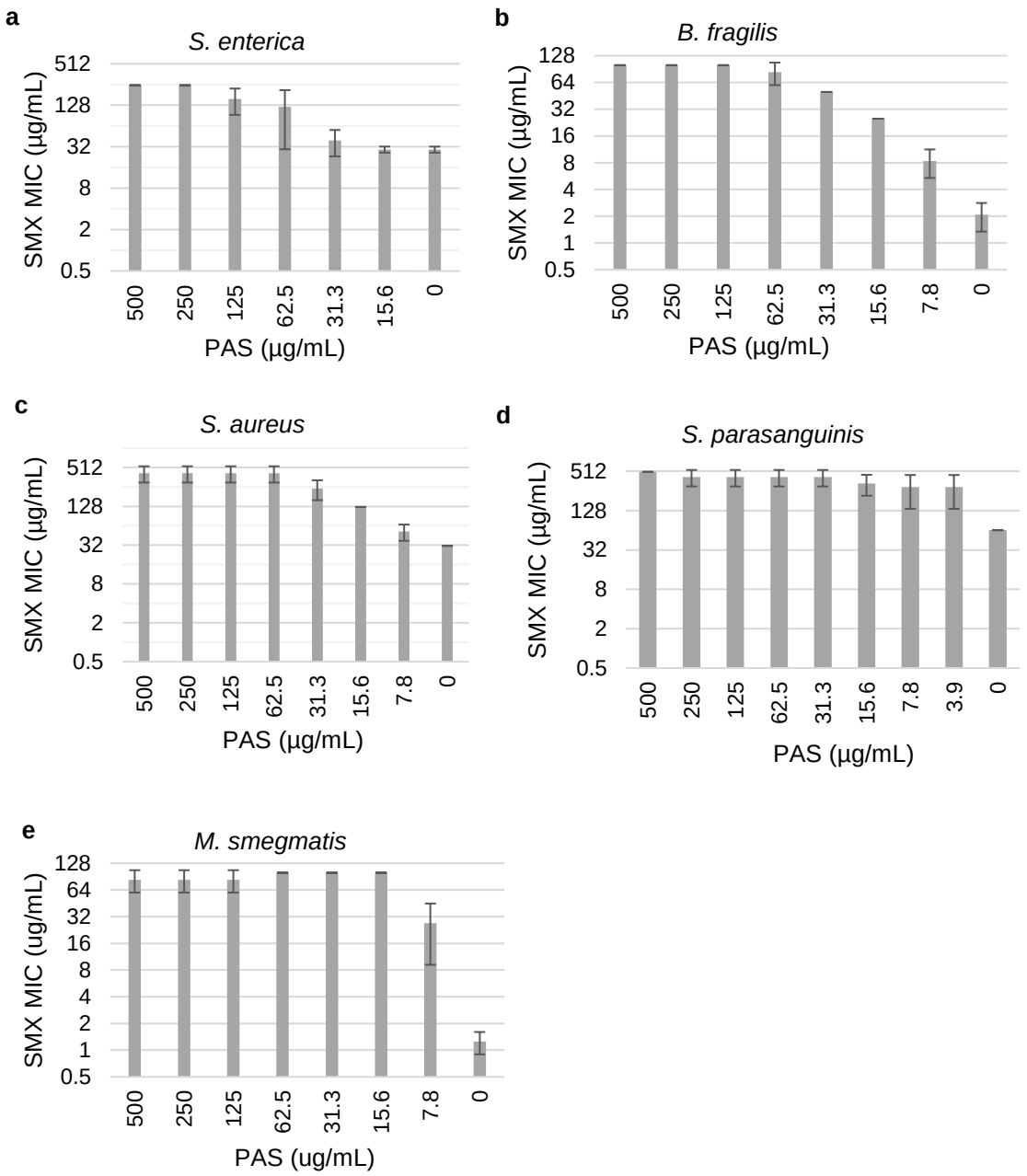

Figure 2.16. PAS, like PABA, can antagonize antifolates in various bacterial species. a) *S. enterica,* b) *B. fragilis,* c) *S. aureus*, d) *S. parasanguinis*, and e) *M. smegmatis* were grown in minimal media, or isosentist broth for *S. parasanguinis*, in the presence of varying concentrations of PAS and SMX at 37 ºC. The data represents the minimum concentration of drug required to inhibit growth in varying PAS concentrations. Each experiment represents an average of three biological replicates, error bar represents standard deviation.

Chapter 3:

The mechanistic basis for *para*-aminosalicylic acid toxicity and resulting antagonism by sulfa-drugs

Specific contributions

Kordus, SL concieved cytotoxicity assay study. Lamont, EA performed the cytotoxicity assays (TABLE 3.4 and 3.5) and wrote the methods for the cytotoxcity assays.

The rest of the chapter has not published when the thesis was submitted. All experiments, experimental design, intellectual contributations were performed by Shannon Lynn Kordus.

Synopsis

Many chemotherapeutic agents cause gastrointestinal distress. These side effects are a result of disturbances within the gut microbiota or off-target effects to the host. *para*-Aminosalicylic acid (PAS) was one of the first chemotherapeutic agents used to treat *Mycobacterium tuberculosis* infections, and its use was highly associated with severe gastrointestinal distress. Consequently, PAS use fell out of favor and it was replaced with better tolerated antitubercular agents. With the emergence of drug-resistant strains of *M. tuberculosis*, PAS has regained clinical use. Thus, there is a renewed interest in understanding the mechanisms that govern PAS toxicity. Human-associated microbiota produce many vitamins and co-factors that are accessible by human cells. Folate, for instance, is produced by bacteria in the small and large intestines and is absorbed by enterocytes, epithelial cells that line the intestines. Based on our observations in Chapter 2, we hypothesized that bacteria in the intestines can utilize PAS for hydroxy-folate synthesis which may be the basis for PAS-mediated gastrointestinal distress in humans. Indeed, we found that hydroxy-folates, but not PAS, are cytotoxic to human cells. Furthermore, we determined that hydroxy-dihydrofolate can be utilized as a substrate by human dihydrofolate reductase at a reduced catalytic rate. We hypothesized that by blocking PAS incorporation into folates in the gut microbiota we could prevent PAS toxicity *in vivo*. By using sulfamethoxazole (SMX), a FolP inhibitor, as a chemical tool we were able to alleviate PAS toxicity in mice. Previous work has demonstrated that

SMX can antagonize the antitubercular activity of PAS *in vitro*. When we examined the interaction between PAS and SMX in a *M. tuberculosis* murine infection model we found that SMX could potently antagonize PAS activity *in vivo*. This antagonism was found to be mediated by alterations in pterin biosynthesis. Taken together, our study is the first to characterize the basis for PAS-mediated toxicity and the mechanistic basis for SMX mediated antagonism of PAS.

Introduction

Folate (vitamin B_9), is required for the *de novo* biosynthesis of thymidylate, purines, coenzyme A and several amino acids. As such, this cofactor is essential for synthesis of new DNA, RNA and proteins in all actively growing cells. In humans, folate deficiency has pleotropic effects, particularly in rapidly dividing tissues including, bone marrow, gastrointestinal (GI), and central nervous system development. Therefore, folate metabolism is an attractive target for treating cancer.

Humans lack many of the enzymes required to synthesize folates and must acquire folates from their diet or other sources. Most, if not all, human cells possess folate receptors which transport the cofactor into the cytosol. The primary system to acquire folates from the diet is in the duodenum and jejunum in the small intestine (Visentin *et. al*., 2014). Most bacteria must produce their own folates, and many bacteria of the human GI tract secrete folates that are accessible by enterocytes, epithelial cells that line the intestines. Once absorbed, these folates can be transported to other areas of the body.

There are a number of solute carriers that possess the ability to transport folates. Two important solute carriers expressed by enterocytes include reduced folate carrier (RFC) and proton-coupled folate transporter (PCFT). Both RFC and PCFT

are specific for folates with distinct roles in transport. RFC is expressed in all tissues and cell lines on the both the apical and basolateral sides of the cell membrane (Wang *et. al*., 2001). RFC binds reduced folates at neutral pH with high affinity but has low affinity for folic acid (Visentin *et. al*., 2014). Furthermore, RFC binds most antifolic acid chemotherapeutic agents including methotrexate, pralatrexate, and premetrexed (Visentin *et. al*., 2014). RFC is the primary solute carrier used to absorb and export reduced folates from the intestines to other areas of the body (Wang *et. al*., 2001). In contrast to RFC, PCFT is expressed and localized only to the apical side of enterocytes in the small intestine and binds folic acid at acidic pH with high affinity (Qiu *et. al*., 2006). PCFT can bind folic acid at neutral pH with lower affinity, however, it cannot bind reduced folates (Qiu *et. al*., 2006). Although PCFT is able to bind some antifolates, it primarily binds premetrexed (Zhao *et. al*., 2008).

Once folate is absorbed into the enterocyte, it can be utilized for one carbon metabolism, or it can be secreted via the basolateral membrane into the portal vein (Visentin *et. al*., 2014). While in the portal vein, folates travel to the liver by merging with the hepatic artery into the hepatic sinusoid. Folates travel to the hepatic vein and are transported to other areas of the body. Folates can also be absorbed by hepatocytes via folate receptors (specifically RFC) on the basolateral membrane. If folates are not utilized by the liver, they can be

secreted via the apical membrane into the bile canaliculus which drains into the small intestine.

Chemotherapy often induces changes in the commensal bacteria of the GI tract as well as changes to the enterocytes (Keefe *et. al*., 1997). Side effects of many chemotherapeutic agents include severe enterocolitis, gastrointestinal ulcerations, diarrhea and anorexia from nutrient malabsorption (Pico and Avila-Garavito, A, Naccache, 1998). Specifically, methotrexate (MTX) and other dihydrofolate reductase (DHFR) inhibitors at high concentration are known to cause mucositis, inflammation and ulcerations along mucosal membranes. Furthermore, these inhibitors are associated with increased intestinal permeability through alteration of tight junction formation (Beutheu Youmba *et. al*., 2012). Tight junctions are transmembrane multi-protein complexes that anchor the peripheral cellular membranes and maintains the intestinal barrier. Recently, MTX was found to modulate tight junction formation by causing alterations in expression of proteins that make up tight junctions (Beutheu Youmba *et. al*., 2012).

para-Aminosalicylic acid (PAS) has been used clinically to treat tuberculosis (TB) for over 70 years. Unfortunately, treatment with PAS was often associated with severe GI distress. In the first clinical trial of PAS, 75% of patients reported

severe GI distress, and 20-25% reported nausea, vomiting and diarrhea (Erdei and Snell, 1948; Vallentin and Tronell, 1950). These side effects were often attributed to the presence of impurities introduced during synthesis or spontaneous deterioration of PAS (Mitchell *et. al*., 1954). In an effort to bypass the associated GI distress, PAS was given intravenously in Europe and was found to be more well-tolerated (Jones, 1954). With the advent of better tolerated and superior chemotherapeutics, PAS fell out of favor to treat TB in the late 1960s.

Use of PAS was revitalized with the emergence of multi-drug resistant strains of *M. tuberculosis* in the 1990s. To help prevent GI distress, PAS was reformulated into a delayed release gastro-resistance formulation. With this formulation, once the granules enter the small intestine, the coating is dissolved at neutral pH which allows for delayed release of PAS, so that the serum levels do not immediately peak. However, patients still must take 10-12 g of PAS per day to reach inhibitory levels in the lung. While this formulation represents an improvement, 20% of patients still discontinue PAS treatment due to GI distress. In response to the revitalization of PAS, there is a need for a better understanding of the molecular basis of PAS toxicity.

Previous work has shown that PAS is converted to hydroxy-dihydrofolate (hydroxy-DHF) via the folate biosynthesis pathway in *M. tuberculosis* (Chakraborty *et. al*., 2013; Zhao *et. al*., 2014; Zheng *et. al*., 2013). Results in chapter 2 indicate the same is true in several other bacterial species. Thus, we hypothesized that bacteria in the GI tract produce hydroxy-folates that might intoxicate gut enterocytes. Consistent with this model, cytotoxicity assays revealed that hydroxy-DHF and hydroxy-folate were toxic for HepG2 and Caco-2 cells while PAS was not toxic. Further, it was found that human DHFR could utilize hydroxy-DHF as a substrate at a compromised rate relative to DHF, suggesting that hydroxy-folates can impair one-carbon metabolism in human cells. Since the first step of hydroxy-DHF synthesis requires dihydropteroate synthase (FolP) (Chakraborty *et. al*., 2013; Zhao *et. al*., 2014; Zheng *et. al*., 2013), the FolP inhibitor sulfamethoxazole was found to be an antagonist of PAS toxicity in mice. These data indicate that PAS-mediated GI distress involves production of hydroxy-DHF by the gut microbiota.

Previous work has shown that PAS activity can be antagonized *in vitro* in *M. tuberculosis* by SMX (Zheng *et. al*., 2013). In the present study, we determined that this antagonism also occurs *in vivo* using a mouse model of *M. tuberculosis* infection. Further, other FolP inhibitors were found to potently antagonize PAS susceptibility in *M. tuberculosis*. The mechanistic basis of antagonism by SMX was probed using strains deficient for synthesis of folate precursors, and it was

found that SMX-mediated PAS antagonism required flux through the pterin biosynthesis pathways. The data from this study can be used to discover novel mechanisms to prevent PAS toxicity. Furthermore, these data can be used to uncover novel antagonism mechanisms that can be used to inform drug development and treatment regimens.

Materials and Methods:

Bacterial strains, media, and growth conditions

All information regarding primers, plasmids, and bacterial can be found in Table 3.1-3.3

M. tuberculosis strains and *Mycobacterium bovis* BCG were grown at 37 ºC in either 7H9 broth (Difco) supplemented with 0.2% (vol/vol) glycerol (Fisher Scientific), 10% (vol/vol) oleic acid-albumin-dextrose-catalase (OADC) (Difco), and 0.05% (vol/vol) tyloxapol (Sigma-Aldrich) or 7H10 agar (Difco) supplemented with 0.2% glycerol and OADC.

All antibiotics were added when appropriate to final concentrations of 50µg/mL for kanamycin, and 150 µg/mL for hygromycin. To eliminate PABA contamination, glassware was baked for a minimum of one hour at 180 ºC. PAS, PABA, trimethoprim (TMP), dapsone (DDS), and methotrexate (MTX) were purchased from Sigma and were dissolved in 100% DMSO (Sigma). 2'-Hydroxy-7,8-dihydrofolate was synthesized as described in Chapter 2. Pterin-PAS was a gift from Dr. Richard Lee and hydroxy-folate was a gift from Dr. Courtney Aldrich. Pterin-PAS and hydroxy-folate were dissolved in 100% DMSO (Sigma).

Cell Lines (Written by Dr. Elise Lamont)

Hep-G2 cell (ATCC HB-8065) and Caco-2 cell (ATCC HTB-37) lines were purchased from the American Type Culture Collection (ATCC; Manassas, VA). Hep-G2 and Caco-2 cell lines were maintained in Minimal Essential Medium (MEM; Gibco, Waltham, MA) and Dulbecco's Modified Eagle Medium (DMEM; Gibco), respectively. Media were supplemented with 10% (Hep-G2) or 20% (Caco-2) fetal bovine serum (FBS) and 1% penicillin/streptomycin (pen/strep) solution. Both cell lines were incubated at 37 ^{o}C in a humidified chamber containing 5% CO_2. Medium was refreshed every 2 days. Once 70% confluency was achieved, cell lines were washed thrice using Dulbecco's phosphate buffered saline (D-PBS) without calcium and magnesium (Gibco) and harvested with TrypLE™ express enzyme (1X; Gibco). Detached cells were subsequently used in cytotoxicity assays.

Cytotoxicity assays (Written by Dr. Elise Lamont)

Unless otherwise noted, cells were incubated at 37 ^{o}C in a humidified chamber containing 5% CO_2. Hep-G2 and Caco-2 cells were seeded separately in tissue culture treated, flat-bottom 96 well plates at a density of 5.0 x 10^4 cells per well in antibiotic free media. The final volume per well was 100 µL. After cells were adhered to the well substrate overnight, cells were washed thrice with D-PBS and incubated with individual drugs and metabolites, methotrexate (MTX; 0-4,000 µM), *para*-aminosalicylic acid (PAS; 0-4,000 µM), hydroxy-folate (0-500 µM), and

hydroxyl-dihydrofolate (0-500 μM) in a two-fold serial dilution using appropriate culture media. Cells were treated for up to 72 h and media containing appropriate drugs were replaced every 24 h. DMSO vehicle control was included for every time point. Cell survival after drug exposure was determined using previously established methods (Mosmann, 1983). Briefly, 200 μL of freshly made 3-(4,5-dimethylthiazol-2-yl)-2,5-diphenyltetrazolium bromide (MTT; 1 mg/mL; Sigma-Aldrich, St. Louis, MO) in serum-free, phenol red-free MEM or DMEM was added to each well and incubated for 3 h. MTT solution was removed and formazan crystals were dissolved in 200 μL of isopropanol. Formazan dye was quantified at 570 nm using the Synergy H1 microtiter plate reader (BioTek; Winooski, VT). Absorbance was normalized for background at OD_{650}. Cell survival was calculated as the percentage absorbance of sample relative to no vehicle control. IC_{50} (half maximal inhibitory concentrations) values for each drug at all time points tested were calculated using GraphPad Prism (San Diego, CA) statistical software. All treatments were conducted in technical triplicate for each time point. All experiments were repeated thrice.

Assessing PAS toxicity in mice

Seven week old C57BL/6 mice were obtained from Jackson Laboratory (Bar Harbor, ME). Female mice (5 per treatment) were orally gavaged every day for two weeks with a vehicle control of phosphate buffered saline (PBS) (pH 7.2) or 750 mg/kg *para*-aminosalicylic acid. Before the mice were gavaged, the cannula

was submerged in a 10% (weight/volume) sucrose (Fisher) solution. Fecal pellets (3-6) were collected from individual mice prior to initiation of treatment, after two weeks of treatment, and after a two week recovery following treatment. Mice were sacrificed and the small and large intestines were harvested and washed in PBS.

Construction and purification of $DHFR_{Human}$

Human DHFR isoform 1 cDNA was codon optimized and purchased as a gene block (Invitrogen) containing 5' *Nde*I and 3' *Bam*HI cut sites. The gene block was digested with *Nde*I and *Bam*HI and ligated into an already digested pET28b(+) (Novagen) using the same restriction enzymes. Expression and purification of $DHFR_{Human}$ was performed as previously described (Tai *et. al*., 2002). Briefly, sequence-verified pET28b(+):*$DHFR_{Human}$* was used to transform competent *E. coli* BL21 (DE3) cells. *E. coli* BL21 pET28b(+):*$DHFR_{Human}$* was inoculated into Lysogeny Broth (LB) and grown overnight at 37 ºC. The cells were diluted 1:1000 into fresh LB (4 L) and were grown until mid-exponential phase (optical density at 600 nm (OD_{600}) 0.4–0.6) at 37 ºC. Next, 1 mM isopropyl β-D-1-thiogalactopyranoside (IPTG) (GoldBio) was added to induce protein expression at 37 ºC for 4 h. The cells were collected by centrifugation at 5,000 rpm (Beckman Coulter, Avanti JXN-30) at 4 ºC. The pellet was resuspended in 10 mL of lysis buffer (100 mM K_2PO_4 (pH 8.0) and 5 mM imidazole) and disrupted by

ultrasonication (Branson Sonifier 450) three times using 20 sec burst and 20 sec cooling (4 ºC). 10 mg chicken egg white lysozyme (MP Biomedicals, LLC) was added and incubated on ice for 30 min. The insoluble fraction was removed by centrifugation (Beckman Coulter, Avanti JXN-30) at 11,000 rpm at 4 ºC for 45 min. The supernatant was applied to 1 ml Ni-NTA Agarose (Qiagen) equilibrated with lysis buffer. $DHFR_{Human}$ was eluted using a step-wise gradient of 10 mL wash buffer containing increasing concentrations of imidazole (10 mM, 15 mM and 20 mM). $DHFR_{Human}$ was eluted with 5 mL of elution buffer (100 mM K_2PO_4 (pH 7.5) and 50 mM imidazole). Fractions containing pure $DHFR_{Human}$ (>90% as judged by running samples on an SDS-PAGE gel) were pooled and using an ultra-centrifugal filter concentrated (Millipore) in storage buffer (50 mM KPO_4, 5 mM β-mercaptoethanol, pH 7.3) to 2.5 mg/ml. The protein was stored at 4 ºC.

Biochemical utilization of DHF and hydroxy-DHF

All enzymatic assays were performed in flat bottom 96 well plates (Corning), with 200 µl reaction volume, and measured in a BioTek Synergy H1 spectrophotometer at 25 ºC. The enzymatic reactions were performed as previously described (White *et. al*., 2004). Enzyme assays were performed using 5 nM enzyme in 50 mM KPO_4, pH 7.3, 5 mM β-mercaptoethanol and 0.01% (vol/vol) Triton-X 100. The enzyme was preincubated with 67 µM of NADPH at room temperature for 5 min. The reaction was initiated with varying

concentrations of DHF or hydroxy-DHF. The decrease in absorbance corresponding to NADPH oxidation was monitored at 340 nm every 10 sec for 10 min. The K_m was determined from 4 independent experiments performed in biological triplicate and analyzed using GraphPad Prism software.

Bacterial enumeration of M. tuberculosis *infected mice during antitubercular oral gavage treatment*

Seven week old C57BL/6 mice were obtained from Jackson Laboratory (Bar Harbor, ME). Mice were infected with ~100 CFU of *M. tuberculosis* H37Rv using an inhalation exposure system (GlasCol) as previously described (Ramakrishnan *et. al*., 2016). The infection was established for 1 week. Following the 1 weeks incubation period, mice were gavaged daily for 13 days with vehicle (PBS), SMX (150 mg/kg), PAS (500 mg/kg or 750 mg/kg), and a combination of SMX (150 mg/kg) and PAS (750 mg/mg). Before gavage, the cannula was submerged in 10% (wt/vol) sucrose (Fisher) solution. Following each daily treatment mice were fed peanut butter. The peanut butter (PB2 powdered peanut butter) (Amazon) was suspended in 50:50 (weight/volume) of sterile water. Infected mice were euthanized by CO_2 overdose. Bacterial CFU were enumerated by plating serially diluted lung, spleen, and liver homogenates on complete Middlebrook 7H10 agar containing 100 µg/ml cycloheximide. The CFU's were enumerated after 3 to 4 weeks of incubation at 37 °C. All animal protocols were reviewed and approved

by the University of Minnesota Institutional Animal Care and Use Committee and were conducted in accordance with recommendations in the National Institutes of Health Guide for the Care and Use of Laboratory Animals. The protocols, personnel and animals used were approved and monitored by the Institutional Animal Care and Use Committee.

M. tuberculosis *antagonism assays*

All assays were performed in round bottom 96-well plates (Corning) except where noted. Minimum inhibitory concentration (MIC_{90}) is defined as the concentration to inhibit 90% of growth compared to a no drug control. Growth was assessed spectrophotometrically (OD_{600}) (BioTek Synergy H1) or visually, when noted. All assays were performed in biological triplicate.

M. *tuberculosis* H37Rv was grown to mid-exponential phase and subcultured to OD_{600} 0.001 in 96 round bottom plates (Corning). The interactions between PABA and PAS, PAS and SMX, PAS and DDS, and pterin-PAS and SMX were evaluated using log_2 serial dilutions. The MIC was determined visually after 14 days of static incubation at 37 ºC. The interactions between TMP and PAS, using log_2 serial dilutions, was performed in *M. tuberculosis* H37Rv grown to mid-exponential phase and subcultured to OD_{600} 0.01 in inkwell bottles at 37 ºC, with

shaking. The MIC_{90} of TMP and PAS was measured spectrophotometrically (GENESYS 20, Thermo Fisher) after 14 days.

M. tuberculosis H37Rv Δ*pabB* was constructed as described in Chapter 2. *M. tuberculosis* H37Rv Δ*pabB* was grown in 7H9 medium containing 1µg/mL of PABA to mid-exponential phase and subcultured to OD_{600} 0.001 in 7H9 media containing 100ng/mL of PABA in round bottom 96-well plates (Corning). The interactions between PAS and SMX was performed using log_2 serial dilutions. The MIC was determined visually after 14 days of static incubation at 37 ºC.

M. bovis BCG and *M. bovis* BCG *ftsH::himar1* was grown in 7H9 medium to mid-exponential phase and subcultured to OD_{600} 0.001 in 7H9 media in round bottom 96-well plates (Corning). The interactions between PAS and SMX was performed using log_2 serial dilutions. The MIC_{90} was determined in a BioTek Synergy H1 spectrophotometer after 14 days of static incubation at 37 ºC.

Statistical analysis

Number of mice required to produce results with statistical significance were determined by a power calculation. A sample size of n≥4 was used detect a 10-fold (1-log_{10}) difference in CFU between groups, assuming standard deviations of

35-40% of sample mean, with a type 1 error rate (α) of 0.05% to achieve a 90% power (Chow *et. al*., 2008). A student's unpaired *t* test (two tailed) was used for comparison between vehicle and treatment groups. *p*-values were calculated using GraphPad Prism 5.0 software (GraphPad Software, Inc.). $p \leq 0.05$ was considered significant.

Results:

Exploring PAS toxicity in humans and in a murine model

Many patients discontinue PAS chemotherapy because of severe GI distress. We have replicated the PAS associated GI toxicity in a mouse model. Mice were treated daily for 14 days, via oral gavage with PAS (750mg/kg). Mice treated with PAS had a 60% mortality rate (Figure 3.1). The fecal pellets in the PAS treatment group were loose, moist, and smaller than the vehicle control fecal pellets (Figure 3.2). After a two week recovery, the size of the fecal pellets from the PAS treatment group returned to the same size as from the vehicle group, however, the pellets were still loose and moist (Figure 3.2). Upon examining the small and large intestines from mice of the PAS treatment group, both the small and large intestine exhibited inflammation and hemorrhaging that was absent in the vehicle treatment group (Figure 3.3).

Based on the observation that bacteria can utilize PAS as a source of folates, we hypothesized that bacteria in the human GI tract were producing a hydroxy-folate species that was causing PAS toxicity. To test this hypothesis, we performed cytotoxicity assays using HepG2 cells (hepatocytes) that are the canonical cell line to test cytotoxicity. We also used Caco-2 cells that are intestinal epithelial cells. Cytotoxicity assays were performed using PAS, hydroxy-DHF and hydroxy-folate. PAS exhibited no cytotoxicity at physiologically relevant concentrations in

HepG2 and Caco-2 cells (IC_{50} 1270 ± 9 µM and 1230 ± 6 µM, respectively) (Table 3.4 and 3.5). Hydroxy-DHF did show some cytotoxicity in HepG2 and Caco-2 cells (IC_{50} 343 ± 4 µM and 370 ± 5 µM, respectively) (Table 3.4 and 3.5). Interestingly, we found that hydroxy-folate is cytotoxic in both HepG2 and Caco-2 cells (IC_{50} 35 ± 5 µM and 44 ± 5 µM, respectively) at similar to concentrations to MTX (IC_{50} 7.2 ± 4.7 µM and 12 ± 6 µM, respectively), a known human-DHFR inhibitor (Table 3.4 and 3.5). We found that purified human-DHFR could use hydroxy-DHF as a suboptimal substrate (K_m 0.16 µM) compared to the native substrate, DHF (K_m 1.26 µM) (Figure 3.4, Table 3.6).

FolP inhibitors antagonize the antitubercular activity of PAS

Since PAS toxicity was mediated by bioactivation of PAS into hydroxy-DHF or hydroxy-folate, we hypothesized toxicity could be prevented by blocking PAS bioactivation. To test this hypothesis we co-treated PAS with SMX because SMX blocks FolP, the first enzyme required to convert PAS into hydroxy-dihydropteroate. TB infected mice were given vehicle control, SMX (150 mg/kg), PAS (500 mg/kg or 750 mg/kg), and SMX and PAS (150 mg/kg and 750mg/kg, respectively) for 13 days. The mice in the vehicle control and SMX treatment group showed a 100% survival rate (Figure 3.5). Mice in the PAS 500 mg/kg group showed an 80% survival rate and mice in the PAS 750 mg/kg group showed a 38% survival rate (Figure 3.5).The mice in the PAS-SMX (PAS 750

mg/kg and SMX 150 mg/kg) treatment groups showed an 87% survival rate (Figure 3.5). These observations demonstrate that SMX can antagonize PAS-mediated toxicity.

Following treatment of the TB infected mice, lung, spleen, and liver were harvested to determine bacterial burden. The vehicle control and SMX treatment groups showed similar bacterial burden in lung liver and spleen (Figure 3.5). PAS treatment was able to reduce the burden of *M. tuberculosis* in the lung of mice and virtually eliminated appearance of bacilli (below limit of detection) in spleen and liver (Figure 3.5). Interestingly, non-mycobacterial growth was observed on liver homogenate plates from the PAS and PAS-SMX treatment groups (Figure 3.6), consistent with the hypothesis that PAS treatment disrupts barrier function of the intestines. Co-treatment with SMX antagonized PAS antitubercular activity and resulted in an increased in bacterial burden in lung, liver and spleen that was statistically indistinguishable from the vehicle control and SMX treatment groups (Figure 3.5).

These observations are consistent with previous work that has shown PAS can be antagonized by SMX *in vitro* (Figure 3.7 and 8) (Zheng *et. al*., 2013). We extended this study to the diaminophenylsulfone, dapsone, (DDS) and found that DDS can antagonize the antitubercular activity of PAS (Figure 3.7 and 3.8).

Trimethoprim (TMP) had no interaction when with PAS *in vitro* (Figure 3.7 and 3.8).

The mechanistic basis for SMX antagonism of PAS

To explore the mechanism of SMX-mediated antagonism of PAS, we tested the hypothesis that SMX might prevent PAS bioactivation to hydroxy-DHF. We used pterin-PAS (PtePAS) an oxidized form of hydroxy-dihydropteroate to bypass the need for FolP (Howe *et. al*., 2018). Thus, co-treatment with PtePAS and SMX should yield either no interaction or a synergistic interaction similar to co-treatment with SMX and TMP. Counter to our expectation, PtePAS activity was antagonized by SMX (Figure 3.7 and 3.8). Since SMX treatment has previously been shown to increase PABA production in bacteria, we reasoned that SMX is causing an increase in PABA biosynthesis and, thereby, driving antagonism of PAS (Minato *et. al*., 2018). We created a deletion in the gene *pabB*, encoding amino-deoxychrosimate synthase. Previous work has shown that strains lacking *pabB* in *M. tuberculosis* are PABA auxotrophs and can only grow with supplemental PABA (Thiede *et. al*., 2016). We found that SMX could still antagonize PAS in the *M. tuberculosis* Δ*pabB* strain (Figure 3.7 and 3.8). This data suggests that SMX antagonism of PAS is not mediated by PAS bioactivation to hydroxy-DHF or through an increase in PABA biosynthesis

Previous studies have shown that FolA inhibitors can also modulate pterin biosynthesis (Minato *et. al*., 2018). We next tested the hypothesis that PAS is causing an increase in pterin production, using a strain containing a transposon disruption in 3' end of *ftsH*, a gene encoding a transmembrane protease. *ftsH::himar1* is directly upstream (150 bp) of the start codon for *folE*, encoding FolE. FolE is required for the first committed step of pterin biosynthesis (Fischer *et. al*., 2003). The insertion is predicted to be in the ribosome binding site for the pterin biosynthesis operon. When we examined if SMX could antagonize PAS in the *ftsH*::*himar*1 mutant we found that antagonism was greatly diminished, relative to that for the wild type strain (Figure 3.9). Taken together, this data suggests the mechanistic basis for SMX antagonism of PAS is mediated through an increase in pterin biosynthesis.

Discussion:

Hydroxy-folates, not PAS, are highly cytotoxic

PAS causes GI distress in humans which can result in patient non-compliance. During PAS treatment in mice, the GI tract showed inflammation and even some bleeding in the small and large intestine compared to the vehicle control (Figure 3.3). Previous work in mice, showed MTX treatment also led to an increase in inflammatory cytokines and the loss of tight junction formation in intestinal epithelial cells (Beutheu Youmba *et. al*., 2012). Therefore, it is possible that PAS is acting by a similar mechanism and is causing inflammation and ultimately reducing tight junction integrity. Furthermore, it was noted that PAS treatment led to a more wet stool compared to controls. Changes in stool integrity could also be indictive of GI disturbances either to the microbiota or to epithelial cells. Currently, a microbiome study is underway to determine bacterial changes (diversity and abundance) in mice treated with vehicle control, PAS, TMP/SMX co-treatment, and PAS/SMX co-treatment.

Based on the observation that bacteria can utilize PAS in the synthesis of folates, we hypothesized that bacteria in the human gut were producing a hydroxy-folate species resulting in PAS associated toxicity. Although it was previously thought that PAS is responsible for the cytotoxicity, we have demonstrated that PAS is not cytotoxic (Table 3.4 and 3.5). Interestingly, hydroxy-folate is cytotoxic at similar concentrations to a known cytotoxic chemotherapeutic agent, MTX (Table

3.4 and 3.5). Hydroxy-DHF was found to be slightly cytotoxic (Table 3.4 and 3.5). It is difficult to assess hydroxy-DHF toxicity because the half-life under an ambient atmosphere is about 6 hours (Dawadi *et. al*., 2017). Since the GI tract is anaerobic, it is possible that hydroxy-DHF is more stable and could exert more cytotoxic effects under physiological conditions.

To determine if hydroxy-DHF showed any inhibitory activity against DHFR in humans, we purified $DHFR_{Human}$ and measured its ability to catalyze reduction of DHF or hydroxy-DHF. We found that $DHFR_{Human}$ could utilize both DHF and hydroxy-DHF as a substrate. Taken together, these data suggest that bacteria in the GI tract could be incorporating PAS in folate synthesis and secreting hydroxy-folate species. Based on the cytotoxicity assays, a hydroxy-folate species could be absorbed into enterocytes. Although hydroxy-DHF does not inhibit $DHFR_{Human}$, it could be inhibitory somewhere downstream in one-carbon metabolism. Furthermore, enterocytes require a large amount of folate for rapid cellular growth and maintenance. Since $DHFR_{Human}$ could not utilize hydroxy-dihydrofolate as efficiently as dihydrofolate, impaired folate reduction could impede cellular processes requiring folates.

There are many experiments that could solidify the hypothesis that the microbiota of mice is producing a toxic byproduct during PAS treatment. One future

experiment would be to treat gnotobiotic mice with a vehicle control, PAS, and MTX. Gnotobiotic mice are born germ-free; therefore, these mice should not succumb to PAS toxicity. Another experiment would be to treat mice with PAS and perform liquid chromatography mass spectrometry/mass spectrometry. This would allow us to determine the hydroxylated folate specie(s) secreted during PAS treatment.

Furthermore, since treatment with MTX depolarizes tight junctions, other follow up experiments would be to determine if tight junction integrity is affected during PAS treatment. Two experiments to test this hypothesis would be to perform transepithelial/transendothelial electrical resistance assay to indirectly measure tight junction integrity during treatment with vehicle control, MTX, PAS, and hydroxy-folate (Srinivasan *et. al*., 2015). Another experiment would be to treat mice with vehicle, MTX, PAS, and hydroxy-folate harvest the small and large intestines and perform immunostaining against tight junction associated proteins zonula occludens-1, occludin, and claudin-1 (Beutheu Youmba *et. al*., 2012). If the GI microbiota are indeed traversing from the lumen into the lamina propria, blood from PAS treated mice could be tested for lipopolysaccharides, a component of bacterial cell wall.

SMX antagonizes the toxicity and activity of PAS.

Many patients discontinue treatment with PAS because of the severe side effects namely GI distress. We treated TB infected mice with a vehicle control, SMX (150 mg/kg), PAS (750 mg/kg), PAS (500 mg/kg), and SMX and PAS (150 mg/kg and 750 mg/kg). A low dose-PAS treatment (500mg/kg) had a higher percent survival (Figure 1b) suggesting that PAS toxicity is dose dependent. PAS and SMX (high dose-750 mg/kg and 150 mg/kg, respectively) co-treatment resulted in increased (87%) survival. Since SMX prevents PAS incorporation into the folate biosynthesis pathway it is likely that PAS mediated toxicity is due to a hydroxylated folate species produced. Taken together, these data suggests that PAS toxicity is dose dependent and toxic metabolite is a product of PAS incorporation in the folate biosynthesis pathway.

Following treatment of the *M. tuberculosis* infected mice, we harvested the lung, spleen, and liver and measured colony forming units. Although we had some bacterial growth in the spleen of PAS treated mice. We tested the colonies for resistance to PAS by plating them on high concentrations of PAS. We found these colonies were resistant to PAS, compared to colonies on plates from the vehicle control (data not shown). Strikingly, SMX (150 mg/kg)/PAS (500 mg/kg) co-treatment allowed for the unrestricted growth of *M. tuberculosis* in the lungs of mice and allowed for the dissemination of *M. tuberculosis* from the lung into the

spleen and liver (Figure 3.5). Taken together, this data suggests that addition of SMX antagonizes the anti-mycobacterial activity of PAS.

Furthermore, we noticed evidence of non-mycobacterial growth in the liver and in some of the spleens in the mice treated with PAS, and some with PAS and SMX co-treatment (Figure 3.6). This growth was absent in the vehicle and SMX treatment groups. As described previously some DHFR inhibitors can impair tight junction formation, we speculate that perhaps hydroxy-DHF/folate produced during PAS treatment can also cause impaired tight junction formation. Depolarization of tight junctions can lead to enterocyte cell death, impaired barrier function and sepsis. The tissue homogenates from the *in vivo* study could also be used and 16S rRNA sequenced to determine if any GI bacteria are represented.

Although we were able to antagonize PAS GI toxicity by co-treatment with SMX, we found that SMX also antagonized the antitubercular activity of PAS *in vivo*. This observation supports previous work that has suggested PAS can be antagonized by SMX (Zheng *et. al*., 2013). We extended this study to DDS and found that DDS can antagonize the antitubercular activity of PAS. TMP did not alter the PAS MIC. As described in Chapter 2, HIV/AIDS infected individuals are prescribed SMX and TMP for lifetime prophylactic therapy. When SMX is not well

tolerated DDS is prescribed. SMX and DDS were found to antagonize the antitubercular activity of PAS. Therefore, HIV/TB co-infected individuals who are prescribed SMX or DDS to protect against opportunistic infections are at risk for treatment failure if using PAS to treat for TB infection. Furthermore, the observations in Chapter 2 suggest that PAS can antagonize the activity of SMX and DDS in treating numerous bacterial infections. Taken together, the combination of SMX/DDS and PAS to treat both TB and opportunistic infections needs to be reevaluated.

The mechanistic basis for SMX antagonism of PAS

To understand the mechanism of SMX mediated antagonism we hypothesized that SMX is preventing PAS bioactivation to hydroxy-DHF. To test this hypothesis we used pterin-PAS (PtePAS) an oxidized form of hydroxy-dihydropteroate, to bypass the need for PAS conversion to hydroxy-dihydropteroate (Howe *et. al*., 2018). Interestingly, PtePAS activity was antagonized by SMX (Figure 3.7 and 3.8). This suggests that SMX mediated antagonism of PAS does not occur by preventing PAS bioactivation.

Since SMX treatment has previously been shown to increase PABA production in bacteria, we reasoned that SMX is causing an increase in PABA biosynthesis and, thereby, antagonism of PAS (Minato *et. al*., 2018). We tested if SMX could

antagonize PAS in *M. tuberculosis* H37Rv Δ*pabB* and found it could still antagonize (Figure 3.7 and 3.8). This data suggests that while SMX could be causing an increase in PABA, the amount of PABA produced is not enough to antagonize the activity of PAS. Therefore, the mechanistic basis of SMX mediated antagonism of PAS is not through an increase in PABA biosynthesis.

When used in combination, TMP and SMX (co-trimoxazole) exhibit highly synergistic antimicrobial activity. For several decades it was presumed that the basis for synergy between SMX and TMP was exclusively due to the ability of SMX to prevent DHF synthesis and enhance the ability of TMP to inhibit FolA (Bushby and Hitchings, 1968; Minato *et. al*., 2018; Wormser *et. al*., 1982). While this model explains how SMX is able to enhance microbial susceptibility to TMP, it is not sufficient to explain the ability of TMP to enhance susceptibility of microbes to SMX (Harvey, 1978). It was recently demonstrated that TMP treatment results in depletion of DHPPP through impairment of GTP synthesis and is the basis for potentiation of SMX susceptibility (Minato *et. al*., 2018). The folate biosynthesis pathway exhibits a cyclic nature that enables the potent synergy between SMX and TMP (Minato *et. al*., 2018). Therefore, we hypothesized that SMX was modulating pterin biosynthesis. We had previously isolated strain with a transposon disruption in 3' end of *ftsH*, a gene encoding a transmembrane protease(Howe *et. al*., 2018). Directly downstream of *ftsH* is *folE*,

a gene encoding FolE required for the first committed step of pterin biosynthesis. We found that SMX could no longer antagonize PAS compared to the parent strain in the *ftsH* mutant. Multiple attempts have been made to create deletions in either *folE* or *folBK*; however, these have not been successful. Currently, more work is underway to determine if SMX increases pterin biosynthesis in the parent strain compared to the *ftsH*::*himar*1 strain using both qPCR and metabolomics. Taken together these data suggest that SMX mediated antagonism of PAS occurs through increasing flux to pterin.

Tables:

Table 3.1. Oligonucleotides used in this study

Primer name	Primer sequence[1]	Source	Restriction enzyme
pabB_Mtb LL	TTTTTTTTCCATAAATTGGCTCGCAAACTCGCGTCGTAGG	This work	*Van91I*
pabB_Mtb LR	TTTTTTTTCCATTTCTTGGGCACCGGACAGGCTCTCATAC	This work	*Van91I*
pabB-Mtb RL	TTTTTTTTCCATAGATTGGAGTGTGGCACCTGGTGTCCAC	This work	*Van91I*
pabB-Mtb RR	TTTTTTTTCCATCTTTTGGACTCCAGCGCGTTAACCGCAA	This work	*Van91I*

[1]Underline corresponds to the restriction enzyme cut site. All primers are written in 5' to 3' orientation

Table 3.2. Plasmids used in this study.

Plasmid	Relevant characteristics	Source
pET28b+	Bacterial high copy plasmid for protein overexpression containing C- and N-terminal 6X histidine tags inducible with *lacI*, Kan^r	Novagen
pET28b-*DHFR*-human	pET28b+ containing $DHFR_{Human}$ with an N-terminal 6x-histidine tag, Kan^r	This work
phAE159	Phasmid used for specialized transduction, Pen^r	(Bardarov *et. al*., 2002)

Table 3.3. Strains used in this study

Strain Name	Relevant characteristics	Source
E. coli		
DH5α	Cloning strain	Lab stock
BL21 (DE3)	Protein purification strain	Lab stock
pET28b-*DHFR*-human	BL21 containing pET28b-*DHFR*-human for overexpression of $FolA_{Mtb}$, Kan^r	This work
M. tuberculosis		
H37Rv	Wild-type strain	Lab stock
Δ*pabB*	H37Rv *pabB*::hygro-*sacB* cassette, $Hygro^r$	This work
M. bovis		
BCG	Wild-type strain	Lab stock
BCG *ftsH*::*himar*1	BCG with a *himar*1 transposon insertion at position 2155 at the 3' end of *ftsH* gene, Kan^r	(Howe *et. al*., 2018)

Table 3.4. Cytotoxicity assays, in HepG2 cells, of MTX, PAS, hydroxy-dihydrofolate, and hydroxy-folate.

	IC_{50} (μM)		
Drug	24 h	48 h	72 h
MTX	823±3	58.2±0.4	7.2±4.7
PAS	1850±10	1480±14	1270±9
Hydroxy-DHF	NA	426±4	343±4
Hydroxy-folate	838±12	166±4	35±5

Table 3.5. Cytotoxicity assays, in Caco-2 cells, of MTX, PAS, hydroxy-dihydrofolate, and hydroxy-folate.

	IC_{50} (μM)		
Drug	24hr	48hr	72hr
MTX	813±12	62±5	12±6
PAS	1850±16	1410±12	1230±6
Hydroxy-DHF	NA	497±4	370±5
Hydroxy-folate	826±7	163±13	44±5

Table 3.6. Mechaelis-Menten kinetics of dihydrofolate and hydroxy-DHF

Organism	DHF (K_m)	Hydroxy-DHF (K_m)
Human	1.26μM	0.16μM

Figures

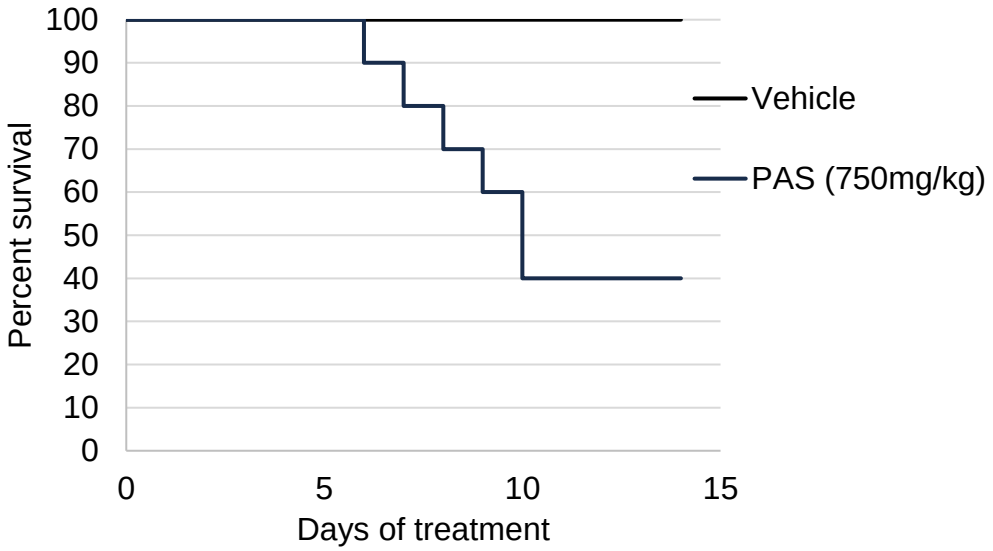

Figure 3.1. Kaplan-Meier kill curve from treatment with PAS. Specific pathogen free C57Bl/6 mice were treated via oral gavage with either a vehicle control (PBS) or 750 mg/kg PAS. The mice were treated every day for 14 days. Mice were assessed daily and examined for signs of distress including shortness of breath, withdrawal from littermates, and lethargy. Any mouse that exhibited these signs was euthanized.

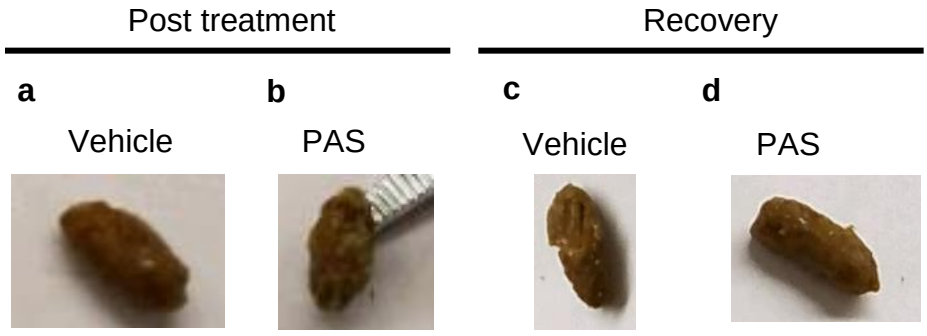

Figure 3.2. Fecal pellets from vehicle and PAS treated mice. Specific pathogen free C57Bl/6 mice were treated via oral gavage with either a vehicle control (PBS) or 750 mg/kg PAS. The mice were treated every day for 14 days. After the treatment the mice were left undisturbed to allow for any recovery in the microbiome to occur. a) and b) fecal pellets post treatment of vehicle and PAS, respectively c) and d) fecal pellets after a 2 week recovery of vehicle and PAS, respectively.

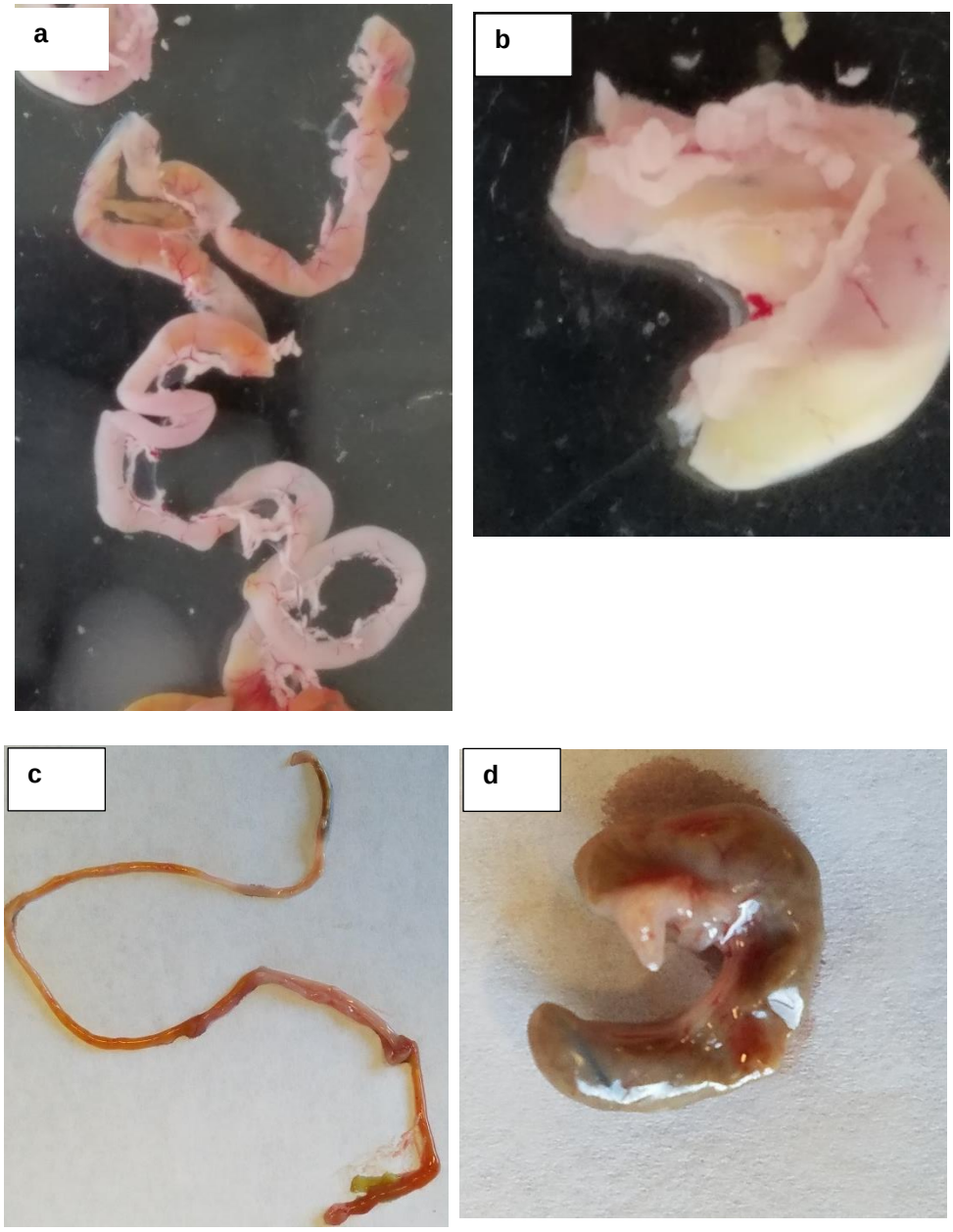

Figure 3.3. Small intestine and cecum from vehicle and PAS treated mice. Specific pathogen free C57Bl/6 mice were treated via oral gavage with either a vehicle control (PBS) or 750 mg/kg PAS. The mice were treated every day for 14 days. After the treatment the mice were euthanized by CO_2 overdose. Vehicle control a) small and b) cecum b). PAS treatment c) small intestine and d) cecum.

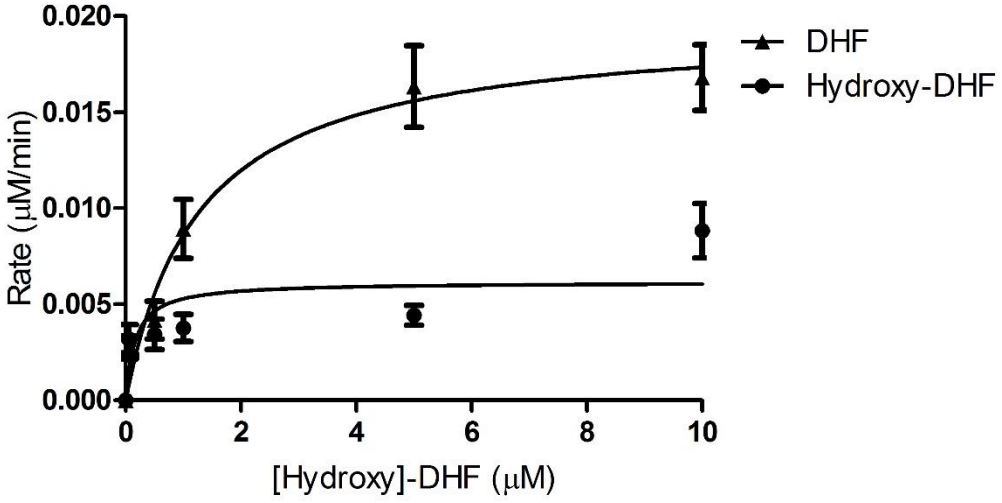

Figure 3.4. DHF and hydroxy-DHF can be utilized as substrates for $DHFR_{Human}$. DHF or hydroxy-DHF utilization was measured in the presence of DHF or hydroxy-DHF using purified recombinant DHFR. The experiment was performed in technical triplicate four times. The error bars represent standard error of the mean.

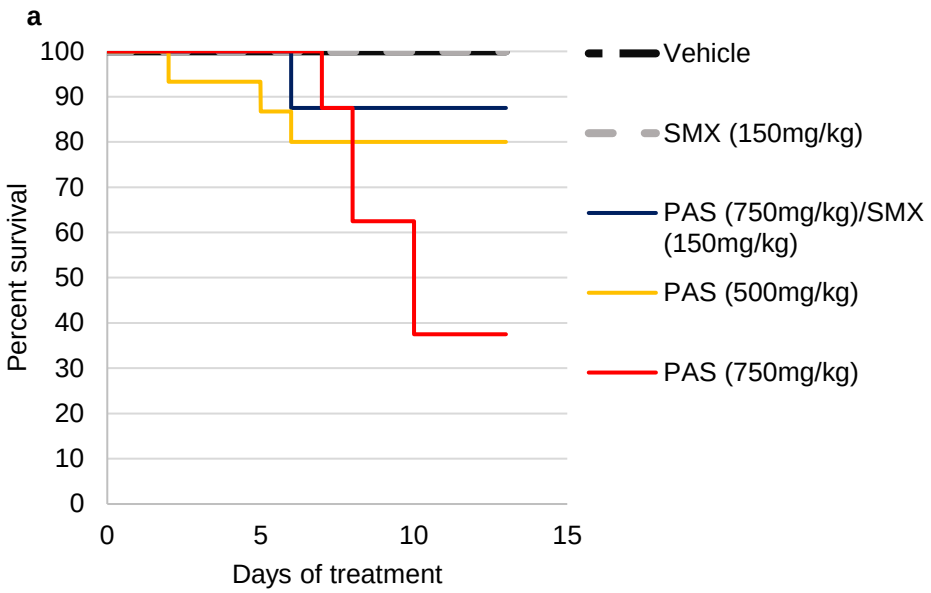
a
100
90
80
70
60
50
40
30
20
10
0
Percent survival
0
5
10
15
Days of treatment
Vehicle
SMX (150mg/kg)
PAS (750mg/kg)/SMX (150mg/kg)
PAS (500mg/kg)
PAS (750mg/kg)

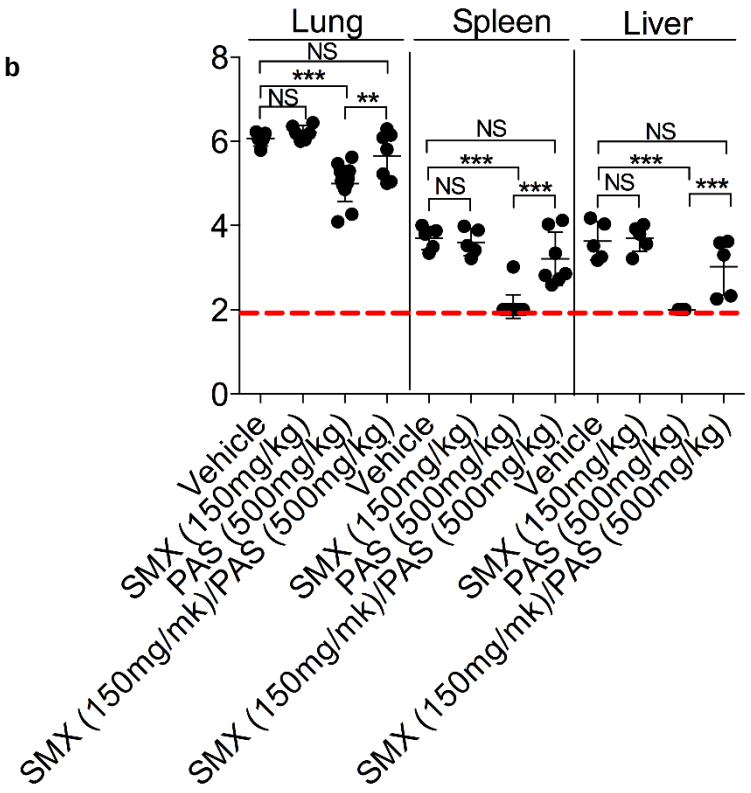
b
Lung
Spleen
Liver
8
6
4
2
0
NS
***
NS
**
NS
***
NS
NS
***
NS
Vehicle
SMX (150mg/kg)
PAS (500mg/kg)
SMX (150mg/mk)/PAS (500mg/kg)

Figure 3.5. SMX antagonizes the anti-tubercular activity of PAS. Analysis of C57Bl/6 mice infected with 100 CFU of *M. tuberculosis* H37Rv. The infection was established for 1 week and the mice were treated for 13 days via oral gavage with vehicle control, SMX, PAS, and SMX/PAS using an acute infection model. a) Kaplan-Meier survival analysis. b) Bacterial burden was enumerated in the lung, spleen, and liver, in mice following treatment. The limit of detection (100 CFU) is marked by dotted red line. ** $p<0.05$, *** $p<0.0001$, NS (not significant).

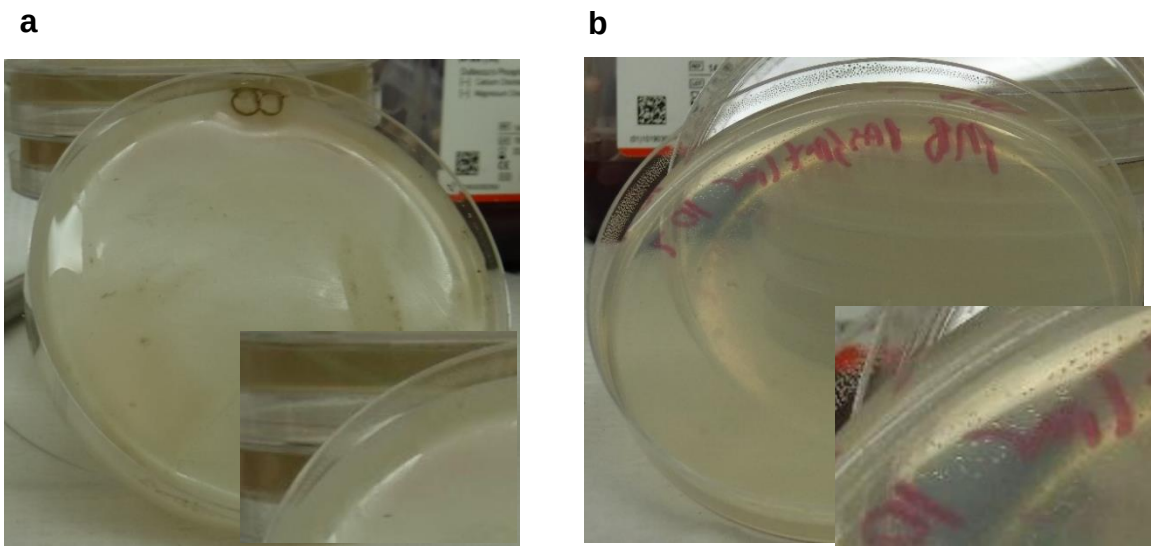

Figure 3.6. Bacterial growth on liver homogenates. These plates are a representative of growth found on plates containing liver homogenates from pictures taken. The plates represent SMX/PAS co-treatment at varying dilutions a) 10^{0} and b) 10^{-1}. Inset shows 800x maginification.

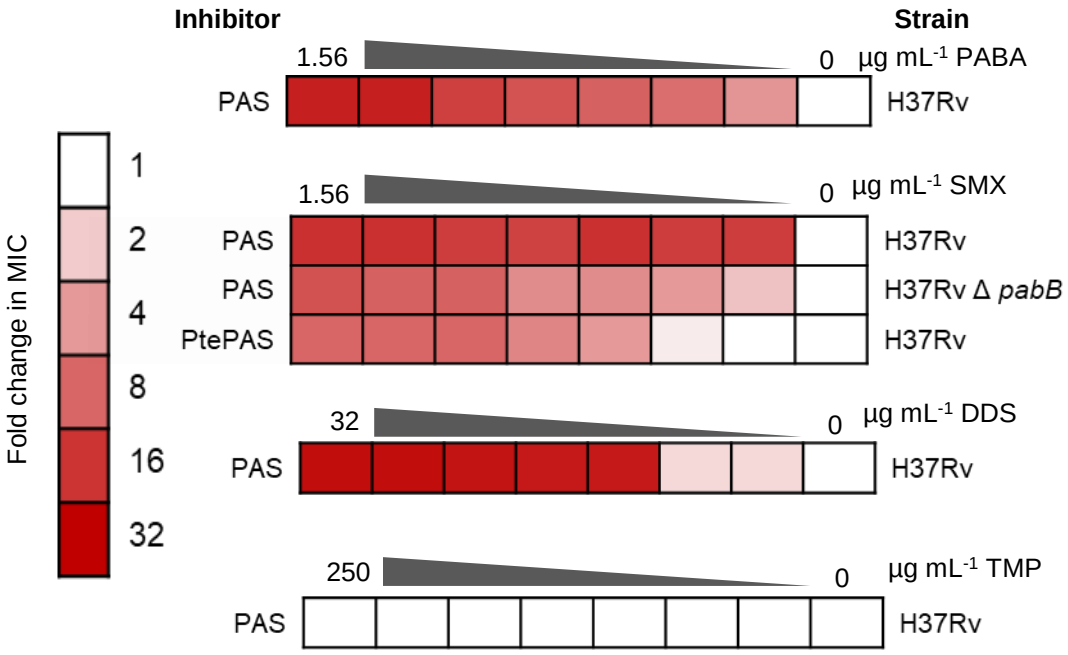

Figure 3.7. FolP inhibitors antagonize the anti-tubercular activity of PAS. *in vitro* interactions between PAS and PABA, PAS and SMX, PAS and DDS, PtePAS and SMX in *M. tuberculosis* H37Rv and H37Rv Δ*pabB*. Data shown represent average of three independent experiments.

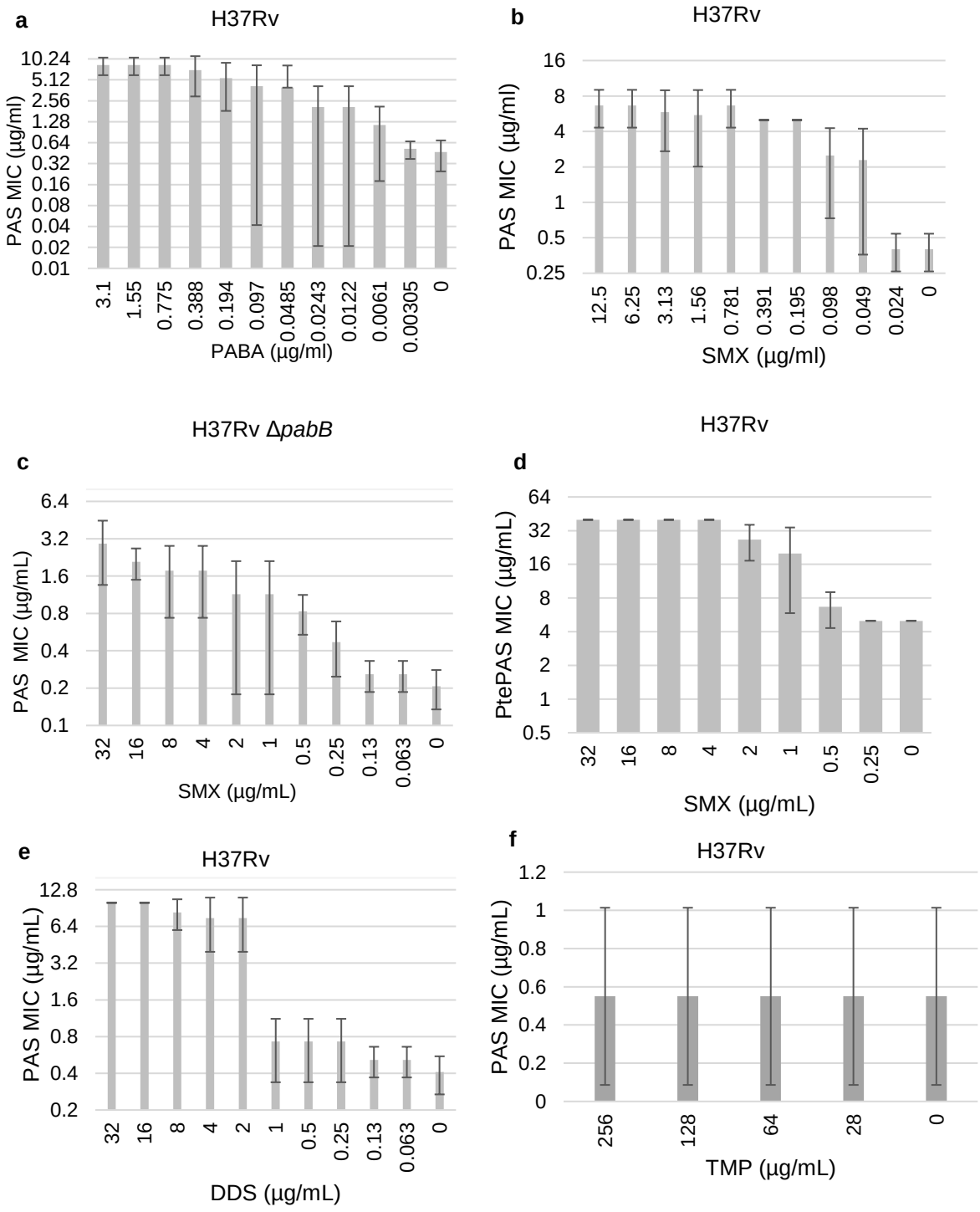
a
H37Rv
PAS MIC (µg/ml)
10.24
5.12
2.56
1.28
0.64
0.32
0.16
0.08
0.04
0.02
0.01
3.1
1.55
0.775
0.388
0.194
0.097
0.0485
0.0243
0.0122
0.0061
0.00305
0
PABA (µg/ml)
b
H37Rv
PAS MIC (µg/ml)
16
8
4
2
1
0.5
0.25
12.5
6.25
3.13
1.56
0.781
0.391
0.195
0.098
0.049
0.024
0
SMX (µg/ml)
c
H37Rv Δ*pabB*
PAS MIC (µg/mL)
6.4
3.2
1.6
0.8
0.4
0.2
0.1
32
16
8
4
2
1
0.5
0.25
0.13
0.063
0
SMX (µg/mL)
d
H37Rv
PtePAS MIC (µg/mL)
64
32
16
8
4
2
1
0.5
32
16
8
4
2
1
0.5
0.25
0
SMX (µg/mL)
e
H37Rv
PAS MIC (µg/mL)
12.8
6.4
3.2
1.6
0.8
0.4
0.2
32
16
8
4
2
1
0.5
0.25
0.13
0.063
0
DDS (µg/mL)
f
H37Rv
PAS MIC (µg/mL)
1.2
1
0.8
0.6
0.4
0.2
0
256
128
64
28
0
TMP (µg/mL)

Figure 3.8. FolP inhibitors antagonize the anti-tubercular activity of PAS. *in vitro* Interactions between PAS and PABA, PAS and SMX, PAS and DDS, PtePAS and SMX in *M. tuberculosis* H37Rv and H37Rv Δ*pabB*. Strains were grown in 7H9 with appropriate supplementations at 37 ºC for 2 weeks. The data represents the minimum concentration of drug required to inhibit growth in varying concentrations. Data shown represent average of three independent experiments. Error bars represent standard deviation.

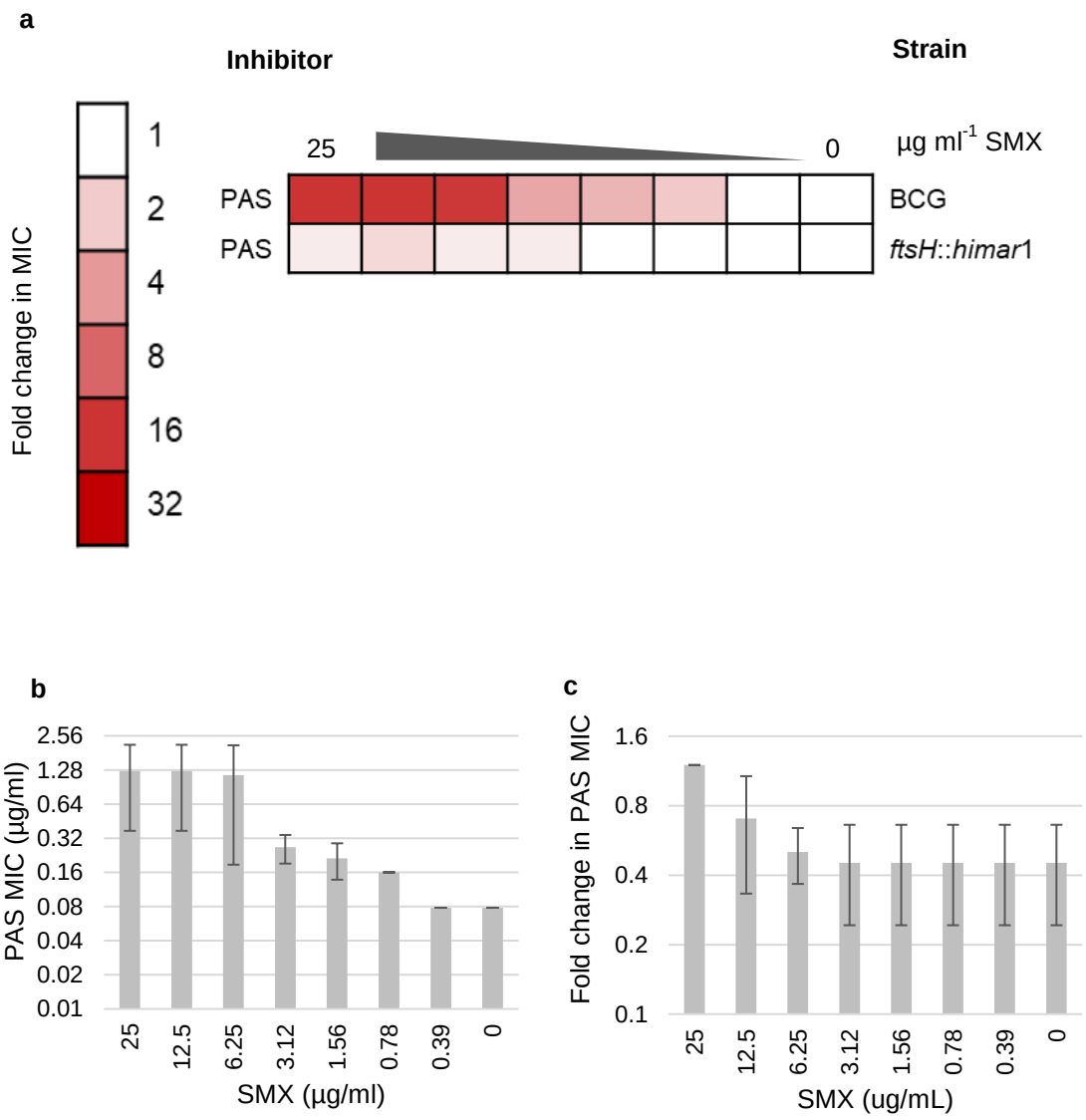

Figure 3.9. SMX antagonizes the anti-tubercular activity of PAS in *M. bovis* BCG but not in *M. bovis* BCG *ftsH*::*himar*1. a) *In vitro* fold change in PAS MIC during SMX treatment. b) *M. bovis* BCG and c) *M. bovis* BCG *ftsH*::*himar*1. Strains were grown in 7H9 with appropriate supplementations at 37 ºC for 2 weeks. The data represents the minimum concentration of drug required to inhibit growth in varying concentrations. Data shown represent average of three independent experiments. Error bars represent standard deviation. Data shown represent average of three independent experiments.

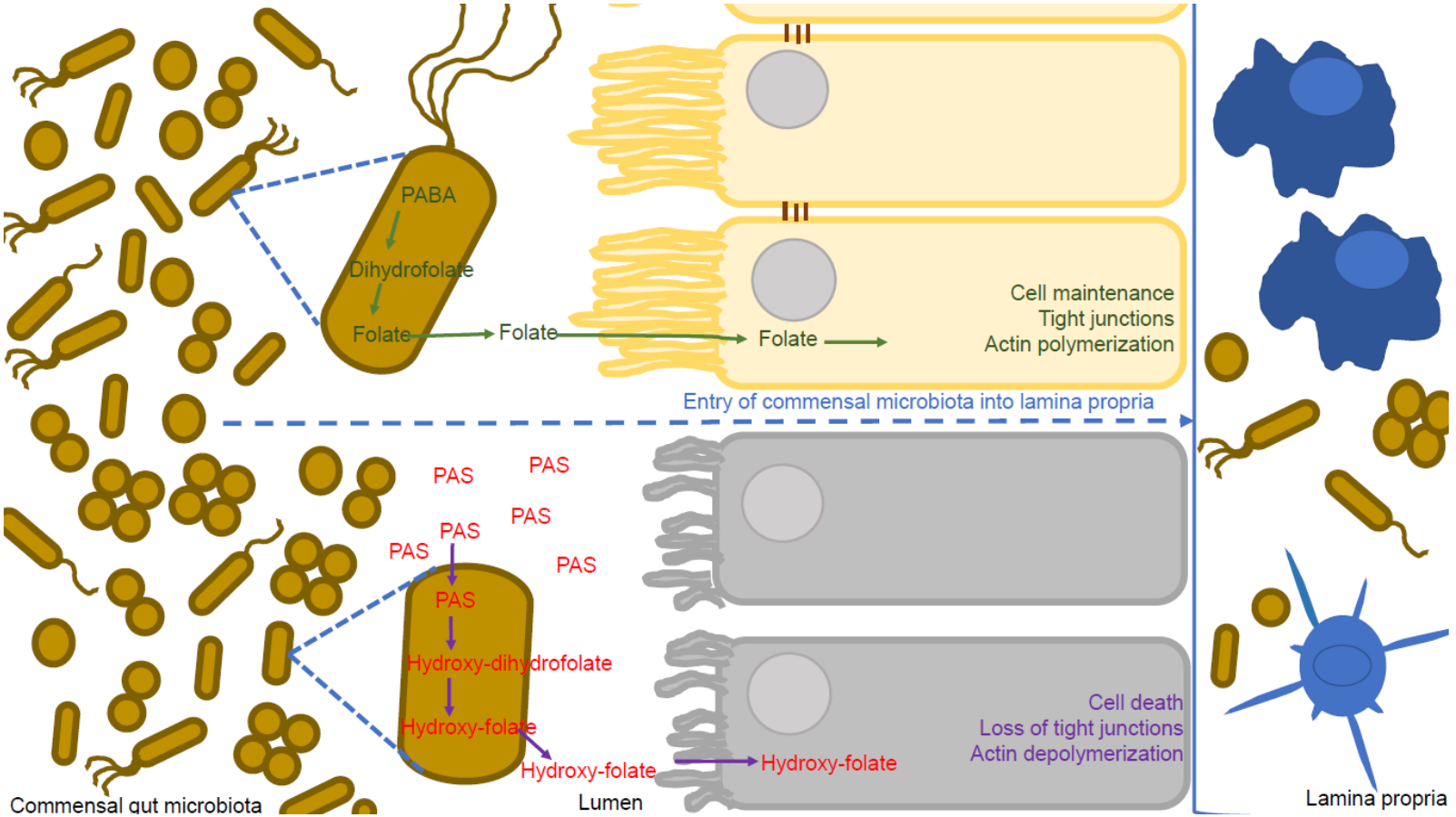
PABA
Dihydrofolate
Folate
Folate
Folate
Cell maintenance
Tight junctions
Actin polymerization
Entry of commensal microbiota into lamina propria
PAS
PAS
PAS
PAS
PAS
PAS
PAS
Hydroxy-dihydrofolate
Hydroxy-folate
Hydroxy-folate
Hydroxy-folate
Cell death
Loss of tight junctions
Actin depolymerization
Commensal gut microbiota
Lumen
Lamina propria

Figure 3.10. Mechanistic basis for PAS toxicity.

Chapter 4: Mechanistic basis for resistance to *para*- aminosalicylic acid in *Mycobacterium tuberculosis*

This chapter is a reprint, with alterations, of a published manuscript.

Thiede JM*, Kordus SL*, Turman BJ, Buonomo JA, Aldrich CC, Minato Y, and Baughn AD. Targeting intracellular p-aminobenzoic acid production potentiates the anti-tubercular action of antifolates. *Scientific Reports* 2016;6.

*Denotes equal contributing

Specific contributions from *Scientific Reports* manuscript

Thiede, JT and Kordus, SL both performed experiments in Figures 4.4 and 4.5.

Kordus, SL performed experiments in Table 4.5 and Figures 4.6 and 4.7.

The rest of the chapter has not published when the thesis was submitted. All experiments, experimental design, intellectual contributations were performed by Shannon Lynn Kordus.

Synopsis

The treatment regimen for *Mycobacterium tuberculosis* involves lengthy, intensive drug therapy that causes severe side-effects. The antimicrobial *para*-aminosalicylic acid (PAS) is used to treat drug resistant *M. tuberculosis* infections. Despite the use of PAS to treat *M. tuberculosis* for over 70 years, the biochemical mechanisms which govern PAS susceptibility and resistance in *M. tuberculosis* are incomplete. In this study we set out to determine novel PAS resistance mutations. We identified mutations in *folC* and *thyA*. We showed *folC* PAS resistant mutants had an increase in expression of *para*-aminobenzoic acid (PABA) biosynthesis genes. We found that disrupting PABA biosynthesis genes resulted in hypersusceptibility to sulfa-drugs and PAS. Furthermore, disruptions in PABA biosynthesis resulted in restoration of PAS susceptibility in *folC* mutant strains. Together, these observations reveal a novel mechanism for PAS resistance.

Introduction:

Resistance to *para*-aminosalicylic acid (PAS) was described shortly after its introduction into the clinic. Therefore, PAS was prescribed in combination with other antitubercular drugs to suppress the emergence of drug resistance. PAS has been discontinued as a first-line agent in treating *Mycobacterium tuberculosis* due to its toxicity and the advent of better tolerated drugs. Currently, PAS is primarily used to treat drug resistant strains of *M. tuberculosis*, but remains a primary chemotherapeutic agent for treating tuberculosis in southeast Asia. With the increase incidence of drug-resistant strains of *M. tuberculosis* a new effort has focused on determining the mechanistic basis for PAS resistance (WHO, 2018).

PAS is a structural analog of the folate precursor metabolite *para*-aminobenzoic acid (PABA). PAS only differs from PABA by the presence of a hydroxyl-group in the *ortho*-position to the carboxylic acid. PAS was thought to disrupt folate biosynthesis based on the observation that exogenous PABA could antagonize PAS inhibition of *M. tuberculosis* growth(Youmans *et. al*., 1947). The folate biosynthesis pathway is composed of three enzymes: dihydropteroate synthase (FolP), dihydrofolate synthase (FolC), and dihydrofolate reductase (FolA). FolP is an essential enzyme required for the condensation of *para*-aminobenzoic acid and 6-hydroxymethyl-7,8-dihydropterin pyrophosphate to form dihydropteroate

(DHP). FolC is required to ligate glutamate to DHP via ATP to produce dihydrofolate (DHF). FolA catalyzes the NADPH-dependent reduction of DHF to tetrahydrofolate (THF).

Initially, PAS was thought to act as a FolP inhibitor similar to sulfonamides(Youmans *et. al*., 1947). However, no cross-resistance between PAS and sulfonamides in *M. tuberculosis* was observed(Yegian and Long, 1951). In contrast to sulfonamides, PAS only weakly inhibited purified FolP enzymatic activity and was later demonstrated to be converted to a hydroxylated version of DHP, hydroxy-DHP (Chakraborty *et. al*., 2013; Zhao *et. al*., 2014; Zheng *et. al*., 2013). FolC was found to catalyze the glutamylation of hydroxy-DHP to hydroxy-DHF. This suggested that FolC is not the target of bioactivated PAS and the target was likely downstream within the folate pathway (Chakraborty *et. al*., 2013; Zhao *et. al*., 2014; Zheng *et. al*., 2013). Indeed, it was predicted and later confirmed that hydroxy-DHF could potently inhibit FolA(Chakraborty *et. al*., 2013; Dawadi *et. al*., 2017; Zheng *et. al*., 2013).

To date, few *folA* missense mutations associated with PAS resistance have been reported(Myllykallio *et. al*., 2002). It is presumed that mutations in the FolA active site can be highly deleterious to the overall enzyme function. Thus, it could be

rare for *folA* point mutations to confer resistance to PAS without compromising FolA enzymatic activity.

Resistance to PAS exclusively arises through the occurrence of spontaneous mutations in genes related to folate synthesis and metabolism. To date, PAS resistance mutations have been identified in *folC*, *ribD*, and *thyA* (Mathys *et. al*., 2009; Zhang *et. al*., 2015; Zhao *et. al*., 2014).

Mutations in *folC* are the most prevalent mutations identified in PAS resistant clinical isolates(Mathys *et. al*., 2009; Zhang *et. al*., 2015). *folC* mutations typically map to positions corresponding to substrate binding and nucleoside binding pockets of the ATP binding domain in FolC(Mathys *et. al*., 2009; Zhang *et. al*., 2015; Zhao *et. al*., 2014). Both of these positions are essential for proper enzymatic function. Purified recombinant FolC variants from resistant strains had reduced enzymatic activity (10 to 20% of wild type activity)(Zhao *et. al*., 2014). These variants were analyzed for the ability to glutamylate hydroxy-DHP to hydroxy-DHF; however, no detectable hydroxy-DHF was observed (Zhao *et. al*., 2014). Similarly, PAS resistant *M. tuberculosis folC* mutant strains were found to produce substantially less hydroxy-DHF than the wild type control(Zhao *et. al*., 2014). Thus, it has been hypothesized that *folC*-linked PAS resistance occurs via impaired synthesis of hydroxy-DHF.

Another common PAS resistance mechanism involves loss-of-function mutations in *thyA*, encoding a non-essential thymidylate synthase (ThyA). In *M. tuberculosis* ThyA is responsible for the 5,10-methylene-tetrahydrofolate dependent conversion of dUMP to dTMP (Mathys *et. al*., 2009; Zhang *et. al*., 2015; Zhao *et. al*., 2014). When functional, ThyA releases DHF that must be re-reduced in order to be utilized in folate metabolism. *M. tuberculosis* encodes an alternate thymidylate synthase (ThyX, encoded by *thyX*) that regenerates THF from 5,10-methylene-THF following catalysis (Myllykallio *et. al*., 2002). Thus, in contrast to ThyA, ThyX places limited demand of FolA for maintaining reduced folate pools. In other bacterial pathogens that do not encode a ThyX ortholog, loss-of-function mutations in *thyA* lead to attenuation due to a resulting thymine auxotrophy (Cersini *et. al*., 1998; Kok *et. al*., 2001). *M. tuberculosis thyA* loss-of-function mutants are not compromised for fitness growth and survival *in vivo* due to the compensatory role of ThyX(Fivian-Hughes *et. al*., 2012; Maisani *et. al*., 2017).

One study recently described five independent PAS resistant clinical isolates containing a deletion of the *folA-thyA* coding sequence(Moradigaravand *et. al*., 2016). These strains were 26 times more resistant to PAS than susceptible control strains. Many bacteria encode a short-chain dehydrogenase/ reductase (FolM, encoded by *folM*)(Pribat *et. al*., 2009). In these bacteria, FolM has the ability to reduce DHF to THF. *M. tuberculosis* does not encode a FolM ortholog

that would be expected to compensate for loss of FolA activity. Instead, this compensation likely comes from a weak DHF reductase activity that is catalyzed by the 5-amino-6-(5-phosphoribosylamino)uracil reductase (encoded by *ribD*, RibD) that normally functions in riboflavin synthesis(Salcedo *et. al*., 2001; Zhao *et. al*., 2014). Consistent with this model, *ribD* promoter mutations have been described that confer PAS resistance and were shown to render *folA* as non-essential in *M. tuberculosis*(Zhang *et. al*., 2015; Zhao *et. al*., 2014).

PAS is prone to exclusion from the cytoplasm by the action of efflux pumps. Overexpression of the major facilitator superfamily protein Tap (encoded by *rv1258c,* Rv1258c) in *Mycobacterium bovis* BCG conferred resistance to PAS(Ramón-García *et. al*., 2012a). Furthermore, overexpression of Tap in *M. tuberculosis* and *M. bovis* BCG conferred resistance to a variety of other antimicrobial agents that do not target folate biosynthesis including streptomycin, vancomycin, and tetracycline(Aínsa *et. al*., 1998; Ramón-García *et. al*., 2012b; Siddiqi *et. al*., 2004).

As described in Chapter 3, the folate biosynthesis pathway has a cyclic nature. FolP inhibitors such as sulfamethoxazole (SMX) increase PABA biosynthesis and could be modulating 6-hydroxymethyl-7,8-dihydropterin pyrophosphate biosynthesis(Minato *et. al*., 2018). We hypothesize one mechanism of PAS resistance is by increasing PABA biosynthesis causing intrinsic resistance to

PAS. To test this hypothesis, *M. tuberculosis* mutants that were resistant to PAS were isolated. PABA biosynthesis gene expression in the PAS resistant mutants were measured. Finally, disruptions in PABA biosynthesis were created to determine if PAS activity could be potentiated and restored in the PAS resistant mutants.

This study found that *folC* mediated resistant to PAS could occur through an increase in PABA biosynthesis causing PAS resistance. PAS susceptibility could be restored by disrupting PABA biosynthesis. These data suggest PABA biosynthesis is a promising drug target to overcome intrinsic resistance to PAS.

Materials and methods:

Bacterial strains, media, and growth conditions

All information regarding primers, plasmids, and bacterial can be found in Table 4.1-4.3

M. tuberculosis strains were grown at 37ºC in either 7H9 broth (Middlebrook) supplemented with 0.2% (wt/vol) glycerol (Fisher Scientific), 10% (vol/vol) oleic acid-albumin-dextrose-catalase (OADC) (Middlebrook), and 0.05% (vol/vol) tyloxapol (Sigma-Aldrich) or 7H10 agar (Middlebrook) supplemented with 0.2% glycerol and 10% OADC. For experiments using *M. tuberculosis* $mc^2$7000, media were supplemented with 50 µg/mL of pantothenate (Sigma).

All antibiotics were added when appropriate to final concentrations of 50 µg/mL for kanamycin, and 150 µg/mL for hygromycin. PABA free mediumwere created by baking glassware for a minimum of one hour at 180ºC and using PABA free reagents. PAS, PABA, trimethoprim (TMP), dapsone (DDS), and methotrexate (MTX) were purchased from Sigma and were dissolved in 100% DMSO (Sigma). Isoniazid was purchased from Sigma and dissolved in water.

Identification of thyA *or* folC *PAS resistance alleles*

PAS resistant mutants were previously isolated from *M. tuberculosis* H37Ra (Zhao *et. al*., 2014) were streaked onto 7H10 containing 1 µg/mL of PAS and

incubated at 37ºC for 3-4 weeks. The genomic DNA from the PAS resistant colonies were isolated and the *folC* and *thyA* genes were amplified using PCR using primers described in table 4.1. The resulting PCR product was purified (Qiagen) and was sequenced using the previously mentioned primers. Corresponding mutations were mapped onto the crystallized FolC (PDB: 2VOR) and ThyA (PDB: 4FOG)(Young *et. al*., 2008). Molecular graphics and analyses were performed with UCSF Chimera, developed by the Resource for Biocomputing, Visualization, and Informatics at the University of California, San Francisco(Pettersen *et. al*., 2004).

Minimum inhibitory concentration determination using PAS resistant isolates

PAS minimum inhibitory concentration (MIC_{90}) is defined as the amount of drug required to inhibit 90% of bacterial growth compared to the no drug control using the log_2 dilution method. All strains were grown in inkwell bottles, with aeration, at 37ºC. The MIC_{90} was determined spectrophotometrically (OD_{600}) (GENESYS 20, Thermo Fisher) and was measured at 7 and 14 days, except when noted. The MIC_{90} was determined in biological triplicate for each strain.

qPCR of PABA and folate biosynthesis pathways of PAS resistance isolates

M. tuberculosis strains PAS6, PAS7, and PAS10 were grown to mid-exponential phase (OD_{600} 0.4-0.6) and subcultured to OD 0.3 in 7H9 complete medium for 24 hr at 37ºC with aeration. The cells were harvested by centrifugation (4,000 x g,

10 min, 4°C). The total RNA was extracted using TRIzol (Invitrogen, CA) with 0.1% polyacryl carrier (Molecular Research Center, Inc.) by bead beating with 0.1-mm zirconia beads (BioSpec Products). The total RNA was treated with Turbo DNase (Invitrogen). cDNA was synthesized and quantitative PCR was performed using QuantiFast SYBR Green RT-PCR (Qiagen). qPCR primers to amplify internal regions of the genes of interest (*trpG, pabB*, *folP*, *folC*, *folA*, *thyA*, and *sigA*) were designed with similar annealing temperatures (58 to 60°C) using Primer3(Koressaar and Remm, 2007; Untergasser *et. al*., 2012). Quantitative RT-PCR mixtures were prepared in technical triplicate using 2 SYBR green master mix, 1µM each primer, and 1 ng RNA. Reactions were run on a LightCycler 480 (Roche). The following real-time cycler conditions were used: reverse transcription 50ºC for 10min; PCR activation step 95°C for 5 min; 40 two-step cycles, denaturation 95°C for 10 sec; combined annealing/extension 60°C for 30 sec; with data collected once per cycle during the extension phase; and one cycle of 95°C for 5 s, 65°C for 1 min, and 97°C with a ramp rate of 0.11°C/s for generation of melting curves. Cycle threshold values (C_p) were normalized to C_p *sigA* values and were normalized to the parent strain wild-type control. qPCRs of *folC* mutants were performed in biological triplicate and *thyA* mutants were performed in biological singlet.

Generation of PABA auxotrophic strains and construction of complemented strains

A transposon mutagenesis screen was performed on *M*. *tuberculosis* mc^{2}7000 (Kriakov *et. al*., 2003) to identify strains that were auxotrophic for PABA. Briefly, transposon mutagenized strains were isolated on supplemented 7H10 agar medium containing 10 µg/ml PABA. Five thousand independent colonies were picked and patched to supplemented 7H10 with or without 10 µg/ml PABA (Sigma). Mutant strains that were unable to grow on the PABA-free medium were purified and rescreened to confirm PABA auxotrophy. Genomic DNA from mutant strains that showed a PABA auxotrophic phenotype was extracted and transposon insertion sites were determined as previously described (Rubin *et. al*., 1999).

M. tuberculosis H37Ra Δ*pabB* was constructed as described in Chapter 2, except *M. tuberculosis* H37Ra was used instead of *M. tuberculosis* H37Rv.

M. tuberculosis H37Ra was used as a template for constructing *pabC* and *pabB* complementation plasmids. Both genes were amplified by PCR, the *pabB* gene was digested with *Nco*I and *Hind*III, the *pabC* gene was digested with *Hind*III and *Eco*RI. The resulting PCR product for *pabC* was ligated into an a previously digested pJT6a, modified from pTIC6a using same restriction enzymes (Glover *et. al*., 2007). The resulting PCR product for *pabB* was ligated into an already digested pMV306 plasmid using the same restriction enzymes(Stover *et. al*., 1992). The resulting plasmids were propagated in *E.*

coli DH5α and were sequenced verified. Once plasmids were sequence verified they were electroporated into the corresponding *M. tuberculosis* strains, the resulting colonies were evaluated by colony PCR to confirm the presence of the plasmid.

Phenotypic validation of PABA auxtrophs

M. tuberculosis $mc^2$7000 *pabC::himar*1 was grown in medium containing 10 ng/mL PABA to mid-exponential phase (OD_{600} 0.4-0.6) and washed three times in PABA free 7H9 medium. The bacterium was subcultured to OD_{600} 0.01 in PABA free complete 7H9 medium with or without 10 µg/mL and was incubated with aeration at 37ºC. The OD_{600} was measured every two to three days as indicated.

M. tuberculosis H37Ra Δ*pabB* was grown in 7H9 medium containing 10 ng/mL of PABA to mid-exponential phase and washed three times in 7H9 PABA free medium. The bacterium was subcultured to OD_{600} 0.01 in 7H9 medium with or without 10 µg/mL of PABA. The cultures were incubated with aeration at 37ºC. The OD_{600} was measured every two to three days as indicated.

A kill curve was generated by growing *M. tuberculosis* H37Ra Δ*pabB* in 7H9 medium containing 10 ng/mL of PABA to mid-exponential phase and washed three times in 7H9 PABA free medium. The bacterium was subcultured to OD_{600}

0.01 in 7H9 PABA free medium. The cultures were incubated with aeration at 37ºC. Every 7, 14, 21, and 28 day aliquots were taken and plated for colony enumeration on 7H10 complete medium with 10 µg/mL PABA. The colonies were counted after 3-4 weeks of growth at 37ºC.

All growth curves were performed in biological triplicate.

Results:

PAS resistance mutations primarily map to folC *and* thyA

Recent findings show that *M. tuberculosis* PAS resistant clinical isolates frequently have mutations that map to folate biosynthesis and metabolism, namely to *thyA* and *folC*(Mathys *et. al*., 2009; Zhang *et. al*., 2015; Zhao *et. al*., 2014). *thyA* encodes a thymidylate synthase that converts dUMP to dTMP with the concomitant conversion of 5,10-methylene-tetrahydrofolate to dihydrofolate. *folC* encodes dihydrofolate synthase, an essential enzyme required for the glutamylation of 7,8-dihydropteroate (DHP) to 7,8-dihydrofolate (DHF). To further investigate molecular mechanisms for PAS resistance, we selected for resistant strains and performed genotypic characterization. Of eight PAS resistant strains that were analyzed, only two were found to have mutations in *folC* (FolC E153A) (Figure 4.1). These isolates had PAS MIC_{90} of 1.2 µg/ml and 4.8 µg/ml (Table 4.4). Five strains were found to have mutations in *thyA* and corresponded to the following positions in the predicted protein S54A, L7V, N134K, H147N, and G15D (Table 4.4 and Figure 4.2). *thyA* mutations had a PAS MIC_{90} ranging from 9.6 µg/ml to 19.2 µg/ml (Table 4.4). One strain did not have mutations in *folC* or *thyA* and had the greatest resistance to PAS with a MIC_{90} of 38.4 µg/ml (Table 4.4).

PAS resistant folC *mutants have increased expression in PABA and folate biosynthesis genes*

Previous work has demonstrated that dihydrofolate reductase inhibitors can cause an increase in PABA biosynthesis through a feedback mechanism(Minato *et. al*., 2018). Based on our previous study of FolC variants associated with PAS resistance, we hypothesized that the *folC* mutants would have compromised DHF synthesis. This defect could result in *M. tuberculosis* synthesizing more PABA and folates for growth, thereby out competing PAS incorporation. To test this hypothesis, we performed qPCR on representative PAS resistant *thyA* and *folC* mutants in the absence of PAS. We found the *folC* PAS resistant strains PAS7 and PAS10 had higher expression of *trpG*, *pabB, folP, folA, and thyA* (roughly 4, 9, 2, 3, and 10 fold respectively) (Figure 4.3). The *thyA* PAS resistant strain PAS6 had increased gene expression of *pabB* and *thyA* (roughly 3 and 3 fold, respectively) (Figure 4.3).

Disruption in PABA biosynthesis genes potentiates activity of PAS and structurally related antifolates

Mutations in *folC* cause an increase in both PABA and folate biosynthesis. Therefore, we hypothesized disruptions in PABA biosynthesis would re-sensitize the *folC* resistant mutants to PAS. First we performed a transposon screen to identify transposon disruptions that would lead to PABA auxotrophy. Our screen yielded a transposon insertion in *pabC*, encoding PabC an amino-deoxychorismate lyase. *M. tuberculosis* $mc^2$7000 *pabC*::*himar*1 was a strict

auxotroph on 7H10 plates in the absence of PABA (data not shown). In liquid medium the strain could grow, albeit at a reduced rate, compared to the wild-type and complemented control (Figure 4.4).

Next, we determined the MIC_{90} of PAS, FolP inhibitors (SMX, STZ, DDS), MTX, TMP, and isoniazid in *M. tuberculosis* $mc^2$7000 *pabC*::*himar*1. PAS and all FolP inhibitors tested showed enhanced activity against *M. tuberculosis* $mc^2$7000 *pabC*::*himar*1 relative to the parental control (Table 4.5). Neither TMP or MTX showed any change in MIC_{90} for *M. tuberculosis* $mc^2$7000 *pabC*::*himar*1 (Table 4.5). Isoniazid, a *M. tuberculosis* cell wall inhibitor, showed no changes in MIC_{90} for *M. tuberculosis* $mc^2$7000 *pabC*::*himar*1 (Table 4.5).

pabB *deletion confers PABA auxotrophy and restores PAS susceptibility in* folC *mutants*

Although *M. tuberculosis* $mc^2$7000 *pabC*::*himar*1 showed enhanced susceptibility to antifolates such as PAS and sulfa-drugs, it is not a PABA auxotroph. We hypothesized the protein upstream of PabC in the PABA synthesis pathway, PabB an amino-deoxychorismate synthase, encoded by *pabB*, would be essential for PABA synthesis. Indeed *M. tuberculosis* H37Ra Δ*pabB* could not grow in the absence of PABA, unless *pabB* was supplied *in trans* (Figure 4.5). Furthermore, *M. tuberculosis* H37Ra Δ*pabB* could be chemically complimented

with the addition of exogenous PABA (Figure 4.5). Interestingly, *M. tuberculosis* H37Ra Δ*pabB* lost viability as early as 7 days without exogenously supplemented PABA (Figure 4.6).

PABA is a known antagonist of PAS. Since *M. tuberculosis* H37Ra Δ*pabB* cannot grow in the presence of exogenous PABA, we performed a dose response with varying concentrations of PABA and determined the MIC_{90} of PAS. In *M. tuberculosis* H37Ra, the PAS MIC_{90} increased with increasing concentrations of supplemental PABA. This trend was also observed in the *M. tuberculosis* H37Ra Δ*pabB*; however, the PAS MIC_{90} was much lower than the parent strain in the presence of 1 ng/ml and 10 ng/ml of PABA (Figure 4.7).

To test if we could restore PAS susceptibility in *folC* mutants we created a *pabB* deletion in *M. tuberculosis* PAS7. *M. tuberculosis* PAS7 also exhibited a dose response increase in the PAS MIC_{90} in the presence of increasing concentrations of PABA (Figure 4.7). This trend was also observed in the *M. tuberculosis* PAS7 Δ*pabB* (Figure 4.7). Notably, the PAS MIC_{90} of *M. tuberculosis* PAS7 Δ*pabB* was near the wild-type drug susceptible parent strain in the presence of 1 ng/ml and 10 ng/ml (Figure 4.7). Furthermore, the PAS MIC_{90} of *M. tuberculosis* PAS7 Δ*pabB* was restored to that of the parent drug resistant strain in the presence of 100 ng/ml of PABA (Figure 4.7).

Discussion:

Characterization of PAS resistant strains

We isolated PAS resistant laboratory strains of *M. tuberculosis* in an effort to discover novel resistance mechanisms. The PAS MIC_{90} of these strains were determined and eight were found to be resistant to PAS. Of these strains, 2 were found to have mutations in *folC*, 5 were found to have mutation in *thyA*, and one did not have mutations that mapped to *folC* or *thyA*. The mutations that mapped to *folC* were found within the active site and resulted in a non-synonymous change from charged, glutamic acid to non-polar alanine. These mutations have been described previously(Zhao *et. al*., 2014). Interestingly, both *folC* strains had mutations in the same location; however, the MIC_{90} were different. This suggests that there could be a secondary mutation somewhere else in the genome and warrants further investigation.

FolC E153A mediated PAS resistance could occur by preventing binding of hydroxy-DHP. Specifically, hydroxy-DHP could form hydrogen bonding or salt bridges via glutamic acid in the native enzyme that is not required for binding DHP. These interactions would be abolished in the presence of alanine. This hypothesis would be difficult to test since hydroxy-DHP is only stable for about 3hrs in ambient oxygen. FolC has a very slow catalytic turnover and previous

FolC enzymatic assays require 24hrs to determine enzymatic activity (Dawadi *et. al*., 2017; Zhao *et. al*., 2014).

Treatment with FolA inhibitors leads to folate starvation in *E. coli*. We have recently shown that treatment with FolA inhibitors resulted in increased production of PABA, in *E. coli*(Minato *et. al*., 2018). FolC E153A mutants had reduced enzymatic activity (~20% of wild-type) utilizing the native substrate, DHP(Zhao *et. al*., 2014). Since FolC mutants had reduced enzymatic activity, we hypothesized that the FolC mutants could be limited for folates. These FolC mutants could be synthesizing more PABA to compensate for the reduced enzymatic activity of FolC E153A.

In contrast to PAS resistant *folC* mutant strains, *thyA* mutant strains were the most prevalent and changes corresponded to the active site residues (S54A and H147N) as well as residues outside of the active site (L7V, G15D, and N134K). ThyA H147N has already been described as a molecular mechanism of resistance to PAS(Zhao *et. al*., 2014). Mutations in ThyA G15 have been described (G15R); however, G15D represents a novel mutation. We also described 3 novel ThyA mutations (S54A, L7V, N134K). Interestingly, all mutations in *thyA* had the greatest PAS resistance (MIC_{90} 9.6-19.6 µg/ml) compared to mutations in *folC* (MIC_{90} 1.2-4.8 µg/ml). Furthermore, we noticed

some of *thyA* mutants had a growth defect. This suggests that *thyA* mediated PAS resistance mechanisms are different than *folC* mediated PAS resistance.

In addition, we isolated one mutant that did not have any mutations that mapped to *thyA* or *folC*. This strain had the highest PAS resistance out of all of the mutants. We have whole genome sequenced this strain and are awaiting sequencing results.

PABA biosynthesis genes are upregulated in folC *mutants*

During treatment with FolA inhibitors PABA levels are increased(Minato *et. al*., 2018). We hypothesized that *folC* mutants are not able to produce enough folates causing an increase in PABA biosynthesis genes. To test this hypothesis, we performed qPCR on the *folC* and *thyA* mutants in the absence of PAS. We found that the *folC* mutants had increased expression of PABA and folate biosynthesis genes. *thyA* mutants only had increased expression of *folA* and *thyA* biosynthesis genes. This also suggests the mechanistic basis for *folC* mediated PAS resistance is different than *thyA*. Specifically, that *folC* causes an increase in PABA and folate biosynthesis. Since it appears that *thyA* increases *folA* and its own expression, we hypothesize that *thyA* mediated resistance is caused by a decreased demand for *folA* expression.

Targeting PABA biosynthesis sensitizes M. tuberculosis *to folP inhibitors and PAS*

We hypothesized we could restore susceptibility to PAS by creating a disruption in PABA biosynthesis in PAS resistant *folC* mutants. First we performed a transposon mutagenesis screen for a PABA auxotrophic phenotype. We isolated a mutant strain with a transposon insertion in *pabC* that could only grow in the presence of PABA on solid medium. Unfortunately, this strain, *M. tuberculosis* $mc^2$7000 pabC::*himar*1 could still grow in the absence of PABA in liquid culture. Since *pabC* encodes an amino-deoxychorismate lyase requiring water to eliminate pyruvate, it is possible that this hydrolysis could occur in the absence of PabC.

M. tuberculosis $mc^2$7000 *pabC*::*himar*1 was tested for susceptibility to a variety of folate biosynthesis inhibitors including and was hypersusceptible to all sulfonamides tested as well as DDS and PAS. There was no change in TMP, MTX and isoniazid susceptibility. As discussed in Chapter 3, sulfonamides, as well as DDS and PAS can be antagonized by exogenous PABA; therefore, this hypersusceptibility is likely due to the decrease in intrinsic PABA production. As discussed in Chapter 3, PABA does not antagonize TMP. Since *M. tuberculosis* does not encode a folate transporter, it is unlikely that MTX was transported into *M. tuberculosis*(Minato *et. al*., 2015).

Although we were anticipating the *pabC* mutant would be a PABA auxotroph, we assessed if a deletion in *pabB* would result in complete PABA auxotrophy. Indeed, a deletion in *pabB* resulted in a complete PABA auxotrophy. Since the strain could not grow in the absence of PABA, we assessed if a deletion in *pabB* was bacteriostatic or bactericidal. We found that a deletion in *pabB* is bactericidal. Therefore, *pabB* represents a novel drug target in treating *M. tuberculosis*.

Since PABA limitation is bactericidal for *M. tuberculosis* H37Ra Δ*pabB*, we added exogenous PABA in order to assess the PAS MIC. Even in the presence of exogenous PABA, *M. tuberculosis* H37Ra Δ*pabB* was hypersusceptible to PAS. The PAS MIC_{90} was restored to the drug-susceptible wild-type level when *pabB* was deleted in a *folC* E153A strain. Taken together this data suggest that the *folC* mutants synthesize more PABA resulting in antagonism of PAS.

In *M. tuberculosis,* (-)-abyssomicin C is a known PabB inhibitor and is bactericidal(Freundlich *et. al*., 2010). A future study could investigate treating *M. tuberculosis* with (-)-abyssomicin C in combination with PAS, sulfonamides, and DDS. We anticipate that the combination of (-)-abyssomicin C would have a synergistic effect. Furthermore, co-treating *folC* PAS resistant strains with (-)-abyssomicin C could restore PAS susceptibility.

Tables:

Table 4.1. Oligonucleotide primers used in this study.

Primer name	Primer sequence[1]	Source	Restriction enzyme
folC seq for	CGTCGGGGGCCCGAGTGATGATG	(Zhao *et. al*., 2014)	NA
folC seq internal	CCTACCGGGAGATCGAGCCG	This work	NA
folC seq rev	GAACCTGCGCGATGCTATCGACG	(Zhao *et. al*., 2014)	NA
thyA seq for	CGCCGCGCTTGCATCGCCCGCT	This work	NA
thyA seq rev	TGTCGCTTGAGCCCAGATCA	This work	NA
trpG qPCR for	ACGGTGTCCAGTTCCATCC	This work	NA
trpG qPCR rev	GTGTCGTCTTGCGTCCATC	This work	NA
pabB qPCR for	GGGTACTGGCGTGTCTGGAA	This work	NA
pabB qPCR rev	CGAACCCGTCGATGAAGAAG	This work	NA
folP qPCR for	TGCCCAGATGGTCAACGA	This work	NA
folP qPCR rev	ATCAACACCCACGGCACA	This work	NA
folC qPCR for	AAGGCGGGCATCATCACT	This work	NA
folC qPCR rev	AGCAGCACCTCCATGACCTT	This work	NA
folA qPCR for	ATTCGCTGCCGGCTAAAG	This work	NA
folA qPCR rev	TCGAGTGAACCGACAACCTC	This work	NA
thyA qPCR for	GTTTCCCGCTGCTCACTACC	This work	NA
thyA qPCR rev	GCCTGTATCACTTGCCCATTC	This work	NA
sigA qPCR for	CGACGAAGACCACGAAGACC	This work	NA
sigA qPCR rev	TCATCCCAGACGAAATCACC	This work	NA
pabB_Mtb LL	TTTTTTTTCCATAAATTGGCTCGCAAACTCGCG TCGTAGG	This work	*Van91I*
pabB_Mtb LR	TTTTTTTTCCATTTCTTGGGCACCGGACAGGC TCTCATAC	This work	*Van91I*
pabB-Mtb RL	TTTTTTTTCCATAGATTGGAGTGTGGCACCTG GTGTCCAC	This work	*Van91I*
pabB-Mtb RR	TTTTTTTTCCATCTTTTGGACTCCAGCGCGTTA ACCGCAA	This work	*Van91I*

pMV306-*pabB* for	TTTTTT CCATGG ACG CCG AGC GTG CTT TTC CTA CT	This work	*Nco*I
pMV306-*pabB* rev	TTTTTT AAGCTT CTA CCG CAC TTT GCT GGC TAA CC	This work	*Hind*III
pJT6a-*pabC* for	TTTTTT AAGCTT ATG TTG AGG CAG ACG GGC GT	This work	*Hind*III
pJT6a-*pabC* rev	TTTTTT GAATTC TCA CCG GTC GCT GAC AAT AGC	This work	*Eco*RI

[1]Underline corresponds to the restriction enzyme cut site. All primers are written in 5' to 3' orientation.

Table 4.2. Plasmids used in this study.

Plasmid	Relevant characteristics	Source
p0004S	Plasmid used for allelic exchange, Hygro^r, *sacB*	(Baughn *et. al*., 2010)
phAE159	Phasmid used for specialized transduction, Pen^r	(Bardarov *et. al*., 2002)
pMV306	Mycobacteria integrating vector, Kan^r	(Stover *et. al*., 1992)
pMV306-*pabB*	pMV306 containing *pabB* and 150bp upstream of *pabB*, Kan^r	This work
pJT6a	Modified pTIC6a (Glover *et. al*., 2007), replacing the Kan^r cassette with hygro^r, tet inducible	This work
pJT6a-*pabC*	pJT6a containing *pabC* under tet inducible expression.	This work

Table 4.3. Strains used in this study.

Strain Name	Relevant characteristics	Source
E. coli		
DH5α	Cloning strain	Lab stock
M. tuberculosis		
H37Ra	Wild-type attenuated strain derived from H37Rv	Lab stock
PAS6	H37Ra PAS^r ThyA S54A	This work
PAS7	H37Ra PAS^r FolC E153A	This work
PAS10	H37Ra PAS^r FolC E153A	This work
PAS39	H37Ra PAS^r ThyA L7V	This work
PAS47	H37Ra PAS^r ThyA N134K	This work
PAS48	H37Ra PAS^r ThyA H147N	This work
PAS54	H37Ra PAS^r ThyA G15D	This work
PAS57	H37Ra PAS^r unknown mutation	This work
Δ*pabB*	H37Ra *pabB*::hygro-sacB cassette, Hygro^r	This work
Δ*pabB*-pMV306-*pabB*	Δ*pabB* containing pPV306-*pabB*, Kan^r, Hygro^r	This work
PAS7Δ*pabB*	PAS7 containing Δ*pabB*, Hygro^r	This work
mc^{2}7000	H37Rv Δ*RD1* Δ*panCD*	(Sambandan *et. al*., 2008)
mc^{2}7000 *pabC*::Tn	mc^{2}7000 with a *magellan4* mini transposon insertion in *pabC*, Kan^r	This work
mc^{2}7000 *pabC*::Tn-pJT6a-*pabC*	mc^{2}7000 *pabC*::Tn containing pJT6a-*pabC*, Kan^r, hygro^r	This work

Table 4.4. Characterization of PAS resistant strains of *M. tuberculosis* H37Ra.

Strain	PAS MIC_{90}[1] (µg/mL)	*folC* mutation	*thyA* mutation
H37Ra	0.3	WT	WT
PAS6	9.6	WT	S54A
PAS7	4.8	E153A	WT
PAS10	1.2	E153A	WT
PAS39[2]	9.6	WT	L7V
PAS47[2]	≥9.6	WT	N134K
PAS48	9.6	WT	H147N
PAS54[2]	19.2	WT	G15D
PAS57[2]	38.4	WT	WT

[1]Defined by the minimum concentration of PAS to inhibit 90% of growth compared to a no drug control after two weeks.

[2] MIC read after three weeks of growth.

Table 4.5. Minimum inhibitory concentration (MIC[1]) of various antifolates in *M. tuberculosis* mc[2]7000 *pabC*::Tn.

Drug	mc[2]7000 MIC_{90} (µg/mL)	mc[2]7000 *pabC*::Tn MIC_{90} (µg/mL)	Fold change
PAS	0.3	≤0.000234	≥1000
Sulfamethoxazole	8	≤1	≥8
Sulfathiazole	4	≤0.06	≥64
Dapsone	64	≤0.13	≥512
Trimethoprim	≥512	≥512	1
Methotrexate	≥512	≥512	1
Isoniazid	0.04	0.04	1

[1]MIC_{90} defined as minimum amount of drug required to inhibit 90% of growth compared to a no-drug control.

Figures:

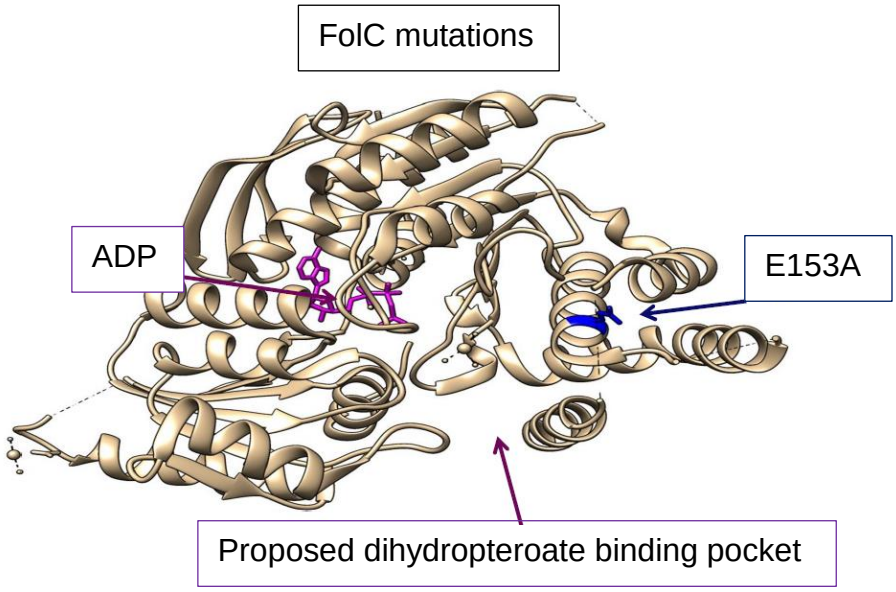

Figure 4.1. Structural consequences of FolC mutations. The FolC mutation described in Table 4.3 was mapped using PDB file 2VOR. The ADP and the proposed dihydropteroate binding pocket are shown.

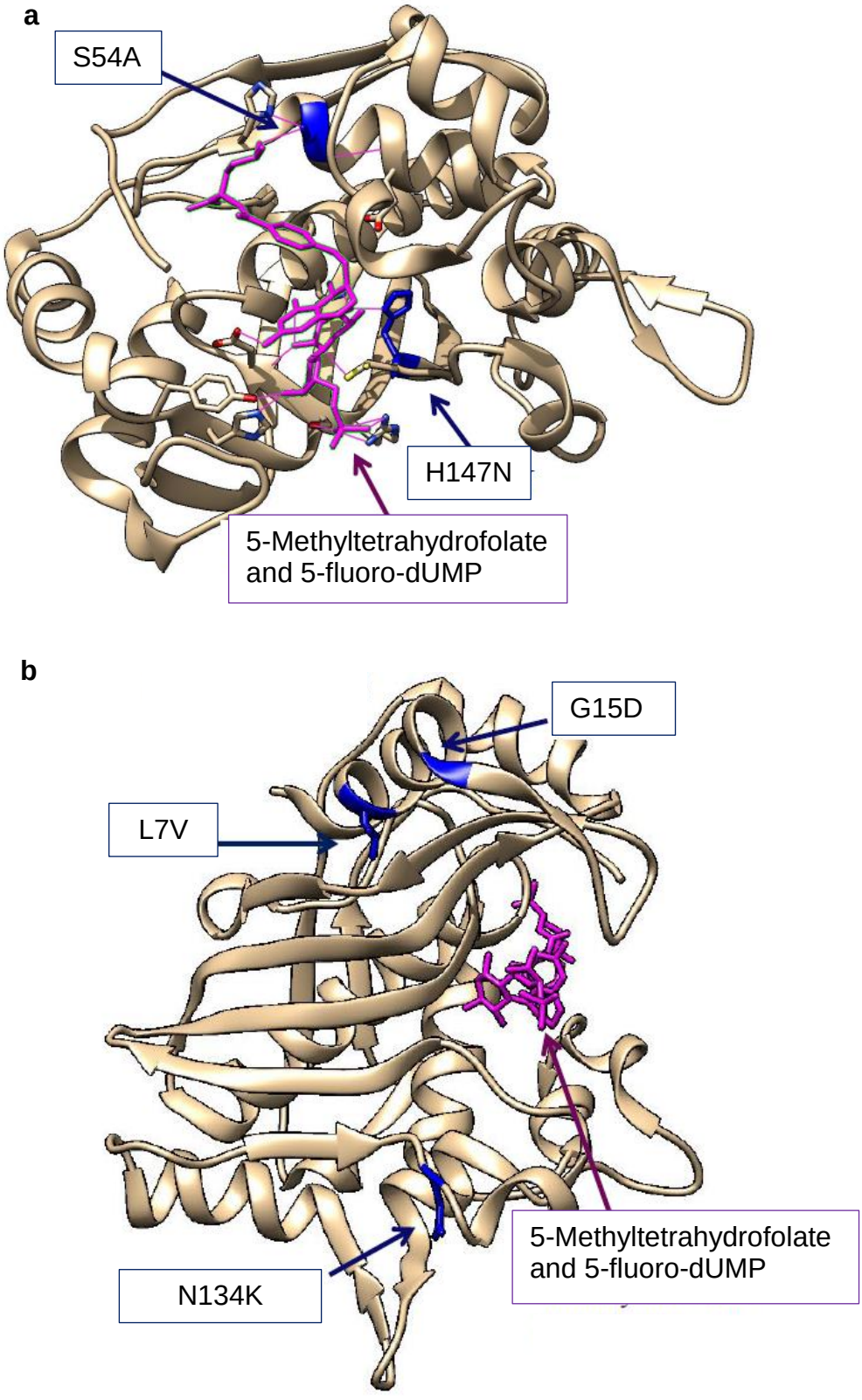
a
S54A
H147N
5-Methyltetrahydrofolate
and 5-fluoro-dUMP
b
G15D
L7V
N134K
5-Methyltetrahydrofolate
and 5-fluoro-dUMP

Figure 4.2. Structural consequences of ThyA mutations inside and outside of the active site. ThyA mutations found within the active site a) and outside of the active site b) are described in Table 4.3 and were mapped using PDB file 4FOG. The substrate binding pocket is shown with 5-methyltetrahydrofolate and 5-fluoro dUMP bound.

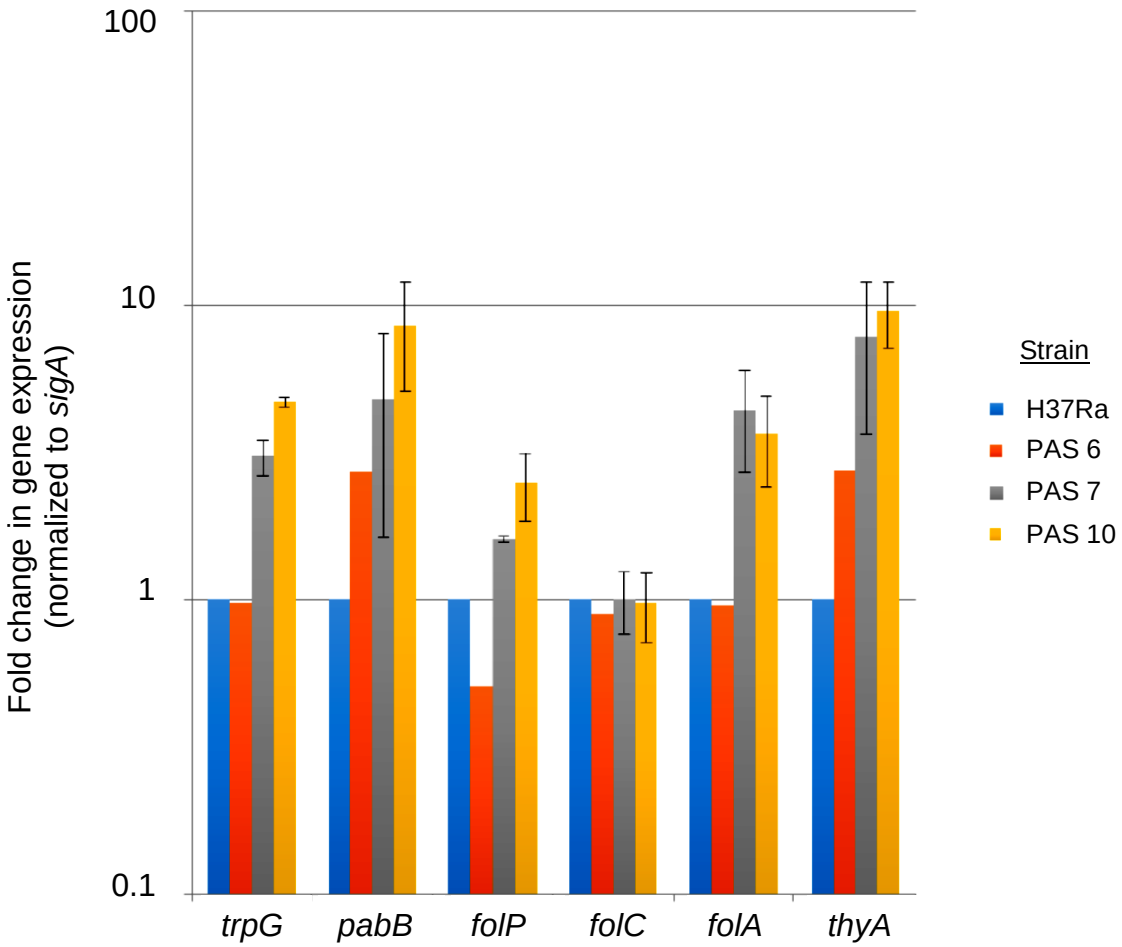

Figure 4.3. PABA and folate biosynthesis genes are upregulated in *folC* PAS resistant mutants but not in *thyA* PAS resistant mutants. *M. tuberculosis* H37Ra was grown to mid-exponential phase (OD 0.4-0.8) in 7H9 complete medium. The RNA was extracted and PABA and folate biosynthesis gene expression was measured. The RNA expression level represented is relative to H37Ra. *folC d*ata represents the average and standard deviation of three independent replicated. *thyA* data represents the average of three technical replicates performed once.

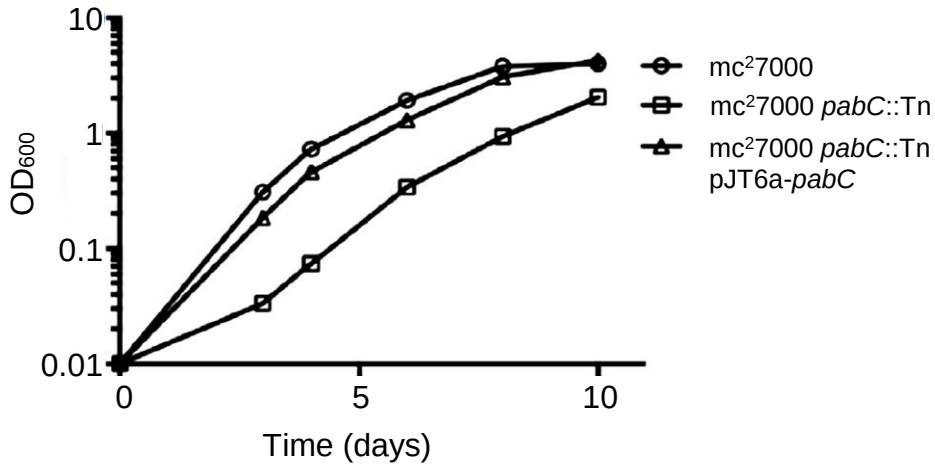

Figure 4.4. mc^{2}7000 *pabC*::Tn is a bradytroph in liquid medium. mc^{2}7000, mc^{2}7000 *pabC*::Tn, and mc^{2}7000 *pabC*::Tn-pJT6a-*pabC* were grown in 7H9 supplemented with 1 ng/ml PABA. The cells were diluted in 7H9 PABA free medium and grown in 37ºC with agitation. OD_{600} measured at indicated time points. Data represents average of three biological replicates. Performed in collaboration with Josh Thiede.

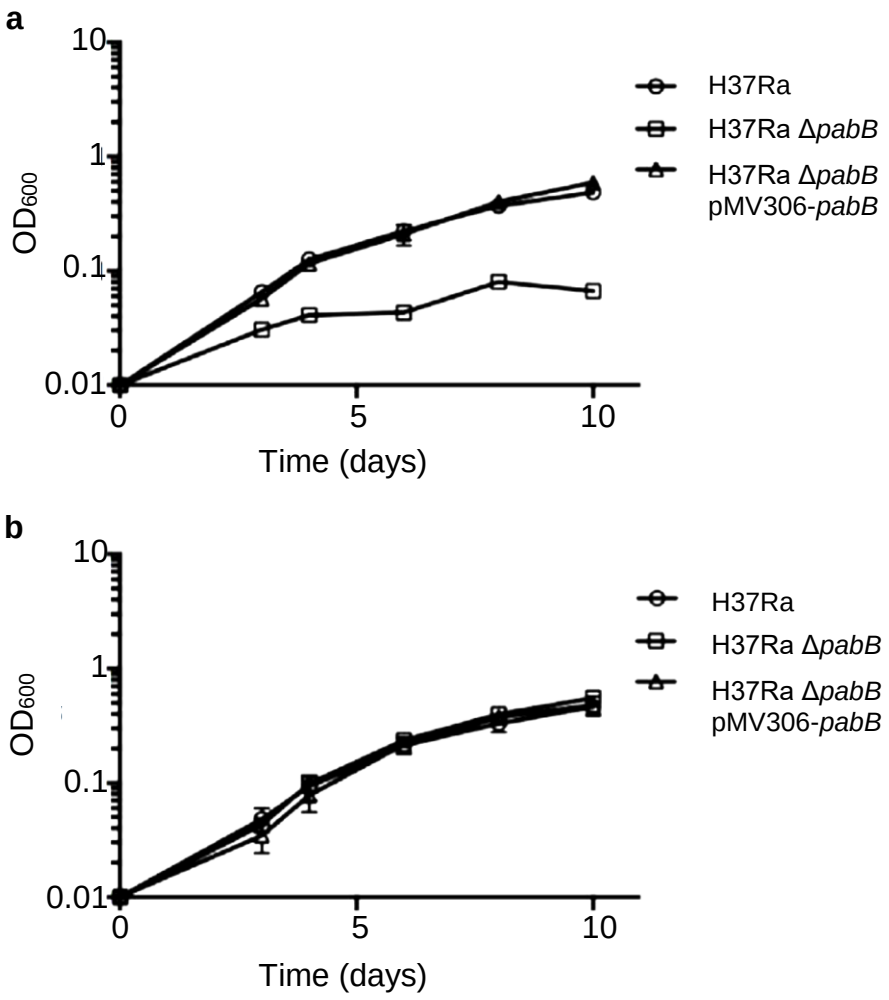

Figure 4.5. H37Ra Δ*pabB* is a PABA auxotroph. H37Ra, H37Ra Δ*pabB*, and H37Ra Δ*pabB*-pMV306-*pabB* were grown in 7H9 supplemented with 1 ng/ml PABA. The cells were diluted in 7H9 a) PABA free medium or b) supplemented with 10 µg/ml PABA and grown in 37ºC with agitation. OD_{600} measured at indicated time points. Data represents average of three biological replicates with standard deviation shown. Performed in collaboration with Josh Thiede.

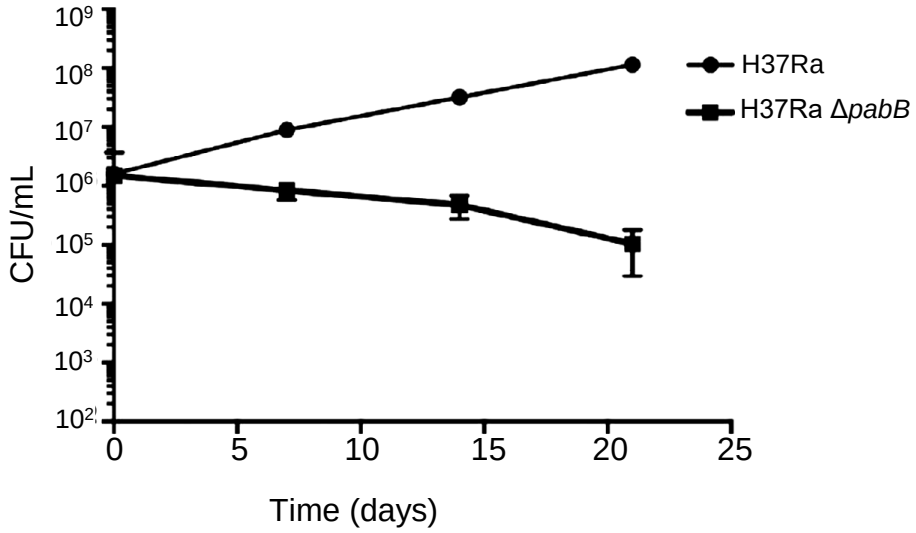

Figure 4.6. H37Ra Δ*pabB* is bacteriocidal. H37Ra and H37Ra Δ*pabB* were grown in 7H9 supplemented with 1 ng/ml PABA. The cells were diluted in 7H9 PABA free medium grown in 37ºC with agitation. CFU's were enumerated every 7 days for 21 days. Data represents average of three biological replicates with standard deviation shown.

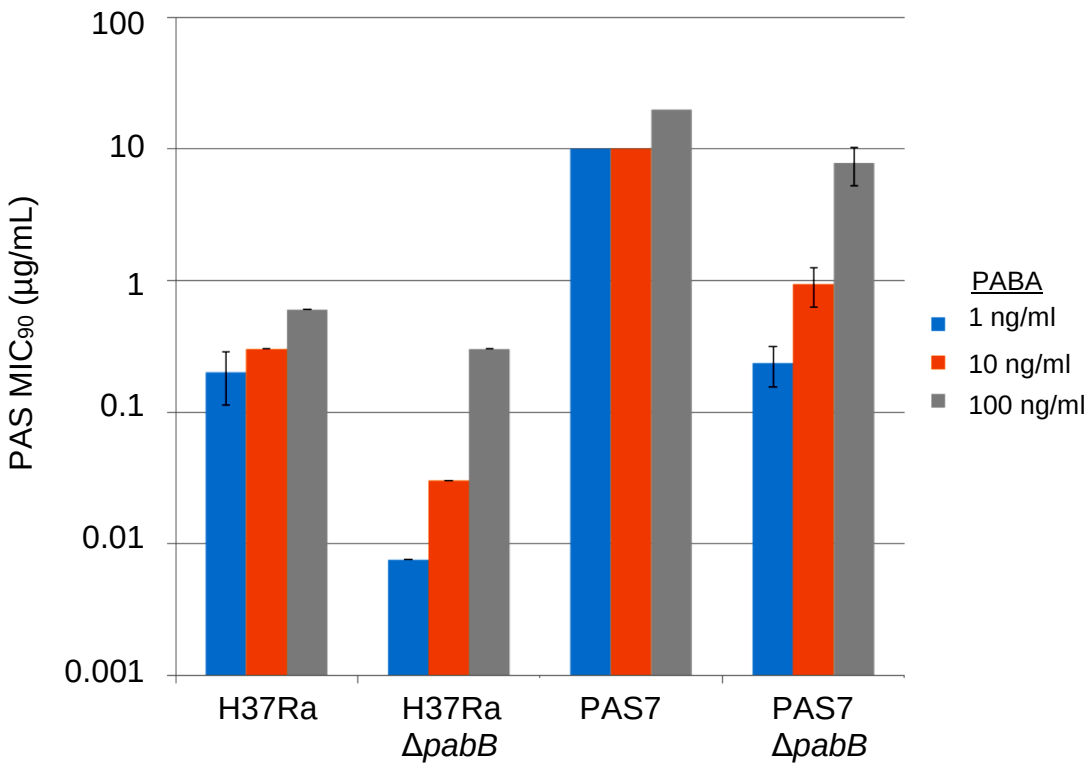

Figure 4.7. Restoration of susceptibility to PAS in *folC* mutant. *M. tuberculosis* strains were in 7H9 containing 1 ng/mL PABA and subcultured in varying concentrations of PABA and the PAS. The minimum inhibitory concentration (MIC_{90}) required to inhibit 90% growth was determined after two weeks of growth. Data represents three biological replicates with standard deviations indicated.

Chapter 5:

Conclusions

para-*Aminosalicylic acid selectively inhibits* Mycobacterium tuberculosis *dihydrofolate reductase*

Many antimicrobial agents have off target effects such as inhibition of commensal bacteria and impairment of human cells. This facet of drug action can present a problem in the context of the human gastrointestinal (GI) microbiota. It has long been known that this consortium of microbes provides protection from opportunistic gut pathogens through competition. Recently, there have been multiple studies showing the human GI microbiota is also important for development and maintenance of an effective and appropriate immune response(Belkaid and Hand, 2014; Cianci *et. al*., 2018; Levy *et. al*., 2017). Perturbations or loss of diversity within the GI microbiota have been shown to dampen the immune response to several pathogens(Belkaid and Hand, 2014; Cianci *et. al*., 2018; Levy *et. al*., 2017). For example, perturbations in the microbiota can promote virulence of the opportunistic pathogen, *Clostridium difficile*, leading to pseudomembranous colitis (Bien *et. al*., 2013). To prevent off target effects on the host and beneficial microbiota, there is an increased need to develop drugs that selectively inhibit a pathogen of interest.

para-Aminosalicylic acid (PAS) has been in clinical use for treatment of tuberculosis for over 70 years. Previous work suggests that PAS targets the folate biosynthesis pathway, specifically by inhibiting dihydrofolate reductase

(FolA) in *Mycobacterium tuberculosis* (Chakraborty *et. al*., 2013; Dawadi *et. al*., 2017; Youmans *et. al*., 1947; Zhao *et. al*., 2014; Zheng *et. al*., 2013). Interestingly, PAS has shown no activity against any other bacterial species that has been evaluated (Ivanovics *et. al*., 1948; Ragaz, 1948; Sievers, 1946; Tobie and Jones, 1949; Wyss, 1943). We built upon these studies and demonstrated that PAS is converted to hydroxy-dihydrofolate (DHF) that subsequently inhibits FolA. Until this study, it was unclear why other bacteria do not show PAS susceptibility. Possible resistance mechanisms to PAS included lack of uptake, exclusion, inactivation, failure to synthesize hydroxy-DHF and lack of inhibition of FolA by hydroxy-DHF. Using biochemical assays, we determined that hydroxy-DHF does not inhibit FolA from other bacterial species that we tested. Rather, FolA from other microbes is able to utilize hydroxy-DHF as a suitable substrate for reduction to hydroxy-tetrahydrofolate. Importantly, we found that these other microbes were able to utilize PAS *in lieu* of PABA in folate synthesis and these PAS-containing folates could be used as a cofactor for one carbon metabolism. Thus, we conclude that PAS selectivity is endowed with a specific structural feature of the *M. tuberculosis* FolA. Interestingly, the broad spectrum FolA inhibitor trimethoprim (TMP) has poor activity against *M. tuberculosis*(Dias *et. al*., 2014). This suggests that FolA could be exploited as a selective target for inhibiting *M. tuberculosis*. These observations will be instrumental in development of more potent next generation FolA inhibitors that maintain selectivity but have fewer off target effects.

There are two hypotheses that could account for PAS selectivity for the *M. tuberculosis* FolA. First, based on our studies, $FolA_{Mtb}$ Q28 is responsible for forming an additional hydrogen bond with hydroxy-DHF. This hydrogen bond is absent in $FolA_{E.coli}$. Second, the active site in $FolA_{Mtb}$ is much smaller and more hydrophilic compared to $FolA_{E.coli}$ that is larger and more hydrophobic. These differences could be utilized to create more potent and selective $FolA_{Mtb}$ inhibitor. One such modification could involve making the hydroxy-group on PAS more electronegative. Replacing the hydroxyl group with a fluorine or chlorine is predicted to allow for stronger hydrogen bond interactions. Another potential approach would be to modify the hydroxyl group on PAS to make it a bulky functional group, such as replacing it with an acetyl group. However, protein structural studies of $FolA_{Mtb}$ and $FolA_{Ec}$ complexed with hydroxy-folate need to be completed before any meaningful structure-based discovery campaigns can be performed.

The mechanistic basis for para*-aminosalicylic acid toxicity and resulting antagonism by sulfa-drugs*

PAS is primarily used to treat drug resistant strains of *M. tuberculosis*, due to its severe side effects. The main side effect is GI distress, causing many patients to

discontinue treatment. Historically, physicians have attributed GI distress to the presence of impurities due to instability of PAS or toxic compounds that arose during synthesis(Mitchell *et. al*., 1954). We determined that bacteria of the GI tract can utilize PAS to produce a cytotoxic hydroxylated folate species, such as hydroxy-DHF and hydroxy-folate. We hypothesize that hydroxylated folates cause the depolarization of tight junctions. The collapse of tight junctions allows for bacteria in the GI tract to transverse into the lamina propria resulting in sepsis. Our data strongly suggest that to avoid GI distress, PAS should not be given orally in its current dosage or in the current form. For PAS to be used as a well-tolerated antitubercular agent it should be modified such that it is not utilized or accessible by GI bacteria.

In an attempt to counter this toxicity, we co-treated mice with SMX to prevent PAS incorporation into hydroxy-folates in the GI tract. This approach prevented toxicity but also demonstrated that SMX can antagonize the antitubercular activity of PAS. Our data suggest that this antagonism was mediated by increased flux through pterin biosynthesis. While these observations indicate that SMX cannot be used to mitigate GI distress caused by PAS, they do provide proof of concept that PAS-mediated GI distress can be mitigated through manipulation of the gut microbiota.

Alternative mechanisms to reduce PAS toxicity

Another mechanism to reduce PAS GI distress may be to orally administer high doses of folinic acid. Folinic acid, also known as leucovorin, is a 5-formyl derivative of tetrahydrofolate and is used with treatment regimens involving drugs that target the folate pathway in humans. Both the cancer chemotherapeutic agent methotrexate (MTX) and the antiprotozoan drug pyrimethamine are given orally and are associated with GI distress and toxicity. To counter this toxicity these drugs are typically prescribed with folinic acid (Goldman and Matherly, 1987). Co-treating with folinic acid prevents some off-target effects of MTX by allowing some synthesis of purines and pyrimidines to occur.

PAS toxicity could also be reduced by administering pro-drug formulations that enable selective release only at the site of infection. This approach would prevent PAS from being taken up by other bacteria and prevent off target effects. One such strategy that has been used in treating cancer involves conjugating drugs to tumor specific antibodies that are taken up via receptor mediated endocytosis(Dan *et. al*., 2018). The antibody-drug conjugate is trafficked to the lysosome where the acidic pH catalyzes release the drug(Ekins, 2014). There are currently two FDA approved antibody-drug conjugates(Ornes, 2013). Using this knowledge, we could design PAS-antibody conjugates that selectively target macrophages. A similar approach would be to conjugate PAS to a nanoparticle

that can be readily phagocytosed by macrophages (Rattan *et. al*., 2017). Drug delivery by nanoparticles has been used to target cancer cells and macrophages (Rattan *et. al*., 2017). Another potential selective release approach could utilize a beta-lactam-PAS conjugate that can only be cleaved by *M. tuberculosis* specific beta-lactamase(Majewski *et. al*., 2016). Beta-lactamases are secreted proteins, therefore the PAS-conjugates would be cleaved to release PAS only in the vicinity of *M. tuberculosis*. Feasibility of these targeted delivery approaches would be dependent upon achieving a critical concentration of PAS at the site of infection.

Other PAS implications for human health

Sulfonamides are used to treat a wide array of bacterial, fungal and protozoan infections. Importantly, SMX is given as prophylactic therapy to prevent opportunistic infections in HIV-positive individuals. The data presented in this dissertation can be used to inform physicians of possible drug-drug interactions between sulfonamides and PAS.

In certain areas of the world HIV-TB co-infections are common. According to the WHO roughly 200,000 people are co-infected with HIV-TB(WHO, 2018). Thus, it is likely that a subset of patients have been prescribed SMX for prophylactic HIV-therapy and PAS to treat MDR-TB. Since co-treatment with SMX antagonized the

activity of PAS in our *in vitro* and *in vivo* studies, we propose that PAS and SMX co-treatment needs to be reevaluated in a clinical setting.

Further, since hydroxy-folates could be causing toxicity in other areas of the body, research focused on measuring hydroxy-folates in the blood stream are warranted. As a folate-rich diet is critical to support normal fetal development in pregnant women, hydroxy-folates found within the circulatory system could pose a complication in this population. If hydroxy-folates can cross the placental barrier they could cause neural defects or other developmental disorders in the fetus. While it is possible that this danger could be mitigated by co-administering PAS and folinic acid, safety of PAS treatment in pregnant women should be evaluated.

Recently, associations have been made between development of autism and mutations in the gene for MTHFR, methylenetetrahydrofolate reductase(Boris *et. al*., 2004). In humans, MTHFR converts 5,10-methylenetetrahydrofolate and NADPH to 5-methyltetrahydrofolate and $NADP^+$. 5,10-methyltetrahydrofolate is the methyl donor for synthesis of methionine from homocysteine via methionine synthase. Pregnant women who carry the *MTHFR* C677T polymorphism have a higher chance of having a child with autism(Boris *et. al*., 2004). Furthermore, infants who are homozygous for this polymorphism are at a higher risk for

developing autism and may be given folinic acid as a preventive measure (Boris *et. al*., 2004). Although a causal association between mutations in MTHFR and autism is still controversial, there are speculations that it may occur via impaired folate metabolism (Boris *et. al*., 2004; Raghavan *et. al*., 2018; Sener *et. al*., 2014). Thus, if hydroxy-folates impair folate metabolism, PAS treatment in pregnant women could contribute to autism or other disorders in the developing fetus. As folates are abundant in breast milk, it may be beneficial to co-administer folinic acid to nursing women taking PAS. A systematic study of the impact of PAS on fetal and childhood development in pregnant or breastfeeding women is essential to address this important concern.

Final Conclusions

My dissertation is the first to determine that PAS selectively inhibits *M. tuberculosis* dihydrofolate reductase enzyme and subsequently, the folate biosynthetic pathway. It was further shown that using PAS and sulfonamides together prevented both drugs from working correctly against *M. tuberculosis* or against in other bacterial species. The results generated from this work will be used to inform the current clinical practices in combination therapy and foster a paradigm shift in the treatment regimen administered to HIV TB co-infected patients, leading to decreased mortality rates among this population.

BIBLIOGRAPHY

Achkar, J.M., Chan, J., and Casadevall, A. (2015). B cells and antibodies in the defense against *Mycobacterium tuberculosis* infection. *Immunol. Rev. 264*, 167–181.

Adamowicz, E.M., Flynn, J., Hunter, R.C., and Harcombe, W.R. (2018). Cross-feeding modulates antibiotic tolerance in bacterial communities. *ISME J. 12*, 2723–2735.

Agarwal, N., Lamichhane, G., Gupta, R., Nolan, S., and Bishai, W.R. (2009). Cyclic AMP intoxication of macrophages by a *Mycobacterium tuberculosis* adenylate cyclase. *Nature*. *460*, 98.

Aínsa, J.A., Blokpoel, M.C.J., Otal, I., Young, D.B., De Smet, K.A.L., and Martín, C. (1998). Molecular cloning and characterization of Tap, a putative multidrug efflux pump present in *Mycobacterium fortuitum* and *Mycobacterium tuberculosis. J. Bacteriol. 180*, 5836–5843.

Akiba, T., Koyama, K., Ishiki, Y., Kimura, S., and Fukushima, T. (1960). On the mechanism of the development of multiple-drug-resistant clones of *Shigella*. *Japanese Jounral Microbiol. 4*, 219–227.

Alsaad, N., Van Altena, R., Pranger, A.D., Van Soolingen, D., De Lange, W.C.M., Van Der Werf, T.S., Kosterink, J.G.W., and Alffenaar, J.W.C. (2013). Evaluation of co-trimoxazole in the treatment of multidrug-resistant tuberculosis. *Eur. Respir. J. 42*, 504–512.

Argyrou, A., Vetting, M.W., Aladegbami, B., and Blanchard, J.S. (2006). *Mycobacterium tuberculosis* dihydrofolate reductase is a target for isoniazid. *Nat. Struct. Mol. Biol*. *13*, 408–413.

Armstrong, J.A., and Hart, P.D. (1975). Phagosome-lysosome interactions in cultured macrophages infected with virulent tubercle bacilli. Reversal of the usual nonfusion pattern and observations on bacterial survival. *J. Exp. Med. 142*, 1–16.

Aschhoff, H.S., and Vergin, H. (1979). Tetroxoprim-a new inhibitor of bacterial dihydrofolate reductase. *J. Antimicrob. Chemother*. *5*, 19–25.

Auerbach, G., Herrmann, A., Bracher, A., Bader, G., Gutlich, M., Fischer, M., Neukamm, M., Garrido-Franco, M., Richardson, J., Nar, H., *et al*. (2000). Zinc

plays a key role in human and bacterial GTP cyclohydrolase I. *Proc. Natl. Acad. Sci*. *97*, 13567–13572.

Baba, T., Ara, T., Hasegawa, M., Takai, Y., Okumura, Y., Baba, M., Datsenko, K.A., Tomita, M., Wanner, B.L., and Mori, H. (2006). Construction of *Escherichia coli* K-12 in-frame, single-gene knockout mutants: The Keio collection. *Mol. Syst. Biol*. *2*. 2006.0008.

Babaoglu, K., Qi, J., Lee, R.E., and White, S.W. (2004). Crystal structure of 7,8-dihydropteroate synthase from *Bacillus anthracis*: Mechanism and novel inhibitor design. *Structure 12*, 1705–1717.

Baca, A.M., Sirawaraporn, R., Turley, S., Sirawaraporn, W., and Hol, W.G.J. (2000). Crystal structure of *Mycobacterium tuberculosis* 6-hydroxymethyl-7,8-dihydropteroate synthase in complex with pterin monophosphate: New insight into the enzymatic mechanism and sulfa-drug action. *J. Mol. Biol*. *302*, 1193–1212.

Balcewicz-Sablinska, M.K., Keane, J., Kornfeld, H., and Remold, H.G. (1998). Pathogenic *Mycobacterium tuberculosis* evades apoptosis of host macrophages by release of TNF-R2, resulting in inactivation of TNF-alpha. *J. Immunol. 161*, 2636–2641.

Banerjee, A., Dubnau, E., Quemard, A., Balasubramanian, V., Um, K.S., Wilson, T., Collins, D., de Lisle, G., and Jacobs, W.R. (1994). *inhA*, a gene encoding a target for isoniazid and ethionamide in *Mycobacterium tuberculosis*. *Science 263*, 227–230.

Banerjee, D., Mayer-Kuckuk, P., Capiaux, G., Budak-Alpdogan, T., Gorlick, R., and Bertino, J.R. (2002). Novel aspects of resistance to drugs targeted to dihydrofolate reductase and thymidylate synthase. *Biochim. Biophys. Acta - Mol. Basis Dis. 1587*, 164–173.

Banerjee, R. V, Shane, B., McGuire, J.J., and Coward, J.K. (1988). Dihydrofolate synthetase and folylpolyglutamate synthetase: direct evidence for intervention of acyl phosphate intermediates. *Biochemistry 27*, 9062–9070.

Barry, C.E., Boshoff, H.I., Dartois, V., Dick, T., Ehrt, S., Flynn, J.A., Schnappinger, D., Wilkinson, R.J., and Young, D. (2009). The spectrum of latent tuberculosis: Rethinking the biology and intervention strategies. *Nat. Rev. Microbiol*. *7*, 845–855.

Bardarov, S., Bardarov, S., Bardarov, S., Pavelka, M.S., Sambandamurthy, V.,

Larsen, M., Tufariello, J., Chan, J., Hartfull, G., and Jacobs W.R. (2002). Specialized transduction : an efficient method for generating marked and unmarked targeted gene disruptions in *Mycobacterium tuberculosis, M. bovis* BCG*,* and *M. smegmatis*. *Microbiology 148*, 3007–3017.

Baughn, A.D., and Malamy, M.H. (2002). A mitochondrial-like aconitase in the bacterium *Bacteroides fragilis*: Implications for the evolution of the mitochondrial Krebs cycle. *Proc. Natl. Acad. Sci*. *99*, 4662–4667.

Baughn, A.D., Deng, J., Vilchèze, C., Riestra, A., Welch, J.T., Jacobs, W.R., and Zimhony, O. (2010). Mutually exclusive genotypes for pyrazinamide and 5-chloropyrazinamide resistance reveal a potential resistance-proofing strategy. *Antimicrob. Agents Chemother*. *54*, 5323–5328.

Behiry, E.M., Luk, L.Y.P., Matthews, S.M., Loveridge, E.J., and Allemann, R.K. (2014). Role of the occluded conformation in bacterial dihydrofolate reductases. *Biochemistry 53*, 4761–4768.

Behr, M.A., Edelstein, P.H., and Ramakrishnan, L. (2018). Revisiting the timetable of tuberculosis. *BMJ 362*, 1-10.

Belkaid, Y., and Hand, T.W. (2014). Role of the microbiota in immunity and inflammation. *Cell 157*, 121–141.

Bennett, B., Langan, P., Coates, L., Mustyakimov, M., Schoenborn, B., Howell, E.E., and Dealwis, C. (2006). Neutron diffraction studies of *Escherichia coli* dihydrofolate reductase complexed with methotrexate. *Proc. Natl. Acad. Sci. 103*, 18493–18498.

Berman, H.M., Westbrook, J., Feng, Z., Gilliland, G., Bhat, T.N., Weissig, H., Shindyalov, I.N., and Bourne, P.E. (2000). The Protein Data Bank Helen. N*ucleic Acids Res*. *28*, 235–242.

Bernheim, F. (1940). The effect of salicylate on the oxygen uptake of the tubercle bacillus. *Science*. *92*, 204.

Beutheu Youmba, S., Belmonte, L., Galas, L., Boukhettala, N., Bôle-Feysot, C., Déchelotte, P., and Coëffier, M. (2012). Methotrexate modulates tight junctions through NF-κB, MEK, and JNK Pathways. *J. Pediatr. Gastroenterol. Nutr*. *54*, 463–470.

Bihelovic, F., Karadzic, I., Matovic, R., and Saicic, R.N. (2013). Total synthesis

and biological evaluation of (-)-*atrop*-abyssomicin C. *Org. Biomol. Chem*. *11*, 5413–5424.

Bien, J., Palagani, V., and Bozko, P. (2013). The intestinal microbiota dysbiosis and *Clostridium difficile* infection: Is there a relationship with inflammatory bowel disease? *Therap. Adv. Gastroenterol*. *6*, 53–68.

Bjartveit, K. (2003). Olaf Scheel and Johannes Heimbeck: their contribution to understanding the pathogenesis and prevention of tuberculosis. *Int. J. Tuberc. Lung Dis. 7*, 306–311.

Blaszczyk, J., Shi, G., Yan, H., and Ji, X. (2000). Catalytic center assembly of HPPK as revealed by the crystal structure of a ternary complex at 1.25 Å resolution. *Structure 8*, 1049–1058.

Blaszczyk, J., Li, Y., Gan, J., Yan, H., and Ji, X. (2007). Structural Basis for the Aldolase and Epimerase Activities of *Staphylococcus aureus* Dihydroneopterin Aldolase. *J. Mol. Biol. 368*, 161–169.

Blau, N., and Niederwieser, A. (1986). The application of 8-aminoguanosine triphosphate, a new inhibitor of GTP cyclohydrolase I, to the purification of the enzyme from human liver. *Biochim. Biophys. Acta 880*, 26–31.

Blum, J.S., Wearsch, P.A., and Cresswell, P. (2013). Pathways of Antigen Processing. *Annu. Rev. Immunol. 31*, 443–473.

Bognar, A.L., Osborne, C., Shane, B., Singer, S.C., and Ferone, R. (1985). Folylpoly-γ-glutamate synthetase-dihydrofolate synthetase. Cloning and high expression of the *Escherichia coli folC* gene and purification and properties of the gene product. *J. Biol. Chem. 260*, 5625–5630.

Boris, M., Goldblatt, A., Galanko, J., and James, S.J. (2004). Association of *MTHFR* Gene Variants with Autism. *J. Am. Physicians Surg*. *9*, 106–108.

Boshoff, H.I., Mizrahi, V., and Barry, C.E. (2002). Effects of Pyrazinamide on Fatty Acid Synthesis by Whole Mycobacterial Cells and Purified Fatty Acid Synthase I. *J. Bacteriol. 184*, 2167–2172.

Bourne, C. (2014). Utility of the Biosynthetic Folate Pathway for Targets in Antimicrobial Discovery. *Antibiotics 3*, 1–28.

Brennan, P.. (2003). Structure, function, and biogenesis of the cell wall of *Mycobacterium tuberculosis*. *Tuberculosis 83*, 91–97.

Brennan, P.J., and Nikaido, H. (1995). The Envelope of *Mycobacteria*. *Annu. Rev. Biochem*. *64*, 29–63.

Brites, D., and Gagneux, S. (2012). Old and new selective pressures on *Mycobacterium tuberculosis. Infect. Genet. Evol*. *12*, 678–685.

Brosch, R., Gordon, S. V., Marmiesse, M., Brodin, P., Buchrieser, C., Eiglmeier, K., Garnier, T., Gutierrez, C., Hewinson, G., Kremer, K., *et al*. (2002). A new evolutionary scenario for the *Mycobacterium tuberculosis* complex. *Proc. Natl. Acad. Sci*. *99*, 3684–3689.

Burchall, J.J., and Hitchings, G.H. (1965). Inhibitor binding analysis of dihydrofolate reductases from various species. *Mol. Pharmacol*. *1*. 126-136.

Bushby, M., and Hitchings, G.H. (1968). Trimethoprim, a sulphonamide poteniator. *Br. J. Pharmacol. Chemother. 90*, 72–90.
Calvori, C., Frontali, L., Leoni, L., and Tecce, G. (1965). Effect of Rifamycin on Protein Synthesis. *Nature 207*, 417–418.

Canfield, C.J., Milhous, W.K., Ager, A.L., Rossan, R.N., and Sweeney, T.R. (1993). PS-15: a potent, orally active antimalarial from a new class of folic acid antagonists. *Am J Trop Med Hyg. 49*, 121–126.

Cannon, W.R., Garrison, B.J., and Benkovic, S.J. (1997). Electrostatic Characterization of Enzyme Complexes: Evaluation of the Mechanism of Catalysis of Dihydrofolate Reductase. *J. Am. Chem. Soc. 119*, 2386–2395.

Carrington, H.C., Crowther, A.F., Davey, D.G., Levi, A.A., and Rose, F. (1951). A metabolite of ’Paludrine’with high antimalarial activity. *Nature 168*, 1080.

Cersini, A., Salvia, A.M., and Bernardini, M.L. (1998). Intracellular multiplication and virulence of *Shigella flexneri* auxotrophic mutants. *Infect. Immun*. *66*, 549–557.

Chakraborty, S., Gruber, T., Barry, C., Boshoff, H., and Rhee, K. (2013). *para*-Aminosalicylic Acid Acts as an Alternative Substrate of Folate Metabolism in *Mycobacterium tuberculosis*. *Science 339*, 88–91.

Chan, J., Xing, Y., Magliozzo, R.S., and Bloom, B.R. (1992). Killing of Virulent *Mycobacterium tuberculosis* by Reactive Nitrogen Intermediates Produced by Activated Murine Macrophages. *Journal Exp. Med. 175*, 1111–1122.

Chang, C.C., Mina, M., Post, J.J., Cameron, B.A., Lloyd, A.R., French, M.A., Lewin, S.R., Chang, C.C., Crane, M., Zhou, J., *et al*. (2013). HIV and co-infections. *Immunol. Rev*. *254*, 114–142.

Chang, J.C., Miner, M.D., Pandey, A.K., Gill, W.P., Harik, N.S., Sassetti, C.M., and Sherman, D.R. (2009). *igr* genes and *Mycobacterium tuberculosis* cholesterol metabolism. *J. Bacteriol*. *191*, 5232–5239.

Chen, Y.Q., Kraut, J., Blakley, R.L., and Callender, R. (1994). Determination by Raman Spectroscopy of the pKa of N5 of Dihydrofolate Bound to Dihydrofolate Reductase: Mechanistic Implications. *Biochemistry 33*, 7021–7026.

Chhabra, S., Dolezal, O., Collins, B.M., Newman, J., Simpson, J.S., Macreadie, I.G., Fernley, R., Peat, T.S., and Swarbrick, J.D. (2012). Structure of S. aureus HPPK and the discovery of a new substrate site inhibitor. *PLoS One 7*. 1-16.

Chhabra, S., Barlow, N., Dolezal, O., Hattarki, M.K., Newman, J., Peat, T.S., Graham, B., and Swarbrick, J.D. (2013). Exploring the Chemical Space around 8-Mercaptoguanine as a Route to New Inhibitors of the Folate Biosynthesis Enzyme HPPK. *PLoS One 4*. 1-14.

Chiaradia, L., Lefebvre, C., Parra, J., Marcoux, J., Burlet-Schiltz, O., Etienne, G., Tropis, M., and Daffé, M. (2017). Dissecting the mycobacterial cell envelope and defining the composition of the native mycomembrane. *Sci. Rep*. *7*, 1–12.

Chisholm, R.H., Trauer, J.M., Curnoe, D., and Tanaka, M.M. (2016). Controlled fire use in early humans might have triggered the evolutionary emergence of tuberculosis. *Proc. Natl. Acad. Sci. 113*, 9051–9056.

Chow, S., Shao, J., and Wang, H. (2008). Sample size calculations in clinical research (Boca Raton, FL: Chapman & Hall/CRC).

Cianci, R., Pagliari, D., Piccirillo, C.A., Fritz, J.H., and Gambassi, G. (2018). The Microbiota and Immune System Crosstalk in Health and Disease. *Mediators Inflamm*. *2018*, 1–3.

Colditz, G.A., Berkey, C.S., Mosteller, F., Brewer, T.F., Wilson, M.E., Burdick, E., and Fineberg, H. V (1995). The Efficacy of Bacillus Calmette-Guérin Vaccination of Newborns and Infants in the Prevention of Tuberculosis: Meta-Analyses of the Published Literature. *Pediatrics 96*, 29–35.

Collins, C.A., De Mazière, A., Van Dijk, S., Carlsson, F., Klumperman, J., and Brown, E.J. (2009). Atg5-independent sequestration of ubiquitinated mycobacteria. *PLoS Pathog*. *5*.

Cronstein, B.N. (2005). Low-Dose Methotrexate: A Mainstay in the Treatment of Rheumatoid Arthritis. *Pharmacol. Rev. 57*, 163–172.

Czekster, C.M., Vandemeulebroucke, A., and Blanchard, J.S. (2011). Kinetic and chemical mechanism of the dihydrofolate reductase from *Mycobacterium tuberculosis*. *Biochemistry 50*, 367–375.

Daher, R., and Therisod, M. (2010). Highly Selective Inhibitors of Class II Microbial Fructose Bis-phosphate Aldolases. *ACS Med. Chem. Lett*. *1*, 101–104.

Dale, G.E., Broger, C., Arcy, A. D', Hartman, P.G., DeHoogt, R., Jolidon, S., Kompis, I., Labhardt, A.M., Langen, H., Locher, H., *et al.* (1997). A single amino acid substitution in *Staphylococcus aureus* dihydrofolate reductase determines trimethoprim resistance. *J. Mol. Biol*. *266*, 23–30.

Dan, N., Setua, S., Kashyap, V.K., Khan, S., Jaggi, M., Yallapu, M.M., and Chauhan, S.C. (2018). Antibody-drug conjugates for cancer therapy: Chemistry to clinical implications. *Pharmaceuticals 11*.

Davenne, T., and McShane, H. (2016). Why don't we have an effective tuberculosis vaccine yet? *Expert Rev. Vaccines 15*, 1009–1013.

Davis, J.M., and Ramakrishnan, L. (2009). The Role of the Granuloma in Expansion and Dissemination of Early Tuberculous Infection. *Cell 136*, 37–49.

Dawadi, S., Kordus, S.L., Baughn, A.D., and Aldrich, C.C. (2017). Synthesis and analysis of bacterial folate metabolism intermediates and antifolates. *Org. Lett. 19*. 5220-5223.

Dennis, M.L., Lee, M.D., Harjani, J.R., Ahmed, M., DeBono, A.J., Pitcher, N.P., Wang, Z.C., Chhabra, S., Barlow, N., Rahmani, R., *et al*. (2018). 8-Mercaptoguanine Derivatives as Inhibitors of Dihydropteroate Synthase. *Chem. A Eur. J*. *24*, 1922–1930.

Desta, Z., Zhao, X., Shin, J.-G., and Flockhart, D.A. (2002). Clinical Significance of the Cytochrome P450 2C19 Genetic Polymorphism. *Clin Pharmacokinet 41*, 913–958.

Dias, M.V.B., Tyrakis, P., Domingues, R.R., Leme, A.F.P., and Blundell, T.L. (2014). *Mycobacterium tuberculosis* dihydrofolate reductase reveals two conformational states and a possible low affinity mechanism to antifolate drugs. *Structure 22*, 94–103.

Diedrich, C.R., and Flynn, J.A.L. (2011). HIV-1/*Mycobacterium tuberculosis* coinfection immunology: How does HIV-1 exacerbate tuberculosis? *Infect. Immun*. *79*, 1407–1417.

Dillon, N.A., Peterson, N.D., Feaga, H.A., Keiler, K.C., and Baughn, A.D. (2017). Anti-tubercular Activity of Pyrazinamide is Independent of *trans*-Translation and RpsA. Sci. Rep. *7*, 1–8.

Divangahi, M., Desjardins, D., Nunes-Alves, C., Remold, H.G., and Behar, S.M. (2010). Eicosanoid pathways regulate adaptive immunity to *Mycobacterium tuberculosis*. *Nat. Immunol*. *11*, 751.

Doitsh, G., Galloway, N.L.K., Geng, X., Yang, Z., Monroe, K.M., Zepeda, O., Hunt, P.W., Hatano, H., Sowinski, S., Muñoz-Arias, I., *et al*. (2013). Cell death by pyroptosis drives CD4 T-cell depletion in HIV-1 infection. *Nature 505*, 509.

Donald, P.R., and Diacon, A.H. (2015). Para-aminosalicylic acid: the return of an old friend. *Lancet Infect. Dis*. *15*, 1091–1099.

Drlica, K., and Zhao, X. (1997). DNA gyrase, topoisomerase IV, and the 4-quinolones. *Microbiol. Mol. Biol. Rev*. *61*, 377–392.

Ebert, D., and Bull, J.J. (2003). Challenging the trade-off model for the evolution of virulence: is virulence management feasible? *Trends Microbiol*. *11*, 15–20.

Ekins, S. (2014). Hacking into the granuloma: Could antibody antibiotic conjugates be developed for TB? *Tuberculosis 94*, 715–716.

Ercikan-Abali, E.A., Mineishi, S., Tong, Y., Nakahara, S., Waltham, M.C., Banerjee, D., Chen, W., Sadelain, M., and Bertino, J.R. (1996). Active site-directed double mutants of dihydrofolate reductase. *Cancer Res*. *56*, 4142–4145.

Erdei, A., and Snell, W.E. (1948). Pulmonary Tuberculosis Treated with *p*-Aminosalicylic Acid: Early Results in 6 Cases. *Lancet 251*, 791–793.

Ernst, J.D. (2012). The immunological life cycle of tuberculosis. *Nat. Rev. Immunol. 12*, 581–591.

Fedrizzi, T., Meehan, C.J., Grottola, A., Giacobazzi, E., Fregni Serpini, G., Tagliazucchi, S., Fabio, A., Bettua, C., Bertorelli, R., De Sanctis, V., *et al.* (2017). Genomic characterization of Nontuberculous *Mycobacteria*. *Sci. Rep*. *7*, 1–14.

Ferebee, S., Doster, B., and Murray, F. (1966). Ethambutol: a substitute for *para*-

aminosalicylic acid in regimens for pulmonary tuberculosis. *Ann N Y Acad Sci 135*, 910–920.

Fierke, C.A., Johnson, K.A., and Benkovic, S.J. (1987). Construction and Evaluation of the Kinetic Scheme Associated with Dihydrofolate Reductase from *Escherichia coli. Biochemistry 26*, 4085–4092.

Fine, P.E.M. (1995). Variation in protection by BCG: implications of and for heterologous immunity. *Lancet 346*, 1339–1345.

Fischer, M., Auerbach, G., Hösl, C., Rebelo, J., Kaiser, J., Schramek, N., Bracher, A., Nar, H., Bacher, A., Bader, G., *et al*. (2003). Biosynthesis of Pteridines. Reaction Mechanism of GTP Cyclohydrolase I. *J. Mol. Biol*. *326*, 503–516.

Fivian-Hughes, A.S., Houghton, J., and Davis, E.O. (2012). *Mycobacterium tuberculosis* thymidylate synthase gene *thyX* is essential and potentially bifunctional, while *thyA* deletion confers resistance to *p*-aminosalicylic acid. *Microbiology 158*, 308–318.

Floyd, J.L., Smith, K.P., Kumar, S.H., Floyd, J.T., and Varela, M.F. (2010). LmrS is a multidrug efflux pump of the major facilitator superfamily from *Staphylococcus aureus. Antimicrob*. *Agents Chemother. 54*, 5406–5412.

Forrellad, M.A., Klepp, L.I., Gioffré, A., y García, J.S., Morbidoni, H.R., de la Paz Santangelo, M., Cataldi, A.A., and Bigi, F. (2013). Virulence factors of the *Mycobacterium tuberculosis* complex. *Virulence 4*, 3–66.

Forsman, L.D., Schön, T., Simonsson, U.S.H., Bruchfeld, J., Larsson, M., Juréen, P., Sturegård, E., Giske, C.G., and Ängebyh, K. (2014). Intra- And extracellular activities of trimethoprim-sulfamethoxazole against susceptible and multidrug-resistant *Mycobacterium tuberculosis*. *Antimicrob. Agents Chemother*. *58*, 7557–7559.

Freilich, E.B., Coe, G.C., and Wien, N.A. (1939). The use of sulfanilamide in pulmonary tuberculosis; Preliminary report. *Ann. Intern. Med. 13*, 1042–1045.

Freisleben, A., Schieberle, P., and Rychlik, M. (2002). Syntheses of Labeled Vitamers of Folic Acid to Be Used as Internal Standards in Stable Isotope Dilution Assays. *J. Agric. Food Chem*. *50*, 4760–4768.

Freundlich, J.S., Lalgondar, M., Wei, J.-R., Swanson, S., Sorensen, E.J., Rubin,

E.J., and Sacchettini, J.C. (2010). The Abyssomicin C family as in vitro inhibitors of *Mycobacterium tuberculosis*. *Tuberculosis 90*, 298–300.

Gabelli, S.B., Bianchet, M.A., Xu, W., Dunn, C.A., Niu, Z.D., Amzel, L.M., and Bessman, M.J. (2007). Structure and Function of the *E. coli* Dihydroneopterin Triphosphate Pyrophosphatase: A Nudix Enzyme Involved in Folate Biosynthesis. *Structure 15*, 1014–1022.

Gagneux, S. (2018). Ecology and evolution of *Mycobacterium tuberculosis*. *Nat. Rev. Microbiol. 16*, 202–213.

Ganguly, N., Siddiqui, I., and Sharma, P. (2008). Role of *M. tuberculosis* RD-1 region encoded secretory proteins in protective response and virulence. *Tuberculosis 88*, 510–517.

Garçon, A., Levy, C., and Derrick, J.P. (2006). Crystal Structure of the Bifunctional Dihydroneopterin Aldolase/6-hydroxymethyl-7,8-dihydropterin Pyrophosphokinase from *Streptococcus pneumoniae*. *J. Mol. Biol*. *360*, 644–653.

Garg, H., Mohl, J., and Joshi, A. (2012). HIV-1 induced bystander apoptosis. *Viruses 4*, 3020–3043.

Gerum, A., Ulmer, J., Jacobus, D., Sherman, D., and Sibley, C. (2002). Novel Saccharomyces cerevisiae screen identifies WR99210 analogues that inhibit *Mycobacterium tuberculosis* dihydrofolate reductase. *Antimicrob. Agents Chemother*. *46*, 3362–3369.

Giladi, M., Altman-Price, N., Levin, I., Levy, L., and Mevarech, M. (2003). FolM, A New Chromosomally Encoded Dihydrofolate Reductase in *Escherichia coli*. *J. Bacteriol*. *185*, 7015–7018.

Glover, R.T., Kriakov, J., Garforth, S.J., Baughn, A.D., and Jacobs, W.R. (2007). The two-component regulatory system *senX3-regX3* regulates phosphate-dependent gene expression in *Mycobacterium smegmatis*. *J. Bacteriol*. *189*, 5495–5503.

Göker, E., Waltham, M., Kheradpour, A., Trippett, T., Mazumdar, M., Elisseyeff, Y., Schnieders, B., Steinherz, P., Tan, C., and Berman, E. (1995). Amplification of the dihydrofolate reductase gene is a mechanism of acquired resistance to methotrexate in patients with acute lymphoblastic leukemia and is correlated with p53 gene mutations. *Blood 86*, 677–684.

Goldman, I.D., and Matherly, L.H. (1987). Biochemical factors in the selectivity of

leucovorin rescue: selective inhibition of leucovorin reactivation of dihydrofolate reductase and leucovorin utilization in purine and pyrimidine biosynthesis by methotrexate and dihydrofolate polyglutamates. *NCI Monogr. a Publ. Natl. Cancer Inst*. *5*, 17–26.

Gonen, N., and Assaraf, Y.G. (2012). Antifolates in cancer therapy: Structure, activity and mechanisms of drug resistance. Drug Resist. Updat. *15*, 183–210.
Grange, J.M., and Yates, M.D. (1995). The time-table of tuberculosis. Respir. Med. *89*, 313–314.

Gräwert, T., Fischer, M., and Bacher, A. (2013). Structures and reaction mechanisms of GTP cyclohydrolases. *IUBMB Life 65*, 310–322.

Green, J.M., and Nichols, B.P. (1991). *p*-Aminobenzoate biosynthesis in *Escherichia coli*: Purification of aminodeoxychorismate lyase and cloning of *pabC*. *J. Biol. Chem*. *266*, 12971–12975.

Green, J.M., Merkel, W.K., and Nichols, B.P. (1992). Characterization and sequence of *Escherichia coli pabC*, the gene encoding aminodeoxychorismate lyase, a pyridoxal phosphate-containing enzyme. *J. Bacteriol*. *174*, 5317–5323.

de Groot, R., Sluijter, M., Bruyn, A., Smith, A.L., and Hermans, P.W.M. (1996). Genetic Characterization of Trimethoprim Resistance in *Haemophilus influenzae*. *Antimicrob. Agents Chemother*. *40*, 2131–2136.

Grzegorzewicz, A.E., De Sousa-D'Auria, C., McNeil, M.R., Huc-Claustre, E., Jones, V., Petit, C., Angala, S.K., Zemanová, J., Wang, Q., Belardinelli, J.M., *et al*. (2016). Assembling of the *Mycobacterium tuberculosis* cell wall core. *J. Biol. Chem*. *291*, 18867–18879.

Guirado, E., Amat, I., Gil, O., Díaz, J., Arcos, V., Caceres, N., Ausina, V., and Cardona, P.J. (2006). Passive serum therapy with polyclonal antibodies against *Mycobacterium tuberculosis* protects against post-chemotherapy relapse of tuberculosis infection in SCID mice. *Microbes Infect*. *8*, 1252–1259.

Hammoudeh, D.I., Zhao, Y., White, S.W., and Lee, R.E. (2013). Replacing sulfa drugs with novel DHPS inhibitors. *Future Med. Chem. 5*, 1331–1340.

Harding, C. V, and Boom, W.H. (2010). Regulation of antigen presentation by *Mycobacterium tuberculosis*: a role for Toll-like receptors. *Nat. Rev. Microbiol*. *8*, 296.

Haruki, H., Pedersen, M.G., Gorska, K.I., Pojer, F., and Johnsson, K. (2013). Tetrahydrobiopterin Biosynthesis as an Off-Target of Sulfa Drugs. *Science 340*,

987–991.

Harvey, R.J. (1978). Interaction of two inhibitors which act on different enzymes of a metabolic pathway. *J. Theor. Biol. 74*, 411–437.

Hawn, T.R., Day, T.A., Scriba, T.J., Hatherill, M., Hanekom, W.A., Evans, T.G., Churchyard, G.J., Kublin, J.G., Bekker, L.G., and Self, S.G. (2014). Tuberculosis Vaccines and Prevention of Infection. *Microbiol. Mol. Biol. Rev*. *78*, 650–671.

Heikkila, E., Sundstrom, L., Skurnik, M., and Huovinen, P. (1991). Analysis of Genetic Localization of the Type I Trimethoprim Resistance Gene from *Escherichia coli* Isolated in Finland. *Antimicrob. Agents Chemother*. *35*, 1562–1569.

Henry, R. (1944). The Mode of Action of Sulfonamides. *J. Am. Chem. Soc*. *66*, 459–464.

Hershberg, R., Lipatov, M., Small, P.M., Sheffer, H., Niemann, S., Homolka, S., Roach, J.C., Kremer, K., Petrov, D.A., Feldman, M.W., *et al*. (2008). High functional diversity in Mycobacterium tuberculosis driven by genetic drift and human demography. *PLoS Biol. 6*, 2658–2671.

Hett, E.C., and Rubin, E.J. (2008). Bacterial Growth and Cell Division: a Mycobacterial Perspective. Microbiol. Mol. Biol. Rev*. 72*, 126–156.

Hevener, K.E., Yun, M., Qi, J., Kerr, I.D., Babaoglu, K., Julian, G., Balakrishna, K., White, S.W., and Lee, R.E. (2011). Structural Studies of Pterin-Based Inhibitors of Dihydropteroate Synthase. *Journal Med. Chem*. *53*, 166–177.

Hill, S.E., Nguyen, E., Ukachukwu, C.U., Freeman, D.M., Quirk, S., and Lieberman, R.L. (2017). Metal ion coordination in the *E . coli* Nudix hydrolase dihydroneopterin triphosphate pyrophosphatase : New clues into catalytic mechanism. *PLoS One 7*, 1–16.

Hitchings, G.H., Elion, G.B., Falco, E.A., Russell, P.B., and VanderWerff, H. (1950). Studies on analogs of purines and pyrimidines. *Ann. New York Acad. Sc. 52*, 1318–1335.

Hoekenga, M.T. (1954). The Treatment of Acute Malaria with Single Oral Doses of Amodiaquin, Chloroquine, Hydroxychloroquine, and Pyrimethamine. *Am. Jounral Trop. Med. Hyg. 3*, 833–836.

Howe, M.D., Kordus, S.L., Cole, M.S., Bauman, A.A., Aldrich, C.C., Baughn, A.D., and Minato, Y. (2018). Methionine Antagonizes *para*-Aminosalicylic Acid

Activity via Affecting Folate Precursor Biosynthesis in *Mycobacterium tuberculosis*. *Front. Cell. Infect. Microbiol*. *8*, 399.

Howell, E.E., Foster, P.G., and Foster, L.M. (1988). Construction of a Dihydrofolate Reductase-Deficient Mutant of *Escherichia coli* by Gene Replacement. *J. Bacteriol*. *170*, 3040–3045.

Huovinen, P., Sundstrom, L., Swedberg, G., and Skold, O. (1995). Trimethoprim and sulfonamide resistance. *Antimicrob. Agents Chemother*. *39*, 279–289.

Ivanovics, G., Csabi, I., and Diczfalusy, E. (1948). Some observations on the antibacterial action of sodium salicylate. *Hungaricaacta Physiol*. *1*, 171–179.

Jang, J., Becq, J., Gicquel, B., Deschavanne, P., and Neyrolles, O. (2008). Horizontally acquired genomic islands in the tubercle bacilli. *Trends Microbiol*. *16*, 303–308.

Jenne, J.W., MacDonald, F.M., and Mendoza, E. (1961). A Study of the Renal Clearances, Metabolic Inactivation Rates, and Serum Fall-Off Interaction of Isoniazid and *para*-Aminosalicylic Acid in Man. *Am. Rev. Respir. Dis*. *84*, 371–378.

JM, G., Yates, M.D., and de Kantor, I.N. (1996). WHO Guidelines for speciation within the *Mycobacterium tuberculosis* complex. 2nd ed. Lab. Equip.

Jones, J.S. (1954). Intravenous P.A.S. in relation to pulmonary tuberculotherapy, with an account of 1,145 transfusions. *Br. J. Tuberc. Dis. Chest 48*, 286–297.

De Jonge, M.I., Pehau-Arnaudet, G., Fretz, M.M., Romain, F., Bottai, D., Brodin, P., Honoré, N., Marchal, G., Jiskoot, W., England, P., et al. (2007). ESAT-6 from *Mycobacterium tuberculosis* dissociates from its putative chaperone CFP-10 under acidic conditions and exhibits membrane-lysing activity. *J. Bacteriol*. *189*, 6028–6034.

Jouanguy, E., Lamhamedi-Cherradi, S., Lammas, D., Dorman, S.E., Fondanèche, M.C., Dupuis, S., Döffinger, R., Altare, F., Girdlestone, J., Emile, J.F., *et al*. (1999). A human *IFNGR1* small deletion hotspot associated with dominant susceptibility to mycobacterial infection. *Nat. Genet*. *21*, 370.

Kang, P.B., Azad, A.K., Torrelles, J.B., Kaufman, T.M., Beharka, A., Tibesar, E., DesJardin, L.E., and Schlesinger, L.S. (2005). The human macrophage mannose receptor directs *Mycobacterium tuberculosis* lipoarabinomannan-mediated phagosome biogenesis. *J. Exp. Med. 202*, 987–999.

Kaplan, J.B., Goncharoff, P., Seibold, A. M., and Nichols, B.P. (1984). Nucleotide sequence of the *Acinetobacter calcoaceticus trpGDC* gene cluster. *Mol. Biol. Evol*. *1*, 456–472.

Kappock, T.J., and Caradonna, J.P. (1996). Pterin-Dependent Amino Acid Hydroxylases. *Chem. Rev*. *96*, 2659–2756.

Keane, J., Remold, H.G., and Kornfeld, H. (2000). Virulent Mycobacterium tuberculosis Strains Evade Apoptosis of Infected Alveolar Macrophages. J. Immunol. *164*, 2016–2020.

Keefe, D.M., Cummins, a G., Dale, B.M., Kotasek, D., Robb, T. a, and Sage, R.E. (1997). Effect of high-dose chemotherapy on intestinal permeability in humans. *Clin. Sci. (Lond). 92*, 385–389.

Keisu, M., Wilholm, B.E., and Palmblad, J. (1990). Trimethoprim-sulphamethoxazole-associated blood dyscrasias. Ten years'experience of the Swedish spontaneous reporting system. *J. Intern. Med*. *228*, 353–360.

Keller, S., Nicholson, G., Drahl, C., Sorensen, E., Fiedler, H.P., and Süssmuth, R.D. (2007a). Abyssomicins G and H and *atrop*-Abyssomicin C from the Marine Verrucosispora Strain AB-18-032. *J. Antibiot. (Tokyo)*. *60*, 391.

Keller, S., Schadt, H.S., Ortel, I., and Süssmuth, R.D. (2007b). Action of *atrop*-abyssomicin C as an inhibitor of 4-amino-4-deoxychorismate synthase PabB. *Angew. Chemie Int. Ed*. *46*, 8284–8286.

Khader, S.A., Pearl, J.E., Sakamoto, K., Gilmartin, L., Bell, G.K., Jelley-Gibbs, D.M., Ghilardi, N., deSauvage, F., and Cooper, A.M. (2005). IL-23 Compensates for the Absence of IL-12p70 and Is Essential for the IL-17 Response during Tuberculosis but Is Dispensable for Protection and Antigen-Specific IFN-ɣ Responses if IL-12p70 Is Available. *J. Immunol*. *175*, 788–7950.

Khader, S.A., Bell, G.K., Pearl, J.E., Fountain, J.J., Rangel-Moreno, J., Cilley, G.E., Shen, F., Eaton, S.M., Gaffen, S.L., Swain, S.L., *et al*. (2007). IL-23 and IL-17 in the establishment of protective pulmonary CD4+ T cell responses after vaccination and during *Mycobacterium tuberculosis* challenge. *Nat. Immunol*. *8*, 369.

Klaus, S.M.J., Wegkamp, A., Sybesma, W., Hugenholtz, J., Gregory, J.F., and Hanson, A.D. (2005). A nudix enzyme removes pyrophosphate from dihydroneopterin triphosphate in the folate synthesis pathway of bacteria and plants. *J. Biol. Chem*. *280*, 5274–5280.

Knöchel, T., Ivens, A., Hester, G., Gonzalez, A., Bauerle, R., Wilmanns, M., Kirschner, K., and Jansonius, J.N. (1999). The crystal structure of anthranilate synthase from *Sulfolobus solfataricus*: functional implications. *Proc. Natl. Acad. Sci. U. S. A*. *96*, 9479–9484.

Kok, M., Michea-Hamzehpour, M., Plesiat, P., Gotoh, N., Nishino, T., Curty, L.K., Pechere, J.C., Köhler, T., Kok, M., Michea-Hamzehpour, M., *et al*. (1996). Multidrug efflux in intrinsic resistance to trimethoprim and sulfamethoxazole in *Pseudomonas aeruginosa*. *Antimicrob Agents Chemother*. *40*, 2288-90.

Kok, M., Bühlmann, E., and Pechère, J.C. (2001). *Salmonella typhimurium thyA* mutants fail to grow intracellularly *in vitro* and are attenuated in mice. *Microbiology 147*, 727–733.

Koressaar, T., and Remm, M. (2007). Enhancements and modifications of primer design program Primer3. *Bioinformatics 23*, 1289–1291.

Koul, A., Arnoult, E., Lounis, N., Guillemont, J., and Andries, K. (2011). The challenge of new drug discovery for tuberculosis. *Nature 469*, 483–490.

Kremer, L., Estaquier, J., Brandt, E., Ameisen, J.C., and Locht, C. (2007). *Mycobacterium bovis* Bacillus Calmette Guérin infection prevents apoptosis of resting human monocytes. *Eur. J. Immunol*. *27*, 2450–2456.

Kriakov, J., Lee, S. hee, and Jacobs, W.R. (2003). Identification of a Regulated Alkaline Phosphatase, a Cell Surface-Associated Lipoprotein, in *Mycobacterium smegmatis*. *J. Bacteriol*. *185*, 4983–4991.

Kumar, A., Guardia, A., Colmenarejo, G., Pérez, E., Gonzalez, R.R., Torres, P., Calvo, D., Gómez, R.M., Ortega, F., Jiménez, E., *et al*. (2015). A Focused Screen Identifies Antifolates with Activity on *Mycobacterium tuberculosis*. *ACS Infect. Dis*. *1*, 604–614.

Kumar, A., Chettiar, S., and Parish, T. (2017). Current challenges in drug discovery for tuberculosis. *Expert Opin. Drug Discov*. *12*, 1–4.

Lange, C., Abubakar, I., Alffenaar, J.W.C., Bothamley, G., Caminero, J.A., Carvalho, A.C.C., Chang, K.C., Codecasa, L., Correia, A., Crudu, V., *et al*. (2014). Management of patients with multi-drug resistant/ extensively drug-resistant tuberculosis in Europe: A TBNET consensus statement. *Eur. Respir. J*. *44*, 23–63.

Lawn, S.D., Bangani, N., Vogt, M., Bekker, L.G., Badri, M., Ntobongwana, M., Dockrell, H.M., Wilkinson, R.J., and Wood, R. (2007). Utility of interferon-γ ELISPOT assay responses in highly tuberculosis-exposed patients with advanced HIV infection in South Africa. *BMC Infect. Dis*. *7*, 1–9.

Lee, J., Yennawar, N.H., Gam, J., and Benkovic, S.J. (2010). Kinetic and structural characterization of dihydrofolate reductase from *Streptococcus pneumoniae*. *Biochemistry 49*, 195–206.

Lee, J.Y. (2015). Diagnosis and treatment of extrapulmonary tuberculosis. *Tuberc. Respir. Dis.* (Seoul). *78*, 47–55.

Lehmann, J. (1946). *para*-Aminosalicylic acid in the treatment of tuberculosis. *Lancet 247*, 15–16.

Levy, C., Minnis, D., and Derrick, J.P. (2008). Dihydropteroate synthase from *Streptococcus pneumoniae* : structure, ligand recognition and mechanism of sulfonamide resistance. *Biochem. J*. *412*, 379–388.

Levy, M., Kolodziejczyk, A.A., Thaiss, C.A., and Elinav, E. (2017). Dysbiosis and the immune system. *Nat. Rev. Immunol. 17*, 219.

Lewinsohn, D.A., Heinzel, A.S., Gardner, J.M., Zhu, L., Alderson, M.R., and Lewinsohn, D.M. (2003). *Mycobacterium tuberculosis*–specific CD8+ T Cells Preferentially Recognize Heavily Infected Cells. *Am. J. Respir. Crit. Care Med*. *168*, 1346–1352.

Li, K., Li, T., Yang, S.-S., Wang, X.-D., Gao, L., Wang, R.-Q., Gu, J., Zhang, X.E., and Deng, J.Y. (2017). Deletion of *nudB* Causes Increased Susceptibility to Antifolates in *Escherichia coli* and *Salmonella enterica*. *Antimicrob. Agents Chemother*. *61*, 1–11.

Li, R., Sirawaraporn, R., Chitnumsub, P., Sirawaraporn, W., Wooden, J., Athappilly, F., Turley, S., and Hol, W. (2000). Three-dimensional structure of *M. tuberculosis* dihydrofolate reductase reveals opportunities for the design of novel tuberculosis drugs. *J Mol Biol 295*, 307–323.

Li, W., Fan, J., Hochhauser, D., Banerjee, D., Zielinski, Z., Almasan, A., Yin, Y., Kelly, R., Wahl, G.M., and Bertino, J.R. (1995). Lack of functional retinoblastoma protein mediates increased resistance to antimetabolites in human sarcoma cell

lines. *Proc. Natl. Acad. Sci. USA 92*, 10436–10440.

Li, W.W., Lin, J.T., Tong, W.P., Trippett, T.M., Brennan, M.F., and Beitino, J.R. (1992). Mechanisms of Natural Resistance to Antifolates in Human Soft Tissue Sarcomas. *Cancer Res*. *52*, 1434–1438.

Lin, J.T., Tong, W.P., Trippett, T.M., Niedzwiecki, D., Tao, Y., Tan, C., Steinherz, P., Schweitzer, B.I., and Bertino, J.R. (1991). Basis for natural resistance to methotrexate in human acute non-lymphocytic leukemia. *Leuk. Res*. *15*, 1191–1196.

Liu, C.T., Layfield, J.P., Stewart, R.J., French, J.B., Hanoian, P., Asbury, J.B., Hammes-Schiffer, S., and Benkovic, S.J. (2014). Probing the Electrostatics of Active Site Microenvironments along the Catalytic Cycle for *Escherichia coli* Dihydrofolate Reductase. *J. Am. Chem. Soc*. *136*, 10349–10360.

Lopez, P., and Lacks, S.A. (1993). A bifunctional protein in the folate biosynthetic pathway of *Streptococcus pneumoniae* with dihydroneopterin aldolase and hydroxymethyldihydropterin pyrophosphokinase activities. *J. Bacteriol*. *175*, 2214–2220.

Luzzatto, L., Apirion, D., and Schlessinger, D. (1968). Mechanism of action of streptomycin in *E. coli*: interruption of the ribosome cycle at the initiation of protein synthesis. *PNAS 60*, 873–880.

M Cristina, G., Brisse, S., Brosch, R., Fabre, M., Omaïs, B., Marmiesse, M., Supply, P., and Vincent, V. (2005). Ancient origin and gene mosaicism of the progenitor of *Mycobacterium tuberculosis*. *PLoS Pathog*. *1*, 0055–0061.

Majewski, M.W., Tiwari, R., Miller, P.A., Cho, S., Franzblau, S.G., and Miller, M.J. (2016). Design, syntheses, and anti-tuberculosis activities of conjugates of piperazino-1,3-benzothiazin-4-ones (pBTZs) with 2,7-dimethylimidazo [1,2-a]pyridine-3-carboxylic acids and 7-phenylacetyl cephalosporins. *Bioorg. Med. Chem. Lett*. *26*, 2068–2071.

Marks, D.S., Hopf, T.A., and Sander, C. (2012). Protein structure prediction from sequence variation. *Nat. Biotechnol*. *30*, 1072–1080.

Mårtensson, I.L., Almqvist, N., Grimsholm, O., and Bernardi, A.I. (2010). The pre-B cell receptor checkpoint. *FEBS Lett*. *584*, 2572–2579.

Mathieu, M., Debousker, G., Vincent, S., Viviani, F., Bamas-Jacques, N., and Mikol, V. (2005). *Escherichia coli* FolC structure reveals an unexpected

dihydrofolate binding site providing an attractive target for anti-microbial therapy. *J. Biol. Chem*. *280*, 18916–18922.

Mathys, V., Wintjens, R., Lefevre, P., Bertout, J., Singhal, A., Kiass, M., Kurepina, N., Wang, X.M., Mathema, B., Baulard, A., et al. (2009). Molecular genetics of para-aminosalicylic acid resistance in clinical isolates and spontaneous mutants of Mycobacterium tuberculosis. Antimicrob. Agents Chemother. *53*, 2100–2109.

Matovic, R., Bihelovic, F., Gruden-Pavlovic, M., and Saicic, R.N. (2014). Total synthesis and biological evaluation of *atrop*-O-benzyl-desmethylabyssomicin C. *Org. Biomol. Chem*. *12*, 7682–7685.

Matthews, D.A., Bolin, J.T., Burridge, J.M., Filman, D.J., Volz, K.W., and Kraut, J. (1985). Dihydrofolate reductase. The stereochemistry of inhibitor selectivity. *J. Biol. Chem*. *260*, 392–399.

Mazurek, G.H., LoBue, P.A., Daley, C.L., Bernardo, J., Lardizabal, A.A., Bishai, W.R., Iademarco, M.F., and Rothel, J.S. (2001). Comparison of a Whole-Blood Interferon γ Assay With Tuberculin Skin Testing for Detecting Latent *Mycobacterium tuberculosis* Infection. *JAMA 286*, 1740–1747.

Milhous, W.K., Weatherly, N.F., Bowdre, J.H., and Desjardins, R.E. (1985). *In Vitro* Activities of and Mechanisms of Resistance to Antifolate Antimalarial Drugs. *Antimicrob. Agents Chemother*. *27*, 525–530.

Minato, Y., Thiede, J.M., Kordus, S.L., Mcklveen, E.J., Turman, B.J., and Baughn, D. (2015). *Mycobacterium tuberculosis* Folate Metabolism and the Mechanistic Basis for *para*-Aminosalicylic Acid Susceptibility and Resistance. *Antimicrob. Agents Chemother*. *59*, 5097–5106.

Minato, Y., Dawadi, S., Kordus, S.L., Sivanandam, A., Aldrich, C.C., and Baughn, A.D. (2018). Mutual potentiation drives synergy between trimethoprim and sulfamethoxazole. *Nat. Commun. 9*, 1–6.

Misumi, M., and Tanaka, N. (1980). Mechanism of inhibition of translocation by kanamycin and viomycin: A comparative study with fusidic acid. *Biochem. Biophys. Res. Commun*. *92*, 647–654.

Mitchell, R.S., Schmidt, J., Capel, L.H., and Scheel, L. (1954). Study of *para*-Aminosalicylic Acid Intolerance in Tuberculosis of Lung. *J. Am. Med. Assoc*. *156*, 124–125.

Molloy, A., Laochumroonvorapong, P., and Kaplan, G. (1994a). Apoptosis, but

not necrosis, of infected monocytes is coupled with killing of intracellular bacillus Calmette-Guérin. *J. Exp. Med*. *180*, 1499 LP – 1509.

Moradigaravand, D., Grandjean, L., Martinez, E., Li, H., Zheng, J., Coronel, J., and Moore, D. (2016). *dfrA thyA* Double Deletion in *para*-Aminosalicylic Acid-Resistant. *60*, 4–7.

Morollo, A.A., and Eck, M.J. (2001). Structure of the cooperative allosteric anthranilate synthase from *Salmonella typhimurium*. *Nat. Struct. Biol*. *8*, 243–247.

Morrison, J.F., and Walsh, C.T. (1988). The behavior and significance of slow-binding enzyme inhibitors. *Adv. Enzyolmology Relat. Areas Mol. Biol*. *61*, 201–301.

Mosmann, T. (1983). Rapid colorimetric assay for cellular growth and survival: Application to proliferation and cytotoxicity assays. *J. Immunol. Methods 65*, 55–63.

Mugumbate, G., Abrahams, K.A., Cox, J.A.G., Papadatos, G., Westen, G. Van, Leli, J., Calus, S.T., Loman, N.J., and Ballell, L. (2015). Mycobacterial Dihydrofolate Reductase Inhibitors Identified Using Chemogenomic Methods and *In Vitro* Validation. *PLoS One 10*, 1–17.

Myllykallio, H., Lipowski, G., Leduc, D., Filee, J., Forterre, P., and Liebl, U. (2002). An Alternative Flavin-Dependent Mechanism for Thymidylate Synthesis. *Science*. *297*, 105–107.

Nopponpunth, V., Sirawaraporn, W., Greene, P.J., and Santi, D. V. (1999). Cloning and expression of *Mycobacterium tuberculosis* and *Mycobacterium leprae* dihydropteroate synthase in *Escherichia coli*. *J. Bacteriol*. *181*, 6814–6821.

Nurjadi, D., Olalekan, A.O., Layer, F., Shittu, A.O., Alabi, A., Ghebremedhin, B., Schaumburg, F., Hofmann-eifler, J., and Genderen, P.J.J. Van (2014). Emergence of trimethoprim resistance gene *dfrG* in *Staphylococcus aureus* causing human infection and colonization in sub-Saharan Africa and its import to Europe. *J. Antimicrob. Chemother*. *27*, 2361–2368.

O'Handley, S.F., Frick, D.N., Dunn, C.A., and Bessman, M.J. (1998). Orf186 represents a new member of the Nudix hydrolases, active on adenosine(5')triphospho(5')adenosine, ADP-ribose, and NADH. *J. Biol. Chem*. *273*, 3192—3197.

Oddo, M., Renno, T., Attinger, A., Bakker, T., MacDonald, H.R., and Meylan, P.R. (1998). Fas ligand-induced apoptosis of infected human macrophages reduces the viability of intracellular *Mycobacterium tuberculosis*. *J. Immunol*. *160*, 5448–5454.

Okoye, A.A., and Picker, L.J. (2013). CD4+ T-cell depletion in HIV infection: mechanisms of immunological failure. *Immunol. Rev*. *254*, 54–64.

Ornes, S. (2013). Antibody-drug conjugates. *Proc. Natl. Acad. Sci*. *110*, 13695

Padayachee, T., and Klugman, K.P. (1999). Novel expansions of the gene encoding dihydropteroate synthase in trimethoprim-sulfamethoxazole-resistant *Streptococcus pneumoniae*. *Antimicrob. Agents Chemother*. *43*, 2225–2230.

Palmer, A.C., and Kishony, R. (2014). Opposing effects of target overexpression reveal drug mechanisms. *Nat. Commun. 5*, 1–8.

Pandey, A.K., and Sassetti, C.M. (2008). Mycobacterial persistence requires the utilization of host cholesterol. *Proc. Natl. Acad. Sci*. *105*, 4376–4380.

Parang, K., and Cole, P.A. (2002). Designing bisubstrate analog inhibitors for protein kinases. *Pharmacol. Ther*. *93*, 145–157.

Peterson, N.D., Rosen, B.C., Dillon, N.A., and Baughn, A.D. (2015). Uncoupling environmental pH and intrabacterial acidification from pyrazinamide susceptibility in *Mycobacterium tuberculosis*. *Antimicrob. Agents Chemother*. *59*, 7320–7326.

Pettersen, E.F., Goddard, T.D., Huang, C.C., Couch, G.S., Greenblatt, D.M., Meng, E.C., and Ferrin, T.E. (2004). UCSF Chimera - A visualization system for exploratory research and analysis. *J. Comput. Chem*. *25*, 1605–1612.

Peyron, P., Vaubourgeix, J., Poquet, Y., Levillain, F., Botanch, C., Bardou, F., Daffé, M., Emile, J.-F., Marchou, B., Cardona, P.J., *et al*. (2008). Foamy Macrophages from Tuberculous Patients' Granulomas Constitute a Nutrient-Rich Reservoir for *M. tuberculosis* Persistence. *PLOS Pathog*. *4*, e1000204.

Pfuetze, K.H., and Pyle, M.M. (1949). Chemotherapy in clinical tuberculosis. *Proc. Staff Meet. Mayo Clin*. *24*, 213–219.

Philips, J.A. (2008). Mycobacterial manipulation of vacuolar sorting. *Cell. Microbiol*. *10*, 2408–2415.

Philips, J.A., and Ernst, J.D. (2012). Tuberculosis Pathogenesis and Immunity. *Annu. Rev. Pathol. Mech. Dis*. *7*, 353–384.

Pico, J.-L., and Avila-Garavito, A, Naccache, V. (1998). Mucositis: Its Occurrence, Consequences, and Treatment in the Oncology Setting. *Oncologist 3*, 446–451.

Pikis, A., Donkersloot, J., Rodriguez, W., and Keith, J. (1998). A conservative amino acid mutation in the chromosome-encoded dihydrofolate reductase confers trimethoprim resistance in *Streptococcus pneumoniae*. *J. Infect. Dis. 178*, 700–706.

van Pinxteren, L.A.H., Cassidy, J.P., Smedegaard, B.H.C., Agger, E.M., and Andersen, P. (2000). Control of latent *Mycobacterium tuberculosis* infection is dependent on CD8 T cells. *Eur. J. Immunol*. *30*, 3689–3698.

Pribat, A., de Crecy-Lagard, V., Lara-Nunez, A., Blaby, I.K., Hanson, A.D., and Gregory, J.F. (2009). FolX and FolM Are Essential for Tetrahydromonapterin Synthesis in *Escherichia coli* and *Pseudomonas aeruginosa*. *J. Bacteriol*. *192*, 475–482.

Qiu, A., Jansen, M., Sakaris, A., Min, S.H., Chattopadhyay, S., Tsai, E., Sandoval, C., Zhao, R., Akabas, M.H., and Goldman, I.D. (2006). Identification of an Intestinal Folate Transporter and the Molecular Basis for Hereditary Folate Malabsorption. *Cell*
127, 917–928.

Ragaz, L. (1948). *p*-Aminosalycylsäure in der Chemother apie der Tuberkulose. *Schweiz. Med. Wochenschr*. *78*, 332–334.

Raghavan, R., Riley, A.W., Volk, H., Caruso, D., Hironaka, L., Sices, L., Hong, X., Wang, G., Ji, Y., Brucato, M., *et al*. (2018). Maternal Multivitamin Intake, Plasma Folate and Vitamin B12 Levels and Autism Spectrum Disorder Risk in Offspring. Paediatr. *Perinat. Epidemiol*. *32*, 100–111.

Ramakrishnan, L. (2012). Revisiting the role of the granuloma in tuberculosis. *Nat. Rev. Immunol*. *12*, 352–366.

Ramakrishnan, P., Aagesen, A.M., McKinney, J.D., and Tischler, A.D. (2016). *Mycobacterium tuberculosis* Resists Stress by Regulating *pe19* Expression. *Infect. Immun*. *84*, 735–746.

Ramón-García, S., Mick, V., Dainese, E., Martín, C., Thompson, C.J., De Rossi, E., Manganelli, R., and Aínsa, J.A. (2012). Functional and Genetic Characterization of the Tap Efflux Pump in *Mycobacterium bovis* BCG. *Antimicrob. Agents Chemother*. *56*, 2074–2083.

Rattan, R., Bhattacharjee, S., Zong, H., Swain, C., Siddiqui, M.A., Visovatti, S.H., Kanthi, Y., Desai, S., Pinsky, D.J., and Goonewardena, S.N. (2017). Nanoparticle-macrophage interactions: A balance between clearance and cell-specific targeting. *Bioorg. Med. Chem*. *25*, 4487–4496.

Reed, M.B., Domenech, P., Manca, C., Su, H., Barczak, A.K., Kreiswirth, B.N., Kaplan, G., and Barry III, C.E. (2004). A glycolipid of hypervirulent tuberculosis strains that inhibits the innate immune response. *Nature 431*, 84.

Rengarajan, J., Sassetti, C., Naroditskaya, V., Sloutsky, A., Bloom, B., and Rubin, E. (2004). The folate pathway is a target for resistance to the drug *para*-aminosalicylic acid (PAS) in mycobacteria. *Mol Microbiol 53*, 275–282.

Rhee, M.S., Wang, Y., Nair, M.G., and Galivan, J. (1993). Acquisition of Resistance to Antifolates Caused by Enhanced γ-Glutamyl Hydrolase Activity. *Cancer Res*. *53*, 2227–2230.

Riedlinger, J., Reicke, A., Zahner, H., Krismer, B., Bull, A.T., Maldonado, L.A., Ward, A.C., Goodfellow, M., Bister, B., Bischoff, D., *et al*. (2004). Abyssomicins, Inhibitors of the *para*-Aminobenzoic Acid Pathway Produced by the Marine Verrucosispora Strain AB-18-032. *J. Antibiot. (Tokyo)*. *57*, 271–279.

Rogall, T., Wolters, J., Flohr, T., and Bottger, E. (1990). Towards a phylogeny and definition of species at the molecular level within the genus *Mycobacterium*. *Int. Jounral Syst. Bacteriol*. *40*, 323–330.

Roux, B., and Walsh, C.T. (1993). *p*-Aminobenzoate Synthesis in *Escherichia coli*: Mutational Analysis of Three Conserved Amino Acid Residues of the Amidotransferase PabA. *Biochemistry 32*, 3763–3768.

Rubin, E.J., Akerley, B.J., Novik, V.N., Lampe, D.J., Husson, R.N., and Mekalanos, J.J. (1999). In vivo transposition of mariner-based elements in enteric bacteria and mycobacteria. *Proc. Natl. Acad. Sci*. *96*, 1645–1650.

Russell, D.G. (2001). *Mycobacterium tuberculosis*: here today, and here tomorrow. *Nat. Rev. Mol. Cell Biol*. *2*, 569.

Salcedo, E., Cortese, J.F., Plowe, C. V., Sims, P.F.G., and Hyde, J.E. (2001). A

bifunctional dihydrofolate synthetase–folylpolyglutamate synthetase in *Plasmodium falciparum* identified by functional complementation in yeast and bacteria. *Mol. Biochem. Parasitol*. *112*, 239–252.

Sambandan, D., Baughn, A.D., Hsu, T., Alahari, A., Kremer, L., Ojha, A.K., Guerardel, Y., Jacobs, W.R., Trivelli, X., and Hatfull, G.F. (2008). Growth of *Mycobacterium tuberculosis* biofilms containing free mycolic acids and harbouring drug-tolerant bacteria. *Mol. Microbiol*. *69*, 164–174.

Samten, B., Wang, X., and Barnes, P.F. (2009). *Mycobacterium tuberculosis* ESX-1 system-secreted protein ESAT-6 but not CFP10 inhibits human T-cell immune responses. *Tuberculosis 89*, 74–76.

Sánchez-Osuna, M., Cortés, P., Barbé, J., and Erill, I. (2019). Origin of the Mobile Di-Hydro-Pteroate Synthase Gene Determining Sulfonamide Resistance in Clinical Isolates. *Front. Microbiol*. *9*, 1–15.

Sander, C., Marks, D.S., Hopf, T.A., Colwell, L.J., Pagnani, A., Sheridan, R., and Zecchina, R. (2011). Protein 3D Structure Computed from Evolutionary Sequence Variation. *PLoS One 6*, e28766.

Sanders, W.J., Nienaber, V.L., Lerner, C.G., McCall, J.O., Merrick, S.M., Swanson, S.J., Harlan, J.E., Stoll, V.S., Stamper, G.F., Betz, S.F., *et al*. (2004). Discovery of Potent Inhibitors of Dihydroneopterin Aldolase Using CrystaLEAD High-Throughput X-ray Crystallographic Screening and Structure-Directed Lead Optimization. *J. Med. Chem*. *47*, 1709–1718.

Schäfer, G., Jacobs, M., Wilkinson, R.J., and Brown, G.D. (2009). Non-opsonic recognition of *Mycobacterium tuberculosis* by phagocytes. *J. Innate Immun*. *1*, 231–243.

Schatz, A., Bugle, E., and Waksman, S.A. (1944). Streptomycin, a Substance Exhibiting Antibiotic Activity Against Gram-Positive and Gram-Negative Bacteria. *Proc. Soc. Exp. Biol. Med*. *55*, 66–69.

Schimke, R.T. (1988). Gene amplification in cultured cells. *J. Biol. Chem*. *263*, 5989–5992.

Schnappinger, D., Ehrt, S., Voskuil, M.I., Liu, Y., Mangan, J.A., Monahan, I.M., Dolganov, G., Efron, B., Butcher, P.D., Nathan, C., et al. (2003). Transcriptional Adaptation of *Mycobacterium tuberculosis* within Macrophages. *J. Exp. Med*. *198*, 693–704.

Schnell, J.R., Dyson, H.J., and Wright, P.E. (2004). Structure, dynamics, and catalytic function of dihydrofolate reductase. *Annu. Rev. Biophys. Biomol. Struct*. *33*, 119–140.

Seidel, H., and Bittner, J. (1902). Darstellung der βm Aminosalicylsäure. *Monatch Chem 23*, 431–433.

Sener, E.F., Oztop, D.B., and Ozkul, Y. (2014). *MTHFR* Gene C677T Polymorphism in Autism Spectrum Disorders . *Genet. Res. Int*. *2014*, 1–5.

Seputiene, V., Povilonis, J., Ruz, M., Pavilonis, A., and Suziedeliene, E. (2010). Prevalence of trimethoprim resistance genes in *Escherichia coli* isolates of human and animal origin in Lithuania. *J. Med. Microbiol*. *59*, 315–322.

Shane, B. (1979). Pteroylpoly (gamma glutamate) Synthesis by *Corynebacterium* Species. *J. Biol. Chem*. *255*, 5655–5662.

Sheng, Y., Khanam, N., Tsaksis, Y., Shi, X., Lu, Q., and Bognar, A.L. (2008). Mutagenesis of Folylpolyglutamate Synthetase Indicates That Dihydropteroate and Tetrahydrofolate Bind to the Same Site. *Biochemistry 47*, 2388–2396.

Shi, G., Shaw, G., Liang, Y.H., Subburaman, P., Li, Y., Wu, Y., Yan, H., and Ji, X. (2012). Bisubstrate analogue inhibitors of 6-hydroxymethyl-7,8-dihydropterin pyrophosphokinase: New design with improved properties. *Bioorganic Med. Chem*. *20*, 47–57.

Shi, W., Zhang, X., Jiang, X., Yuan, H., Lee, J.S., Barry, C.E., Wang, H., Zhang, W., and Zhang, Y. (2011). Pyrazinamide Inhibits *Trans*-Translation in *Mycobacterium tuberculosis*. *Science*. *333*, 1630–1632.

Shin, H.W., Lim, J., Kim, S., Kim, J., Kwon, G.C., and Koo, S.H. (2014). Characterization of trimethoprim-sulfamethoxazole resistance genes and their relatedness to class 1 integron and insertion sequence common region in gram-negative bacilli. *J. Microbiol. Biotechnol*. *25*, 137–142.

Siddiqi, N., Das, R., Pathak, N., Banerjee, S., Ahmed, N., Katoch, V.M., and Hasnain, S.E. (2004). *Mycobacterium tuberculosis* Isolate with a Distinct Genomic Identity Overexpresses a Tap-Like Efflux Pump. *Infection 32*, 109–111.

Sievers, O. (1946). No. Sven. *Lakartidn*. *204*, 2041.

Sincak, C.A., and Schmidt, J.M. (2009). Iclaprim, a novel diaminopyrimidine for the treatment of resistant gram-positive infections. *Ann. Pharmacother*. *43*, 1107–1114.

Sköld, O. (2000). Sulfonamide resistance: mechanisms and trends. *Drug Resist. Updat*. *3*, 155–160.

Slock, J., Stahly, D.P., Han, C.Y., Six, E.W., and Crawford, I.P. (1990). An apparent *Bacillus subtilis* folic acid biosynthetic operon containing *pab*, an amphibolic *trpG* gene, a third gene required for synthesis of *para*-aminobenzoic acid, and the dihydropteroate synthase gene. *J. Bacteriol*. *172*, 7211–7226.

Sly, L.M., Hingley-Wilson, S.M., Reiner, N.E., and McMaster, W.R. (2014). Survival of Mycobacterium tuberculosis in Host Macrophages Involves Resistance to Apoptosis Dependent upon Induction of Antiapoptotic Bcl-2 Family Member Mcl-1. J*. Immunol*. *170*, 430–437.

Smilack, J. (1999). Trimethoprim-sulfamethoxazole. *Mayo Clin Proc 74*, 730–734.

Smith, C.A., Cross, J.A., Bognar, A.L., and Sun, X. (2006). Mutation of Gly51 to serine in the P-loop of *Lactobacillus casei* folylpolyglutamate synthetase abolishes activity by altering the conformation of two adjacent loops. *Acta Crystallogr. Sect. D 62*, 548–558.

Srinivasan, B., Kolli, A.R., Esch, M.B., Abaci, H.E., Shuler, M.L., and Hickman, J.J. (2015). TEER Measurement Techniques for In Vitro Barrier Model Systems. *J. Lab. Autom*. *20*, 107–126.

Srimatkandada, S., Schweitzer, B.I., Moroson, B.A., Dube, S., and Bertino, J.R. (1989). Amplification of a polymorphic dihydrofolate reductase gene expressing an enzyme with decreased binding to methotrexate in a human colon carcinoma cell line, HCT-8R4, resistant to this drug. *J. Biol. Chem*. *264*, 3524–3528.

Stanley, S.A., Raghavan, S., Hwang, W.W., and Cox, J.S. (2003). Acute infection and macrophage subversion by *Mycobacterium tuberculosis* require a specialized secretion system. *Proc. Natl. Acad. Sci*. *100*, 13001–13006.

Stone, D., and Smith, S.L. (1979). The amino acid sequence of the trimethoprim-resistant dihydrofolate reductase specified in *Escherichia coli* by R-plasmid R67. *J. Biol. Chem*. *254*, 10857–10861.

Stover, C.K., da la Cruiz, V.F., P., B.G., Hanson, M.S., Fuerst, T.R., Jacobs, W.R.J., and Bloom, B.R. (1992). Use of recombinant BCG as a vaccine delivery vehicle. *Adv. Exp. Med. Biol*. *327*, 175–182.

Strevel, E.L., Kuper, A., and Gold, W.L. (2006). Severe and protracted

hypoglycaemia associated with co-trimoxazole use. *Lancet Infect. Dis*. *6*, 178–182.

Sudimack, J., and Lee, R.J. (2000). Targeted drug delivery via the folate receptor. *Adv. Drug Deliv. Rev*. *41*, 147–162.

Sun, X., Cross, J.A., Bognar, A.L., Baker, E.N., and Smith, C.A. (2001). Folate-binding triggers the activation of folylpolyglutamate synthetase. *J. Mol. Biol*. *310*, 1067–1078.

Supply, P., Marceau, M., Mangenot, S., Roche, D., Rouanet, C., Khanna, V., Majlessi, L., Criscuolo, A., Tap, J., Pawlik, A., *et al*. (2013). Genomic analysis of smooth tubercle bacilli provides insights into ancestry and pathoadaptation of *Mycobacterium tuberculosis*. *Nat. Genet*. *45*, 172–179.

Suthar, A.B., Lawn, S.D., del Amo, J., Getahun, H., Dye, C., Sculier, D., Sterling, T.R., Chaisson, R.E., Williams, B.G., Harries, A.D., *et al*. (2012). Antiretroviral therapy for prevention of tuberculosis in adults with hiv: A systematic review and meta-analysis. *PLoS Med*. *9*. e1001270.

Swedberg, G., Ringertz, S., and Sköld, O. (1998). Sulfonamide resistance in Streptococcus pyogenes is associated with differences in the amino acid sequence of its chromosomal dihydropteroate synthase. *Antimicrob. Agents Chemother*. *42*, 1062–1067.

Tai, N., Ding, Y., Schmitz, J.C., and Chu, E. (2002). Identification of critical amino acid residues on human dihydrofolate reductase protein that mediate RNA recognition. *Nucleic Acids Res*. *30*, 4481–4488.

Takayama, K., and Kilburn, J.O. (1989). Inhibition of synthesis of arabinogalactan by ethambutol in *Mycobacterium smegmatis*. *Antimicrob. Agents Chemother*. *33*, 1493–1499.

Tanaka, Y., Nakagawa, N., Kuramitsu, S., Yokoyama, S., and Masui, R. (2005). Novel reaction mechanism of GTP cyclohydrolase I. High-resolution X-ray crystallography of Thermus thermophilus HB8 enzyme complexed with a transition state analogue, the 8-oxoguanine derivative. *J. Biochem*. *138*, 263–275.

Thiede, J.M., Kordus, S.L., Turman, B.J., Buonomo, J.A., Aldrich, C.C., Minato, Y., and Baughn, A.D. (2016). Targeting intracellular *p*-aminobenzoic acid production potentiates the anti-tubercular action of antifolates. Sci. Rep. *6*. 38083.

Thijssen, H.H.W. (1973). A simple method for preparing 2-amino-4-hydroxy-6-formylpteridine, a precursor of the pteridine substrate of dihydropteroate biosynthesis. *Anal. Biochem*. *54*, 609–611.

Tiemersma, E.W., van der Werf, M.J., Borgdorff, M.W., Williams, B.G., and Nagelkerke, N.J.D. (2011). Natural History of Tuberculosis: Duration and Fatality of Untreated Pulmonary Tuberculosis in HIV Negative Patients: A Systematic Review. PLoS One *6*, 1–13.

Tobie, W., and Jones, M. (1949). *para*-Aminosalicylic acid in the metabolism of bacteria. *J. Bacteriol*. *57*, 573.

Tomich, M., and Mohr, C.D. (2004). Genetic characterization of a multicomponent signal transduction system controlling the expression of cable pili in *Burkholderia cenocepacia*. *J. Bacteriol*. *186*, 3826–3836.

Trippett, T., Schlemmer, S., Elisseyeff, Y., Goker, E., Wachter, M., Steinherz, P., Tan, C., Berman, E., Wright, J., and Rosowsky, A. (1992). Defective transport as a mechanism of acquired resistance to methotrexate in patients with acute lymphocytic leukemia. *Blood 80*, 1158–1163.

Untergasser, A., Cutcutache, I., Koressaar, T., Ye, J., Faircloth, B.C., Remm, M., and Rozen, S.G. (2012). Primer3-new capabilities and interfaces. *Nucleic Acids Res*. *40*, 1–12.

Vallentin, G., and Tronell, E. (1950). *p*-Amino-salicylic acid in pulmonary tuberculosis. *Tubercle 31*, 2–10.

Vandal, O.H., Nathan, C.F., and Ehrt, S. (2009). Acid resistance in *Mycobacterium tuberculosis*. *J. Bacteriol*. *191*, 4714–4721.

VanderVen, B.C., Huang, L., Rohde, K.H., and G, R.D. (2017). The Minimal Unit of Infection: *Mycobacterium tuberculosis* in the Macrophage. In Tuberculosis and the Tubercle Bacillus, O.I. Jacobs, Jr. W, McShane H, Mizrahi V, ed. (ASM Press, Washington, DC.), pp. 635–652.

Vilchèze, C., and Jacobs, W.R. (2012). The combination of sulfamethoxazole, trimethoprim, and isoniazid or rifampin is bactericidal and prevents the emergence of drug resistance in *Mycobacterium tuberculosis*. *Antimicrob. Agents Chemother*. *56*, 5142–5148.

Vincent, A.T., Nyongesa, S., Morneau, I., Reed, M.B., Tocheva, E.I., and Veyrier, F.J. (2018). The Mycobacterial Cell Envelope: A Relict From the Past or the Result of Recent Evolution? *Front. Microbiol*. *9*, 2341.

Visentin, M., Unal, E.S., Zhao, R., and Goldman, I.D. (2013). The membrane transport and polyglutamation of pralatrexate: A new-generation dihydrofolate reductase inhibitor. *Cancer Chemother. Pharmacol*. *72*, 597–606.

Viswanathan, V.K., Green, J.M., and Nichols, B.P. (1995). Kinetic characterization of 4-amino 4-deoxychorismate synthase from *Escherichia coli*. *J. Bacteriol*. *177*, 5918–5923.

Volkman, H.E., Pozos, T.C., Zheng, J., Davis, J.M., Rawls, J.F., and Ramakrishnan, L. (2010). Tuberculous Granuloma Induction via Interaction of a Bacterial Secreted Protein with Host Epithelium. *Science*. *327*, 466–469.

Volpe, F., Ballantine, S.P., and Delves, C.J. (1993). The multifunctional folic acid synthesis fas gene of *Pneumocystis carinii* encodes dihydroneopterin aldolase, hydroxymethyldihydropterin pyrophosphokinase and dihydropteroate synthase. *Eur. J. Biochem 458*, 449–458.

Wang, J.F., Dai, H.Q., Wei, Y.L., Zhu, H.J., Yan, Y.M., Wang, Y.H., Long, C.L., Zhong, H.M., Zhang, L.X., and Cheng, Y.X. (2010a). Antituberculosis agents and an inhibitor of the *para*-aminobenzoic acid biosynthetic pathway from *Hydnocarpus anthelminthica* seeds. *Chem. Biodivers*. *7*, 2046–2053.

Wang, J.Y., Chou, C.H., Lee, L.N., Hsu, H.L., Jan, I.S., Hsueh, P.R., Yang, P.C., and Luh, K.T. (2007). Diagnosis of tuberculosis by an enzyme-linked immunospot assay for interferon-γ. *Emerg. Infect. Dis*. *13*, 553–558.

Wang, P., Wang, Q., Yang, Y., Coward, J.K., Nzila, A., Sims, P.F.G., and Hyde, J.E. (2010). Characterisation of the bifunctional dihydrofolate synthase–folylpolyglutamate synthase from *Plasmodium falciparum*; a potential novel target for antimalarial antifolate inhibition. *Mol. Biochem. Parasitol*. *172*, 41–51.

Wang, Y., Li, Y., and Yan, H. (2006). Mechanism of dihydroneopterin aldolase: Functional roles of the conserved active site glutamate and lysine residues. *Biochemistry 45*, 15232–15239.

Wang, Y., Zhao, R., Russell, R.G., and Goldman, I.D. (2001). Localization of the murine reduced folate carrier as assessed by immunohistochemical analysis. *Biochim. Biophys. Acta - Biomembr*. *1513*, 49–54.

Watson, M., Liu, J.-W., and Ollis, D. (2007). Directed evolution of trimethoprim resistance in *Escherichia coli*. *FEBS J*. *274*, 2661–2671.

van der Wel, N., Hava, D., Houben, D., Fluitsma, D., van Zon, M., Pierson, J.,

Brenner, M., and Peters, P.J. (2007). *M. tuberculosis* and *M. leprae* Translocate from the Phagolysosome to the Cytosol in Myeloid Cells. *Cell 129*, 1287–1298.

Wen, X., Wang, J.-S., Backman, J.T., Laitila, J., and Neuvonen, P.J. (2002). Trimethoprim and Sulfamethoxazole are Selective Inhibitors of CYP2C8 and CYP2C9, Respectively. *Drug Metab. Dispos*. *30*, 631–635.

White, E.L., Ross, L.J., Cunningham, A., and Escuyer, V. (2004). Cloning, expression, and characterization of *Mycobacterium tuberculosis* dihydrofolate reductase. *FEMS Microbiol. Lett*. *232*, 101–105.

WHO (2018). Who, Global report 2018.

Williams, B.G., Granich, R., De Cock, K.M., Glaziou, P., Sharma, A., and Dye, C. (2010). Antiretroviral therapy for tuberculosis control in nine African countries. *Proc. Natl. Acad. Sci*. *107*, 19485–19489.

Williams, J.W., Morrison, J.F., and Duggleby, R.G. (1979). Methotrexate, a High-Affinity Pseudosubstrate of Dihydrofolate Reductase. *Biochemistry 18*, 2567–2573.

Wolf, A.J., Linas, B., Trevejo-Nunez, G.J., Kincaid, E., Tamura, T., Takatsu, K., and Ernst, J.D. (2007). *Mycobacterium tuberculosis* Infects Dendritic Cells with High Frequency and Impairs Their Function In Vivo. *J. Immunol*. *179*, 2509–2519.

Wolf, A.J., Desvignes, L., Linas, B., Banaiee, N., Tamura, T., Takatsu, K., and Ernst, J.D. (2008). Initiation of the adaptive immune response to *Mycobacterium tuberculosis* depends on antigen production in the local lymph node, not the lungs. *J. Exp. Med*. *205*, 105–115.

Wormser, G., Keusch, G., and Heel, R. (1982). Co-trimoxazole (Trimethoprim-sulfamethoxazole). *Drugs 24*, 459–518.

Wyss, O. (1943). Antibacterial action of a pyridine analogue of thiamine. *J. Bacteriol. 52*, 346.

Yang, S., Jan, Y.-H., Mishin, V., Richardson, J.R., Hossain, M.M., Heindel, N.D., Heck, D.E., Laskin, D.L., and Laskin, J.D. (2015). Sulfa Drugs Inhibit Sepiapterin Reduction and Chemical Redox Cycling by Sepiapterin Reductase. *J. Pharmacol. Exp. Ther*. *352*, 529–540.

Yegian, D., and Long, R.T. (1951). The Specific Resistance of Tubercle Bacilli to *para*-Aminosalicylic acid and Sulfonamides. *J. Bacteriol*. *61*, 747 LP – 749.

Youmans, G.P., Raleigh, G.W., and Youmans, A.S. (1947). The Tuberculostatic Action of *para*-Aminosalicylic Acid. *J. Bacteriol*. *54*, 409–416.

Young, D.B., Gideon, H.P., and Wilkinson, R.J. (2009). Eliminating latent tuberculosis. *Trends Microbiol*. *17*, 183–188.

Young, P., Smith, C., Metcalf, P., and Baker, E. (2008). Structures of *Mycobacterium tuberculosis* folylpolyglutamate synthase complexed with ADP and AMPPCP. *Acta Crystallogr D Biol Crystallogr 64*, 745–753.

Yun, M.-K., Wu, Y., Li, Z., Zhoa, Y., Waddell, M.B., Ferreira, A.M., Lee, R.E., Bashford, D., and White (2012). Catalysis and Sulfa Drug Resistance in Dihydropteroate Synthase. *Science 335*, 1110–1115.

Zhang, X., Liu, L., Zhang, Y., Dai, G., Huang, H., and Jina, Q. (2015). Genetic determinants involved in *p*-aminosalicylic acid resistance in clinical isolates from tuberculosis patients in northern China from 2006 to 2012. *Antimicrob. Agents Chemother*. *59*, 1320–1324.

Zhao, F., Wang, X. De, Erber, L.N., Luo, M., Guo, A.Z., Yang, S.S., Gu, J., Turman, B.J., Gao, Y.R., Li, D.F., *et al*. (2014). Binding pocket alterations in dihydrofolate synthase confer resistance to *para*-aminosalicylic acid in clinical isolates of *Mycobacterium tuberculosis*. *Antimicrob. Agents Chemother*. *58*, 1479–1487.

Zhao, Y., Hammoudeh, D., Yun, M.K., Qi, J., White, S.W., and Lee, R.E. (2012). Structure-Based Design of Novel Pyrimido[4,5-c]pyridazine Derivatives as Dihydropteroate Synthase Inhibitors with Increased Affinity. *ChemMedChem 7*, 861–870.

Zhao, Y., Shadrick, W.R., Wallace, M.J., Wu, Y., Griffith, E.C., Qi, J., Yun, M.-K., White, S.W., and Lee, R.E. (2016). Pterin–sulfa conjugates as dihydropteroate synthase inhibitors and antibacterial agents. *Bioorg. Med. Chem. Lett*. *26*, 3950–3954.

Zheng, J., Rubin, E.J., Bifani, P., Mathys, V., Lim, V., Au, M., Jang, J., Nam, J., Dick, T., Walker, J.R., et al. (2013). *para*-Aminosalicylic acid is a prodrug targeting dihydrofolate reductase in *Mycobacterium tuberculosis*. *J. Biol. Chem*. *288*, 23447–23456.

Zimhony, O., Cox, J.S., Welch, J.T., Vilchèze, C., and Jacobs Jr., W.R. (2000). Pyrazinamide inhibits the eukaryotic-like fatty acid synthetase I (FASI) of *Mycobacterium tuberculosis*. *Nat. Med*. *6*, 1043.

Zimmerman, M., Tolman, R., Morman, H., Graham, D., and Rogers, E. (1977). Inhibitors of folate biosynthesis. 1. Inhibition of dihydroneopterin aldolase by pteridine derivatives. *J. Med. Chem*. *20*, 1213–1215.

Zlitni, S., Ferruccio, L.F., and Brown, E.D. (2013). Metabolic suppression identifies new antibacterial inhibitors under nutrient limitation. *Nat. Chem. Biol*. *9*, 796–804.

Zuniga, E.S., Early, J., and Parish, T. (2015). The future for early-stage tuberculosis drug discovery. *Future Microbiol. 10*, 217–229.